Signaling in Retinal Degeneration and Neuroprotection – the Role of JAK/STAT and HIF

DISSERTATION

zur Erlangung der naturwissenschaftlichen Doktorwürde

(Dr. sc. Nat.)

vorgelegt der

Mathematisch-naturwissenschaftlichen Fakultät der Universität Zürich

von

Christina Lange

aus Deutschland

Promotionskomitee:

Prof. Dr. Stephan Neuhaus (Vorsitz)

Prof. Dr. Christian Grimm (Leitung)

Prof. Dr. Wolfgang Berger

Prof. Dr. Stephan Christen

Zürich 2010

Summary

Photoreceptor cell death is a leading cause of blindness in human patients and no treatment options are available to date. To develop therapeutic approaches, it is mandatory to understand the molecular mechanisms, which are initiated in response to retinal injury either to protect cells or to initiate and execute photoreceptor apoptosis.

Activation of the Janus Kinase/Signal Transducer and Activator of Transcription (JAK/STAT) signaling is common to many retinal degenerative diseases. The cytokine Leukemia inhibitory factor (LIF) was shown to induce a survival pathway during photoreceptor degeneration that implies JAK/STAT signaling. This pathway is suppressed and degeneration is accelerated in retinas lacking LIF.

In this thesis I show that expression of Janus kinase 3 (*Jak3*), but not of the other members of the Janus kinase family, is induced in four mouse models for retinal degeneration. Furthermore, *Jak3* induction correlates with the induction of *Lif* in stressed retinas even in the absence of photoreceptor degeneration. I also show that LIF is essential and sufficient to induce *Jak3* but that JAK3 is not needed for the neuroprotective LIF signaling. We suggest that LIF induces an additional, yet unknown, retinal stress response, which involves JAK3.

Hypoxic preconditioning protects murine photoreceptors from degeneration in the model of light induced retinal degeneration. It is characterized by the activation of hypoxia inducible factors (HIFs), which control the expression of a variety of target genes including genes encoding anti-apoptotic factors. Erythropoietin (EPO) is a hypoxia-inducible gene that was shown to be protective against light induced retinal degeneration. With the activation of HIFs in normoxia (by knocking down von Hippel Lindau (VHL) protein) we aimed to test their capacity to protect photoreceptors against degeneration.

In the second part of my thesis I show that normoxic stabilization of HIFs in rod-photoreceptors transiently protects against light induced degeneration. However this stabilization was not enough to rescue photoreceptors from final death. This might be partly attributed to the missing induction of *Epo* expression in the retinas of those mice. Furthermore, activation of HIF-target genes in other cell layers of the retina

may be additionally important for the neuroprotection achieved by hypoxic preconditioning. Moreover I show that the long-term hypoxia like response in rod photoreceptors leads to cell death in aged mice.

In the third part of my thesis I show that the sustained activation of HIFs in most cells of the peripheral retina leads to disturbances in the retinal vasculature and to severe retinal degeneration in the periphery and moderate loss of photoreceptor nuclei also in the central retina. The degeneration activated the LIF-controlled endogenous survival pathway, expression of genes connected to the extracellular matrix and expression of caspase 1 and 8. This *Vhl* knockdown mouse may provide a good model to study the connection between proper vasculature development and the integrity and function of the retina. The targeted inactivation of VHL can also be used to study pathological mechanisms of the VHL disease that is accompanied by hemangioblastomas in the retina.

Zusammenfassung

Photorezeptorzelltod ist eine der Hauptursachen für Blindheit beim Menschen und bis heute sind noch keine Behandlungsmöglichkeiten verfügbar. Um therapeutische Mittel für diese Krankheit zu entwickeln, ist das Verständnis der durch eine Verletzung der Netzhaut ausgelösten Mechanismen, die entweder die Zellen vor dem Tod schützen oder den Zelltod einleiten und ausführen, zwingend erforderlich.

Bei vielen Netzhautdegenerationskrankheiten wird der „Janus kinase/Signal Transducer and Activator of Transcription“ (JAK/STAT) Signalweg ausgelöst. Es wurde gezeigt, dass das Zytokin „Leukemia inhibitory factor“ (LIF) bei Photorezeptordegeneration einen Signalweg auslösen kann, der JAK/STAT Signale beinhaltet. In Mäusen, die kein LIF haben, wird dieser Signalweg unterbunden und die Netzhautdegeneration beschleunigt.

In dieser Doktorarbeit zeige ich, dass nur die Expression von Janus kinase 3 (*Jak3*) in vier Mausmodellen für Netzhautdegeneration induziert wird, und die Expression der anderen Janus Kinase Familienmitglieder gegenüber einer gesunden Kontrolle gleich bleibt. Darüberhinaus korreliert die *Jak3* Induktion mit der Induktion von *Lif* in gestressten Netzhäuten unabhängig davon, ob Photorezeptoren absterben oder nicht. Weiterhin zeige ich, dass LIF zwar essentiell und ausreichend ist für die Induktion von *Jak3*, JAK3 aber nicht für den neuroprotektiven LIF-Signalweg gebraucht wird. Wir schlagen deshalb vor, dass LIF einen weiteren, noch unbekannten Signalweg auslösen kann, der JAK3 einschliesst.

Hypoxische Präkonditionierung schützt Mausphotorezeptoren vor dem Absterben im Modell der lichtinduzierten Netzhautdegeneration. Dabei werden Transkriptionsfaktoren, so genannte „hypoxia inducible factors“ (HIFs), aktiviert, welche die Expression einer Vielzahl von Zielgenen einschliesslich antiapoptotischen Genen kontrollieren. Erythropoietin (EPO) ist ein durch Hypoxie induzierbares Gen, von dem gezeigt wurde, dass es gegen lichtinduzierte Degeneration schützt.

Im zweiten Teil meiner Doktorarbeit zeige ich, dass die normoxische Stabilisierung von HIFs in Stäbchen vorübergehend vor lichtinduzieter Degeneration schützt. Diese Stabilisierung reichte jedoch letztlich nicht aus, um die Sehzellen vor dem Tod zu bewahren. Dies könnte teilweise durch die ausbleibende *Epo* Hochregulierung in den

Netzhäuten dieser Mäuse erklärbar sein. Zusätzlich könnte die Aktivierung von Zielgenen in anderen Zellschichten der Netzhaut ebenfalls wichtig sein für eine Neuroprotektion wie sie bei hypoxischer Präkonditionierung vorkommt. Ausserdem zeige ich, dass der langanhaltende hypoxie-ähnliche Zustand zu Zelltod in Netzhäuten von älteren Mäusen führt.

Im dritten Teil meiner Dissertation zeige ich, dass die anhaltende Aktivierung einer hypoxie-ähnlichen Antwort in den meisten Zellen der peripheren Netzhaut zu Beeinträchtigungen in den Blutgefässen der Netzhaut, zu schwerwiegender Netzhautdegeneration in der Peripherie und zu leichtem Absterben von Sehzellen in der zentralen Netzhaut führt. Die Degeneration aktivierte den LIF-gesteuerten endogenen Überlebenssignalweg, sowie die Expression von Genen die für Proteine der extrazellulären Matrix und für Caspase 1 und Caspase 8 kodieren. Die *Vhl* Knockdown-Maus könnte als Modell dienen, um den Zusammenhang zwischen einer korrekten Blutgefässentwicklung und dem Aufbau und Funktion der Netzhaut zu untersuchen. Die gezielte Ausschaltung von VHL könnte auch zur Aufklärung von pathologischen Mechanismen der VHL Krankheit, die von Hämangioblastomen in der Netzhaut begleitet wird, dienen.

Contents

1. Introduction

It doesn't need much of an explanation for how much eyesight is needed to lead a normal life. Vision depends on many things from an intact eye structure to functional protein machinery. The importance of vision only really appears when it is impaired or lost. Various eye diseases – environmental or hereditary - exist that impair vision or lead to blindness. To understand the processes that lead to such diseases is a major goal and a prerequisite to develop successful therapeutic strategies.

1.1. The visual system

1.1.1. The eye

The eye is a central nervous system organ that detects light stimuli and translates them into electrical signals that are computed by the brain. The vertebrate eyeball consists of three layers: the sclera, the choroid and the retina (Fig.1). Light can enter the eye through the pupil, which is build by a hole in the iris. The lens, which consists of avascular tissue, is able to accommodate so that the light from the object one wants to see hits directly on the fovea. The fovea is the place of sharp central vision in the retina (see 1.1.2.). It represents the most central part of the macula, which is found in higher primates. Zonular fibres of the ciliary muscle accomplish accommodation of the lens. To view objects that are far away, the ciliary muscle relaxes so that the lens takes up a flat shape. To view very close objects, the ciliary muscle contracts and the lens becomes more concave (Fig.2). The anterior chamber, filled with aqueous humour, covers lens and iris and supplies lens, iris and corneal epithelium with essential nutrients. Additionally, it serves to dampen immune responses to allergic grafts. The cornea constitutes a protective layer over all these structures. It contributes the most to the refractive power of the eye. Out of 59 diopters for the unaccomodated eye, 43 are accounted to the cornea and only 16 to the lens. The vitreous humour, which fills the eyeball, consists mostly of water enriched with salt and sugar and a collagen network. It contains some phagocytes to remove unwanted debris, but it

lacks blood vessels. Unlike the aqueous humour it is never replenished. Therefore everything that gets into the vitreous humour will stay there for a lifetime unless surgically removed. The vitreous humour serves also to hold the retina in place by pressing it against the choroid. Thereby it touches the retina in only three places: the anterior border of the retina, the macula and the optic nerve disc. The optic disc is the place where the optic nerve exits the eyeball. It is also referred to as the blind spot because at this position there are no photoreceptors. In the middle of the eye resides the hyaloid canal, which is the leaving from the hyaloid artery that serves to nourish the growing lens during development and from where retinal blood vessel start to invade deeper retinal layers. It regresses before birth in humans (see 1.1.6.).

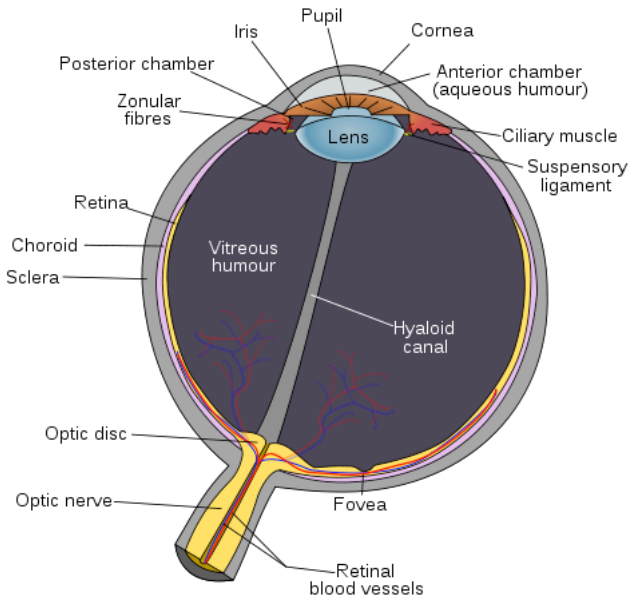

Fig.1: Schematic representation of a human eye.
http://en.wikipedia.org/wiki/File:Schematic_diagram_of_the_human_eye_en.svg

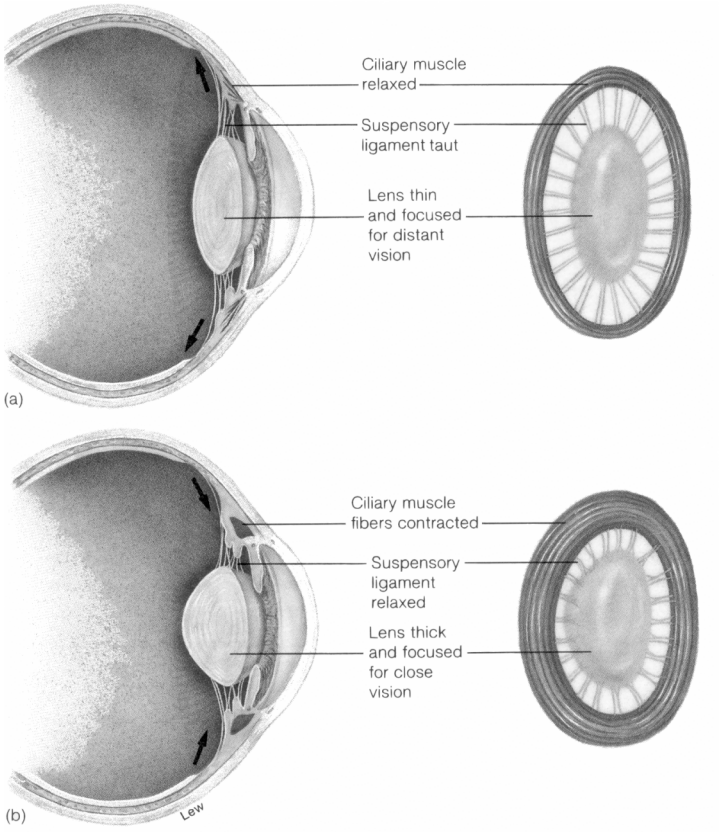

Fig.2: Schematic representation of the contraction and relaxation the ciliary muscle for accommodation of the lens.
http://projects.cbe.ab.ca/Diefenbaker/Biology/Bio%20Website%20Final/notes/nervous_system/Image51.gif

1.1.2. The architecture of the retina

The retina consists of six layers (Fig.3). The single cell layer of the retinal pigment epithelium (RPE) is the outermost layer. Its main role is the phagocytosis of photoreceptor outer segments and renewal of the visual pigment (see 1.1.4.). The photoreceptor cell bodies are located in the outer nuclear layer (ONL). They span their inner and outer segments towards the RPE. Between the photoreceptor cell bodies and the segments, the outer limiting membrane is located. In the outer plexiform layer (OPL) the photoreceptors build synapses to bipolar cells for signal transduction or to horizontal cells for signal modulation (see 1.1.5.). These cells are located in the inner nuclear layer (INL) together with amacrine cells. Amakrine cells form synaptic complexes to bipolar and ganglion cells in the inner plexiform layer (IPL). Apart from neurons, there are also glial cells in the retina: astrocytes, microglia

and Müller cells. Astrocytes are restricted to the nerve fibre layer. Together with pericytes, they are particularly important in the development of the retinal vasculature (see 1.1.6.) and later on they build an important component of the blood-retinal-barrier. Microglia reside dormant in the retina until they get stimulated into macropagic function upon retinal injury. The third kind of glial cells, the Müller-glial cell (or Müller cell) spans from the outer limiting membrane to the inner limiting membrane, which rounds of the retina at the border of the ganglion cell layer (GCL). These cells fulfill a wide range of physiological functions to support the functioning and survival of retinal neurons. Resent research showed that they may also act as optical fibres to guide the light all the way through the retina to the photoreceptors (Franze et al., 2007). The cell bodies of ganglion cells are located in the GCL. The axons of the ganglion cells gather at the optic disc and constitute the optic nerve, which exits the retina at the blind spot leading to the brain.

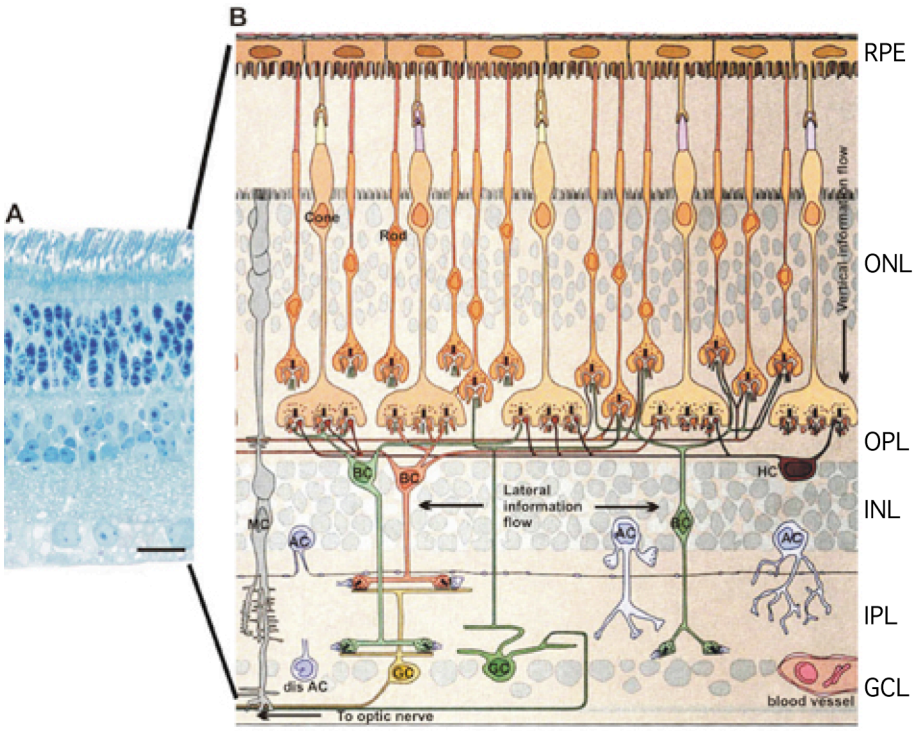

Fig.3: Morphological section of a guinea pig retina (A) and schematic representation (B) of a mouse retina. PE: pigment epithelium. PR: photoreceptor inner and outer segments. ONL: outer nuclear layer. OPL: outer plexiform layer. INL: inner nuclear layer. IPL: inner plexiform layer. GCL: ganglion cell layer. ON: optic nerve. AC: amacrine cell. BC: bipolar cell. GC: ganglion cell. HC: horizontal cell. MC: Müller cell. Scale bar: 25µm. Adapted from:
http://www.anatomy.unimelb.edu.au/researchlabs/rees/images/retina.jpg

There are two different kinds of photoreceptors, rods and cones (Fig.4). Rod photoreceptor outer segments consist of enclosed discs, whereas cone discs are infolds of the cell membrane. Cones are shorter than rods and are outnumbered by them. In the human retina around 120 million rods exist and only 6-7 million cones. Only in the central region of the retina, the macula, and in the innermost center, the fovea (around 1.5 mm in diameter in the human eye), the ratio of cones is higher. The center of the fovea, the foveola (around 0.33 mm in diameter in the human eye), is even rod-free. Rods can detect very low levels of light intensity, whereas cones only function at higher light intensities. Consequently, rods are there to see rough shapes in dim light whereas cones are there to see color with a high visual acuity in bright light. Three different kinds of cones exist in the human retina (S-, M- and L-cones), that perceive light from different wavelengths (blue, green and red respectively; Fig.5). Mice do not have L-cones, i.e. they cannot see light in the red part of the spectrum. Mice are also devoid of a macula and therefore they also have a lower percentage of cones (around 3%) and no cone-rich region in their retina.

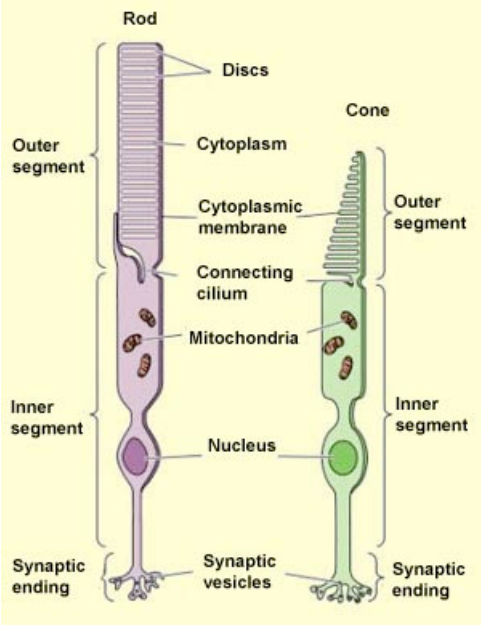

Fig.4: Schematic representation of rod and cone photoreceptors.
http://thebrain.mcgill.ca/flash/d/d_02/d_02_m/d_02_m_vis/d_02_m_vis_1a.jpg

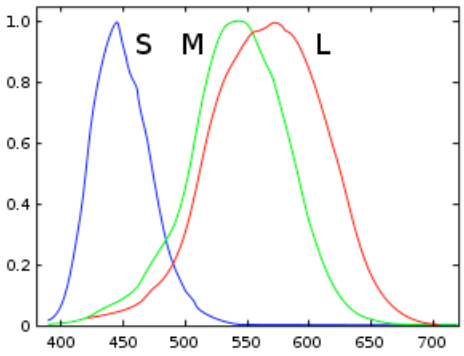

Fig.5: Absorbance spectrum and maxima of S-, M-, and L-cones (blue, green and red, respectively). http://en.wikipedia.org/wiki/File:Cones_SMJ2_E.svg

1.1.3. Phototransduction

The discs in the outer segments of rod and cone photoreceptors harbor special membrane proteins called opsin (rod opsin or cone opsin, respectively). Together with the chromophore 11-*cis*-retinal they build the light sensitive visual pigment. Most of what is known about the molecular events of phototransduction has been learned from experiments in rods, in which the photopigment is rhodopsin (Fig.6). When light enters the retina and a photon hits the visual pigment, the chomophore undergoes a conformational change from 11-*cis*- to all-*trans*-retinal (first step Fig.6). This change causes activation of rhodopsin and the G-protein transducin. Several steps are executed (Fig. 6) that in the end lead to closure of cyclic guanosine monophosphate (cGMP)-gated Ca^{2+}-channels. In darkness cGMP binds to these channels leaving them open for a constant influx of Ca^{2+} and Na^{+}. This leaves the cell partially depolarized leading to a constant release of the neurotransmitter glutamate. When, during light conditions, cGMP is hydrolysed (step 4 in Fig. 6) to GMP, it cannot bind to the channels anymore. The channels will close and positively charged ions will stop to enter the cell. However, positive charge will still exit the cell due to the ongoing K^{+}-current. Therefore the cell hyperpolarizes leading to a decrease of the release of glutamate from the photoreceptor synaptic ending (see 1.1.5.). In order to switch off the system and not to react again until the chromophore is recycled, rhodopsin is phosphorylated by rhodopsin kinase. The S-antigen arrestin can bind to phosphorylated opsins and thereby block further G-protein signaling. This also

facilitates the release of all-*trans* retinal. All-*trans* retinal is now entering the visual cycle to be reisomerized to 11-*cis* retinal (see 1.1.4.).

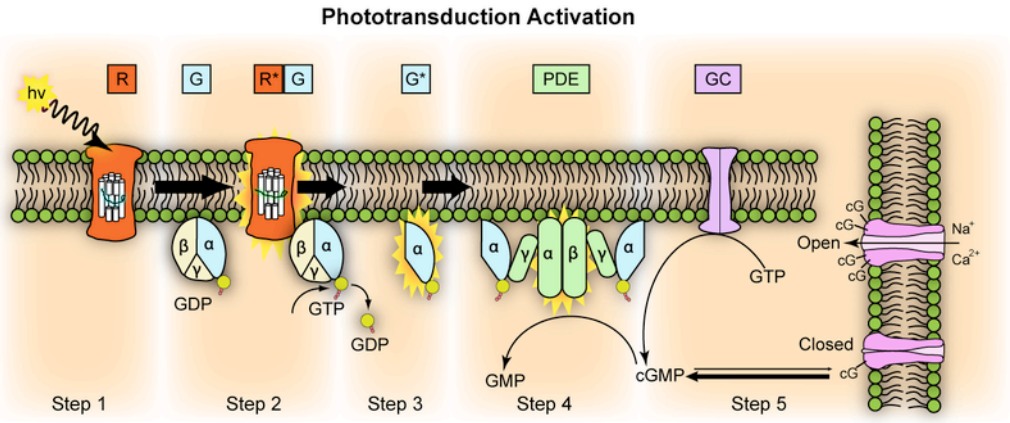

Fig.6: Schematic drawing of the events happening during phototransduction. When light enters the retina and a photon hits rhodopsin, the chomophore undergoes a conformational change from 11-*cis*- to all-*trans*-retinal (Step 1). This change causes activation of rhodopsin upon which transducin can bind to it. After binding, transducin releases guanosine-5 diphosphate (GDP) and exchanges it to guanosine-5 triphosphate (GTP) (Step 2). Then the α-subunit of transducin, which has the GTP bound, is released and binds to the γ-subunit of a phosphodiesterase (PDE) activating its α- and β-subunits (Step 4). These activated subunits hydrolyze cyclic guanosine monophosphate (cGMP, cG), which is synthesized by the guanyl cyclase (GC) (Step 5). R: rhodopsin. G: G-protein (transducin). R*: activated rhodopsin. G*: activated transducin. GMP: guanosine monophosphate.
http://en.wikipedia.org/wiki/File:Phototransduction.png

1.1.4. The visual cycle

After photon absorbtion, all-*trans* retinal is transported to the RPE where different enzymatic reactions lead to its reisomerization into the photosensitive 11-*cis* retinal (Redmond et al., 1998) (Fig.7). The most important step in this visual cycle is the reisomerisation carried out by the enzyme retinal pigment epithelium 65 (RPE65). If this protein is mutated it leads to loss of function and blindness in a disease called Leber's congenital amaurosis (see 1.2.). Furthermore, only one aminoacid substitution in RPE65 influences the light damage susceptibility in mouse models for induced retinal degeneration (see 1.3.).

The visual cycle has been described mostly for rods. Recent studies suggest that there might be a different visual cycle in cone photoreceptors involving Müller cells (Wolf, 2004; Fleisch et al., 2008; Wang and Kefalov, 2009).

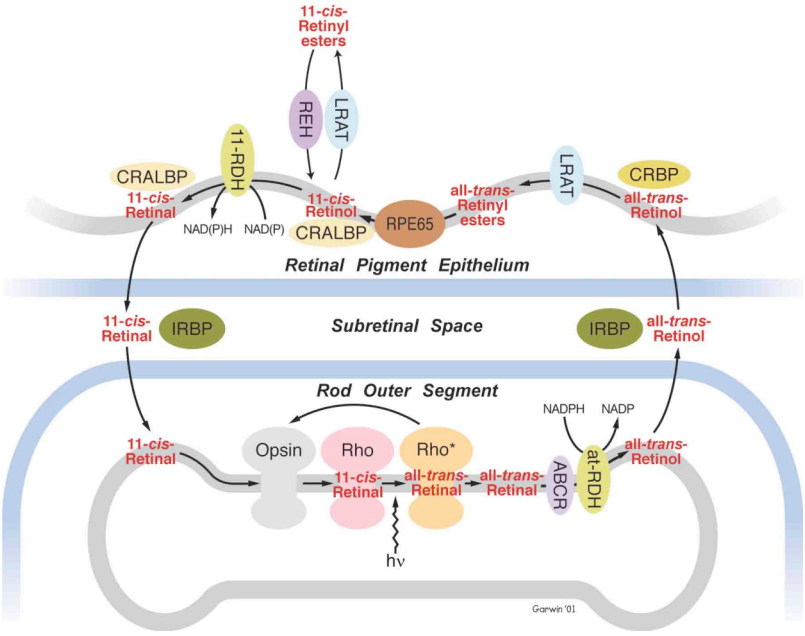

Fig.7: Schematic drawing of the events happening during the rod visual cycle. all-*trans* retinal is first transported from the disc membrane to the cytosol of the rod outer segment by the ATP binding cassette protein (ABCA). In the cytosol the all-*trans* retinol dehydrogenase (atRDH) reduces the aldehyde to all-*trans* retinol. This form binds to the inter photoreceptor retinol binding protein (IRBP) which facilitates the transport to the RPE. In the RPE all-*trans* retinol binds to the cellular retinol binding protein (CRBP). The lecithin retinol acyl transferase (LRAT) esterifies all-*trans* retinol to all-*trans* retinyl ester. This ester is hydrolyzed and isomerized to 11-*cis* retinol by RPE65. The 11-*cis* retinol dehydrogenase (11-RDH) then oxidizes 11-*cis* retinol to 11-*cis* retinal in a reaction accelerated by the cellular retinaldehyde binding protein (CRALBP). 11-*cis* retinal is finally transported back to a rod outer segment to bind to opsin and therefore form a new light sensitive rhodopsin molecule.
Rho: rhodopsin. Rho*: activated rhodopsin. REH: retinyl ester hydrolase.

1.1.5. The visual pathway

Light enters the retina from the innermost layer, the GCL, and has to travel all the way through the cell layers in order to reach the photoreceptors in the ONL. There it causes phototransduction, which leads to activation of bipolar cells in the INL. For cones, there are two kinds of bipolar cells, on-centre bipolar cells (or on-bipolar cells) and off-centre bipolar cells (or off-bipolar cells) (Fig.8). The area in the visual field

that one ganglion cell can detect is called receptive field. This is basically the same area that the corresponding bipolar cell can detect except for information that is gained or lost by lateral communication with horizontal or amacrine cells. On-bipolar cells are activated when light hits at the center of their receptive field. Off-bipolar cells react to dark receptive field centers and light in the surroundings. Like this, edges and structures can be visualized. Rods connect only to on-bipolar cells so that every little light can be detected. Furthermore, many rods connect to only one bipolar cell thereby amplifying very low light signals. Cones in the foveola connect to bipolar cells in a one-to-one ratio to establish a high visual acuity. On-bipolar cells depolarize when glutamate release from photoreceptors decreases (when light hits the photoreceptor cell) and off-bipolar cells depolarize upon high glutamate release from an unexited photoreceptor. Like most other cells in the retina (except ganglion cells) bipolar cells have graded potentials rather than action potentials. That means that depolarization of on-center bipolar cells leads to an increase of transmitter-released at their synaptic terminals and consequent depolarization (activation) of on-centre ganglion cells without the need of a threshold value.

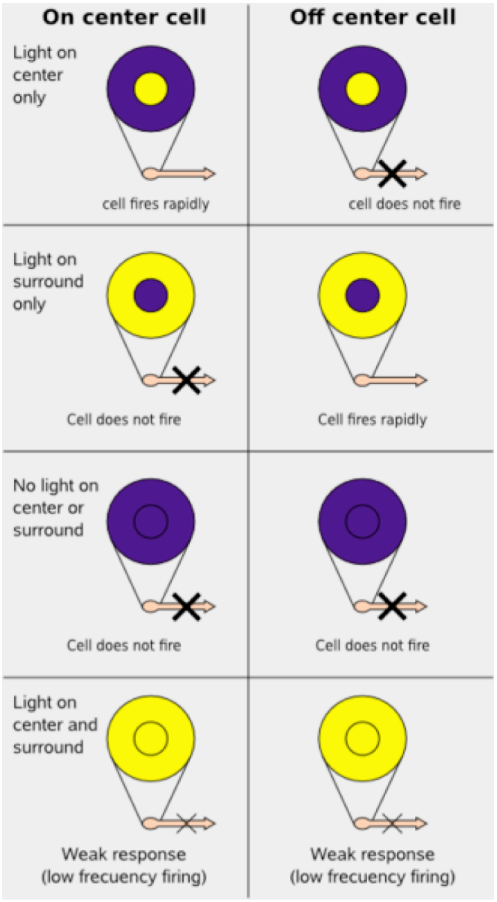

Fig.8: Schematic drawing of the receptive fields and reactions of on and off center bipolar cells. http://en.wikipedia.org/wiki/File:Receptive_field.png

The signal is then transferred to ganglion cells. Interneurons in the INL either modify the signal from photoreceptors to bipolar cells (horizontal cells) or the signal from bipolar cells to ganglion cells (amacrine cells). Rod bipolar cells don't connect directly to ganglion cells, they always connect over an amacrine cell. Modification can be either signal amplification/inhibition or it can result in more complex receptive fields that especially detect either motion or color. This ends in different on- and off-center ganglion cells that are responsible for either motion or color. When the optic nerve exits the eye it first crosses at the optic chiasm (Fig.9) and enters the laterate geniculate nucleus (LGN) as the optic tract. The LGN is the first relay station in the brain before the signal is transferred to the visual cortex.

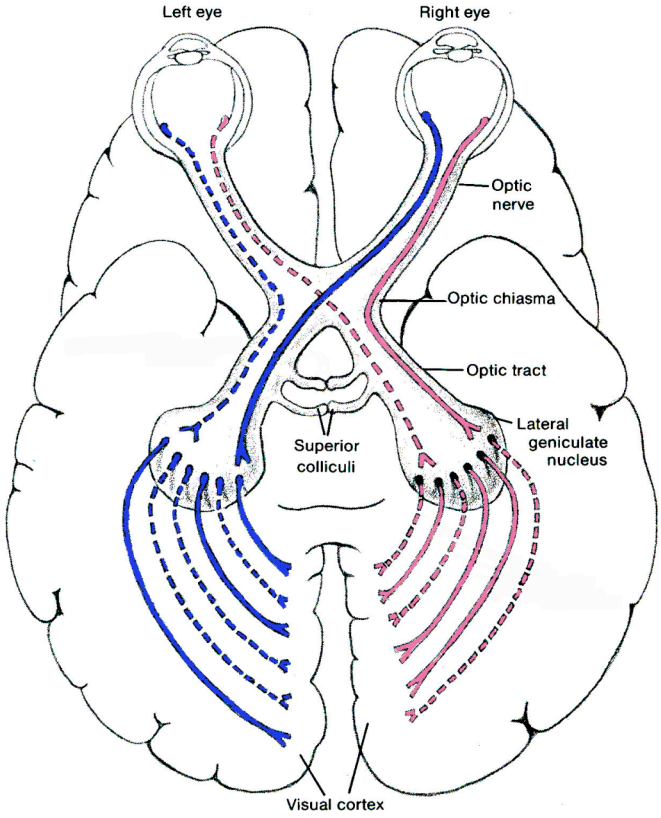

Fig.9: Schematic representation of optic nerve fibers on their way to the visual cortex. http://www.skidmore.edu/~hfoley/images/Brain.top.jpg

Another pathway is initiated by intrinsically photosensitive ganglion cells (ipGCs). These cells contain the photosensitive pigment melanopsin (Freedman et al., 1999; Gooley et al., 2003). This system regulates the circadian rhythm and other functions depending on the light-dark cycle and thus fullfills non-image forming tasks. The axons of the ipGCs project via the optic nerve to areas of the thalamus before projecting to other brain areas like motor cortex or areas for regulation of sleeping behavior (Hattar et al., 2006).

1.1.6. The retinal vasculature

Correct function of the retinal network requires supplementation of the cells with nutrients and oxygen. The retinal blood vessel system supplies the inner retinal layers whereas the choroidal vascular system nourishes the outer retinal layers. Unlike the retinal vessels, which are part of the blood-retinal-barrier and therefore contain tight junctions, the choroidal vessels are fenestrated. To maintain a blood-retinal-barrier in

the outer retina, choroidal capillaries are separated from the neural retina by the Bruch's membrane and the RPE, which contains tight junctions (Fig 10).

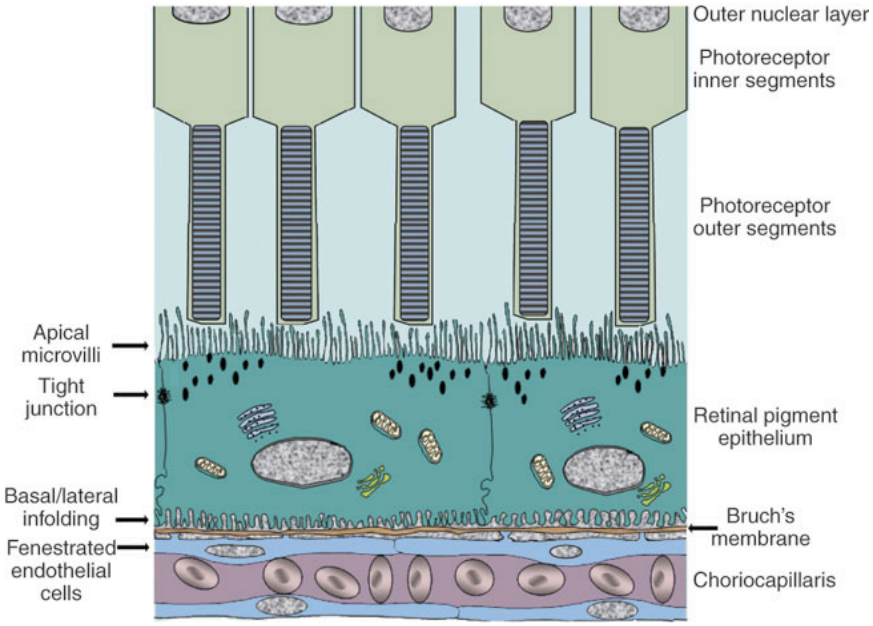

Fig.10: Schematic representation of the choroidal blood-retinal-barrier built by Bruch's membrane and the RPE.
Nature Protocols 4, 662 - 673 (2009)

The retinal vasculature develops in the fourth month after gestation in human and after birth in mice. Before that time, the hyaloid vascular system nourishes the developing retina. This arterial network in the vitreous is characterized by the absence of veins. Blood enters through the hyaloid artery in the optic nerve, runs through hyaloidal vessels in the vitreous and exits through the choroidal vein (Fig.11A). As long as the retinal thickness is below 90µm, the choroidal and hyaloidal blood supply are sufficient. In some mammals, e.g. the guinea pig, the retina remains so thin that it never develops a retinal vasculature. In most mammals however, as the retina grows, a superficial retinal vascular plexus (or primary plexus) starts to develop (Fig.11B). The new built blood vessels grow along an astrocyte network. The driving force for this is tissue hypoxia (see 1.4.). The further growth of the retina promotes the development of the deep (in OPL) and the intermediate vascular plexus (in IPL). The primary plexus consists of arteries and veins. The deeper plexi develop from veins, venules and capillaries of the primary plexus. The hyaloidal vessels regress as the retinal vessels start to build (Fig.11C).

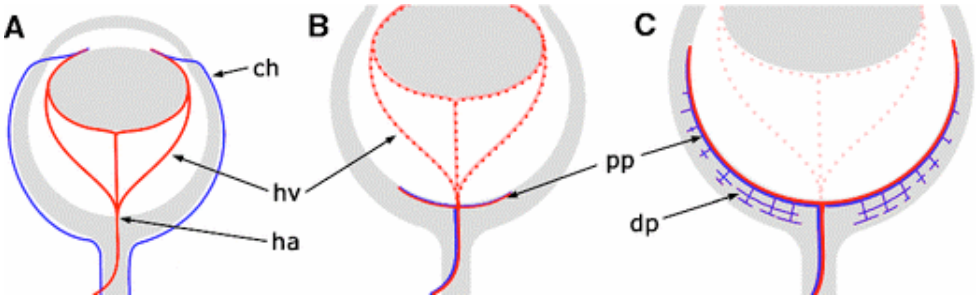

Fig.11: Schematic drawing of the regression of the hyaloid vessels and the development of the retinal vasculature. A: The hyaloid vasculature (hv) is supplied by the hyaloid artery (ha). It drains into the choroidal net (ch). B: The hyaloid vasculature regresses when the primary plexus (pp) starts to grow into the retina. C: The deeper plexi (dp) develop from veins, venules and capillaries in the primary plexus.
From Fruttiger, M., Development of the retinal vasculature, Angiogenesis 2007, 10:77-88, Figure 1.

1.2. Blinding diseases of the retina

The complex network of the visual system requires precise function of a multitude of different proteins. Not surprisingly things go wrong sometimes. Hereditary vision impairments like myopia and hyperopia, which are caused by an abnormal shape of the eyeball, are in most cases correctible by glasses. The most frequent eye disease is cataract (lense disease) followed by glaucoma (ganglion cells affected) and age related macular degeneration (macula, photoreceptors affected) (see 1.2.1.). These diseases are complex diseases involving gene mutations but also environmental factors. They develop at later ages due to certain risk factors like smoking or malnutrition. The leading cause of blindness in working age people in the western world is diabetic retinopathy, which is a secondary cause of diabetes. It develops after hyperglycemia-induced vasoregression that leads to retinal hypoxia causing activation of angiogenic genes and subsequent neovascularization in the retina (Aiello et al., 1994; Frank, 2004). These neovascularizations can rapture and cause intra-retinal bleeding and detachment of the retina. Retinitis pigmentosa (RP) (see 1.2.2.) represents a group of hereditary diseases, which especially affect photoreceptors or the RPE.

1.2.1. Age related macular degeneration

Age related macular degeneration (AMD) is the major cause of visual impairment in people over 50 years of age. It results in loss of vision in the macula, the center of the visual field, due to degeneration of the neuronal retina and the RPE (Fig.12). AMD starts with characteristic yellow deposits, called drusen, in the macula between the RPE and the choroid (Fig.13). Dry (non-exudative) AMD (also called geographic atrophy) is the most frequent and initial form of AMD. The disease can develop into the wet (exudative) and more severe form. Here, blood vessels from the choroid, which supplies the macula, grow into the retina and can cause its detachment. The blood vessels derived from neovascularization are usually leaky causing strong damage to photoreceptors. The wet form of AMD is more seldom than the dry form of AMD. It develops in only 10-15% of all AMD cases but it is nonetheless responsible for about 80% of severe visual impairment in AMD patients (Jager et al., 2008).

Fig.12: Left: an image that a healthy human can see. Right: the same image as it would be seen by an AMD patient. http://en.wikipedia.org/wiki/Macular_degeneration

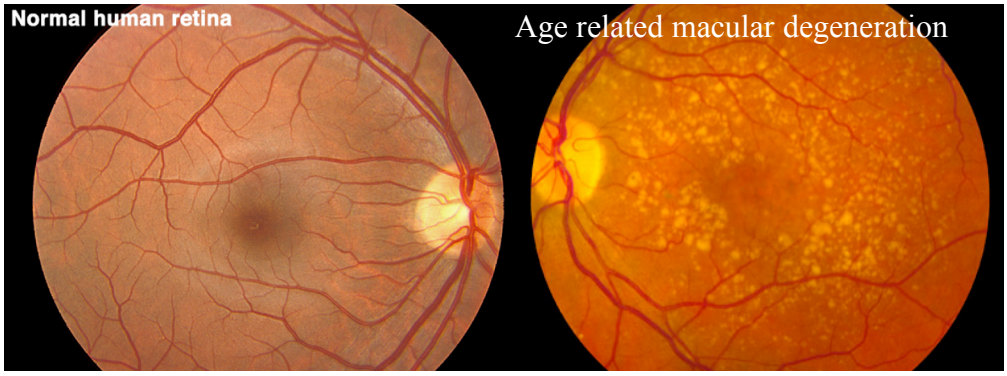

Fig.13: Left: fundus image from a healthy human. Right: fundus from an AMD patient. The yellow dots are drusen between the choroid and the RPE.
http://webvision.med.utah.edu/ClinicalERG.html#ERGs%20in%20retinitis%20pigmentosalike%20diseases and http://en.wikipedia.org/wiki/Macular_degeneration

1.2.2. Retinitis pigmentosa

Retinitis pigmentosa (RP) represents a group of hereditary diseases, which especially affect photoreceptors or the RPE classically leading to night blindness (rods are affected) and tunnel vision during adolescence (Fig. 14) until, at a later stage, the patient becomes completely blind (cones are then also affected). RP is mostly a monogenic disease. Up to now, 46 genes have been identified which, when mutated can cause RP (http://www.sph.uth.tmc.edu/Retnet/disease.htm). These genes are for example important for the visual cycle (e.g. RPE65, ABCA, LRAT) or phototransduction (e.g. SAG, RHO, PDE6A, PDE6B). Many gene mutations are still unknown and the number of identified mutations is growing constantly. Furthermore, there is increasing evidence that modifier genes – mutated genes that indirectly cause a disease by acting on another gene - also play an important role in the disease onset and progression. Statistically, 1 in 4000 humans suffers from RP, which numbers the total affected humans to more than 1.5 million worldwide. RP can be inherited in an autosomal-dominant, an autosomal recessive or in an X-linked manner. RP is a variably developing disorder, which can lead to loss of vision between childhood/birth and mid-adulthood. A characteristic of RP is the intraretinal pigmentation that can be seen in the fundus of patients (Fig.15). This pigmentation results from RPE cells that invade the neural retina due to lesions caused by dying photoreceptor cells. The

pigmentation starts in the periphery of the retina, because rods, which reside in the peripheral retina, are the first cells affected.

Fig.14: Left: an image that a healthy human can see. Right: the same image as it would be seen by an RP patient. http://en.wikipedia.org/wiki/Retinitis_pigmentosa

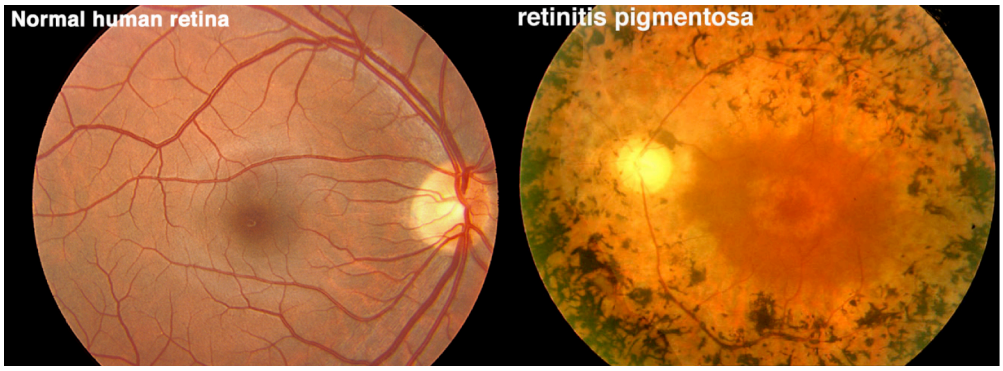

Fig.15: Left: fundus image from a healthy human. Right: fundus from an RP patient. The dark lesions represent the pigment of RPE cells that invade the retina.
http://webvision.med.utah.edu/ClinicalERG.html#ERGs%20in%20retinitis%20pigmentosalike%20diseases

1.3. Mouse models for retinal degeneration

To find out more about the molecular mechanisms underlying retinal degeneration diseases like AMD or RP different models are utilized. Cell culture models are in most cases the most unobjectionable models due to ethical reasons. However, since the retina is a very complex, multilayered neuronal tissue, it is not possible to date to use cell culture for all the studies. The mouse is a well-established model and with some exceptions the only mammal, which can be genetically modified. Using genetically modified mice it is possible to mimic human genetic diseases and study mechanisms of disease development or possibilities for therapeutic treatment.

Several mouse models, induced (see 1.3.1.) and inherited (see 1.3.2.), exist to mimic human retinal degenerations like RP or AMD. The common feature of these diseases is the loss of visual cells by apoptosis. The events taking place after the induction of the death signal share some features in induced and inherited models. But whereas induced models lead to a very synchronized cell death, inherited degenerations always represent photoreceptors in different stages of demise. Some examples for induced and inherited degeneration are described below.

1.3.1. The light exposure model

Light induced photoreceptor degeneration represents a very suitable model to study the mechanisms of degeneration. It is a fast experimental model and cell death occurs almost synchronously in all photoreceptor cells. In this model mice are exposed to very bright fluorescent white light for a specific time frame (for example 1 hour to 5000 lux for albino mice) (Reme et al., 1998; Grimm et al., 2000a; Wenzel et al., 2005). This causes very rapid photoreceptor degeneration (Fig. 16). It has been elucidated that apoptosis after light induced degeneration occurs in four phases: the induction phase, the death signal transduction phase, the execution phase and the clearance phase (Wenzel et al., 2005). Already 12 hours after exposure first pyknotic nuclei (rounded black nuclei in Fig. 16) are visible. 24 hours after the light insult disintegration of outer and inner segments can be seen and a reduced number of photoreceptor nuclei is visible at 3 days. Resident microglia get activated around 3 to 5 days after light exposure and blood macrophages enter the retina through the optic nerve and the ciliary body to phagocytose dead cells (Joly et al., 2009). Most photoreceptor debris are cleared away from the subretinal space at 10 days after exposure. However, the severity of damage can be tuned by changing duration and intensity of the insult. The susceptibility of mouse eyes to a light (and often also an inherited) insult depends closely on the amino acid at position 450 in the RPE65 isomerohydrolase (Wenzel et al., 2001). If the leucine at this position is substituted by a methionine ($Rpe65_{450Met}$) the animal is less sensitive to light. The mutation occurs naturally and renders for example the C57BL/6 mouse strain resistant against light induced degeneration. This genetic modifier also alters the speed of rhodopsin regeneration (Wenzel et al., 2001). Constant reisomerization of the chromophore is

required for light damage susceptibility (Grimm et al., 2000b; Keller et al., 2001). Mice without a functional visual cycle are resistant to light damage. Additionally, in several inherited mouse models the time course of degeneration is accelerated by light, thus the light exposure model has also relevance for inherited degenerations.

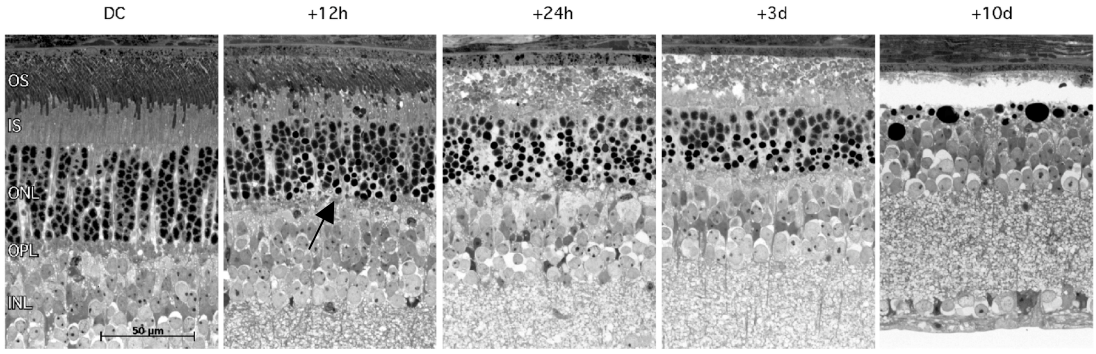

Fig. 16: Light induced retinal degeneration. Shown are morphological sections of retinas from light exposed mice. OS: outer segments. IS: inner segments. ONL: outer nuclear layer. OPL: outer plexiform layer. INL: inner nuclear layer. DC: dark control, unexposed mouse. +12h - +10d: timepoint after light exposure. h: hours. d: days. Arrow: pyknotic nucleus (example).

1.3.2. Inherited mouse models

Among the inherited models the VPP mouse (Naash et al., 1993) is a model for autosomal dominant RP. It expresses a rod opsin transgene with three mutations (V20G, P23H, P27L). Photoreceptor apoptosis starts around postnatal day 15 and procedes slowly (Fig. 17) (Samardzija et al., 2006a). The rd1 (retinal degeneration 1) mouse (Bowes et al., 1990) is a model for autosomal recessive RP. It carries a naturally occurring nonsense mutation in the β-subunit of the cGMP-phosphodiesterase (PDE). This leads to accumulation of calcium in photoreceptor outer segments that causes photoreceptor degeneration by an unknown mechanism. Already at 21 days of age most photoreceptor nuclei are lost in this mouse (onset of degeneration is around 11 days of age) (Fig. 17). The rd10 mouse (Chang et al., 2007) carries a missense mutation in the β-subunit of the PDE leading to a similar degeneration as in the rd1 mouse but with a later onset (around 15 days of age) and a slower progression. The $RPE65_{R91W}$ knock-in mouse (Samardzija et al., 2008) carries a point mutation in the *Rpe65* gene that leads to substitution of the arginine at position 91 by a tryptophan in the isomerohydrolase RPE65. This reduces reisomerization of

the chromophore 11-*cis*-retinal leading to accumulation of retinyl esters in the RPE and subsequent degeneration of first cone and then rod photoreceptors (Samardzija et al., 2009). The same mutation is found in humans with Leber congenital Amaurosis, a severe form of retinal degeneration.

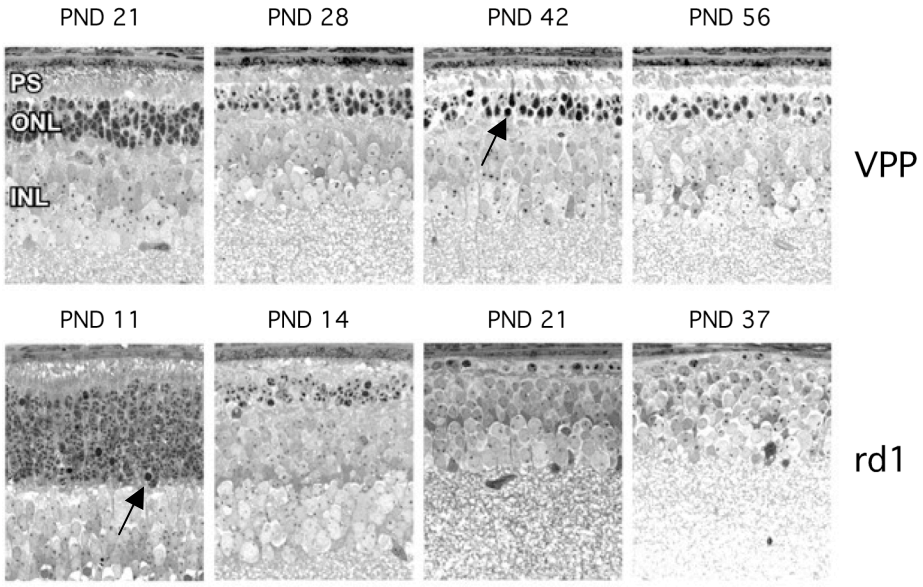

Fig. 17: Examples for inherited retinal degenerations. Pictures of retinal morphology of the VPP and the rd1 mouse model. PND: postnatal day. PS: photoreceptor segments. ONL: outer nuclear layer. INL: inner nuclear layer. Arrow: pyknotic nucleus (example).

1.4. Signaling in the retina: the JAK/STAT pathway

The Janus kinase/Signal Transducer and Activator of Transcription (JAK/STAT) signaling pathway takes part in the regulation of cellular responses to cytokines and growth factors. Six classes and different subclasses of cytokine receptors are known to date (Table 1). All cytokine receptors are composed of two or more polypeptide chains. Some cytokine receptor chains are specific to a particular cytokine receptor (e.g. LIFR for the Leukemia inhibitory factor (LIF) receptor), whereas others are shared among several such receptors (e.g. GP130 for LIF receptor and Interleukin 6 receptor). Type I and type II cytokine receptors are always associated with one or more Janus kinases (JAKs). In mammals, the JAK family compromises four members (TYK2, JAK1, JAK2 and JAK3). Of the STAT transcription factors seven members (STAT1, STAT2, STAT3, STAT4, STAT5a, STAT5b and STAT6) are known (Schindler et al., 2007). Binding of an extracellular cytokine enables trans-phosphorylation of JAKs. Upon phosphorylation they execute the subsequent phosphorylation of tyrosine residues on the receptor creating docking sites for STAT proteins. After STATs have bound to the receptor, they are phosphorylated by JAKs. This phosphorylation enables dimerization of STATs and translocation to the nucleus where they activate gene transcription. Janus kinases are crucial for the transduction of cytokine signals and are therefore often essential for survival (see also chapter 3.1.1.).

Type	Example	Special feature
Type I cytokine receptor	- Type I interleukin receptors - Erythropoietin receptor - Leukemia inhibitory factor receptor	Use JAK/STAT signaling
Type II cytokine receptor	- Type II interleukin receptors - Interferon-α/β receptor - Interferon-γ receptor	Use JAK/STAT signaling
Members of Immunoglobulin superfamily	- Interleukin 1 receptor - Interleukin 18 receptor	
Tumor necrosis factor receptor family	- FAS receptor - Nerve growth factor receptor	
Chemokine receptors	- Interleukin 8 receptor - CXCR4 (HIV)	G-protein coupled
TGF-β receptors	- TGF-β receptor 1 - TGF-β receptor 2	

Table 1: The six classes of cytokine receptors.

The JAK/STAT pathway can be negatively regulated on multiple levels (Fig. 18). Suppressors of Cytokine Signaling (SOCS) inhibit STAT phosphorylation by binding to and inhibiting JAKs or competing with STATs for phosphotyrosine binding sites on cytokine receptors (Krebs and Hilton, 2001). They are also able to interact with the elongin B/C complex and cullin 2 to build a E3 ubiquitinase complex that serves for ubiquitination of JAKs (Kile and Alexander, 2001). STATs are also negatively regulated by Protein Inhibitors of Acitvated STATs (PIAS), which act in the nucleus through several mechanisms, including blocking the DNA accessibility of STATs, recruiting transcriptional co-repressors or promoting protein sumoylation (Shuai, 2006). Protein tyrosine phosphatases (PTPs) remove phosphates from phosphorylated

tyrosine residues and can therefore inhibit activated JAKs or STATs (Sun and Tonks, 1994).

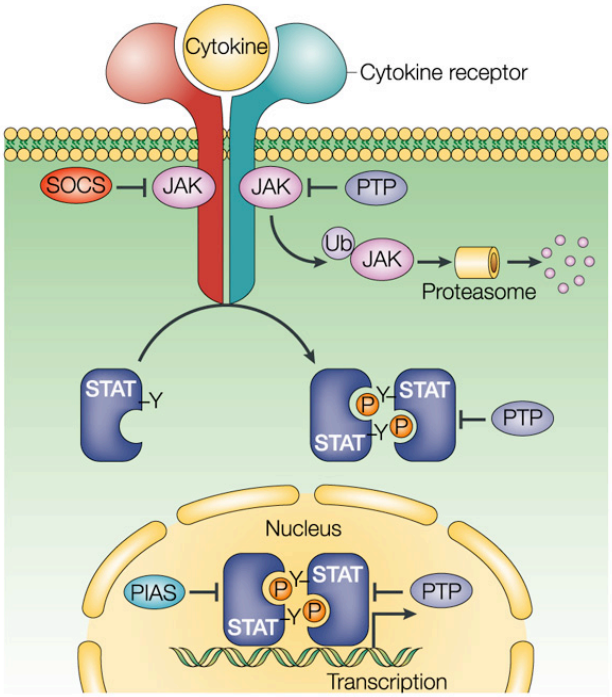

Fig.18: Schematic drawing of components of the JAK/STAT signaling pathway. SOCS: suppressor of cytokine signaling. JAK: Janus kinase. PTP: protein tyrosine phosphatase. Ub: Ubiquitination signal. STAT: Signal transducer and activator of Transcrition. PIAS: protein inhibitor of activated STATs. http://www.nature.com/nri/journal/v3/n11/images/nri1226-f2.jpg

Genes of the JAK/STAT pathway are activated during retinal degeneration (Samardzija et al., 2006a; Lange et al., 2010a) (last reference refers to chapter 3.2.3.). Their signaling has been associated with retinal stress, neuroprotection and other yet unknown functions (Joly et al., 2008; Ueki et al., 2008; Lange et al., 2010b) (last reference refers to chapter 3.1.1.).

1.5. Hypoxia and HIF

In conditions of reduced oxygen availability (hypoxia) the organs of the body need to accommodate. Therefore expression of genes for survival, metabolism and growth has to be adjusted. Special transcription factors called hypoxia inducible factors (HIFs)

serve for the upregulation of potentially protective genes during hypoxia. Three family members have been identified (HIF1, HIF2 and HIF3) with HIF1 being the best characterized (Bruick and McKnight, 2001). HIF1 controls predominantly anaerobic glycolysis (Hu et al., 2003), HIF2 appears to be the main regulator of erythropoietin (EPO) (Haase, 2010) and the role of HIF3 is until today less clear. HIFs consist of two subunits, an α-subunit, which is different for every HIF, and a common β-subunit, called arryl-hydrocarbon receptor nuclear translocator (ARNT). Both subunits belong to the basic helix-loop-helix PER/ARNT/SIM (bHLH-PAS) family. The HIF-β-subunit is located in the nucleus and is constitutively expressed. In conditions of normal oxygen availability (normoxia) HIF-α-subunits are constantly degraded (Wang and Semenza, 1993). They are hydroxylized at certain proline residues by prolyl hydroxylases (PHDs) (Bruick and McKnight, 2001; Ivan et al., 2001; Jaakkola et al., 2001) (Fig. 19). Upon this hydroxylation the proteins are recognized by the Von Hippel-Lindau (VHL) complex (see 1.7.), which targets them for proteasomal degradation through ubiquitination (Salceda and Caro, 1997; Huang et al., 1998). Another hydroxylase, the factor inhibiting HIF (FIH), hydroxylates HIF at an asparagine residue leading to a blockade of the p300 co-activator recruitment (Mahon et al., 2001). In order to function, PHDs and FIH both depend on oxygen as a substrate (Jaakkola et al., 2001; Mahon et al., 2001). Hence, during hypoxia, hydroxylation does not occur, HIF-α is stabilized and can enter the nucleus, bind HIF-β and the co-activator, and carry out transcriptional activity.

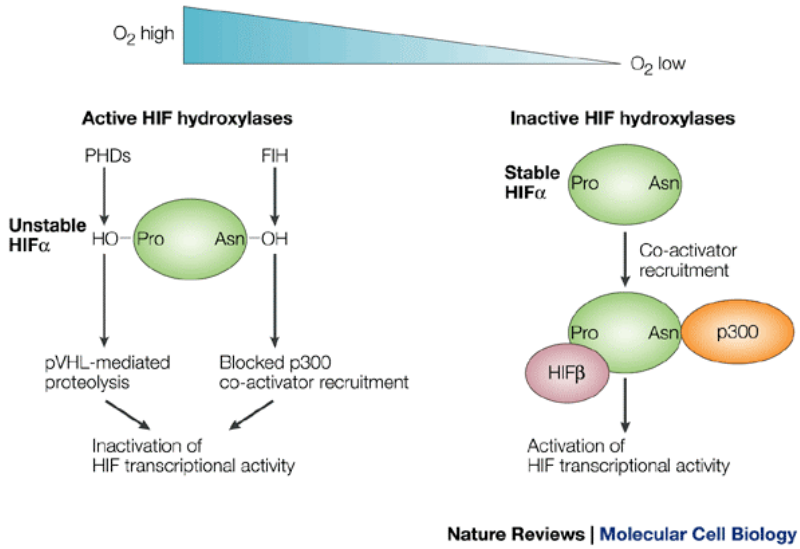

Fig.19: Schematic drawing of the events taking place during hypoxic stabilization of HIFα. PHDs: prolyl hydroxylases. FIH: factor inhibiting HIF.
http://www.nature.com/nrm/journal/v5/n5/images/nrm1366-f3.gif

Apart from heterodimerization with HIF-β, HIF-α can bind to non-PAS domain proteins and inhibit their function. Proteins like the tumor suppressor p53, the c-Myc proto-oncogene or the Notch intracellular domain have been shown to be inhibited by HIF-α binding (An et al., 1998; Koshiji et al., 2004; Gustafsson et al., 2005).

1.6. Neuroprotection by hypoxic preconditioning

The body can experience hypoxia in many different ways. Physiologically, during development of blood vessels (angiogenesis) for instance, tissue hypoxia is essential (Risau, 1997). HIF1 and its target genes like vascular endothelial growth factor (*Vegf*) and other pro- and also anti-angiogenic genes are thought to play a major role in this process (Carmeliet, 2003). In other situations hypoxia and VEGF are considered to act rather pathophysiologically, for example in tumor biology (Senger et al., 1983). There, angiogenesis is induced by the growing tumor. Blood vessels nourish the tumor promoting its further growth leading to more hypoxic tissue and again enhanced angiogenesis.

Nevertheless, hypoxia can also have beneficial effects. An exposure of mice to hypoxia before light exposure (hypoxic preconditioning) protects photoreceptors from

degeneration (Grimm et al., 2002; Grimm et al., 2005). Preconditioning – the exposure of a tissue or an organism to sublethal stress conditions – is a very successful strategy to diminish neuro- and retinal degeneration in animal models. It induces pro-survival pathways that protect against future injury. Preconditioning stimuli like light or ischemia have been shown to prevent very efficiently neuronal degeneration (Liu et al., 1998; Zhang et al., 2002). Whereas hypoxic preconditioning reduces the oxygen availability, ischemic preconditioning inhibits the blood flow preventing nutrition exchange and waste disposal.

The level of retinal neuroprotection in mice preconditioned by hypoxia correlates with the oxygen levels. A 6-hour exposure to an oxygen concentration of 6 to 10% provides complete protection against light induced retinal degeneration. 14% oxygen shows an intermediate level of protection and no protection is observed in retinas of mice exposed to 18% oxygen (normal room air has around 21% oxygen). The protection is also time-limited. After 16 h of reoxygenation the retina regains light damage susceptibility (Grimm et al., 2002; Grimm et al., 2005). This implies, that potential neuroprotective factors induced by hypoxic preconditioning are short-lived and rapidly degraded or inactivated during reoxygenation.

Erythrpoietin (EPO) is one of the proteins that is induced upon hypoxic preconditioning and has been shown to have a protective role on the retina even when applied systemically as a recombinant protein before light exposure (Grimm et al., 2006). EPO is mainly regulated by HIF2 (Haase, 2010).

1.7. VHL

The von Hippel Lindau protein (VHL) forms a multimeric protein complex together with Cullin-2, ring box1 (RBX1), and the Elongins B and C, which act as a E3 ubiquitinase (Kibel et al., 1995; Pause et al., 1997; Iwai et al., 1999; Kamura et al., 1999; Stebbins et al., 1999) (Fig.20).

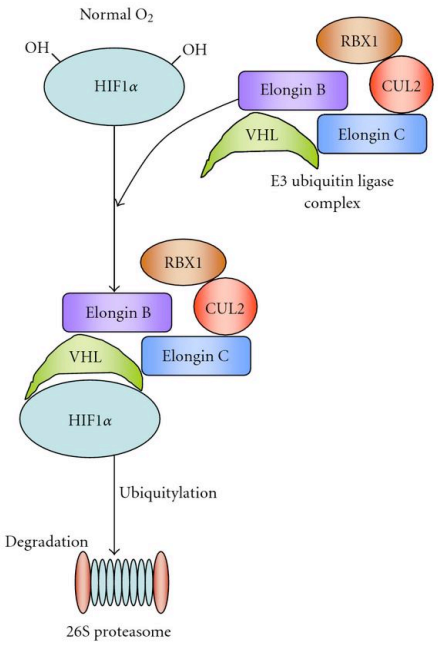

Fig.20: Schematic drawing of the events taking place during ubiquitination and degradation of HIFα. RBX1: ring box 1. CUL2: cullin 2.
http://www.hindawi.com/floats/720840/figures/720840.fig.001.jpg

VHL is the substrate recognition component of the complex. It is the master regulator of HIF transcription factors. It binds with its β-domain directly to the region where HIF-α is hydroxylated (Ohh et al., 2000). Ubiquitination of the HIF-α-subunit is exhibited by the elongin B/C-cullin2 ligase and enhanced by the RBX1 protein. Apart from regulating HIF activity, VHL has been shown to regulate microtubule stability and to be important for cilia maintenance (Hergovich et al., 2003; Thoma et al., 2007). Furthermore, VHL has been shown to be important for extracellular matrix assembly by binding to fibronectin (Ohh et al., 1998; Ohh and Kaelin, 1999) or to collagen IV without acting as an E3 ubiquitinase (Kurban et al., 2008). Additionally, it controls the stability of the plant homedomain protein Jade-1 (Zhou et al., 2004). This links VHL to the oncogenic β-catenin signaling pathway, because VHL has been also shown to suppress β-catenin through Jade-1 (Chitalia et al., 2008). VHL has also been implicated in the assembly of intracellular junctions (Calzada et al., 2006), in the signaling through atypical protein kinase C isoforms (Okuda et al., 2001) or NF-kappaB (Yang et al., 2007), in the c-Met receptor responsiveness to hepatocyte growth factor (Koochekpour et al., 1999; Peruzzi et al., 2006) and in the regulation of p53 transcriptional activity (Roe et al., 2006). Additionally, interaction of VHL with

proteins, whose function is not yet clear in tumor pathogenesis, has been suggested. These proteins include KRAB-A domain protein, VHLaK, that represses HIF transcriptional activity (Li et al., 2003), de-ubiquitylating enzymes (Li et al., 2002), the large subunit of RNA polymerase II (Kuznetsova et al., 2003) and the RNA-binding protein hnRNP A2 (Pioli and Rigby, 2001).

The VHL Syndrome is an autosomal dominant disease that manifests itself by hemangioblastomas (benign tumor of blood vessel stem cells) in the cerebellum, spinal cord and the retina. Often also renal angiomas (benign tumor of vessel wall components), renal cell carcinomas and pheochromocytomas (tumor of the adrenal gland) are part of the disease. It results from a mutation in the tumor suppressor gene VHL. Tumor development during the disease is thought to be mainly due to overactivation of HIF transcrition factors and the subsequent upregulation of angiogenic and growth related genes. However the roles of other VHL-regulated genes in this disease become more and more evident.

VHL is also important in embryogenesis, since germline inactivation of VHL results in embryonic death (Gnarra et al., 1997).

2. Aims of the thesis

Hypoxic preconditioning stabilizes photoreceptors and protects them against the toxic insult during light exposure (Grimm et al., 2002; Grimm et al., 2005). Gene expression analysis has shown that the expression of different genes changes after light exposure and/or hypoxia (Samardzija et al., 2006a; Thiersch et al., 2008). After light exposure some genes from the JAK/STAT pathway are induced. This induction led to the assumption that this signaling pathway could be important during retinal degeneration. The thesis had three specific aims:

1. To analyze the expression of the different Janus kinases in four mouse models for retinal degeneration. Special attention was then given to JAK3, because its expression was induced in all of the models (3.1.1.).
2. To analyze the role of hypoxia inducible factors in photoreceptors for neuroprotection during hypoxic preconditioning (3.1.2.).
3. To analyze the effect of early and sustained activation of hypoxia inducible factors for retinal development including retinal vasculature and potentially neuroprotection (3.1.3.).

3. Results

3.1. First author publications

3.1.1. LIF-dependent JAK3 activation is not essential for retinal degeneration

Christina Lange[1], Markus Thiersch[1], Marijana Samardzija[1], Sandra Bürgi[1], Sandrine Joly[1] and Christian Grimm[1,2]

[1]Lab for Retinal Cell Biology, Department Ophthalmology, University of Zurich
[2]Zurich Center for Integrative Human Physiology (ZIHP)

J. Neurochem. 2010, 113:1210-20

LIF-dependent JAK3 activation is not essential for retinal degeneration

Christina Lange,* Markus Thiersch,* Marijana Samardzija,* Sandra Bürgi,* Sandrine Joly* and Christian Grimm*,†

*Lab for Retinal Cell Biology, Department Ophthalmology, University of Zurich, Zurich, Switzerland
†Zurich Center for Integrative Human Physiology (ZIHP), University of Zurich, Zurich, Switzerland

Abstract
Retinal degeneration causes the induction of a leukemia inhibitory factor (LIF)-controlled survival pathway which includes Janus kinase/signal transducer and activator of transcription signaling. Lack of LIF prevents activation of this signaling cascade and accelerates disease progression leading to a fast loss of photoreceptor cells. In this study, we show that expression of Janus kinase 3 (*Jak*3), but not of the other members of the family of Janus kinases, is induced in four different models of retinal degeneration and that LIF is essential and sufficient to activate *Jak*3 gene expression. We also show that the induction of *Jak*3 and *Lif* may not depend directly on cell death but rather on the retinal stress during photoreceptor degeneration. However, despite its dependence on LIF, JAK3 is not essential for LIF-mediated photoreceptor protection or gene expression. Also, absence of JAK3 in knockout mice did not affect immune-related responses in the degenerating retina. JAK3 may therefore play a different, yet unknown, role in the retinal response to photoreceptor injury.
Keywords: retinal degeneration, JAK/STAT signaling, leukemia inhibitory factor, Janus kinase 3, neuroprotection.
J. Neurochem. (2010) **113**, 1210–1220.

Retinal degenerative diseases like retinitis pigmentosa are a frequent cause of severe visual impairment or blindness in humans. Most diseases are characterized by a progressive loss of visual cells by apoptosis. Understanding the molecular mechanisms which lead to photoreceptor cell death and identifying endogenous rescue pathways for photoreceptor survival is of fundamental importance to develop successful therapeutic strategies for the treatment of patients.

To study photoreceptor degeneration, a variety of inducible and inherited mouse models have been established. Among the inducible models, exposure of mice to high levels of white light induces photoreceptor cell death depending on light intensity and duration of exposure (Reme *et al.* 1998; Grimm *et al.* 2000a; Wenzel *et al.* 2005). After light exposure, photoreceptor cells die almost synchronously and are cleared from the subretinal space within 10 days. Rd1 [retinal degeneration 1 (Bowes *et al.* 1990)], rd10 (Chang *et al.* 2007), and the transgenic VPP (Naash *et al.* 1993) mice are examples for inherited models of retinal degeneration. Rd1 and rd10 mice carry a spontaneous and recessive nonsense or missense mutation, respectively, in the β-subunit of the cGMP-phosphodiesterase. Retinal degeneration in rd1 mice is characterized by an early onset [around post-natal day (PDN) 11] and rapid progression whereas degeneration in rd10 mice has a later onset (around PND 15) with a slower progression. The VPP mouse line carries a transgene encoding a mutant mouse rod opsin protein with three amino acid substitutions (V20G, P23H, P27L). Expression of the mutant protein causes an autosomal dominant disease (onset around PND 15) with a slow progression (Samardzija *et al.* 2006a).

A mechanism common to different degenerative models is the activation of the Janus kinase/signal transducer and

Received February 19, 2010; revised manuscript received March 9, 2010; accepted March 9, 2010.

Address correspondence and reprint requests to Christian Grimm, Lab for Retinal Cell Biology, Department of Ophthalmology, University of Zurich, Frauenklinikstrasse 24, CH-8091 Zurich, Switzerland.
E-mail: cgrimm@opht.uzh.ch

Abbreviations used: GCL, ganglion cell layer; INL, inner nuclear layer; JAK, janus kinase; LIF, leukemia inhibitory factor; ONL, outer nuclear layer; PBS, phosphate-buffered saline; PFA, paraformaldehyde; PND, post-natal day; rLIF, recombinant LIF; RPE, retinal pigment epithelium; STAT, signal transducer and activator of transcription.

activator of transcription (JAK/STAT) signaling pathway in the retina (Samardzija *et al.* 2006b). The JAK/STAT signaling pathway is known to be part of the cellular response to cytokines and growth factors and to play a central role in cell proliferation, differentiation and apoptosis. (Leonard and O'Shea 1998; Rawlings *et al.* 2004). Binding of cytokines or growth factors to their respective transmembrane receptors induces trans-phosphorylation and thus activation of receptor-bound JAKs. Once activated, JAKs phosphorylate specific tyrosine residues on the receptor to allow docking of STAT proteins. After binding, STATs are phosphorylated by JAKs, leading to their dimerization and translocation to the nucleus for gene transcription. In mammals, the JAK family of proteins contains four members: TYK2, JAK1, JAK2 and JAK3 (Schindler *et al.* 2007). JAK1 is mostly associated with class II growth factor receptors. Probably because of neurologic deficits and problems in lymphopoiesis, JAK1 knockout mice die prenatally (Rodig *et al.* 1998; Ghoreschi *et al.* 2009). JAK2 binds mainly to type I cytokine receptors like the erythropoietin receptor and is therefore critical for erythropoiesis. Consequently JAK2 knockout mice die embryonically (O'Shea *et al.* 2002). TYK2 binds to various types of cytokine receptors and primarily plays a role in allergies and the antimicrobial defense. Mutations in TYK2 cause disturbances in the human immune response (Watford and O'Shea 2006). Unlike the other JAKs that exhibit broad expression patterns, JAK3 is pre-dominantly produced in hematopoietic cells and binds specifically to the (γ_c-subunit of the IL-2-receptor subfamily of cytokine receptors. Mice lacking the subdomains I–IV of the kinase domain of JAK3 (*Jak*3−/− mice) show no JAK3 kinase activity (Thomis *et al.* 1995). They develop a severe combined immune deficiency-like phenotype with disturbed B- and T-cell maturation.

Leukemia inhibitory factor (LIF) has been shown to activate JAK/STAT signaling in the degenerating retina (Joly *et al.* 2008). LIF has been associated with protection of photoreceptors from light damage and from degeneration in the VPP mouse (Joly *et al.* 2008; Ueki *et al.* 2008) suggesting that JAK/STAT signaling may be important for the determination of photoreceptor cell fate upon damage or stress. To specifically address the role of Janus kinases in retinal degeneration, we analyzed the four JAK family members during retinal degeneration in the light-induced and in the inherited rd1, rd10 and VPP mouse models. Special attention was given to JAK3 as expression of this family member was strongly up-regulated in all of the disease models.

Materials and methods

Mice

Animals were treated in accordance with the regulations of the Veterinary Authority of Zurich and with the statement of 'The Association for Research in Vision and Ophthalmology' for the use of animals in research. Wild type 129S6/SvEvTac mice were purchased from Taconics (Eiby, Denmark), C57BL/6 were from RCC (Füllinsdorf, Switzerland), BALB/c and rd1 from Harlan (Horst, The Netherlands), and rd10 and *Jak*3–/– mice from Jackson laboratory (Bar Harbor, USA). VPP mice were obtained from Muna Naash (Naash *et al.* 1993) and mice heterozygous for *Lif* (*Lif*+/–) were a generous gift of Bettina Holtmann and Michael Sendtner (University of Wuerzburg, Wuerzburg, Germany). $Rpe65_{R91W}$ mice were generated previously in our own lab (Samardzija *et al.* 2008). To increase light damage susceptibility of *Lif*–/–, *Jak*3–/–, and their respective control mice (*Lif*+/+ and *Jak*3+/+ respectively), the light sensitive $Rpe65_{450Leu}$ allele was crossed in by breeding animals with 129S6/SvEvTac mice (Wenzel *et al.* 2001; Burgi *et al.* 2009). All mice were maintained as breeding colonies at the University of Zurich in a 12 h : 12 h light-dark cycle (60 lux).

Light exposure

Six- to eight-week-old mice were dark adapted overnight (16 h). Pupils of pigmented animals were dilated with 1% cyclogyl (Alcon, Cham, Switzerland) and 5% phenylephrine (Ciba Vision, Niederwangen, Switzerland) 45 min before exposure. BALB/c mice were exposed to 5000 lux of white fluorescent light for 1 h and pigmented animals to 13 000–15 000 lux for 2 h. After light exposure mice were kept in darkness until the next day before they were returned to cyclic light until killing and removal of the retina. Mice that were dark-adapted but not exposed to light served as controls.

Hypoxic pre-conditioning

Hypoxic pre-conditioning (6–7% O_2 for 6 h) was performed as described previously (Grimm *et al.* 2002). After hypoxia mice were dark adapted for 4 h before light exposure (see above).

Semi-quantitative real-time PCR

Retinas were removed through a slit in the cornea and immediately frozen in liquid nitrogen. Total RNA was prepared using the RNeasy RNA isolation kit (Qiagen, Hilden, Germany) according to the manufacturer's directions including a Dnase treatment to digest residual genomic DNA. Equal amounts of RNA were used for reverse transcription using oligo(dT) primer and M-MLV reverse transcriptase (Promega, Madison, WI, USA). Relative quantification of cDNA was done by semi-quantitative real time-PCR using the LightCycler 480 Sybr Green I Master kit, a LightCycler 480 instrument (Roche Diagnostics, Basel, Switzerland) and specific primer pairs (Table 1). Three animals per time point were analyzed in duplicates and normalized to β-*actin* using the Light Cycler 480 software (Roche Diagnostics, Basel, Switzerland). Values of experimental retinas were expressed relative to their respective controls, which were set to 1.

Intravitreal injection of recombinant LIF (rLIF)

Intravitreal injections were performed as described (Joly *et al.* 2008). Briefly, animals were anesthetized and 1 µL of rLIF in phosphate-buffered saline (PBS) (10 ng/µL; Chemicon, Temecula, CA, USA), or of PBS alone was injected within 5 to 10 s using a 34G needle mounted on a 10 µL Hamilton syringe. The empty needle was kept in place for additional 30 s before it was slowly withdrawn. The injection site was just behind the limbus on the

Table 1 Primers and conditions for real-time PCR

Gene	Up-stream	Down-stream	Annealing temperature (°C)	Product (bp)
*Jak*1	tgagctttgatcggatcctt	gcagggtcccagaatagatatg	60	90
*Jak*2	gaacctacagatacggagtgtcc	caaaatcatgccgccact	60	96
*Jak*3	cacagtgcatggcctatgat	aggtgtggggtctgagagg	60	66
*Tyk*2	cctgtgtcaccttgctctca	ggaatgagggatgcagttct	60	85
*Gnat*1	gaggatgctgagaaggatgc	tgaatgttgagcgtggtcat	58	209
*Gnat*2	gcatcagtgctgaggacaaa	ctaggcactcttcgggtgag	58	192
*Chx*10	ccagaagacaggatacaggtg	ggctccatagagaccatact	60	111
β-*actin*	caacggctccggcatgtgc	ctcttgctctgggcctcg	62	153
*Opn*4	ccagcttcacaaccagtcct	cagcctgatgtgcagatgtc	58	457
Lif	aatgccacctgtgccatacg	caacttggtcttctctgtcccg	60	216
*Fgf*2	tgtgtctatcaagggagtgtgtgc	accaactggagtatttccgtgaccg	62	158
*Edn*2	agacctcctccgaaagctg	ctggctgtagctggcaaag	60	64
Gfap	ccaccaaactggctgatgtctac	ttctctccaaatccacacgagc	62	240
*Stat*3	tgcggagaagcattgtgagtg	ttttccagacggtccaggcagatg	62	159

superior part of the eye. Intravitreal placement of the needle was observed through the pupil. Mice were killed 24 h after injection.

Morphology and cell death detection ELISA

For light microscopy, eyes were fixed in 2.5% glutaraldehyde in 0.1 M cacodylate buffer (pH 7.3) at 4°C overnight. For each eye, the superior and the inferior retina were prepared, washed in cacodylate buffer, incubated in osmium tetroxide for 1 h, dehydrated, and embedded in Epon 812. Sections (0.5 μm) were prepared from the lower central retina and counter-stained with methylene blue. Cell death was quantified 24 h after light exposure in isolated retinas using the ELISA-based cell death detection kit (Roche Diagnostics) according to the manufacturer's recommendation.

Immunofluorescence

Mice were perfused transcardially with 4% paraformaldehyde (PFA) in 0.1 M phosphate buffer (pH 7.4). After enucleation, eyes were fixed for 2 h in 4% PFA at 4°C before cornea and lens were removed. The remaining ocular tissue was post-fixed for additional 2 h in 4% PFA at 4°C, followed by cryoprotection in 30% sucrose in PBS, pH 7.4, at 4°C. Eyecups were embedded in tissue freezing medium (Leica Microsystems Nussloch GmbH, Nussloch, Germany) and frozen in a 2-methylbutane bath cooled by liquid nitrogen. Retinal sections (12 μm) were cut and blocked in 3% normal goat serum, 0.3% Triton X-100 in 0.1 M PBS (pH 7.4) for 1 h at 22°C. Sections were then incubated in blocking solution at 4°C overnight with one of the following primary antibodies: anti F4/80 (#T-2028 BMA biomedicals, Augst, Switzerland, 1 : 500) or anti Iba1 (#019-19741 Wako, Richmond, USA, 1 : 1000). After washing thrice with PBS, slides were incubated with the appropriate secondary antibody coupled to Cy3 for 1 h at 22°C, counter-stained with DAPI and mounted with MOWIOL anti-fade medium (10% Mowiol 4-88 (w/v) (Calbiochem, San Diego, CA, USA), in 100 mM Tris, pH 8.5, 25% glycerol (w/v) and 0.1% 1,4-diazabicyclo [2.2.2] octane. Signals on sections were analyzed with a digitalized Axiovision microscope (Carl Zeiss, Jena, Germany).

Lasercapture microdissection and detection of gene expression

Mice were killed, eyes enucleated and immediately embedded in tissue freezing medium (Leica Microsystems Nussloch GmbH) and frozen in a 2-methylbutane bath cooled by liquid nitrogen. Retinal sections (20 μm) were fixed (5 min acetone), air dried (5 min), and dehydrated (30 s 100% ethanol, 5 min xylene). Microdissection was performed using an Arcturus XT Lasercapture device (Molecular devices, Silicon Vally, USA). RNA was isolated using the Arcturus kit for RNA isolation (Molecular devices) according to the manufacturer's directions including a Dnase treatment to digest residual genomic DNA. Equal amounts of RNA were used for reverse transcription using oligo(dT) and M-MLV reverse transcriptase (Promega). Resulting cDNA was used for conventional PCR to detect layer-specific gene expression. Primers are given in Table 1. Conditions for conventional PCR included an initial denaturation step (95°C, 5 min) and 40 cycles of denaturing (95°C, 45 s), annealing (specific temperatures indicated in Table 1, 30 s) and extension (72°C, 30 s), followed by a final extension step (72°C, 10 min). Amplified products were analyzed on a non-denaturing polyacrylamide gel.

Western blotting

Retinas were homogenized by sonication in 100 mM Tris/HCl, pH 8.0, and analyzed for protein content using Bradford reagent. Standard sodium dodecyl sulfate–polyacrylamide gel electrophoresis (10%) and western blotting of 40 μg of total retinal extracts were performed. For immunodetection, the following antibodies were used: anti-STAT3 (#9132 Cell Signaling Technology, Beverly, MA, USA, 1 : 1000), anti-STAT1 (#9171 Cell Signaling Technology, 1 : 1000), anti-STAT5 (#sc835 Santa Cruz Biotechnology, Santa Cruz, CA, USA, 1 : 1000), anti-pSTAT3 (#9131 Cell Signaling Technology, 1 : 500), anti-pSTAT1 (#9171, Cell Signaling Technology, 1 : 1000), anti-pSTAT5 (#9359 Cell Signaling Technology, 1 : 1000) and anti-β-*actin* (#A5441 Sigma, St. Louis, MO, USA, 1 : 5000). Blots were incubated overnight at 4°C with primary antibodies followed by a 1 h incubation at 22°C with horseradish peroxidase-conjugated secondary antibodies. Immunoreactivity was

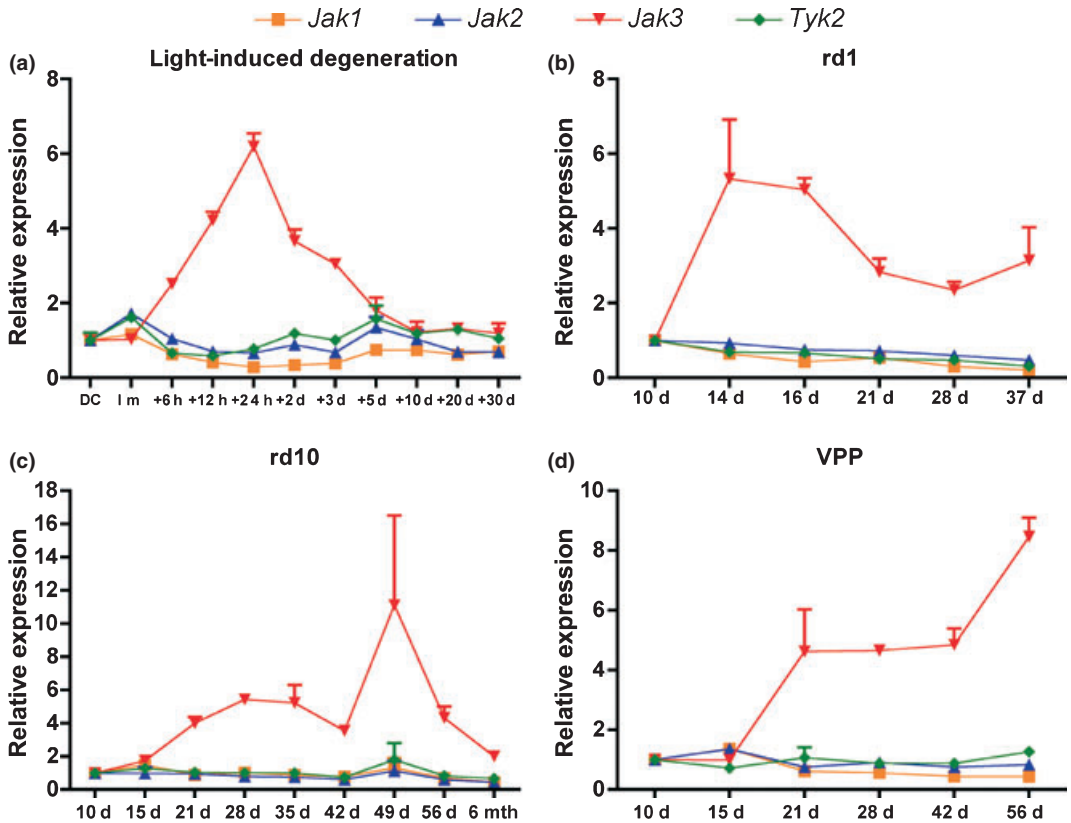

Fig. 1 Photoreceptor degeneration induces expression of *Jak*3. Expression of *Jak*1, *Jak*2, *Jak*3 and *Tyk*2 (as indicated) was detected by semi-quantitative real-time PCR after light exposure (a), in the rd1 (b), the rd10 (c) and the VPP mouse (d). Values were normalized to β-*actin* and expressed relatively to their respective controls (b–d) and to the first timepoint (a–d), which was set to 1 for each gene. Shown are means ± SD of three retinas per time point amplified in duplicates. DC, dark control; Im, immediately after light exposure; h, hours; d: days; mth, months.

visualized using the Western Lightning Chemiluminescence reagent (Perkin–Elmer, Boston, MA, USA).

Results

Photoreceptor degeneration induces expression of *Jak*3

Semi-quantitative real-time PCR analysis of the expression of the four members of the Janus kinase family of proteins (*Jak*1, *Jak*2, *Jak*3 and *Tyk*2) showed that *Jak*3 is induced in all of the models for retinal degeneration (Fig. 1). Expression peaked at 24 h after light exposure (Fig. 1a), at PND 14 in the rd1 mouse (Fig. 1b), at PND 49 in the rd10 mouse (Fig. 1c) and at the last time point tested in the VPP mouse (Fig. 1d). In contrast, expression of the other kinases did not increase but even slightly decreased. This was most obvious for *Jak*1 in the light damage model with reduced expression between 12 h and 3 days after light exposure and for *Jak*1, *Jak*2 and *Tyk*2 in the rd1 mouse, which displays the most severe degeneration phenotype. Expression of these genes in the rd1 retina continuously decreased over the period analyzed. The consistent induction of *Jak*3 expression in the retina of all models suggested that JAK3 might play an important role either in the degenerative process or in the retinal response to photoreceptor injury and thus in neuroprotection.

Janus kinases are expressed in all nuclear layers of the retina

To analyze the expression pattern of the Janus kinases in the retina, we isolated the outer nuclear layer (ONL), the inner nuclear layer (INL) and the ganglion cell layer (GCL) using lasercapture microdissection. Conventional endpoint PCR of cDNA generated from RNA isolated from each layer determined presence or absence of individual genes. Possible cross-contamination of layers was tested using layer-specific marker genes: *Gnat*1 (ONL), *Chx*10 (INL) and *Opn*4 (GCL). The amplification pattern of the marker genes showed that INL and GCL samples were pure and the ONL samples had a slight, but for our purpose negligible, INL contamination (Fig. 2). All members of the Janus kinase family of proteins were expressed in all nuclear layers of the retina in dark conditions and at 24 h after light exposure.

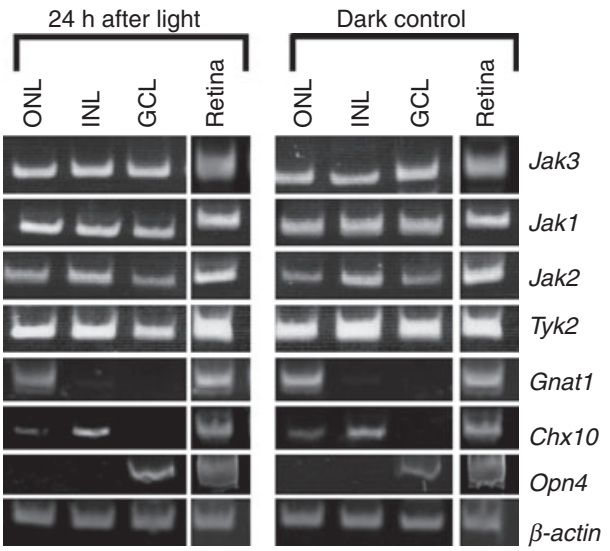

Fig. 2 Janus kinases are expressed in all nuclear layers of the retina. Outer nuclear layer (ONL), inner nuclear layer (INL) and ganglion cell layer (GCL) were isolated by lasercapture microdissection. Gene expression was tested in the individual layers or in total retina (retina) by conventional reverse transcription PCR. *Gnat*1 served as marker for the ONL, *Chx*10 for the INL, and *Opn*4 for GCL. β-*actin* was used as positive control. All members of the family of Janus kinases were expressed in all cell layers in dark conditions (dark control) and at 24 h after light exposure.

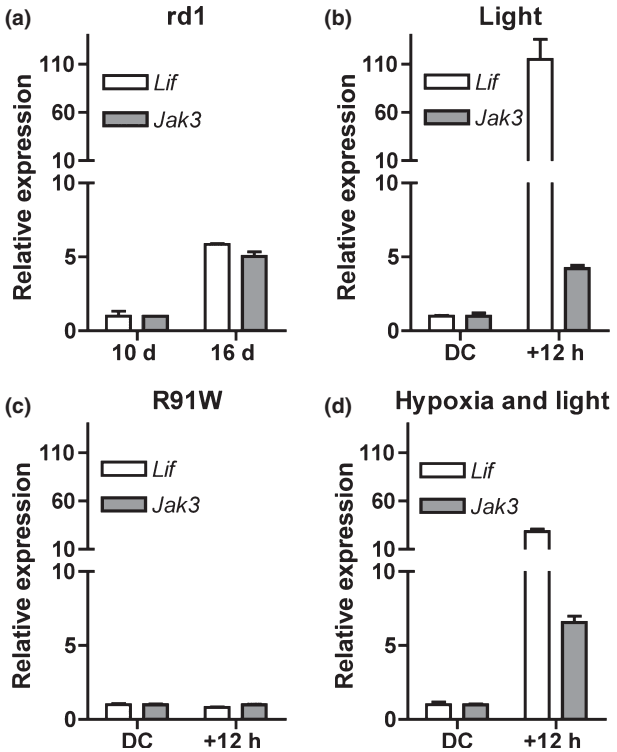

Fig. 3 Janus kinase (*Jak*) 3 and leukemia inhibitory factor (*Lif*) are similarly expressed in the stressed retina. Gene expression of *Lif* and *Jak*3 was analyzed by semi-quantitative real-time PCR. (a) Expression levels in retinas of 10 and 16-day-old rd1 mice. (b) Expression levels in wild type retinas of dark controls (DC) and at 12 h after light exposure. (c) Expression levels in $Rpe65_{R91W}$ retinas of dark controls (DC) and at 12 h after light exposure. (d) Expression levels in retinas of hypoxia pre-conditioned wild type mice not exposed to light (DC) or at 12 h after light exposure. Shown are means ± SD of three retinas per condition, amplified in duplicates. Values were normalized to β-*actin* and expressed relatively to the respective wild type control and to levels at 10 days (a) or to levels of dark controls (b–d), respectively, which were set to 1.

Jak3 and LIF are similarly expressed in the stressed retina

We and others showed that LIF is neuroprotective to the retina after light exposure and in the VPP mouse (Wenzel *et al.* 2001; Joly *et al.* 2008; Ueki *et al.* 2008; Burgi *et al.* 2009). Interestingly, *Lif* was induced along with *Jak*3 in the degenerative retina of the rd1 mouse (Fig. 3a), at 12 h after light exposure (Fig. 3b), in the VPP mouse (Joly *et al.* 2008; Ueki et al. 2008) and the rd10 retina (not shown) suggesting a regulatory connection between the two genes. To test the basis of such a potential connection and of the induction of the two genes, we used two mouse models which are protected against light damage.

The $Rpe65_{R91W}$ knockin mouse expresses a mutant form of the retinal pigment epithelium 65 (RPE65) isomerohydrolase. RPE65 is expressed in the pigment epithelium and is essential for the isomerization of all-*trans*-retinal to 11-*cis*-retinol in the visual cycle (Lamb and Pugh 2004; Jin *et al.* 2005; Moiseyev *et al.* 2005; Redmond *et al.* 2005). The R91W amino acid substitution reduces levels and activity of RPE65 leading to highly diminished amounts of 11-*cis*-retinal and thus of bleachable rhodopsin in photoreceptors (Samardzija *et al.* 2008). As light damage depends on photon absorption by rhodopsin (Noell and Albrecht 1971; Grimm *et al.* 2000b) and on the visual cycle (Wenzel *et al.* 2001), $Rpe65_{R91W}$ mice are protected from light-induced degeneration (not shown). Another model for retinal protection is hypoxic pre-conditioning (Grimm *et al.* 2002). Pre-conditioning of wild type mice renders photoreceptors resistant against light damage even though levels of bleachable rhodopsin are normal and the visual cycle is functional.

Exposure of $Rpe65_{R91W}$ mice to high levels of white light did not induce *Jak*3 or *Lif* expression (Fig. 3c). This suggests that expression of these genes depends either on photon absorption by rhodopsin and/or on photoreceptor cell death. Exposure of mice pre-conditioned by hypoxia, however, led to an increased expression of both genes (Fig. 3d). Taken together, these results demonstrate that (i) induction of *Lif* and *Jak*3 expression requires photon absorption by rhodopsin, and (ii) does not depend on photoreceptor death. Thus, our data suggest that absorption of an excessive amount of photons induces a stress-related signaling system which is sufficient to up-regulate *Lif* and *Jak*3 expression even in the absence of photoreceptor degeneration.

LIF is essential and sufficient to induce *Jak3* expression

Importantly, light induced *Jak3* up-regulation was absent in *Lif*−/− mice (Fig. 4a). We previously reported that lack of LIF prevented induction of *Jak3* also in the VPP retina (Joly *et al.* 2008). This indicates that LIF is generally required to induce *Jak3* during retinal degeneration. To test whether LIF is directly involved in the regulation of *Jak3* expression, we injected rLIF into the vitreous of wild type mice. Analysis of *Jak3* mRNA levels at 24 h after injection showed that application of rLIF induced expression of *Jak3* approximately 15-fold (Fig. 4b). Thus, LIF is essential and sufficient to induce *Jak3* expression in the degenerating mouse retina. These results suggested that JAK3 might be part of the LIF-controlled neuroprotective response in the mouse retina.

JAK3 is not essential to induce LIF-mediated neuroprotection

We recently showed that photoreceptor degeneration induces expression of *Lif* in a subset of Muller glia cells by an unknown mechanism. We proposed that Muller-cell derived LIF induces endothelin 2 (*Edn2*) expression in photoreceptors. EDN2 in turn activates expression of fibroblast growth factor 2 (*Fgf2*), which finally supports survival of damaged photoreceptors (Joly *et al.* 2008). To analyze whether JAK3 was part of this mechanism, we tested the regulation of the LIF-controlled signaling system in light-exposed *Jak3*+/+ and *Jak3*−/− mice (Fig. 5a). All genes tested were similarly induced in the presence or absence of JAK3. Furthermore, the phosphorylation pattern of STAT1, STAT3 and STAT5 after light exposure was similar in both types of mice. Total protein expression of these three STATs also remained at steady state levels in the two genotypes (Fig. 5b).

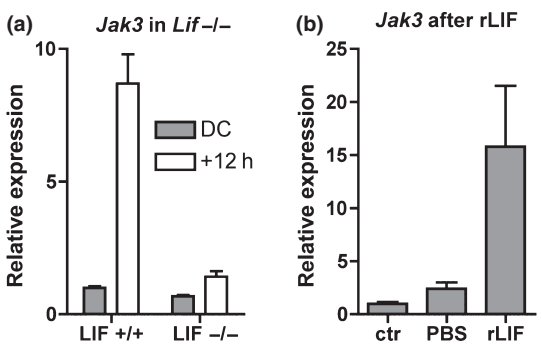

Fig. 4 Leukemia inhibitory factor (LIF) is essential and sufficient to induce *Jak3* expression. Gene expression of *Jak3* was analyzed by semi-quantitative real-time PCR. (a) Comparison of *Jak3* expression levels in *Lif+/+* and *Lif*−/− retinas of dark controls (DC) and of mice at 12 h after light exposure. (b) *Jak3* expression levels in retinas of wild type (129S6) mice which were untreated (ctr), or at 24 h after intravitreal injection of phosphate-buffered saline (PBS) or recombinant LIF, as indicated. Shown are means ± SD of three retinas per condition, amplified in duplicates. Values were normalized to β-*actin* and expressed relatively to dark control levels (a) or to levels in untreated controls (b).

Intravitreal injection of rLIF into eyes of *Jak3*+/− and *Jak3*−/− mice had comparable effects on the expression levels of genes involved in the LIF-controlled signaling pathway (Fig. 5c). Taken together, our results show that LIF is essential and sufficient to induce *Jak3* expression (Fig. 4) but that JAK3 is not necessary for *Lif* expression and/or the regulation of the members of the LIF-controlled survival pathway (Fig. 5). This suggests that LIF induced by photoreceptor damage not only activates a survival pathway but also a second signaling system of unknown function involving JAK3. Alternatively, it might be possible that there is a redundancy among the members of the JAK family of proteins with another kinase substituting for the lack of JAK3 in the retina. Although this possibility cannot be excluded, it seems rather unlikely because other JAK family members did not show an increased retinal expression in the absence of JAK3 (data not shown).

JAK3 ablation does not influence retinal degeneration

Even though JAK3 did not seem to be specifically involved in the LIF-mediated survival pathway, JAK3 might still be important for the regulation of photoreceptor cell fate after injury. Thus, we tested whether ablation of JAK3 would influence retinal degeneration. Retinal morphology of light-exposed *Jak3*+/+ and *Jak3*−/− littermates was comparable with first pyknotic nuclei visible at 12 h after exposure, outer and inner segment disintegration at 24 h, reduced number of photoreceptor nuclei at 3 d and clearance of most debris from the subretinal space at 10 days after exposure (Fig. 6a). These observations were supported by the quantification of cell death at 24 h after exposure. The generation of free nucleosomes, as they are generated during apoptotic cell death, was not significantly different in *Jak3*+/+ and *Jak3*−/− mice (Fig. 6c).

Lack of JAK3 did also not noticeably modify the course of degeneration in the VPP mouse. At 6 months of age, both VPP and VPP;*Jak3*−/− littermates had four to five rows of photoreceptor nuclei left in the ONL (Fig. 6b). Accordingly, there was no difference in the expression levels of rod and cone transducins (*Gnat1* and *Gnat2*, respectively) in 6 months old VPP and VPP;*Jak3*−/− littermates (Fig. 6d). These findings strongly suggest that JAK3 does not play an essential role in retinal degeneration.

Lack of JAK3 does not influence macrophage infiltration or microglia activation in the retina

Photoreceptor death during retinal degeneration activates resident microglia and attracts bone marrow-derived macrophages to the subretinal space (Joly *et al.* 2009a). These cells are thought to assist in the clearance of cellular debris from the space between ONL and RPE. Bone marrow progenitors from *Jak3* knockout mice show a reduced response to chemotactic stimuli (Soldevila *et al.* 2004) and LIF was reported to influence macrophage recruitment (Sugiura *et al.*

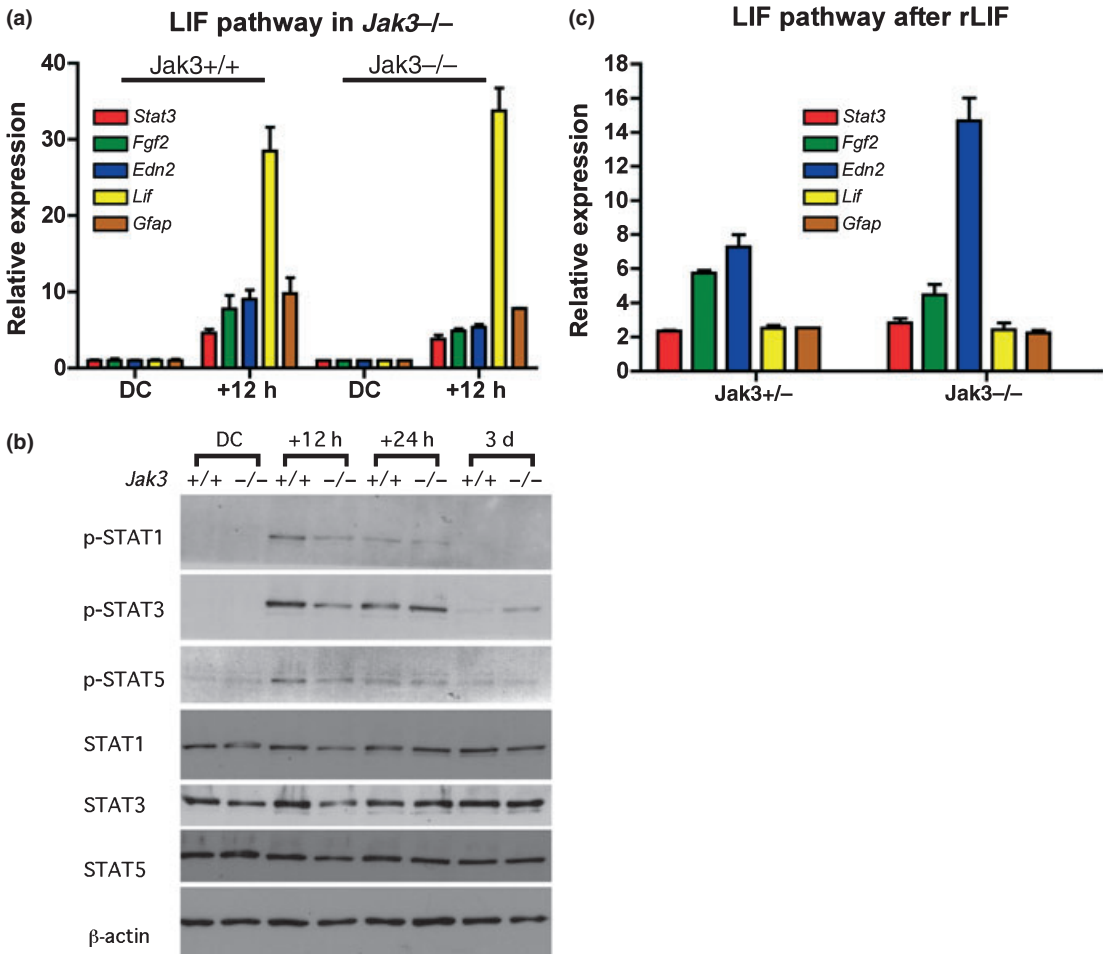

Fig. 5 Janus kinase (JAK) 3 is not essential to induce leukemia inhibitory factor (LIF)-mediated neuroprotection. Gene expression was analyzed by semi-quantitative real-time PCR and western blotting. (a) Expression levels of indicated genes in retinas of *Jak3+/+* and *Jak3–/–* mice before (DC) and at 12 h after light exposure (+ 12 h). Shown are means ± SD of three retinas per condition, amplified in duplicates. Values were normalized to β-*actin* and expressed relatively to dark control levels for each gene and genotype. (b) Levels of phosphorylated and of total signal transducer and activator of transcription (STAT) 1, STAT3 and STAT5 proteins were tested in total retinal homogenates from *Jak3+/+* and *Jak3–/–* mice without light exposure (dark controls, DC) or at 12 h (+ 12 h), 24 h (+ 24 h) and 3 days (3 days) after illumination. β-*actin* served as control for equal loading. (c) Expression levels of indicated genes in retinas of *Jak3+/–* and *Jak3–/–* mice at 24 h after intravitreal injection of recombinant LIF. Shown are means ± SD of three retinas per condition, amplified in duplicates. Values were normalized to β-*actin* and expressed relatively to phosphate-buffered saline-injection levels for each gene (set to 1, not shown).

2000; Kerr and Patterson 2004; Linker *et al.* 2008). Given the connection between LIF and JAK3 (see above), we tested whether invasion or activation of macrophages and microglia, respectively, might be impaired in the damaged retinas of *Jak3–/–* mice. We used anti-F4/80 antibodies to specifically detect macrophages (Fig. 7a) and anti-Iba1 antibodies to label activated microglia in addition to macrophages (Fig. 7b) in retinas of *Jak3+/+* and *Jak3–/–* mice at 5 days post-exposure. Peak invasion of macrophages and activation of microglia occurs around 3 and 5 days after light exposure (Joly *et al.* 2009a). A similar number of macrophages was detected (Fig. 7a and b; arrows) in retinas of *Jak3+/+* and *Jak3–/–* mice. Similarly, the distribution of activated microglia was not noticeably different in the light exposed *Jak3+/+* and *Jak3–/–* retinas (Fig. 7b, arrowheads). This suggests that JAK3 is not involved in the recruitment of bone marrow-derived macrophages or the activation of microglia in the retina and that stress dependent activation of *Jak3* expression was not required for the clearance of photoreceptor debris from the subretinal space.

Discussion

Photoreceptor degeneration induces *Lif* expression which controls an endogenous survival pathway including JAK/STAT signaling (Samardzija *et al.* 2006b; Joly *et al.* 2008).

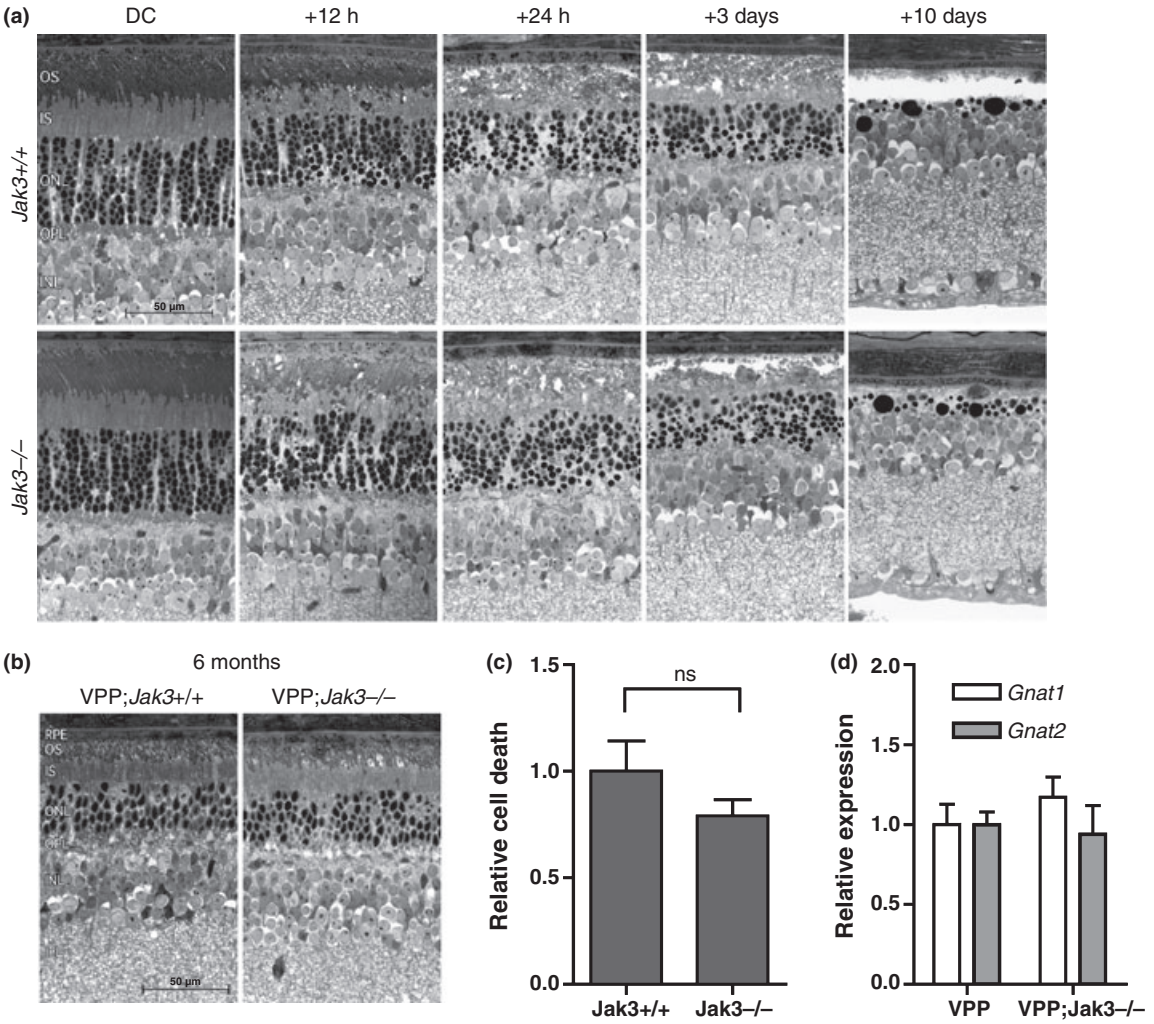

Fig. 6 Janus kinase (JAK) 3 ablation does not influence retinal degeneration. (a) Retinal morphology of *Jak3+/+* and *Jak3–/–* mice was tested before (DC) and at different time points after light exposure as indicated. Shown are representative sections of the most affected regions of three mice. (b) Retinal morphology of VPP; *Jak3+/+* and VPP; *Jak3–/–* mice at 6 months of age. Shown are representative sections of the most affected regions of three mice. OS, outer segments; IS, inner segments; ONL, outer nuclear layer; OPL, outer plexiform layer; INL, inner nuclear layer; IPL, inner plexiform layer. (c) Quantification of apoptosis in retinas of *Jak3+/+* and *Jak3–/–* retinas at 24 h after light exposure. Shown are mean values ± SD of three retinas per genotype. Cell death in *Jak3–/–* was expressed relative to *Jak3+/+*, which was set to 1. Ns, not significantly different (Student's *t*-test). (d) expression of *Gnat1* (rod transducin) and *Gnat2* (cone transducin), determined by semi-quantitative real-time PCR in retinas of 6-month-old VPP; *Jak3+/+* and VPP; *Jak3–/–* retinas as indicated. Shown are mean values ± SD of three retinas per genotype. Values were normalized to β-*actin* and expression levels in VPP; *Jak3–/–* were calculated relatively to levels in VPP; *Jak3+/+*, which were set to 1.

Lack of LIF prevents activation of this signaling cascade and accelerates disease progression leading to a fast loss of photoreceptor cells (Joly *et al.* 2008). In this study, we analyzed the expression of the four members of the family of Janus kinases in four models for retinal degeneration. We show that *Jak3* is induced in all of the models and that its expression is dependent on the presence of LIF.

Our data link increased expression of *Jak3* to retinal stress and, in the case of light-induced photoreceptor degeneration, to excessive photon absorption by rhodopsin. Photon absorption by rhodopsin is the first step in a cascade leading to photoreceptor degeneration after light exposure (Grimm *et al.* 2000b). Hypoxic pre-conditioning protects photoreceptors from light damage even though photon absorption is normal. As *Jak3* was induced after light exposure of hypoxia pre-conditioned mice, *Jak3* activation might be an early event in the cascade and may not depend on photoreceptor death but rather on the stress induced by excessive absorption of photons. This conclusion is further supported by our finding that *Jak3* was not induced in the $Rpe65_{R91W}$ mouse

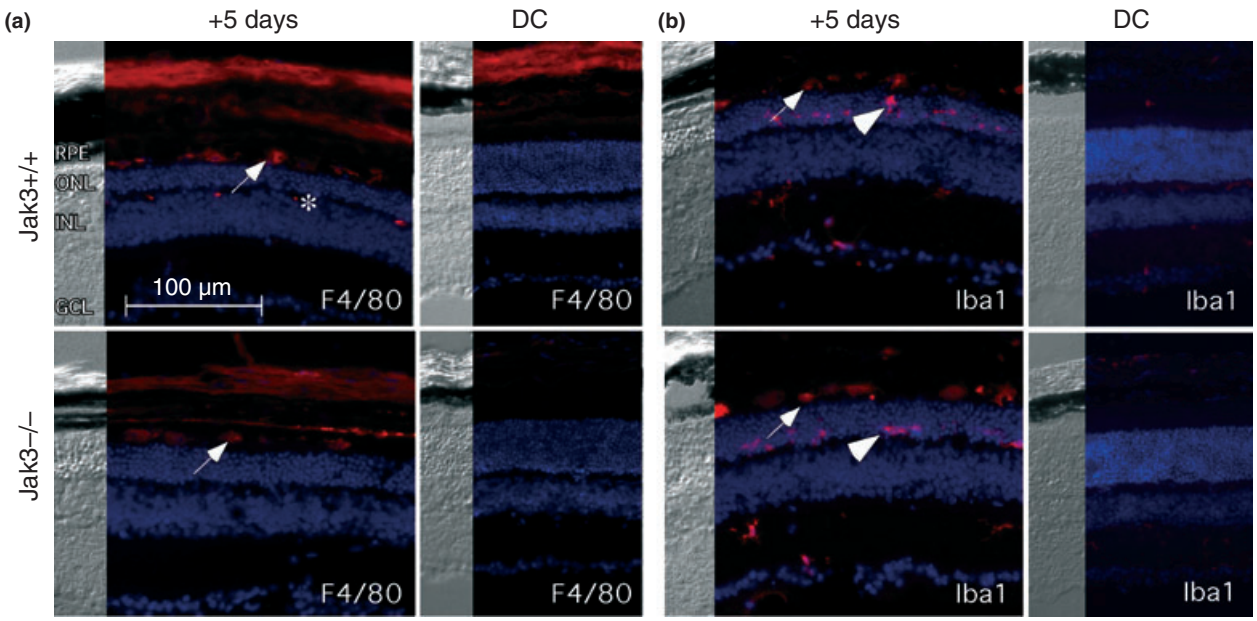

Fig. 7 Lack of Janus kinase (JAK) 3 does not influence macrophage infiltration or microglia activation in the retina. Immunostainings of macrophages (F4/80, red, a) and microglia (Iba1, red, b) in *Jak*3−/− and *Jak*3+/+ retinas of dark controls (DC) and at 5 days after light exposure (+ 5 days). Arrows point to macrophages, arrowheads to activated microglia. * marks artificially labeled blood vessels of the deep vascular plexus. DAPI (blue) was used to counterstain nuclei. Nomarski pictures (gray) give an impression of the different cell layers. RPE, retinal pigment epithelium; ONL, outer nuclear layer; INL, inner nuclear layer; GCL, ganglion cell layer.

which has only 5% of normal rhodopsin levels and thus a much reduced photon catch capacity.

Interestingly, *Jak*3 showed an expression pattern similar to *Lif* in induced and several inherited models of retinal degeneration [Fig. 3 and (Joly *et al.* 2008) data not shown]. In a recent study, we showed that *Lif* is induced in a subset of Muller glia cells in response to photoreceptor injury and that LIF controls an endogenous survival pathway which includes increased expression of *Edn*2 and *Fgf*2. It has also been shown that LIF signaling through the JAK/STAT pathway is neuroprotective (Joly *et al.* 2008; Ueki *et al.* 2008). The similar expression pattern of *Jak*3 and *Lif* in susceptible and protected models of retinal degeneration therefore suggested that JAK3 might also be involved in a neuroprotective pathway. This hypothesis was further strengthened by the observation that LIF was both essential and sufficient to induce expression of *Jak*3 (Fig. 4). Basic expression levels of *Jak*3, however, were similar in wild type and *Lif*−/− mice and thus independent of LIF [Fig. 4 and (Joly *et al.* 2008)]. This suggests that activation of *Jak*3 in the degenerating retina was highly specific and important for the general, LIF-mediated response of the retina to photoreceptor injury. However, LIF-mediated neuroprotective signaling was not affected in *Jak*3−/− retinas and rLIF was sufficient to induce the expression of *Edn*2 and *Fgf*2 in the absence of JAK3. Furthermore, absence of JAK3 did not influence induction or progression of photoreceptor degeneration. In summary, our results show that *Jak*3 expression depends on LIF but that JAK3 is not involved in the neuroprotective pathway controlled by the LIF cytokine. This result implies that LIF has multiple functions in the degenerative retina controlling a protective response and an as yet unidentified mechanism which involves JAK3. Alternatively, *Jak*3 up-regulation might be needed for protection of cells different from photoreceptors. Injury of other retinal cells (e.g. ganglion cells) may induce the same LIF controlled signaling system but protection of these cells may require JAK3. In such a scenario, repression of JAK3 signaling in a model of exclusive photoreceptor death would not lead to a detectable phenotype.

It has been reported that *Jak*3 is mainly expressed in hematopoietic cells but also in vascular cells and other non-lymphoid and myeloid tissue (Verbsky *et al.* 1996). Through the involvement in common cytokine receptor γ-chain (γ_c) signaling, *Jak*3 is important for both the innate and adaptive immune response (Ghoreschi *et al.* 2009). *Jak*3−/− mice were shown to have a blockade in B-cell development and abnormal T-cells. They also show symptoms similar to severe combined immune deficiency (Thomis *et al.* 1995; Thomis and Berg 1997). As a result of the ocular immune privilege (Streilein 2003; Taylor 2009) and the blood retinal barrier, T- and B-cells or antibodies are normally not able to enter the retina and to activate immune responses or inflammation. Nevertheless, retinal degeneration induces immune-like responses in the retina including activation of resident microglia, infiltration of bone-marrow derived

macrophages (Ng and Streilein 2001; Joly *et al.* 2009b) and the activation of several genes involved in innate and acquired immune systems (Rohrer *et al.* 2007). LIF has been shown to be important for immune-like responses in models of central or peripheral nervous system injury (Sugiura *et al.* 2000; Linker *et al.* 2008), for macrophage recruitment in a late phase of autoimmune encephalomyelinitis (Linker *et al.* 2008) and for the stimulation of macrophage and microglia proliferation (Kerr and Patterson 2004). Even though LIF controls activation of *Jak*3 expression (Fig. 4), our data indicate that LIF influences those systems through other signaling pathways and that JAK3 is not required for macrophage infiltration, microglia activation (Fig. 7), or the induction of genes related to the innate immune response in the retina (not shown). Whether ocular immunity in the absence of JAK3 would be impaired in other models remains a target for further research.

Immunologic challenges up-regulate *Jak*3 expression in blood monocytes but JAK3 ablation has no influence on monocyte function (Villa *et al.* 1996). Thus, it was suggested that JAK3 function can be redundant in certain situations and that other proteins may substitute for JAK3 to some extent. To address this possibility in the mouse retina, we tested whether any of the other JAK family kinases would show higher expression levels in *Jak*3−/− mice to compensate for the absence of JAK3. However, expression of *Jak*1, *Jak*2 and *Tyk*2 remained at basic levels in *Jak*3−/− mice and was comparable to wild types (data not shown). Although this does not exclude the possibility of a certain redundancy on the protein level, our data indicate that *Jak*3 does not play a unique role in LIF mediated photoreceptor neuroprotection.

In summary, we show that the degenerating retina induced expression of *Jak*3. LIF was essential and sufficient for *Jak*3 induction, even in the absence of photoreceptor death. However, JAK3 was not essential for survival or death of injured photoreceptors and did not influence immune-related responses in the retina. We suggest that LIF not only activates a neuroprotective signaling pathway through *Edn*2 and *Fgf*2 but also induces an additional retinal stress response of unknown function which involves JAK3.

Acknowledgements

The authors thank Coni Imsand, Hedwig Wariwoda, Philipp Huber and Corinne Britschgi for excellent technical assistance. This work was supported by the Swiss National Science Foundation (Grant 3100A0–117760), the Fritz Tobler Foundation and the H. Messerli Foundation.

References

Bowes C., Li T., Danciger M., Baxter L. C., Applebury M. L. and Farber D. B. (1990) Retinal degeneration in the rd mouse is caused by a defect in the beta subunit of rod cGMP-phosphodiesterase. *Nature* **347**, 677–680.

Burgi S., Samardzija M. and Grimm C. (2009) Endogenous leukemia inhibitory factor protects photoreceptor cells against light-induced degeneration. *Mol. Vis.* **15**, 1631–1637.

Chang B., Hawes N. L., Pardue M. T. *et al.* (2007) Two mouse retinal degenerations caused by missense mutations in the beta-subunit of rod cGMP phosphodiesterase gene. *Vision Res.* **47**, 624–633.

Ghoreschi K., Laurence A. and O'Shea J. J. (2009) Janus kinases in immune cell signaling. *Immunol. Rev.* **228**, 273–287.

Grimm C., Wenzel A., Hafezi F. and Reme C. E. (2000a) Gene expression in the mouse retina: the effect of damaging light. *Mol. Vis.* **6**, 252–260.

Grimm C., Wenzel A., Hafezi F., Yu S., Redmond T. M. and Reme C. E. (2000b) Protection of Rpe65-deficient mice identifies rhodopsin as a mediator of light-induced retinal degeneration. *Nat. Genet.* **25**, 63–66.

Grimm C., Wenzel A., Groszer M., Mayser H., Seeliger M., Samardzija M., Bauer C., Gassmann M. and Reme C. E. (2002) HIF-1-induced erythropoietin in the hypoxic retina protects against light-induced retinal degeneration. *Nat. Med.* **8**, 718–724.

Jin M., Li S., Moghrabi W. N., Sun H. and Travis G. H. (2005) Rpe65 is the retinoid isomerase in bovine retinal pigment epithelium. *Cell* **122**, 449–459.

Joly S., Lange C., Thiersch M., Samardzija M. and Grimm C. (2008) Leukemia inhibitory factor extends the lifespan of injured photoreceptors in vivo. *J. Neurosci.* **28**, 13765–13774.

Joly S., Samardzija M., Wenzel A., Thiersch M. and Grimm C. (2009a) Nonessential role of beta3 and beta5 integrin subunits for efficient clearance of cellular debris after light-induced photoreceptor degeneration. *Invest. Ophthalmol. Vis. Sci.* **50**, 1423–1432.

Joly S., Francke M., Ulbricht E. *et al.* (2009b) Cooperative phagocytes: resident microglia and bone marrow immigrants remove dead photoreceptors in retinal lesions. *Am. J. Pathol.* **174**, 2310–2323.

Kerr B. J. and Patterson P. H. (2004) Potent pro-inflammatory actions of leukemia inhibitory factor in the spinal cord of the adult mouse. *Exp. Neurol.* **188**, 391–407.

Lamb T. D. and Pugh Jr E. N. (2004) Dark adaptation and the retinoid cycle of vision. *Prog. Retin. Eye Res.* **23**, 307–380.

Leonard W. J. and O'Shea J. J. (1998) Jaks and STATs: biological implications. *Annu. Rev. Immunol.* **16**, 293–322.

Linker R. A., Kruse N., Israel S. *et al.* (2008) Leukemia inhibitory factor deficiency modulates the immune response and limits autoimmune demyelination: a new role for neurotrophic cytokines in neuroinflammation. *J. Immunol.* **180**, 2204–2213.

Moiseyev G., Chen Y., Takahashi Y., Wu B. X. and Ma J. X. (2005) RPE65 is the isomerohydrolase in the retinoid visual cycle. *Proc. Natl Acad. Sci. USA* **102**, 12413–12418.

Naash M. I., Hollyfield J. G., al-Ubaidi M. R. and Baehr W. (1993) Simulation of human autosomal dominant retinitis pigmentosa in transgenic mice expressing a mutated murine opsin gene. *Proc. Natl Acad. Sci. USA* **90**, 5499–5503.

Ng T. F. and Streilein J. W. (2001) Light-induced migration of retinal microglia into the subretinal space. *Invest. Ophthalmol. Vis. Sci.* **42**, 3301–3310.

Noell W. K. and Albrecht R. (1971) Irreversible effects on visible light on the retina: role of vitamin A. *Science* **172**, 76–79.

O'Shea J. J., Gadina M. and Schreiber R. D. (2002) Cytokine signaling in 2002: new surprises in the Jak/Stat pathway. *Cell* **109**(Suppl), S121–S131.

Rawlings J. S., Rosler K. M. and Harrison D. A. (2004) The JAK/STAT signaling pathway. *J. Cell Sci.* **117**, 1281–1283.

Redmond T. M., Poliakov E., Yu S., Tsai J. Y., Lu Z. and Gentleman S. (2005) Mutation of key residues of RPE65 abolishes its enzymatic

role as isomerohydrolase in the visual cycle. *Proc. Natl Acad. Sci. USA* **102**, 13658–13663.

Reme C. E., Grimm C., Hafezi F., Marti A. and Wenzel A. (1998) Apoptotic cell death in retinal degenerations. *Prog. Retin. Eye Res.* **17**, 443–464.

Rodig S. J., Meraz M. A., White J. M. *et al.* (1998) Disruption of the Jak1 gene demonstrates obligatory and nonredundant roles of the Jaks in cytokine-induced biologic responses. *Cell* **93**, 373–383.

Rohrer B., Demos C., Frigg R. and Grimm C. (2007) Classical complement activation and acquired immune response pathways are not essential for retinal degeneration in the rd1 mouse. *Exp. Eye Res.* **84**, 82–91.

Samardzija M., Wenzel A., Naash M., Reme C. E. and Grimm C. (2006a) Rpe65 as a modifier gene for inherited retinal degeneration. *Eur. J. Neurosci.* **23**, 1028–1034.

Samardzija M., Wenzel A., Aufenberg S., Thiersch M., Reme C. and Grimm C. (2006b) Differential role of Jak-STAT signaling in retinal degenerations. *FASEB J.* **20**, 2411–2413.

Samardzija M., von Lintig J., Tanimoto N., Oberhauser V., Thiersch M., Reme C. E., Seeliger M., Grimm C. and Wenzel A. (2008) R91W mutation in Rpe65 leads to milder early-onset retinal dystrophy due to the generation of low levels of 11-cis-retinal. *Hum. Mol. Genet.* **17**, 281–292.

Schindler C., Levy D. E. and Decker T. (2007) JAK-STAT signaling: from interferons to cytokines. *J. Biol. Chem.* **282**, 20059–20063.

Soldevila G., Licona I., Salgado A., Ramirez M., Chavez R. and Garcia-Zepeda E. (2004) Impaired chemokine-induced migration during T-cell development in the absence of Jak 3. *Immunology* **112**:191–200.

Streilein J. W. (2003) Ocular immune privilege: the eye takes a dim but practical view of immunity and inflammation. *J. Leukoc. Biol.* **74**, 179–185.

Sugiura S., Lahav R., Han J., Kou S. Y., Banner L. R., de Pablo F. and Patterson P. H. (2000) Leukaemia inhibitory factor is required for normal inflammatory responses to injury in the peripheral and central nervous systems in vivo and is chemotactic for macrophages in vitro. *Eur. J. Neurosci.* **12**, 457–466.

Taylor A. W. (2009) Ocular immune privilege. *Eye (Lond)* **23**, 1885–1889.

Thomis D. C. and Berg L. J. (1997) The role of Jak3 in lymphoid development, activation, and signaling. *Curr. Opin. Immunol.* **9**, 541–547.

Thomis D. C., Gurniak C. B., Tivol E., Sharpe A. H. and Berg L. J. (1995) Defects in B lymphocyte maturation and T lymphocyte activation in mice lacking Jak3. *Science* **270**:794–797.

Ueki Y., Wang J., Chollangi S. and Ash J. D. (2008) STAT3 activation in photoreceptors by leukemia inhibitory factor is associated with protection from light damage. *J. Neurochem.* **105**, 784–796.

Verbsky J. W., Bach E. A., Fang Y. F., Yang L., Randolph D. A. and Fields L. E. (1996) Expression of Janus kinase 3 in human endothelial and other non-lymphoid and non-myeloid cells. *J. Biol. Chem.* **271**, 13976–13980.

Villa A., Sironi M., Macchi P., Matteucci C., Notarangelo L. D., Vezzoni P. and Mantovani A. (1996) Monocyte function in a severe combined immunodeficient patient with a donor splice site mutation in the Jak3 gene. *Blood* **88**:817–823.

Watford W. T. and O'Shea J. J. (2006) Human tyk2 kinase deficiency: another primary immunodeficiency syndrome. *Immunity* **25**, 695–697.

Wenzel A., Reme C. E., Williams T. P., Hafezi F. and Grimm C. (2001) The Rpe65 Leu450Met variation increases retinal resistance against light-induced degeneration by slowing rhodopsin regeneration. *J. Neurosci.* **21**, 53–58.

Wenzel A., Grimm C., Samardzija M. and Reme C. E. (2005) Molecular mechanisms of light-induced photoreceptor apoptosis and neuroprotection for retinal degeneration. *Prog. Retin. Eye Res.* **24**, 275–306.

3.1.2. Normoxic activation of hypoxia inducible factors in photoreceptors provides transient protection against light induced retinal degeneration

Christina Lange[1], Markus Thiersch[1], Naoyuki Tanimoto[3], Severin Heynen[1], Gesine Huber[3], Susanne C. Beck[3], Sandrine Joly[1], Mathias W. Seeliger[3] Marijana Samardzija[1] and Christian Grimm[1,2]

[1]Lab for Retinal Cell Biology, Department Ophthalmology, University of Zurich
[2]Zurich Center for Integrative Human Physiology (ZIHP), [3]Institute of Ophthalmic Research, Centre of Ophthalmology, Devision of Ocular Neurodegeneration, Tubingen, Germany

Manuscript in preparation

Normoxic activation of hypoxia inducible factors in photoreceptors provides transient protection against light induced retinal degeneration

Christina Lange[1], Markus Thiersch[1], Naoyuki Tanimoto[3], Severin Heynen[1], Gesine Huber[3], Susanne C. Beck[3], Sandrine Joly[1], Yun-Zheng Le[4], Mathias W. Seeliger[3], Marijana Samardzija[1] and Christian Grimm[1,2]

[1]Lab for Retinal Cell Biology, Department Ophthalmology, University of Zurich
[2]Zurich Center for Integrative Human Physiology (ZIHP)
[3]Institute of Ophthalmic Research, Centre of Ophthalmology, Division of Ocular Neurodegeneration, Tubingen, Germany
[4]Department of Cell Biology and Dean A. McGee Eye Institute, Oklahoma City, OK

Keywords: hypoxia, HIF, VHL, retina, light induced retinal degeneration, EPO, hypoxic preconditioning

Corresponding author:

Christian Grimm
Lab for Retinal Cell Biology
Department Ophthalmology
University of Zurich,
CH 8091 Zurich, Switzerland
Email: cgrimm@opht.uzh.ch
Tel: 0041 44 255 39 05
FAX:0041 44 255 43 85

ABSTRACT

Hypoxic preconditioning protects photoreceptors from light induced retinal degeneration. Hypoxia inducible factors (HIFs) are stabilized in the whole retina of preconditioned mice and may regulate expression of potentially protective genes. In a cre-lox approach we knocked down the von Hippel Lindau (VHL) protein to stabilize HIF1A and HIF2A specifically in rod photoreceptors under normoxic conditions. We show that the retinas of rod specific *Vhl* knockdowns are normal in morphology and function and that the stabilized HIFs can activate hypoxia target genes. 36 hours after exposure to excessive light levels, *Vhl* knockdowns show significantly less photoreceptor cell death than wild type controls. However this protection is only transient, since 10 days after light exposure, photoreceptors of *Vhl* knockdowns had degenerated to a similar extent as in control animals. Therefore, activation of HIF transcription factors in rods alone is not sufficient to render the same neuroprotective response as observed after hypoxic preconditioning. Interestingly, some hypoxia target genes, like erythropoietin (*Epo*) were not induced in rod specific *Vhl* knockdown mice. Hence, hypoxic preconditioning might induce neuroprotective genes in retinal cells other than photoreceptors. Products of these genes might act in a paracrine manner to protect photoreceptors from degeneration.

Analysis of 1-year-old *Vhl* knockdowns showed that lack of VHL and/or long-term stabilization of HIF transcription factors in photoreceptors leads to retinal degeneration with time. In conclusion, a short hypoxic exposure may shift cells into a protective state, whereas prolonged activation of a hypoxia-like response or a prolonged downregulation of VHL function may lead to cell death.

INTRODUCTION

Retinitis pigmentosa (RP) is a major cause of severe visual disturbances or blindness in humans. It is characterized by progressive loss of photoreceptors. Not much is known about the mechanisms of degeneration and how inhibition of cell death can be achieved. Different mouse models, induced and inherited, have been developed to mimic the cell death occurring during RP. The model of light-induced photoreceptor cell death is widely used to analyze immediate changes in gene expression during degeneration or to test the efficacy of neuroprotective strategies. Hypoxic preconditioning - the exposure of mice to low oxygen concentrations before a toxic insult - stabilizes photoreceptors and protects them from light-induced degeneration (Grimm et al., 2002).

In conditions of reduced oxygen availability (hypoxia) cells need to accommodate to cope with the imposed stress. Therefore expression of genes for survival, growth or metabolism has to be regulated. This regulation is achieved mainly by special transcription factors called hypoxia inducible factors (HIFs). HIFs consist of two subunits, an α- and a β-subunit. The HIF-β-subunit, also called aryl-hydrocarbon receptor nuclear translocator (ARNT), is located in the nucleus and is constitutively expressed. In conditions of normal oxygen availability (normoxia) HIF-α-subunits are constantly degraded. Hydroxylation of proline residues by prolyl hydroxylases (egl nine family, EGLNs) leads to the recognition of the HIF-α subunits by the von Hippel-Lindau (VHL) protein complex, which acts as a E3-ubiquitinase targeting them to proteasomal degradation (Ohh et al., 2000). VHL forms a multimeric protein complex together with Cullin-2, RBX1, and the Elongins B and C (Kibel et al., 1995; Iwai et al., 1999; Kamura et al., 1999). Another hydroxylase, the factor inhibiting HIF (FIH), hydroxylates HIF-α at an asparagine residue inhibiting the p300 co-activator recruitment and transcriptional activity (Mahon et al., 2001). There are 3 isoforms of HIF-α known, HIF1A, HIF2A and HIF3A.

In order to function, PHDs and FIH both depend on oxygen as a substrate (Jaakkola et al., 2001; Mahon et al., 2001). Hence, during hypoxia, hydroxylation does not occur, HIF-α subunits are not recognized by VHL and thus stabilized, can enter the nucleus, bind HIF-β and the co-activator, and carry out transcriptional activity.

It has been shown that during hypoxic preconditioning HIF1A and HIF2A are stabilized and that HIF-target genes are differentially regulated in the retina (Grimm et al., 2002; Thiersch et al., 2008; Thiersch et al., 2009). One of these target genes, erythropoietin (*Epo*), has been shown to be induced during hypoxia and recombinant EPO is protective if injected before light exposure (Grimm et al., 2002). To test whether stabilization of HIF transcription factors in photoreceptors is responsible for the neuroprotective effect seen after hypoxic preconditioning, we aimed at the stabilization of HIFs during normoxic conditions specifically in rod photoreceptors and at the determination whether this stabilization of HIFs renders the same neuroprotective effect as hypoxic preconditioning. To achieve normoxic stabilization of HIF-α proteins, we generated photoreceptor specific *Vhl* knockdown mice using the Cre-lox system. In the absence of VHL protein, HIF-α subunits are not targeted to degradation and may therefore act as transcriptional regulators mimicking the hypoxic response (Haase et al., 2001).

MATERIALS AND METHODS

Mice and genotyping

Mice were treated in accordance with the regulations of the Veterinary Authority of Zurich and with the statement of 'The Association for Research in Vision and Ophthalmology' for the use of animals in research. All mice were maintained as breeding colonies at the University of Zurich in a 12 h : 12 h light-dark cycle (60 lux).

129S-Vhlh^{tm1jae}/J-mice (from now on referred to as *Vhl*$^{flox/flox}$ mice), which have *lox*P sites flanking exon 1 and part of the promoter of the *Vhl* gene (Haase et al., 2001) were purchased from Jackson Laboratory (Bar Harbor, USA). To generate rod photoreceptor specific *Vhl* knockdown mice *Vhl*$^{flox/flox}$ mice were crossed with mice expressing Cre-recombinase under the control of the opsin promoter (LMOPC1, from now on called opsin-cre mice), which activates Cre expression in rods starting around postnatal day 7. Expression increases up to 6 weeks of age (Le et al., 2006). The breeding colonies were kept on the light sensitive Rpe65$_{450Leu}$ background (Seeliger et al., 2001). The following primers were used to detect wt and *Vhl*-flox alleles: forw (5'-TGAGTATGGGATAACGGGTTGAAC-3') and rev (5'-

AGAACTGACTGACTTCCACTGATGC-3'). The wt allele was identified as a 125-bp PCR fragment and the *Vhl*-flox as a 317-bp fragment after electrophoresis through a 1.5% agarose gel. Presence of the opsin-cre transgene was tested by PCR using the following primer pair: forw (5'-AGGTGTAGAGAAGGCACTTAGC-3') and rev (5'-CTAATCGCCATCTTCCAGCAGG-3'). In the presence of the transgene, the amplification reaction resulted in the production of a 411 bp fragment. To detect excision of floxed sequences in the *Vhl* gene, genomic DNA was isolated from retinas and tested by PCR using the following primers: forw_un-excised (5'-CTGGTACCCACGAAACTGTC-3'), forw_excised (5'-CTAGGCACCGAGCTTAGAGGTTTGCG-3') and rev_both (5'-CTGACTTCCACTGATGCTTGTCACAG-3'). The excised allele was identified as a 260 bp and the un-excised allele as a 460 bp fragment.

Lasercapture microdissection

Mice were sacrificed, eyes enucleated, immediately embedded in tissue freezing medium (Leica Microsystems Nussloch GmbH, Nussloch, Germany), and frozen in a 2-methylbutane bath cooled by liquid nitrogen. Retinal sections (20 μm) were fixed (5 min acetone), air dried (5 min), and dehydrated (30 sec 100% ethanol, 5 min xylene). Microdissection was performed using an Arcturus XT Lasercapture device (Molecular devices, Silicon Vally, USA). RNA was isolated using the Arcturus kit for RNA isolation (Molecular devices) according to the manufacturer's directions including a DNase treatment to digest residual genomic DNA. Equal amounts of RNA were used for reverse transcription using oligo(dT) and M-MLV reverse transcriptase (Promega, Madison, WI, USA).

Semi-quantitative real time PCR

Retinas were removed through a slit in the cornea and immediately frozen in liquid nitrogen. Total RNA was prepared using the RNeasy RNA isolation kit (Qiagen, Hilden, Germany) according to the manufacture's directions including a DNase treatment to digest residual genomic DNA. Equal amounts of RNA were used for reverse transcription using oligo(dT) and M-MLV reverse transcriptase (Promega). Relative quantification of cDNA was carried out by real-time PCR using the LightCycler 480 Sybr Green I Master kit, a LightCycler 480 instrument (Roche Diagnostics, Basel, Switzerland) and specific primer pairs (Table 1). Expression was

normalized to β-actin and relative quantification was calculated using the Light Cycler 480 software (Roche).

Western blotting

Retinas were homogenized in 0.1M Tris/HCl (pH8) at 4°C and protein content was determined using Bradford reagent. Standard SDS-PAGE and Western blotting were performed. For immunodetection, the following antibodies were used: anti-HIF1A (#Nb100-479 Novus Biologicals, Cambridge, United Kingdom, 1:1000), anti-HIF2A (#Nb100-122, Novus Biologicals, 1:1000), anti-pSTAT3 (#9131 Cell Signaling Technology, 1:500) and anti-ACTB (#A5441 Sigma, St. Louis, MO, USA, 1:5000). Blots were incubated overnight at 4°C with primary antibodies followed by a 1 hour incubation with HRP-conjugated secondary antibodies. Immunoreactivity was visualized using the Renaissance-Western blot detection kit (Perkin Elmer Life Sciences, Emeryville, CA, USA).

Electroretinographic analysis

Electroretinograms (ERGs) were recorded according to previously described procedures (Seeliger et al., 2001; Tanimoto et al., 2009). The ERG equipment consisted of a Ganzfeld bowl, a direct current amplifier, and a PC-based control and recording unit (Multiliner Vision; VIASYS Healthcare GmbH, Hoechberg, Germany). Mice were dark-adapted overnight and anaesthetized with ketamine (66.7 mg/kg body weight) and xylazine (11.7 mg/kg body weight). Pupils were dilated and single flash ERG responses were obtained under dark-adapted (scotopic) and light-adapted (photopic) conditions. Light adaptation was accomplished with a background illumination of 30 candela (cd) per square meter starting 10 minutes before recording. Single white-flash stimulus intensity ranged from –4 to 1.5 log cd*s/m^2 under scotopic and from –2 to 1.5 log cd*s/m^2 under photopic conditions, divided into 10 and 8 steps, respectively. Ten responses were averaged with an inter-stimulus interval (ISI) of either 5 seconds (for –4, –3, –2, –1.5, –1, and –0.5 log cd*s/m^2) or 17 seconds (for 0, 0.5, 1, and 1.5 log cd*s/m^2).

Light exposure, cell death detection and morphology

Mice were dark-adapted overnight and exposed to white fluorescent light (13’000 lux) for 1 hour. Pupils of pigmented mice were dilated 1 hour before light exposure

with 1% Cyclogyl (Alcon, Cham, Switzerland) and 5% phenylephrine (Ciba vision, Niederwangen, Switzerland).

After light exposure mice were placed in darkness for 24 hours and put back to cyclic light thereafter until they were sacrificed. To quantify apoptosis mice were sacrificed 36 hours after light exposure. Nucleosomal release was determined using a cell death detection (CDD) kit (Roche Diagnostics) according to the manufacture's recommendations.

For light microscopy, eyes were fixed in 2.5% glutaraldehyde in 0.1 M cacodylate buffer (pH 7.3) at 4°C overnight. For each eye, the superior and the inferior retina were prepared, washed in cacodylate buffer, incubated in osmium tetroxide for 1h, dehydrated, and embedded in Epon 812. Sections (0.5 μm) were prepared from the lower central retina and counterstained with methylene blue.

Rhodopsin measurements

Mice were dark adapted overnight. Retinas were removed through a slit in the cornea under dim red light and placed in 1 ml of distilled H_2O for 1 min. After 3 min of centrifugation at 15,000 × g, the supernatant was discarded and 700 μl of 1% hexadecyltrimethylammonium bromide (Fluka Chemie, Buchs, Switzerland) in H_2O was added to the pellet. Retinas were mechanically homogenized with a Polytron (20 s, 3,000 rpm), centrifuged for 3 min at 15,000 × g, and the supernatant was collected. The absorption at 500 nm was measured before and after exposure to bright white light (20,000 lux for 1 min). The amount of rhodopsin present per retina was calculated using the following formula derived from the Lambert-Beer equation: rho = vol × c = vol ×Δabs500/(∈500 × l × n). rho is the amount of rhodopsin per retina (in moles); vol, the volume of the sample (in liters); c, the concentration of rhodopsin per retina (in mol/liters); Δabs500 is the difference between absorption before and after bleaching measured at 500 nm; ∈500 is the extinction coefficient of rhodopsin at 500 nm (4.2 × 104 cm × molar); l is the path length of the cuvette (in cm); and n is the number of retinas.

RESULTS

Successful knockdown of Vhl in photoreceptors of 10-week-old $Vhl^{flox/flox}$;opsin-cre mice

Analysis of genomic DNA from retinal tissue showed excision of floxed DNA sequences in 10-week-old mice expressing Cre recombinase but not in control mice (Fig. 1A). Because excision does only take place in rod photoreceptors (Le et al., 2006), whole retinal samples contain both the floxed (unexcised; from retinal cells without Cre-expression) and the excised allele. Semi-quantitative real time PCR on samples obtained by lasercapture microdissection revealed downregulation of *Vhl* expression in the ONL of $Vhl^{flox/flox}$;opsin-cre mice (CRE+) compared to their wild type ($Vhl^{flox/flox}$, CRE-) littermates (Fig. 1B). The reason for the upregulation of *Vhl* expression in the other cell layers is unclear, but might involve some compensatory effects.

Stabilization of HIF-α proteins and increased expression of HIF target genes in 10-week-old $Vhl^{flox/flox}$;opsin-cre mice

Further, we tested whether the downregulation of *Vhl* in photoreceptors led to a stabilization of HIF-α proteins in normoxic conditions. Indeed, increased expression and thus stabilization of HIF1A and HIF2A was detected in retinas of 10-week-old $Vhl^{flox/flox}$;opsin-cre mice (CRE+) (Fig. 2A). At 6 weeks of age, such a stabilization was not yet observable (data not shown). This might be explained by the slowly increasing expression of Cre-recombinase in opsin-cre mice (Le et al., 2006). In addition to HIF-α stabilization we saw phosphorylation of STAT3, which is reported to be part of the HIF-pathway (Jung et al., 2005). To determine whether the stabilized HIFs are transcriptionally active, we analyzed the expression of several hypoxia response genes (Thiersch et al., 2008) in 10-week-old $Vhl^{flox/flox}$;opsin-cre mice (Fig. 2B). Compared to $Vhl^{flox/flox}$ mice, expression of adrenomedullin (*Adm*), prolyl hydroxylase 2 (*Egln1*), BCL2/adenovirus E1B 19kDa interacting protein 3 (*Bnip3*), solute carrier family 2 (facilitated glucose transporter) member 1 (*Slc2a1*, also called *Glut1*) and vascular endothelial growth factor (*Vegf*) was induced in $Vhl^{flox/flox}$;opsin-cre mice approximately to the same level as in hypoxic wild type mice (after 6 hours

of hypoxia in 7% oxygen) (Fig. 2B). Regulation of these hypoxia response genes is largely attributed to HIF1-regulation activity (Garayoa et al., 2000; Warnecke et al., 2008; Zhang et al., 2008). Expression of metallothionin 1 (*Mt1*) and metallothionin 2 (*Mt2*) was also upregulated in $Vhl^{flox/flox}$;opsin-cre mice but to a lower extent as compared to hypoxic wild types mice. Expression of erythropoietin (*Epo*), which is reported to be activated by HIF2 (Haase, 2010), was not induced in $Vhl^{flox/flox}$; opsin-cre mice. This either means that the stabilized HIF2 is not transcriptionally active or that induction of *Epo* during hypoxia is regulated by cells other than rod photoreceptors (see also discussion).

Normal retinal function and morphology up to 17 weeks of age in Vhl knockdown mice

Before using the *Vhl* knockdown mice for neurodegeneration experiments we analyzed their retinas in physiological conditions. ERG measurements were recorded in 17-week-old $Vhl^{flox/flox}$;opsin-cre and $Vhl^{flox/flox}$ littermates (Fig. 3). Scotopic and photopic recordings of both genotypes were comparable to those of wild type mice (Tanimoto et al., 2009). There was no difference in the b-wave amplitudes of scotopic and photopic responses between $Vhl^{flox/flox}$;opsin-cre and $Vhl^{flox/flox}$ (Fig. 3C,D). Furthermore, expression of the photoreceptor markers rod transducin (*Gnat1*), cone transducin (*Gnat2*), S-antigen (*Sag*) and rod opsin (*Rho*) was the same in 10-week-old $Vhl^{flox/flox}$;opsin-cre (gray bars) and $Vhl^{flox/flox}$ mice (white bars) (Fig. 3E). Similarly, retinal morphologies of untreated $Vhl^{flox/flox}$;opsin-cre and $Vhl^{flox/flox}$ control mice were comparable (see Fig. 4A).

Reduced photoreceptor cell damage 36 hours after light exposure in Vhl knockdown mice

To test whether stabilization of HIFs in photoreceptors during normoxic conditions has a neuroprotective potential similar to the effect seen after hypoxic preconditioning, we exposed 10-week-old $Vhl^{flox/flox}$;opsin-cre mice to excessive light. Retinal morphology was analyzed and cell death quantified biochemically 36 hours after the exposure (Fig. 4). Morphological sections of light exposed $Vhl^{flox/flox}$;opsin-cre mice showed a better preservation of the structure of photoreceptor outer segments and fewer pyknotic nuclei than sections of the $Vhl^{flox/flox}$ controls (Fig. 4A). Furthermore, although cell death was variable within groups, light exposed

Vhl$^{flox/flox}$;opsin-cre mice showed significantly less cell death compared to their light exposed *Vhl*$^{flox/flox}$ littermates (Fig. 4B). The reason for the variability in cell death within the groups is not clear, but might be attributed to the mixed genetic background of the animals. To make sure that the protection in *Vhl*$^{flox/flox}$;opsin-cre mice was not due to the opsin-transgene expression, we also exposed 10-week-old opsin-cre mice to light and quantified cell death 36 hours thereafter. The cell death in these mice was comparable to *Vhl*$^{flox/flox}$ mice and significantly higher than in *Vhl*$^{flox/flox}$;opsin-cre mice. Hence, the expression of the Cre recombinase had no influence on the cell death observed after light exposure.

Transient protection in Vhl$^{flox/flox}$*;opsin-cre*

Although we observed a significant rescue in *Vhl*$^{flox/flox}$*;*opsin-cre mice 36 hours after light exposure, morphological sections of light exposed *Vhl*$^{flox/flox}$*;*opsin-cre mice at 10 days after light exposure revealed that photoreceptors had degenerated to a similar extent as in *Vhl* $^{flox/flox}$ controls (Fig. 5A). Accordingly, both genotypes showed a comparable reduction in rhodopsin levels (as a measure for intact photoreceptors) in the retina at 10 days post exposure (Fig. 5B). This observation suggests that the protection observed early after light exposure (Fig. 4) was only transient.

We also noted that non-exposed *Vhl*$^{flox/flox}$*;*opsin-cre mice had basal rhodopsin levels which were approximately 25% lower than in control mice (Fig. 5C). Again, this cannot be attributed to the transgene expression, because opsin-cre mice had similar rhodopsin levels as *Vhl*$^{flox/flox}$ mice and significantly different levels to *Vhl* knockdown mice. Since expression of *Gnat1* and of *Rho* were not significantly different in *Vhl*$^{flox/flox}$*;*opsin-cre and *Vhl* $^{flox/flox}$ mice (Fig. 3E), this result may suggest that the rod opsin protein synthesis and/or the formation of bleachable rhodopsin is affected in rods lacking VHL. However, the reduced amount of rhodopsin in the retinas of *Vhl*$^{flox/flox}$;opsin-cre mice did obviously not influence the final outcome of light-induced degeneration, because 10 days after light exposure the extent of photoreceptor-loss was comparable in *Vhl*$^{flox/flox}$;opsin-cre and *Vhl*$^{flox/flox}$ mice (Fig. 5B).

Long term stabilization of HIFs in photoreceptors leads to degeneration

ERG measurements on one-year-old *Vhl*$^{flox/flox}$;opsin-cre mice revealed a reduction of a- and b-wave amplitudes under both scotopic and photopic conditions (Figure 6

A-D). The reduction in the a-wave amplitude suggested that photoreceptors might be injured or lost. This was confirmed by the morphological analyses of one-year old retinas (Fig. 6E). As compared to the ONL of one-year-old *Vhl*$^{flox/flox}$ control mice, the ONL of *Vhl*$^{flox/flox}$;opsin-cre mice was severely thinned with only about 4 rows of photoreceptor nuclei remaining. In addition, the structure of inner and outer segments appeared severely disintegrated.

DISCUSSION

Hypoxic preconditioning protects photoreceptors from a subsequent light insult (Grimm et al., 2002). The exact mechanism of this neuroprotection is not known. Hypoxia inducible factors like HIF1 and HIF2 are activated during hypoxic preconditioning in the whole retina (Thiersch et al., 2009) and at least one product of their target genes, EPO, has been shown to be protective to photoreceptors (Grimm et al., 2002). Here we show that a sustained activation of HIF transcription factors in normoxic photoreceptors induced a hypoxia-like response and provided protection against light induced cell death. However, this protection was only transient and did not reach the level observed after hypoxic preconditioning.

Knockdown of *Vhl* strongly stabilized HIF1A and HIF2A and induced phosphorylation of STAT3 leading to the activation of target genes (*Adm*, *Egln1*, *Bnip3*, *Slc2a1* and *Vegf*), a reaction similar to a short hypoxic exposure of wild type mice (Fig. 2). This suggests that expression of these genes can be regulated by HIFs and/or pSTAT3 in rod photoreceptors but does not exclude expression of these genes in various additional cell types in response to hypoxic exposure. *Mt1* and *Mt2* showed a reduced induction in *Vhl* knockdowns as compared to hypoxic wild type mice. Therefore, hypoxia might induce transcription of *Mt1* and *Mt2* primarily in other retinal cell types and/or might use additional or different transcription factors for their regulation. *Epo* was the only tested gene that was not induced in *Vhl*$^{flox/flox}$;opsin-cre mice. It is unlikely that artificial activation of HIFs by the *Vhl* knockdown is not sufficient to increase *Epo* gene expression in normoxia since a pan knockdown of *Vhl* in *Vhl*$^{flox/flox}$;α-Cre mice resulted in a strong increase of *Epo* expression (Lange C, in print). Hence, hypoxic expression of *Epo* may not occur in rods but in other cell types in the retina.

It was shown earlier that injection of recombinant EPO is protective against light damage (Grimm et al., 2002). The fact that *Epo* was not induced in *Vhl* knockdown mice might thus be part of the explanation for the reduced and only transient protection in $Vhl^{flox/flox}$;opsin-cre mice. Alternatively, long-term stabilization of HIFs by the *Vhl* knockdown might cause a general downregulation of the neuroprotective cellular response through negative feedback loops. It has been shown for example that prolonged hypoxia downregulates levels of HIF1A and reduces the expression of some hypoxic responsive genes (Holmquist-Mengelbier et al., 2006) probably as an adaptational mechanism of the cells or tissues. However, hypoxic preconditioning also fully protected $Vhl^{flox/flox}$;opsin-cre mice from light induced degeneration (data not shown), indicating that retinal cells of *Vhl* knockdown mice are still able to react to acute hypoxia arguing against a permanent downmodulation of the neuroprotective response.

The *Vhl* knockdown *per se* might not only trigger a protective reaction but may simultaneously alter the physiology of rods in a way that imposes a cellular stress making the photoreceptors more vulnerable. VHL has been shown for example to play a role in extracellular matrix assembly (Ohh et al., 1998) and in the regulation of transcriptional activity of the tumor suppressor gene *p53* (Roe et al., 2006). An indication of cellular stress might be the slightly elevated levels of *caspase-1* expression already in young *Vhl* knockdowns (data not shown). Such an effect of the knockdown might antagonize a protective function of stabilized HIF transcription factors. Indeed, mouse models of inherited retinal degeneration showed slightly enhanced cell death when combined with the $Vhl^{flox/flox}$;opsin-cre mice (data not shown) and long-term lack of VHL induced photoreceptor degeneration in aged mice. Hence, only a short hypoxic period may be tolerated by the retina and, in fact be protective. Long-term hypoxia (Neubauer, 2001) or a long-term hypoxia-like response (this work) may lead to cell death.

Interestingly, $Vhl^{flox/flox}$;opsin-cre mice had reduced levels of rhodopsin. However, this may not account for the only transient protection of photoreceptors after light damage. Firstly, it is the rate of rhodopsin regeneration rather than the amount of dark adapted rhodopsin which determines light damage susceptibility (Seeliger et al., 2001). Secondly, an influence on light damage susceptibility would affect the amount of cell death and might not cause a delay in the progression of degeneration. The reason for the reduced amount of rhodopsin in retinas of *Vhl* knockdowns remains

unclear. It cannot be accounted for by a reduced number of photoreceptor cells because expression of rod and cone markers, retinal function (ERG) and morphology were normal in 10-week-old *Vhl*$^{flox/flox}$;opsin-cre mice (Figs. 3 and 4A). Although VHL was shown to be involved in the stability of ciliary structures (Thoma et al., 2007), we did not detect mislocalization of rod opsin in the retinas of *Vhl*$^{flox/flox}$;opsin-cre mice (data not shown) as might be expected if the connecting cilium of photoreceptors and therefore opsin transport to the outer segments would have been affected by the knockdown.

In summary, we showed that a photoreceptor specific *Vhl* knockdown induced a hypoxia-like response which protected photoreceptors against light induced cell death in 10-week-old mice. However, protection was only transient and did not reach the level detected after hypoxic preconditioning. This argues that the full and sustained protection of photoreceptors after hypoxic exposure requires regulation of factors in addition to the ones observed here, and/or that hypoxia-mediated protection of photoreceptors is mainly controlled by other retinal cells in a paracrine fashion.

ACKNOWLEDGEMENTS

The authors thank Coni Imsand and Hedwig Wariwoda for excellent technical assistance. This work was supported by the Swiss National Science Foundation (Grant 3100A0–117760), the Fritz Tobler Foundation, the H. Messerli Foundation, the Deutsche Forschungsgemeinschaft (DFG, grants Se837/5-2, Se837/6-1, Se837/7-1) and the German Ministry of Education and Research (BMBF, grant 0314106).

FIGURE LEGENDS

Figure 1: Vhl was successfully knocked down in photoreceptors of 10-week-old *Vhl*$^{flox/flox}$;opsin-cre mice.

(A) PCR amplification of genomic DNA isolated from retinal tissue from 10-week-old *Vhl*$^{flox/flox}$ (CRE -) and *Vhl*$^{flox/flox}$;opsin-cre (CRE +) mice. The un-excised allele (floxed) has a length of 460 bp in both *Vhl*$^{flox/flox}$ and *Vhl*$^{flox/flox}$;opsin-cre mice. The excised allele (excised) was identified as a 260 bp band in *Vhl*$^{flox/flox}$;opsin-cre mice.

(B) Semi-quantitative real time PCR after lasercapture microdissection showing *Vhl* expression in the different retinal layers (as indicated) of $Vhl^{flox/flox}$ (CRE -) and $Vhl^{flox/flox}$;opsin-cre (CRE +) mice. ONL: outer nuclear layer, INL: inner nuclear layer, GCL: ganglion cell layer. Given are mean values ± SD of 3 samples amplified in duplicates. Values were normalized to *β-actin* and expressed relatively to the respective value of $Vhl^{flox/flox}$ mice, which was set to 1.

Figure 2: HIF1A is stabilized and target genes are activated in 10-week-old $Vhl^{flox/flox}$;opsin-cre mice.
(A) Western blots showing protein expression of HIF1A, HIF2A and phosphorylated STAT3 (p-STAT3) in 10-week-old $Vhl^{flox/flox}$ (CRE -) and $Vhl^{flox/flox}$;opsin-cre (CRE +) mice. ACTB served as a control for equal loading. (B) Semi-quantitative real time PCR for hypoxia response genes (as indicated) amplified from retinas of 10-week-old $Vhl^{flox/flox}$, $Vhl^{flox/flox}$;opsin-cre and hypoxic wild type mice. Given are mean values ± SD of 4 retinas amplified in duplicates. Values were normalized to *β-actin* and expressed relatively to the values of normoxic wild type controls (not shown). For comparison, the value of $Vhl^{flox/flox}$ was artificially set to 1 and values of $Vhl^{flox/flox}$; opsin-cre were represented relative to the values of $Vhl^{flox/flox}$.

Figure 3: *Vhl* knockdown mice show no abnormalities up to 17 weeks of age.
(A) Representative scotopic (dark-adapted) and (B) photopic (light-adapted) single flash ERGs with increasing light intensities recorded from 17-week-old $Vhl^{flox/flox}$ control and $Vhl^{flox/flox}$;opsin-cre mice as indicated. The vertical line crossing each trace shows the time point of the light flash. (C) Scotopic and (D) photopic b-wave amplitudes from control (black, n=3) and $Vhl^{flox/flox}$;opsin-cre mice (red, n=3) as a function of the logarithm of the flash intensity. Boxes indicate the 25% and 75% quantile range, whiskers indicate the 5% and 95% quantiles, and the asterisks indicate the median of the data. (E) Semi-quantitative real-time PCR for photoreceptor-specific genes (as indicated) in $Vhl^{flox/flox}$ (white bars) and $Vhl^{flox/flox}$;opsin-cre (gray bars). Given are mean values ± SD of 4 retinas amplified in duplicates. Values were normalized to *β-actin* and expressed relatively to the value of $Vhl^{flox/flox}$ mice, which was set to 1.

Figure 4: *Vhl* knockdown mice show less photoreceptor cell damage 36 hours after light exposure.

(A) Morphological sections of dark controls (DC) and at 36 hours after light exposure (+36h) from $Vhl^{flox/flox}$ and $Vhl^{flox/flox}$;opsin-cre mice. Shown are representative sections of the lower central retina, the most affected region in our light damage setup. Examples of pyknotic nuclei are pointed out by arrows. (B) Cell death quantification ELISA of dark controls (DC) and at 36 hours after light exposure (+36h) from opsin-cre, $Vhl^{flox/flox}$ and $Vhl^{flox/flox}$;opsin-cre mice as indicated. Sown are boxblots representing the median, the lower and upper quantil and lower and upper "whiskers", representing the lower and upper 25%-quartil of 7 (DC, $Vhl^{flox/flox}$), 5 (DC, $Vhl^{flox/flox}$;opsin-cre), 4 (+36h, opsin-cre), 9 (+36h, $Vhl^{flox/flox}$) and 6 (+36h, $Vhl^{flox/flox}$;opsin-cre) retinas. As comparison, we show a single value of dark control opsin-cre mice. Values were calculated in percentage to the value of a positive control (provided by the kit), which was set to 100%. *: $p<0.05$. Significance was calculated by an unpaired t test. RPE: retinal pigment epithelium, OS: photoreceptor outer segments, IS: photoreceptor inner segments, ONL: outer nuclear layer, INL: inner nuclear layer.

Figure 5: Protection in $Vhl^{flox/flox}$;opsin-cre mice is transient.

(A) Morphological sections of dark controls (DC) and at 10 days after light exposure (+10d) from $Vhl^{flox/flox}$ and $Vhl^{flox/flox}$;opsin-cre mice. Shown are representative sections of the lower central retina, the most affected region in our light damage setup. (B) Rhodopsin content of retinas at 10 days after light exposure (LE) from $Vhl^{flox/flox}$ (white bars) and $Vhl^{flox/flox}$;opsin-cre mice (gray bars) expressed relatively to the corresponding dark controls (DC), which were set to 100%. (C) Rhodopsin content of retinas of dark adapted opsin-cre, $Vhl^{flox/flox}$ and $Vhl^{flox/flox}$;opsin-cre mice, as indicated. Values are expressed relatively to the values of $Vhl^{flox/flox}$ mice, which were set to 1. Sown are mean values ± SD of 6 retinas. **: $p<0.01$. Significance was calculated by an unpaired t test. RPE: retinal pigment epithelium, OS: photoreceptor outer segments, IS: photoreceptor inner segments, ONL: outer nuclear layer, INL: inner nuclear layer.

Figure 6: Long term stabilization of HIFs in photoreceptors leads to degeneration.

(A) Representative scotopic (dark-adapted) and (B) photopic (light-adapted) single flash ERGs with increasing light intensities recorded from one-year-old *Vhl*$^{flox/flox}$ control and *Vhl*$^{flox/flox}$;opsin-cre mice as indicated. The vertical line crossing each trace shows the timing of the light flash. (C) Scotopic and (D) photopic b-wave amplitudes from control (black, n=3) and *Vhl*$^{flox/flox}$;opsin-cre mice (red, n=3) as a function of the logarithm of the flash intensity. Boxes indicate the 25% and 75% quantile range, whiskers indicate the 5% and 95% quantiles, and the asterisks indicate the median of the data. (E) Representative morphological sections from the lower central retina of one-year-old *Vhl*$^{flox/flox}$ and *Vhl*$^{flox/flox}$;opsin-cre mice. RPE: retinal pigment epithelium, OS: photoreceptor outer segments, IS: photoreceptor inner segments, ONL: outer nuclear layer, INL: inner nuclear layer.

REFERENCES

Garayoa M, Martinez A, Lee S, Pio R, An WG, Neckers L, Trepel J, Montuenga LM, Ryan H, Johnson R, Gassmann M, Cuttitta F (2000) Hypoxia-inducible factor-1 (HIF-1) up-regulates adrenomedullin expression in human tumor cell lines during oxygen deprivation: a possible promotion mechanism of carcinogenesis. Mol Endocrinol 14:848-862.

Grimm C, Wenzel A, Groszer M, Mayser H, Seeliger M, Samardzija M, Bauer C, Gassmann M, Reme CE (2002) HIF-1-induced erythropoietin in the hypoxic retina protects against light-induced retinal degeneration. Nat Med 8:718-724.

Haase VH (2010) Hypoxic regulation of erythropoiesis and iron metabolism. Am J Physiol Renal Physiol 299:F1-13.

Haase VH, Glickman JN, Socolovsky M, Jaenisch R (2001) Vascular tumors in livers with targeted inactivation of the von Hippel-Lindau tumor suppressor. Proc Natl Acad Sci U S A 98:1583-1588.

Holmquist-Mengelbier L, Fredlund E, Lofstedt T, Noguera R, Navarro S, Nilsson H, Pietras A, Vallon-Christersson J, Borg A, Gradin K, Poellinger L, Pahlman S (2006) Recruitment of HIF-1alpha and HIF-2alpha to common target genes is differentially regulated in neuroblastoma: HIF-2alpha promotes an aggressive phenotype. Cancer Cell 10:413-423.

Iwai K, Yamanaka K, Kamura T, Minato N, Conaway RC, Conaway JW, Klausner RD, Pause A (1999) Identification of the von Hippel-lindau tumor-suppressor protein as part of an active E3 ubiquitin ligase complex. Proc Natl Acad Sci U S A 96:12436-12441.

Jaakkola P, Mole DR, Tian YM, Wilson MI, Gielbert J, Gaskell SJ, Kriegsheim A, Hebestreit HF, Mukherji M, Schofield CJ, Maxwell PH, Pugh CW, Ratcliffe PJ (2001) Targeting of HIF-alpha to the von Hippel-Lindau ubiquitylation complex by O2-regulated prolyl hydroxylation. Science 292:468-472.

Jung JE, Lee HG, Cho IH, Chung DH, Yoon SH, Yang YM, Lee JW, Choi S, Park JW, Ye SK, Chung MH (2005) STAT3 is a potential modulator of HIF-1-mediated VEGF expression in human renal carcinoma cells. Faseb J 19:1296-1298.

Kamura T, Koepp DM, Conrad MN, Skowyra D, Moreland RJ, Iliopoulos O, Lane WS, Kaelin WG, Jr., Elledge SJ, Conaway RC, Harper JW, Conaway JW (1999) Rbx1, a component of the VHL tumor suppressor complex and SCF ubiquitin ligase. Science 284:657-661.

Kibel A, Iliopoulos O, DeCaprio JA, Kaelin WG, Jr. (1995) Binding of the von Hippel-Lindau tumor suppressor protein to Elongin B and C. Science 269:1444-1446.

Lange C, Caprara C, Tanimoto N, Beck S, Huber G, Samardzija M, Seeliger M, Grimm C (in print) Retina specific activation of a sustained hypoxia-like response leads to severe retinal degeneration and loss of vision. Neurobiol Dis.

Le YZ, Zheng L, Zheng W, Ash JD, Agbaga MP, Zhu M, Anderson RE (2006) Mouse opsin promoter-directed Cre recombinase expression in transgenic mice. Mol Vis 12:389-398.

Mahon PC, Hirota K, Semenza GL (2001) FIH-1: a novel protein that interacts with HIF-1alpha and VHL to mediate repression of HIF-1 transcriptional activity. Genes Dev 15:2675-2686.

Neubauer JA (2001) Invited review: Physiological and pathophysiological responses to intermittent hypoxia. J Appl Physiol 90:1593-1599.

Ohh M, Park CW, Ivan M, Hoffman MA, Kim TY, Huang LE, Pavletich N, Chau V, Kaelin WG (2000) Ubiquitination of hypoxia-inducible factor requires direct binding to the beta-domain of the von Hippel-Lindau protein. Nat Cell Biol 2:423-427.

Ohh M, Yauch RL, Lonergan KM, Whaley JM, Stemmer-Rachamimov AO, Louis DN, Gavin BJ, Kley N, Kaelin WG, Jr., Iliopoulos O (1998) The von Hippel-Lindau tumor suppressor protein is required for proper assembly of an extracellular fibronectin matrix. Mol Cell 1:959-968.

Roe JS, Kim H, Lee SM, Kim ST, Cho EJ, Youn HD (2006) p53 stabilization and transactivation by a von Hippel-Lindau protein. Mol Cell 22:395-405.

Seeliger MW, Grimm C, Stahlberg F, Friedburg C, Jaissle G, Zrenner E, Guo H, Reme CE, Humphries P, Hofmann F, Biel M, Fariss RN, Redmond TM, Wenzel A (2001) New views on RPE65 deficiency: the rod system is the source of vision in a mouse model of Leber congenital amaurosis. Nat Genet 29:70-74.

Tanimoto N, Muehlfriedel RL, Fischer MD, Fahl E, Humphries P, Biel M, Seeliger MW (2009) Vision tests in the mouse: Functional phenotyping with electroretinography. Front Biosci 14:2730-2737.

Thiersch M, Raffelsberger W, Frigg R, Samardzija M, Wenzel A, Poch O, Grimm C (2008) Analysis of the retinal gene expression profile after hypoxic preconditioning identifies candidate genes for neuroprotection. BMC Genomics 9:73.

Thiersch M, Lange C, Joly S, Heynen S, Le YZ, Samardzija M, Grimm C (2009) Retinal neuroprotection by hypoxic preconditioning is independent of hypoxia-inducible factor-1 alpha expression in photoreceptors. Eur J Neurosci 29:2291-2302.

Thoma CR, Frew IJ, Krek W (2007) The VHL tumor suppressor: riding tandem with GSK3beta in primary cilium maintenance. Cell Cycle 6:1809-1813.

Warnecke C, Weidemann A, Volke M, Schietke R, Wu X, Knaup KX, Hackenbeck T, Bernhardt W, Willam C, Eckardt KU, Wiesener MS (2008) The specific contribution of hypoxia-inducible factor-2alpha to hypoxic gene expression in vitro is limited and modulated by cell type-specific and exogenous factors. Exp Cell Res 314:2016-2027.

Zhang H, Bosch-Marce M, Shimoda LA, Tan YS, Baek JH, Wesley JB, Gonzalez FJ, Semenza GL (2008) Mitochondrial autophagy is an HIF-1-dependent adaptive metabolic response to hypoxia. J Biol Chem 283:10892-10903.

Figure 1

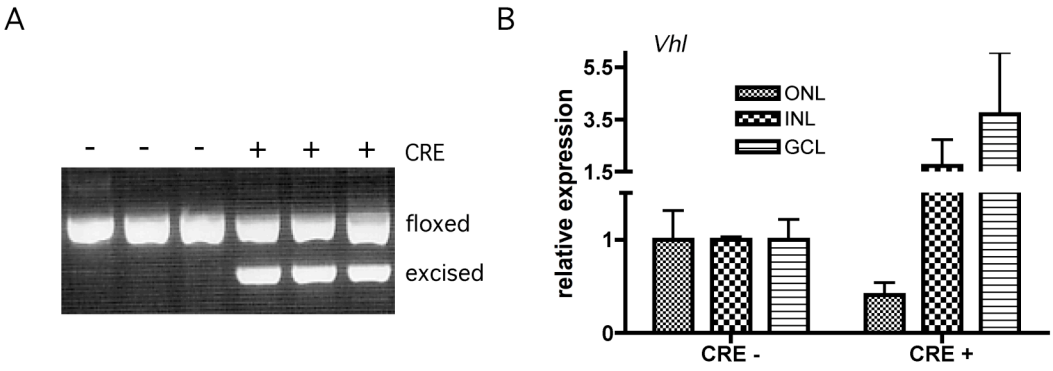
A
- - - + + + CRE
floxed
excised
B
Vhl
ONL
INL
GCL
relative expression
5.5
3.5
1.5
1
0
CRE -
CRE +

Figure 2

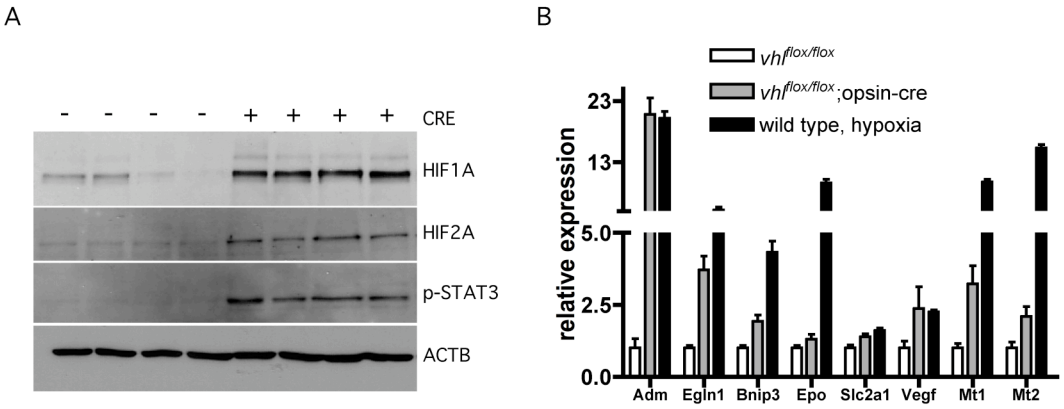
A
- - - - + + + + CRE
HIF1A
HIF2A
p-STAT3
ACTB
B
vhl flox/flox
vhl flox/flox ;opsin-cre
wild type, hypoxia
relative expression
23
13
5.0
2.5
0.0
Adm
Egln1
Bnip3
Epo
Slc2a1
Vegf
Mt1
Mt2

Figure 3

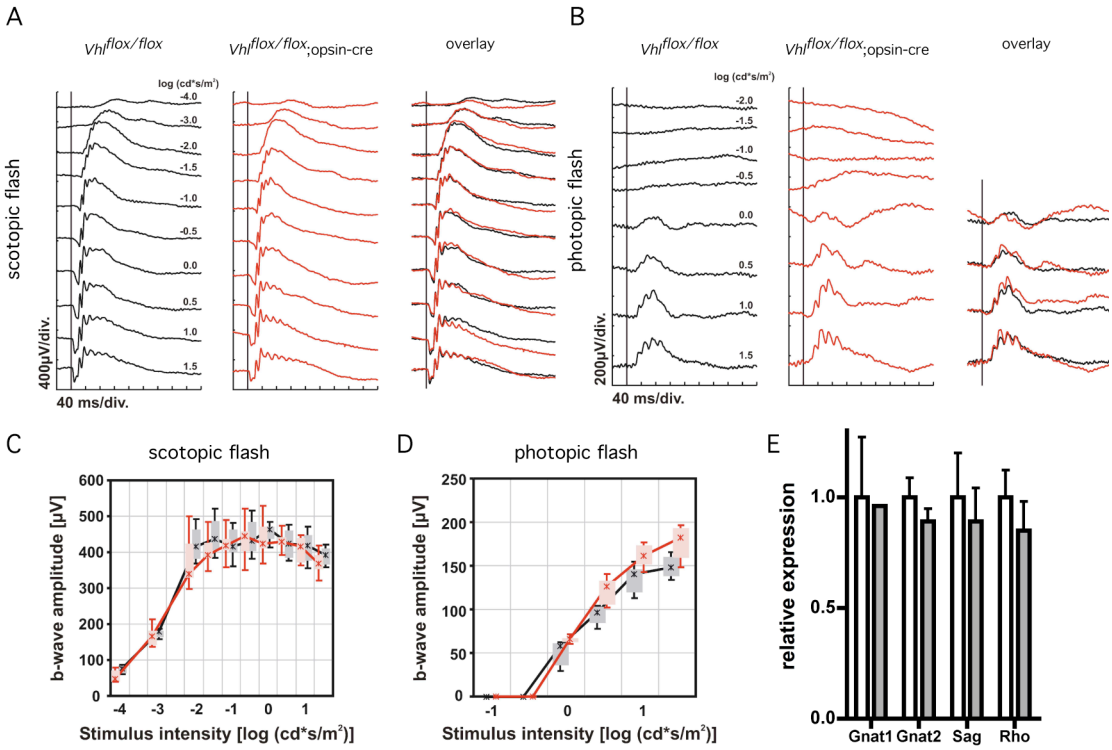
A
Vhl flox/flox
Vhl flox/flox;opsin-cre
overlay
scotopic flash
log (cd*s/m²)
-4.0
-3.0
-2.0
-1.5
-1.0
-0.5
0.0
0.5
1.0
1.5
400µV/div.
40 ms/div.
B
Vhl flox/flox
Vhl flox/flox;opsin-cre
overlay
photopic flash
log (cd*s/m²)
-2.0
-1.5
-1.0
-0.5
0.0
0.5
1.0
1.5
200µV/div.
40 ms/div.
C
scotopic flash
b-wave amplitude [µV]
600
500
400
300
200
100
0
-4
-3
-2
-1
0
1
Stimulus intensity [log (cd*s/m²)]
D
photopic flash
b-wave amplitude [µV]
250
200
150
100
50
0
-1
0
1
Stimulus intensity [log (cd*s/m²)]
E
relative expression
1.0
0.5
0.0
Gnat1
Gnat2
Sag
Rho

Figure 4

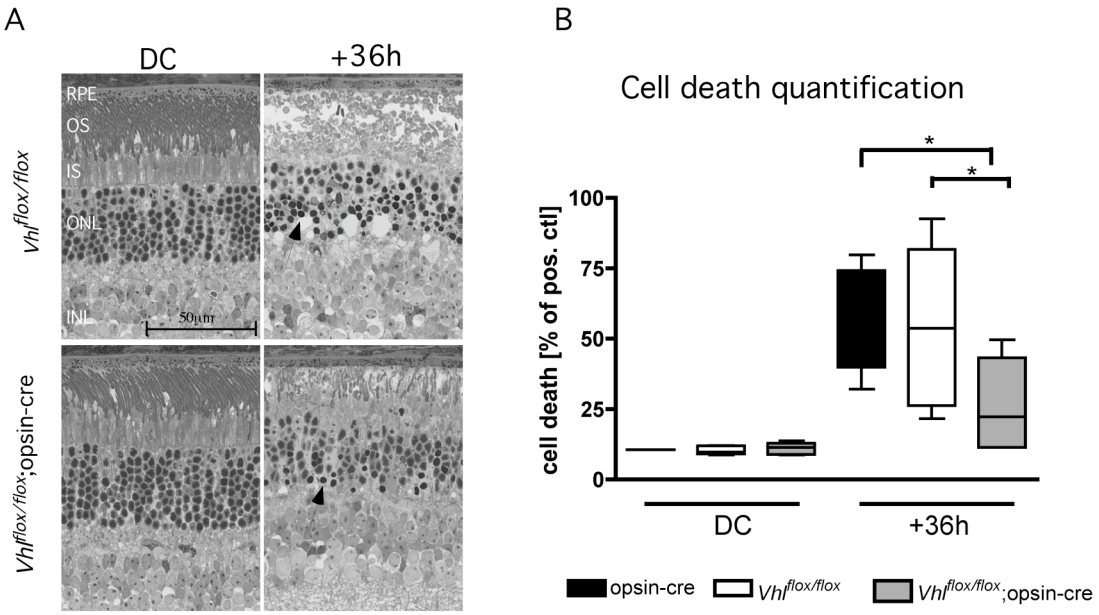
A
DC
+36h
RPE
OS
IS
ONL
INL
50µm
Vhlflox/flox
Vhlflox/flox;opsin-cre
B
Cell death quantification
cell death [% of pos. ctl]
100
75
50
25
0
*
*
DC
+36h
opsin-cre
Vhlflox/flox
Vhlflox/flox;opsin-cre

Figure 5

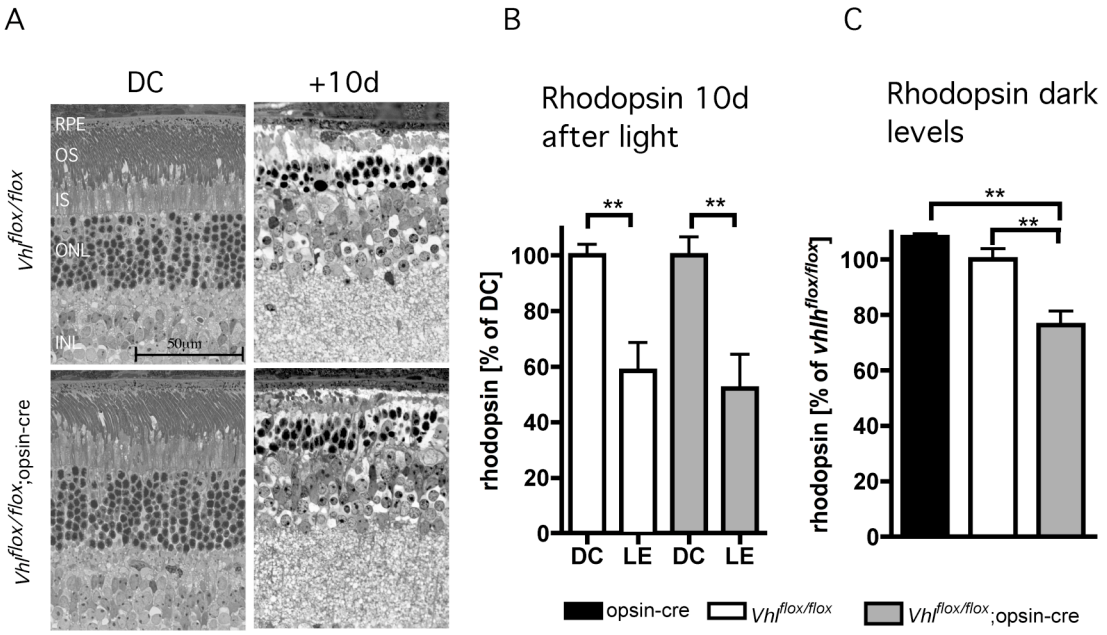
A
B
C
DC
+10d
RPE
OS
IS
ONL
INL
50µm
Vhl flox/flox
Vhl flox/flox;opsin-cre
Rhodopsin 10d after light
rhodopsin [% of DC]
100
80
60
40
20
0
**
**
DC
LE
DC
LE
Rhodopsin dark levels
rhodopsin [% of vhlh flox/flox]
opsin-cre
Vhl flox/flox
Vhl flox/flox;opsin-cre

Figure 6

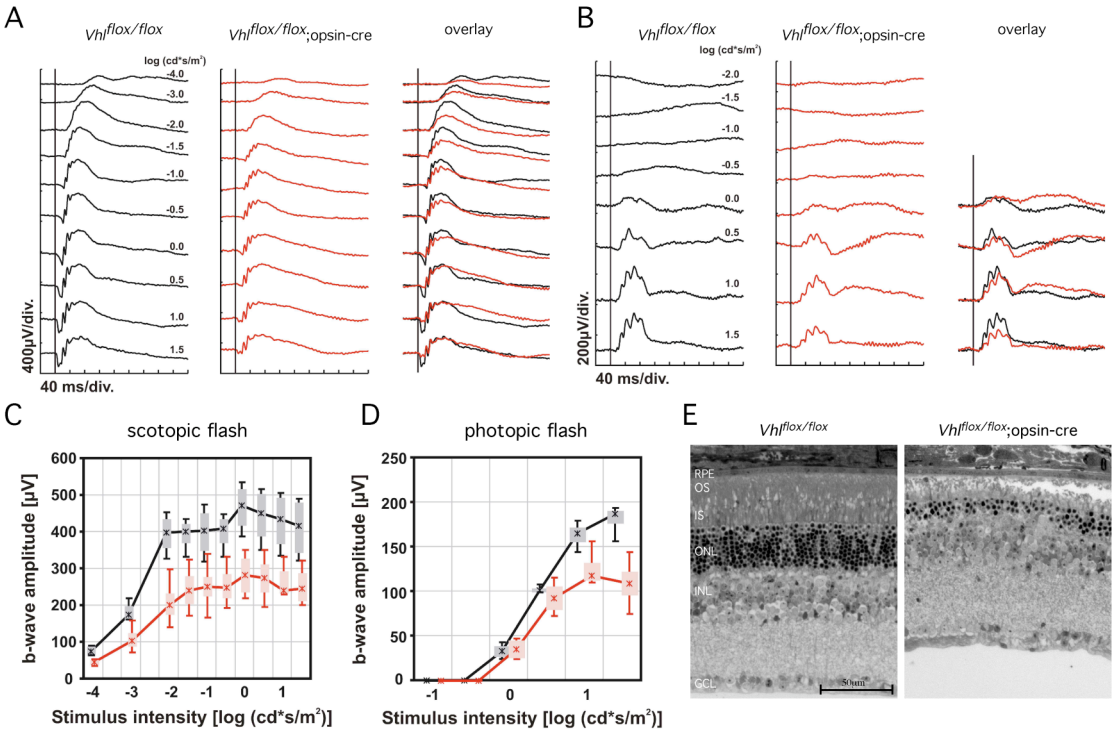
A
Vhlflox/flox
Vhlflox/flox;opsin-cre
overlay
log (cd*s/m²)
-4.0
-3.0
-2.0
-1.5
-1.0
-0.5
0.0
0.5
1.0
1.5
400µV/div.
40 ms/div.
B
Vhlflox/flox
Vhlflox/flox;opsin-cre
overlay
log (cd*s/m²)
-2.0
-1.5
-1.0
-0.5
0.0
0.5
1.0
1.5
200µV/div.
40 ms/div.
C
scotopic flash
b-wave amplitude [µV]
600
500
400
300
200
100
0
-4
-3
-2
-1
0
1
Stimulus intensity [log (cd*s/m²)]
D
photopic flash
b-wave amplitude [µV]
250
200
150
100
50
0
-1
0
1
Stimulus intensity [log (cd*s/m²)]
E
Vhlflox/flox
Vhlflox/flox;opsin-cre
RPE
OS
IS
ONL
INL
GCL
50µm

Table 1. Primers used for real-time PCR

Gene	Upstream (5' – 3')	Downstream (5' – 3')	Annealing	Product
Adm	ttcgcagttccgaaagaagt	ggtagctgctggatgcttgta	62°C	77bp
β-actin	cgacatggagaagatctggc	caacggctccggcatgtgc	62°C	153bp
Bnip3	cctgtcgcagttgggttc	gaagtgcagttctacccaggag	60°C	93bp
Egln1	cattgttggcagaaggtgtg	caaaggactacagggtctcca	62°C	70bp
Epo	gccctgctagccaattcc	gccctgctagccaattcc	60°C	128bp
Gnat1	gaggatgctgagaaggatgc	tgaatgttgagcgtggtcat	58°C	209bp
Gnat2	gcatcagtgctgaggacaaa	ctaggcactcttcgggtgag	58°C	192bp
Mt1	gaatggaccccaactgctc	gcagcagctcttcttgcag	62°C	104bp
Mt2	tgtacttcctgcaagaaaagctg	acttgtcggaagcctctttg	62°C	94bp
Sag	ttacaagccttccaacctctgac	accagcacaacaccatctacag	64°C	189bp
Scl2a1	cagtgtatcctgttgcccttctg	gccgaccctcttctttcatctc	62°C	151bp
Rho	cttcacctggatcatggcgtt	ttcgttgttgacctcaggcttg	62°C	130bp
Vegfa	acttgtgttgggaggaggatgtc	aatgggtttgtcgtgtttctgg	60°C	171bp
Vhl	gagggacccgttccaataat	ttggcaaaaataggctgtcc	60°C	364bp

3.1.3. Retina specific activation of a sustained hypoxia-like response leads to severe retinal degeneration and loss of vision

Christina Lange[1], Christian Caprara[1], Naoyuki Tanimoto[3], Susanne C. Beck[3], Gesine Huber[3], Marijana Samardzija[1], Mathias W. Seeliger[3] and Christian Grimm[1,2]

[1]Lab for Retinal Cell Biology, Department Ophthalmology, University of Zurich
[2]Zurich Center for Integrative Human Physiology (ZIHP), [3]Institute of Ophthalmic Research, Centre of Ophthalmology, Devision of Ocular Neurodegeneration, Tübingen, Germany

Manuscript accepted for publication in Neurobiology of Disease

Retina specific activation of a sustained hypoxia-like response leads to severe retinal degeneration and loss of vision

Christina Lange[1], Christian Caprara[1], Naoyuki Tanimoto[3], Susanne Beck[3], Gesine Huber[3], Marijana Samardzija[1], Mathias Seeliger[3] and Christian Grimm[1,2]

[1] Lab for Retinal Cell Biology, Department Ophthalmology, University of Zurich, Zurich, Switzerland
[2] Zurich Center for Integrative Human Physiology (ZIHP), University of Zurich, Zurich, Switzerland
[3] Institute of Ophthalmic Research, Centre of Ophthalmology, Division of Ocular Neurodegeneration, Tübingen, Germany

Keywords: Von Hippel Lindau, HIF, Caspase, retinal degeneration, vasculature, retina, photoreceptor

Corresponding author:

Christina Lange
Lab for Retinal Cell Biology
Department Ophthalmology
University of Zurich,
CH 8091 Zurich, Switzerland
Email: christina.lange@usz.ch
Tel: 0041 44 255 38 72
FAX:0041 44 255 43 85

Abstract

Loss of vision and blindness in human patients is often caused by the degeneration of neuronal cells in the retina. In mouse models, photoreceptors can be protected from death by hypoxic preconditioning. Preconditioning in low oxygen stabilizes and activates hypoxia inducible transcription factors (HIFs), which play a major role in the hypoxic response of tissues including the retina. We show that a tissue-specific knockdown of von Hippel Lindau protein (VHL) activated HIF transcription factors in normoxic conditions in the retina. Sustained activation of HIF1 and HIF2 was accompanied by persisting embryonic vasculatures in the posterior eye and the iris. Embryonic vessels persisted into adulthood and led to a severely abnormal mature vessel system with vessels penetrating the photoreceptor layer in adult mice. The sustained hypoxia-like response also activated the Leukemia inhibitory factor (LIF)-controlled endogenous molecular cell survival pathway. However, this was not sufficient to protect the retina against massive cell death in all retinal layers of adult mice. Caspases 1, 3 and 8 were upregulated during the degeneration as were several VHL target genes connected to the extracellular matrix. Misregulation of these genes may influence retinal structure and may therefore facilitate growth of vessels into the photoreceptor layer. Thus, an early and sustained activation of a hypoxia-like response in retinal cells leads to abnormal vasculature and severe retinal degeneration in the adult mouse retina.

Introduction

Retinitis pigmentosa (RP) is a major cause of severe visual impairment or blindness in humans. It is characterized by an initial loss of photoreceptors in the peripheral retina causing tunnel vision. As photoreceptor degeneration progresses, affected patients loose vision also in the center leading to complete blindness. Although mechanisms of cell death in RP and other degenerative diseases of the retina have been a subject of intense investigations, the exact molecular events leading to loss of photoreceptors have not been defined. As a consequence, only little is known about possible ways to inhibit cell death by neuroprotective approaches. In experimental model systems, preconditioning by hypoxia or light - the pre-exposure of mice to low oxygen concentrations or to non-damaging levels of light, respectively - protects photoreceptors from light induced degeneration (Grimm et al., 2002; Grimm et al., 2006; Chollangi et al., 2009). These systems may thus be valuable tools to study and develop neuroprotective measures to delay photoreceptor apoptosis.

Conditions of low oxygen availability (hypoxia) activate hypoxia inducible transcription factors (HIFs), which may regulate potentially protective genes during hypoxic preconditioning. HIFs are heterodimeric factors consisting of an α- and a β-subunit. Three isoforms of the α-subunit, HIF1A, HIF2A and HIF3A, and one form of the β-subunit, called aryl-hydrocarbon receptor nuclear translocator (ARNT), are known. ARNT is constitutively expressed and located in the nucleus. In conditions of normal oxygen availability (normoxia) HIF-α subunits are constantly degraded through the proteasomal pathway. Prolyl hydroxylases (PHDs or EGLNs) hydroxylate HIF-α subunits turning them into a binding substrate for the von Hippel-Lindau (VHL) protein complex that includes VHL, Cullin-2, Rbx1, the Elongins B and C and an E3-ubiquitinase (Kibel et al., 1995; Iwai et al., 1999; Kamura et al., 1999). Subsequent ubiquitination targets the HIF-α subunits to proteasomal degradation (Huang et al., 1998; Ivan et al., 2001). The function of PHDs depends on oxygen as a substrate. Hence, during hypoxia, hydroxylation does not occur and the VHL complex cannot bind to HIF-α. HIF-α is stabilized, enters the nucleus, binds ARNT and p300 as a transcriptional co-activator, and participates in the regulation of gene expression.

It has been shown that hypoxic exposure of mice stabilizes and activates HIF1A and HIF2A in the retina (Grimm et al., 2002; Thiersch et al., 2009). However, it is

unknown whether activation of HIF transcription factors is sufficient to protect photoreceptors from light induced degeneration as observed after hypoxic preconditioning. Inactivation of VHL prevents degradation of HIF-α subunits and leads to constitutively active HIFs even in normoxia (Haase et al., 2001). Long-term stabilization of HIF transcription factors during normoxia in the retina might provide information about the contribution of HIF to neuroprotection by hypoxic preconditioning. However, overactivation of HIFs may lead to excessive blood vessel growth, a phenomenon particularly important in tumor biology (Senger et al., 1983). In addition, a recent report shows that untimely activation of HIFs during retinal development causes a severely disturbed retinal vasculature (Kurihara et al.).

To activate HIFs in normoxia, we generated a *Vhl* knockdown mouse using the Cre-lox system with Cre-recombinase being expressed under the control of the α-element of the Pax6-promotor. This promoter is active as early as E10.5 and leads to the deletion of floxed sequences in the distal retina and in the iris, but not in the lens or the retinal pigment epithelium (Marquardt et al., 2001). In accordance with a recent report, we show that development of the retinal vasculature is severely disturbed early during development in the *vhl* knockdown mouse (Kurihara et al.). In addition we show that embryonic vasculature persists into adulthood and that the *vhl* knockdown also results in severe cell death in the ageing retina with an increase of *Casp-8* and *Casp-1* expression and induction of HIF-independent stress response pathways.

Materials and Methods

Mice and genotyping

Mice were treated in accordance with the regulations of the Veterinary Authority of Zurich and with the statement of 'The Association for Research in Vision and Ophthalmology' for the use of animals in research. 129S-Vhlh^{tm1jae}/J-mice (from now on referred to as *vhl*$^{flox/flox}$ mice), which have *lox*P sites flanking exon 1 and part of the promoter of the *Vhl* gene (Haase et al., 2001) were purchased from Jackson Laboratory (Bar Harbor, USA). To generate retina specific *Vhl* knockdown mice, *vhl*$^{flox/flox}$ mice were crossed with mice expressing Cre-recombinase under the control of the α-element of the Pax6-promotor (α-Cre), which leads to the deletion of floxed sequences in the distal retina and in the iris (Marquardt et al., 2001). Breeding pairs were established to generate *vhl*$^{flox/flox}$;α-cre and *vhl*$^{flox/flox}$ control littermates. The following primers were used to detect wild type (wt) and *Vhl*-flox alleles: forw (5'-TGAGTATGGGATAACGGGTTGAAC-3') and rev (5'-AGAACTGACTGACTTC CACTGATGC-3'). The wt allele was identified as a 125 bp and the *Vhl*-flox allele as a 317 bp long fragment on a 1.5% agarose gel. Presence of the α-Cre transgene was tested by PCR using the following primer pair: forw (5'-AGGTGTAGAGAAGG CACTTAGC-3') and rev (5'-CTAATCGCCATCTTCCAGCAGG-3'). Amplification resulted in a 411 bp fragment.

To detect excision of floxed sequences in the *Vhl* gene, genomic DNA from retina was isolated and tested by PCR using the following primers: forw_un-excised (5'-CTGGTACCCACGAAACTGTC-3'), forw_excised (5'-CTAGGCACCGAGCTTAG AGGTTTGCG-3') and rev_both (5'-CTGACTTCCACTGATGCTTGTCACAG-3'). The excised allele was identified as a 260 bp and the un-excised allele as a 460 bp fragment.

RNA, DNA and protein preparation

Retinas were removed through a slit in the cornea and immediately frozen in liquid nitrogen. Total RNA was prepared using the RNeasy RNA isolation kit (Qiagen, Hilden, Germany) according to the manufacturer's directions including a DNase treatment to digest residual genomic DNA. Equal amounts of RNA were used for

reverse transcription using oligo(dT) primer and M-MLV reverse transcriptase (Promega, Madison, WI, USA).

For retinal genomic DNA isolation 10 µl of the homogenate prepared for RNA isolation (RNeasy RNA isolation; see above) were processed with the QIAamp DNA Blood Mini Kit (Qiagen) according to the manufacturer's directions but without proteinase K treatment and heating.

For protein isolation retinas were homogenized by sonication in 100 mM Tris/HCl, pH 8.0, and analyzed for protein content using Bradford reagent. 4x Laemmli buffer was added and samples were heated for 10 min at 75°C before loading onto an SDS-PAGE gel for Western blotting (see below).

Semi-quantitative real time polymerase chain reaction (PCR)

Relative quantification of cDNA was done by semi-quantitative real time PCR using the LightCycler 480 SybrGreen I Master kit, a LightCycler 480 instrument (Roche Diagnostics, Basel, Switzerland) and specific primer pairs (Table 1). Three animals per time point were analyzed in duplicates and normalized to *β-Actin* using the Light Cycler 480 software (Roche Diagnostics, Basel, Switzerland). Values of experimental retinas were expressed relative to the first time point tested, which was set to 1. Significance of differences between expression levels at specific time points in wild type and knockdown mice was tested using an unpaired student's t-test.

Western blotting

Standard SDS-PAGE (10%) and Western blotting of 40 µg of total retinal extracts were performed. For immunodetection, the following antibodies were used: anti-HIF1A (#Nb100-479 Novus Biologicals, Cambridge, United Kingdom, 1:1000), anti-HIF2A (#Nb100-122, Novus Biologicals, 1:1000), anti-pSTAT3 (#9131 Cell Signaling Technology, 1:500), anti-STAT3 (#9132 Cell Signaling Technology, 1: 1000), anti-GFAP (MAB302 Chemicon/Millipore, Billerica, USA, 1:500), CASP1, CASP3, CASP8 (all kindly provided by Peter Vandenabeele, Ghent University, Belgium, all 1:10000), CASP9 (#9504, Cell Signaling Technology, 1:500) and anti-ACTB (#A5441 Sigma, St. Louis, MO, USA, 1:5000). Blots were incubated overnight at 4°C with primary antibodies followed by a one hour incubation at room temperature (22°C) with HRP-conjugated secondary antibodies. Immunoreactivity

was visualized using the Western Lightning Chemiluminescence reagent (Perkin-Elmer, Boston, MA, USA).

Confocal scanning laser ophthalmoscopy (cSLO)

cSLOs were obtained according to previously reported procedures (Seeliger et al., 2005). Briefly, mice were anaesthetized by a subcutaneous injection of ketamine (66.7 mg/kg) and xylazine (11.7 mg/kg). Pupils were dilated with tropicamide eye drops (Mydriaticum Stulln, Pharma Stulln, Stulln, Germany) in anesthesia. cSLO imaging was performed with a Heidelberg Retina Angiograph (HRA I) equipped with an argon laser featuring two wavelengths (488 nm and 514 nm) in the short wavelength range and two infrared diode lasers (795 nm and 830 nm) in the long wavelength range. The 488 nm and 795 nm lasers were used for fluorescein (FL) and indocyanine green (ICG) angiography, respectively. FL angiography was performed using a subcutaneous injection of 75 mg/kg body weight fluorescein-Na (University pharmacy, University of Tuebingen, Germany), and ICG angiograhy following an s.c. injection of 50 mg/kg body weight ICG (ICG-Pulsion, Pulsion Medical Systems AG, Munich, Germany).

Spectral domain optical coherence tomography (SD-OCT)

SD-OCT imaging was done in the same session as cSLO, i.e. animals remained anaesthetized using identical preparatory steps. Mouse eyes were subjected to SD-OCT using the commercially available Spectralis™ HRA+SD-OCT device (Heidelberg Engineering, Heidelberg, Germany) featuring a broadband superluminescent diode at λ = 870 nm as low coherent light source. Each two-dimensional B-Scan recorded at 30° field of view consists of 1536 A-Scans, which are acquired at a speed of 40,000 scans per second. Optical depth resolution is around 7 µm with digital resolution reaching 3.5 µm (Huber et al., 2009). The optical adjustments to permit the use in mice were described previously (Fischer et al., 2009). Imaging was performed using the proprietary software package Eye Explorer version 3.2.1.0. The combination of scanning laser retinal imaging and SD-OCT allows for real-time tracking of eye movements and real-time averaging of SD-OCT scans, reducing speckle noise in the SD-OCT images considerably (Huber et al., 2009).

Retinal flat mounts and immunofluorescence

Eyes were collected and fixed for 3-5 minutes in 2% (w/v) paraformaldehyde (PFA) in PBS. The sclera was dissected from the eyes in PBS and lens, iris and vitreous were removed. The retina was flattened and stored in methanol at -20°C. Before use, the retina was post-fixed in 4% (*w/v*) PFA in PBS for 10 minutes. For immunofluorescence, the flat-mounted retina was washed in PBS and incubated in blocking buffer (1% fetal bovine serum, 0.1% Triton X-100 in PBS) for 1 hour at room temperature (22°C). Flat mounts were incubated with Alexa594-coupled isolectin-A4 (#I21413, Invitrogen, Basel, Switzerland, 1:50) at 4°C overnight, washed and mounted in MOWIOL anti-fade medium (10% Mowiol 4-88 (*w/v*) (Calbiochem, San Diego, CA, USA), in 100 mM Tris, pH 8.5, 25% glycerol (*w/v*) and 0.1% 1,4-diazabicyclo [2.2.2] octane (DABCO)), Calbiochem, San Diego, CA, USA). Signals on sections were analyzed with a digitalized Axiovision microscope (Carl Zeiss AG, Feldbach, Switzerland).

Retinal sections and immunofluorescence

After enucleation, eyes were fixed for 2 h in 4% PFA (w/v) at 4°C before cornea and lens were removed. The remaining ocular tissue was post-fixed for an additional 2 hours in 4% PFA at 4°C, followed by cryoprotection in 30% sucrose in PBS, pH 7.4, at 4°C over night. Eyecups were embedded in tissue freezing medium (Leica Microsystems Nussloch GmbH, Nussloch, Germany) and frozen in a 2-methylbutane bath cooled by liquid nitrogen. Retinal sections (12 µm) were cut and blocked in 3% normal goat serum, 0.3% Triton X-100 in 0.1 M PBS (pH 7.4) for 1 hour at room temperature. Sections were incubated in blocking solution at 4°C over night with one of the following primary antibodies: anti-IBA1 (#019-19741, Wako, Richmond, USA, 1:1000), isolectin-A4 (# L1509; Sigma, St. Louis, MO, USA, 1:50, coupled to FITC), anti-rod opsin (kindly provided by David Hicks, 1:100) and anti-swl-cone opsin (#sc-14363, Santa Cruz Biotechnology, Santa Cruz, CA, USA, 1:500). After 3 washes with PBS, slides were incubated with the appropriate secondary antibody coupled to Cy3 for 1 hour at room temperature, counterstained with DAPI and mounted with MOWIOL anti-fade medium (10% Mowiol 4-88 (*w/v*)). Signals on sections were analyzed with a digitalized Axiovision microscope (Carl Zeiss AG, Feldbach, Switzerland).

Morphology

For light microscopy, eyes were fixed in 2.5% glutaraldehyde in 0.1 M cacodylate buffer (pH 7.3) at 4°C overnight. For each eye, the superior and the inferior retina were prepared, washed in cacodylate buffer, incubated in osmium tetroxide for 1h, dehydrated, and embedded in Epon 812. Sections (0.5 µm) were prepared from the lower central retina and counterstained with methylene blue.

Electroretinographic analysis

Electroretinograms (ERGs) were recorded according to previously described procedures (Seeliger et al., 2001; Tanimoto et al., 2009). The ERG equipment consisted of a Ganzfeld bowl, a direct current amplifier, and a PC-based control and recording unit (Multiliner Vision; VIASYS Healthcare GmbH, Hoechberg, Germany). Mice were dark-adapted overnight and anaesthetized with ketamine (66.7 mg/kg body weight) and xylazine (11.7 mg/kg body weight). Pupils were dilated and single flash ERG responses were obtained under dark-adapted (scotopic) and light-adapted (photopic) conditions. Light adaptation was accomplished with a background illumination of 30 candela (cd) per square meter starting 10 minutes before recording. Single white-flash stimulus intensity ranged from –4 to 1.5 log cd*s/m^2 under scotopic and from –2 to 1.5 log cd*s/m^2 under photopic conditions, divided into 10 and 8 steps, respectively. Ten responses were averaged with an inter-stimulus interval (ISI) of either 5 seconds (for –4, –3, –2, –1.5, –1, and –0.5 log cd*s/m^2) or 17 seconds (for 0, 0.5, 1, and 1.5 log cd*s/m^2).

Results

Tissue specific knockdown of Vhl leads to HIFα stabilization in the retina.

Analysis of genomic DNA from retinal tissue showed that excision of floxed DNA sequences was obvious in mice expressing Cre recombinase but not in control mice (Fig. 1A). Accordingly, expression of *Vhl* was significantly reduced in retinas of $vhl^{flox/flox}$;α-cre mice as compared to $vhl^{flox/flox}$ littermates. Strongest reduction was observed at 28 days of age (P=0.0044, Fig. 1B). Surprisingly, expression of *Hif1a,* but not of *Hif2a (Epas1)* was also affected by the *Vhl* knockdown. *Hif1a* was significantly down-regulated up to 1.7 fold (at 28 d, P=0.0094) in $vhl^{flox/flox}$;α-cre mice until 42 days of age (Fig. 1B). In contrast, expression of the prolyl hydroxylases *Phd2* (*Egln1*) and especially of *Phd3* (*Egln3*) was significantly and strongly induced in the *Vhl* knockdown retinas at early timepoints (*Egln1*) or throughout the analyzed period (*Egln3*). Expression of *Phd1* (*Egln2*) was not affected by the knockdown. Since VHL controls levels of HIF-α transcription factors by regulating protein stability, we tested levels of HIF1A and HIF2A (EPAS1) in retinas of 10 and 28 days old knockdown mice and wild type littermates. Retinal HIF1A levels are high after birth and decrease with the development of the retinal vasculature (Grimm et al., 2005). In knockdown mice, HIF1A and HIF2A levels were increased at both ages tested (Fig. 1C). Levels of HIF1A decreased with time in retinas of both control and knockdown mice (cross-compare 10d and 28d). Whereas this was expected for wild type retinas (Grimm et al., 2005), the reduction in HIF1A stability in adult *Vhl* knockdowns probably reflects the restricted loss of VHL activity in the peripheral but not central retina (see below). Thus, in the adult knockdown mice HIF1A is only stabilized in the retinal periphery, in contrast to retinas at 10 days of age where normal development additionally stabilizes HIF1A also in the central retina.

Abnormal vasculature in retina and iris of Vhl knockdown mice

The retinal vasculature of $vhl^{flox/flox}$;α-cre mice was assessed with confocal scanning laser ophthalmoscopy (cSLO) in conjunction with fluorescein (FL) and indocyanine green (ICG), which are clinically established dyes to visualize the retinal and choroidal circulation, respectively. ICG angiography depicts both retinal and choroidal structures, whereas FL angiography imaging yields particularly detailed

information about retinal capillaries, but not choroidal vessels (Seeliger et al., 2005). We found no indications that either the retinal or the choroidal vascular system of *vhl*$^{flox/flox}$ mice at the age of 10 weeks was abnormal; they were rather comparable to that of wild-type strains like C57BL/6 (Seeliger et al., 2005). However, in *vhl*$^{flox/flox}$;α-cre mice, abnormal retinal vessels and persistent remnants of the developmental hyaloidal vascular system (Ito and Yoshioka, 1999) were found (Fig. 2A), while choroidal structures appeared unaltered. Retinal vessel density was particularly reduced in the peripheral retina, probably because topographical differences in Cre activity translated into differences in the excision efficiency of floxed sequences (Kurihara et al., ; Marquardt et al., 2001). Persistent hyaloidal vessels originating from the optic disc were still present in the vitreous just above the retinal surface at 10 weeks of age. These vessels were functional as they filled with dye in angiography. SD-OCT imaging confirmed the optic disc area as the region of origin of these persisting hyaloidal vessels in *vhl*$^{flox/flox}$;α-cre mice (Fig. 2B). These results extend observations made by Kurihara *et al.*, who reported persistent hyaloidal vessels only up to postnatal day 6 in the *vhl*$^{flox/flox}$;α-cre mouse (Kurihara et al.). In addition to the abnormal retinal and hyaloidal vessels, 10-week-old *vhl*$^{flox/flox}$;α-cre mice also had an extremely under-developed iris vasculature and a persisting pupillary membrane (Ito and Yoshioka, 1999) (Fig. 2A, white arrow).

Normally, the mature retinal vasculature is fully developed at postnatal day 35 (Fruttiger, 2002) (Fig. 3A). Retinal flatmounts (stained with isolectin-A4) of *vhl*$^{flox/flox}$ mice showed normal vascular architecture (Fig. 3A upper panels). However, the vasculature of *vhl*$^{flox/flox}$;α-cre mice at 35 days of age was severely under-developed with a strongly reduced density of the capillary network in the retinal periphery. Immunofluorescence stainings of retinal cryosections from *vhl*$^{flox/flox}$;α-cre mice revealed that the capillaries in the deep plexi did not or not completely develop (Fig. 3B, isolectin-A4 staining in green, and data not shown). Instead some retinal vessels in the periphery grew into the outer nuclear layer (ONL; Fig. 3B, arrow). These vessels originated from the retinal vasculature because we did not detect any sprouting vessels in the choroid or vessels penetrating the RPE layer (Fig. 3B and data not shown). This angiogenic vessel-growth activated resident microglia. In wild type controls, microglia are located mostly to the GCL and IPL (Fig. 3B, IBA1 staining in red). In the *Vhl* knockdown mice, however, many microglia were found in the OPL

and along ingrown vessels. Some microglia were even located in the layer of the photoreceptor segments (Fig. 3B, arrowheads). In the central retina, the vasculature of *vhl*$^{flox/flox}$;α-cre mice was comparable to controls (Fig. 3A and data not shown).

The abnormal development of the retinal vasculature may have partly been caused by the increased and sustained expression of the pro-angiogenic genes *Vegfa* and *Epo* (Fig. 3C). Both genes are known to be strongly regulated by HIF transcription factors, which were stabilized in the *Vhl* knockdown retinas (see above). *Serpinf1* encodes pigment epithelium derived factor (PEDF), a neuroprotective and anti-angiogenic protein (Barnstable and Tombran-Tink, 2004). Its increased expression (Fig. 3C) may suggest that the retinal response to the disturbed vascular development involves activation of endogenous protective systems (see also below). Other HIF-inducible and angiogenesis-related genes (*Tie1*, *Tie2* (*Tek*) and *Fzd4*), however, were not or only slightly induced in *vhl*$^{flox/flox}$;α-cre compared to *vhl*$^{flox/flox}$ mice.

These data show, that lack of functional VHL during development and in the mature retina leads to an upregulation of several angiogenic factors, the persistence of the embryonic ocular vasculature (hyaloidal vessels, pupillary membrane) deep into adulthood and to a disturbed and severely under-developed vessel system in the mature retina and iris.

Degeneration of photoreceptors in vhl$^{flox/flox}$;α-cre *mice*

Ongoing angiogenesis and growth of vessels into the ONL may affect retinal morphology and function, as well as cell physiology and survival. Retinal sections from 2-week-old (Fig. 4A, B) and 10-week-old (Fig. 4C, D) mice were prepared and analyzed by light microscopy. The peripheral retina of 2-week-old *vhl*$^{flox/flox}$;α-cre mice showed structural abnormalities especially in the ONL. Photoreceptor nuclei were not aligned properly affecting also the layering of the cells in the INL (Fig. 4B upper right panel). In 10-week-old *vhl*$^{flox/flox}$;α-cre mice parts of the peripheral retina had completely degenerated and cells of the ONL, the INL and the GCL had been lost (Fig. 4D upper right pannel). Degeneration in the retinal periphery of 10-week-old *vhl*$^{flox/flox}$;α-cre mice was not always as severe as shown here but was very pronounced in all animals analyzed. The central retina of 2-week-old *Vhl* knockdowns was comparable to controls, although one or two rows of photoreceptor nuclei were missing (Fig. 4B lower panels). In the central retina of 10-week-old *vhl*$^{flox/flox}$;α-cre

mice, however, at least three rows of photoreceptor nuclei were missing and outer and inner segments seemed to be shortened compared to *vhl*$^{flox/flox}$ controls (Fig. 4D lower panels).

Immunofluorescence analysis of sections prepared from less severely damaged regions in the peripheral ventral retina of 10-week-old animals showed reduced expression of rod opsin and S-cone opsin in knockdown retinas (Fig. 5A). S-cone opsin positive cells were especially sparse, even in the ventral retina, the region of highest S-cone density in mice (Applebury et al., 2000). If all retinal cells were similarly affected by the degeneration, one might expect that expression levels of markers for specific cell types would remain roughly constant when normalized to *β-Actin*. This was indeed observed for expression of *Chx10*, a marker for bipolar cells and for *Opn4*, a marker for ganglion cells (data not shown). However, levels of short wave length cone opsin (*Opn1sw*), middle wavelength cone opsin (*Opn1mw*), rod opsin (*Rho*), rod transducin (*Gnat1*) and cone transducin (*Gnat2*) were significantly reduced in *vhl*$^{flox/flox}$;α-cre mice compared to *vhl*$^{flox/flox}$ littermates (Fig. 5B). This suggests that rod and cone photoreceptors are the most strongly affected cell types by the degeneration and that they may be lost even outside of the severely degenerated peripheral retina (as it is also suggested by the morphology of the central retina, Fig. 4D). Thus, these cells seem to be more sensitive to the abnormal retinal vasculature than cells of the other layers and retinal function may thus be strongly affected.

Reduction of retinal function in vhl$^{flox/flox}$;α-cre *mice*

To investigate functional properties of *vhl*$^{flox/flox}$;α-cre mice, flash ERGs were recorded from 10-week-old *vhl*$^{flox/flox}$;α-cre and control *vhl*$^{flox/flox}$ mice under scotopic and photopic conditions (Fig. 6). *Vhl*$^{flox/flox}$;α-cre mice showed strongly reduced scotopic (Fig. 6A, C) and photopic ERG (Fig. 6B, D) responses, indicating alterations of both rod and cone system components. As the initial portion of the a-wave reflects the primary light response in photoreceptors, the attenuation of the a-wave up to the highest intensity observed in *vhl*$^{flox/flox}$;α-cre mice indicates strong photoreceptor dysfunction/degeneration. The b-wave and the oscillatory potentials, generated by downstream retinal circuitry, were also strongly reduced, but this is presumably mainly a consequence of the primary effect on photoreceptors. Rod and cone signaling were about equally affected.

Stress-activated signaling and cell death pathways in vhl$^{flox/flox}$;α-cre mice

Degeneration of photoreceptors was shown to activate the JAK/STAT signaling pathway (Samardzija et al., 2006a; Joly et al., 2008; Ueki et al., 2008; Burgi et al., 2009), an endogenous survival system, which is mainly controlled by LIF expression in a subset of Muller glia cells (Joly et al., 2008). So far, however, regulation of this signaling system was only tested in conditions of pure photoreceptor injury. We therefore asked, whether the broader retinal degeneration in the Vhl knockdown mice would trigger the same molecular response. Semi-quantitative real time PCR analysis showed that expression of *Lif*, *Gfap*, *Edn2* and *Fgf2* was strongly induced starting around 10 days of age in *vhl$^{flox/flox}$*;α-cre mice. Expression remained high during the degenerative phase and lasted at least until 10 weeks of age (Fig. 7A). In addition, STAT3 was phosphorylated in *vhl$^{flox/flox}$*;α-cre but not *vhl$^{flox/flox}$* control mice (Fig. 7B). This suggests that the same, LIF-dependent signaling system was activated as in models of pure photoreceptor degeneration leading to the hypothesis that the LIF-system may be activated in response to most retinal injuries in a general attempt to protect neurons from degeneration. *Cntf*, another endogenous survival factor was also induced in the *Vhl* knockdown retina. In conditions of pure photoreceptor injury, expression of *Cntf* was not (Joly et al., 2008) or only slightly activated late during the degeneration (Samardzija et al., 2006a). CNTF may thus be a factor, which mainly responds to cellular damage in the INL and/or GCL.

Several pro-apoptotic genes can be regulated in a VHL-dependent manner not involving HIF transcription factors. Among those, expression of Kruppel-like transcription factor 10 (*Klf10*), transforming growth factor β induced (*Tgfbi*) and fibronectin 1 (*Fn1*) was significantly upregulated in *vhl$^{flox/flox}$*;α-cre mice (Fig. 8A). In contrast, hepatocyte growth factor (*Hgf*), a VHL-controled gene related to cancer (Peruzzi et al., 2006) was expressed similarly in *vhl$^{flox/flox}$*;α-cre mice and *vhl$^{flox/flox}$* littermates (data not shown).

Apoptotic cell death is frequently executed through caspase activation. Two general pathways are distinguished. Procaspase-8 is activated through the cell surface death receptor pathway whereas activation of procaspase-9 is the first step in the mitochondrial pathway (Budihardjo et al., 1999). Caspase-3 is the main executor caspase of many apoptotic processes and also suspected to be involved in

programmed cell death during postnatal development of the mouse retina (Zeiss et al., 2004; O'Driscoll et al., 2006). In the *vhl*$^{flox/flox}$;α-cre mouse, expression of *caspase-1 (Casp1*) and of *caspase-8* (*Casp8)* was significantly upregulated whereas expression of *caspase-3* (*Casp3*) and of *caspase-9* (*Casp9*) was similar to control animals (Fig. 8A). Although expression of tumor necrosis factor α (*Tnf*), which can induce *Casp8* upon binding to death receptors (Guicciardi and Gores, 2009), showed a strong variation between animals, the pattern of expression nevertheless suggested increased levels of *Tnf* in knockdown animals. Western blots detecting the proforms of Caspases 1, 3, 8 and 9 indicated increased protein levels of CASP1 and CASP3 in 28 day-old knockdown retinas when compared to the wild type littermates (Fig. 8B). Protein levels of CASP8 were not or only slightly elevated in the knockdown and levels of CASP9 were similar in controls and knockdowns. We did not detect activated (cleaved) forms of the caspases in our blots. The reason why protein levels not always paralleled RNA expression profiles is unclear but may be explained by potential differences in RNA and/or protein stability in young and mature mouse retinas.

Discussion:

Hypoxic preconditioning stabilizes HIF transcription factors in the retina of the adult mouse and protects photoreceptors against a subsequent toxic light insult (Grimm et al., 2002). Inactivation of VHL in the peripheral retina by the Cre mediated deletion of floxed *Vhl* gene sequences led to a normoxic and long-lasting activation of HIF1A and HIF2A during retinal development ((Kurihara et al.); Fig. 1). As a consequence, several pro-angiogenic genes like *Vegfa* and *Epo* but also anti-angiogenic factors like *Pedf* (*Serpinf1*) were upregulated. This misregulated gene expression may have led to the severe abnormalities of the retinal vasculature with persisting hyaloidal vessels ((Kurihara et al.); Figs 2 and 3), reduced density of the capillary network in the peripheral retina and retinal vessels penetrating the photoreceptor layer of the adult mouse (Fig. 3). These ingrown vessels severely disturbed the architecture of the inner and outer nuclear layer and were accompanied by increased numbers of activated microglia, which may migrate along these vessels towards the outer retina (Fig. 3B). Since *Vhl* is also inactivated in iris tissue, iris vasculature was also heavily affected and almost absent in adult knockdown mice (Fig. 2A). Similar to the hyaloidal vessels in the vitreous, the pupillary membrane, which is the embryonic system for nutrient supply to the lens, also persisted. These data support results of a recent publication by Kurihara et al. (Kurihara et al.), which showed in the same *Vhl* knockdown mouse as used here that proper expression of VHL is required for the transition from fetal to adult vasculature in the eye.

Retinal degeneration

Here, we focused on the consequences of *Vhl* knockdown for the retina of the adult mouse. Our data indicate that the lack of VHL not only induced a strong vascular phenotype but also a progressive and severe degeneration of neuronal cells in all peripheral retinal cell layers (Fig. 4). This degeneration might be a direct consequence of the *Vhl* knockdown or, alternatively, might be secondary to the loss of normal retinal vasculature and to the resulting disturbed oxygenation of neuronal cells. In addition, the activation of inflammatory responses – like the microglia activation – might also contribute to the cell death. Since inactivation of VHL in adult rod-photoreceptors did not disturb development of retinal vasculature and only resulted in a late onset and very slow photoreceptor degeneration (Lange C, manuscript in

preparation), loss of VHL activity may not, or at least not strongly affect viability of photoreceptor cells directly. We therefore hypothesize that the disturbed vasculogenesis during development, in connection with the up-regulation of pro-apoptotic genes and genes connected to the extracellular matrix might be the main factors contributing to the very severe degeneration observed in $Vhl^{flox/flox}$; α-cre mice.

S-cones appeared to be especially affected by the degeneration as shown by the strongly reduced expression of *Opn1sw* and the very low abundance of S-cones in the ventral retina of 10-week-old knockdown mice. The morphological abnormalities were also reflected in the recordings of retinal function. Under all tested conditions, the magnitude of responses to light flashes under both scotopic and photopic conditions was severely reduced in the knockdowns (Fig. 5). Since the sensitivity was roughly regular, it suggests that the reduced retinal function was caused by a severe reduction in the number of cells rather than by a primary photoreceptor defect. However, the functional loss is larger than one would expect based on histological data showing that about 50% of photoreceptors are left (as judged from expression of photoreceptor markers and from retinal morphology). Therefore additional mechanisms might account for the severely reduced function in *Vhl* knockdown mice. Possible mechanisms include a reduction of tissue oxygenation due to the abnormal vasculature in the $vhl^{flox/flox}$;α-cre mice, which has been shown to reduce functionality of retinal cells (Braun and Linsenmeier, 1995). Additionally, it has been shown that increased levels of CNTF can negatively influence the ERG in wild type mice (Schlichtenbrede et al., 2003). Thus, the elevated expression of *Cntf* in *Vhl* knockdown mice (Fig. 7) may also contribute to the reduced retinal function.

Mechanisms of degeneration

Retinal stress imposed by the *Vhl* knockdown strongly activated a neuroprotective response in the retina. In the light-damaged retina as well as during inherited retinal degeneration, a subset of Muller glia cells expresses LIF, which controls an endogenous neuroprotective signaling system. This signaling pathway includes increased expression of *End2*, *Gfap* and p-STAT3, and culminates in the production of the growth and survival factor FGF2 in an attempt to protect cells from death (Samardzija et al., 2006a; Joly et al., 2008; Burgi et al., 2009). The development of an abnormal retinal vasculature and the induction of retinal degeneration strongly

induced the same protective system in the *Vhl* knockdown (Fig. 7). However, activation of this pathway was obviously not sufficient to protect retinal cells against execution of cell death and to maintain visual function. In several models of retinal degeneration, caspase-1 was the only caspase associated with the cell death (Doonan et al., 2003; Samardzija et al., 2006b). Here, we observed increased expression of *caspase-8* in addition to *caspase-1*. This suggests a role for the cell surface death receptor pathway in the degenerative process, a hypothesis supported by the increased expression of *Tnf* in the retina of *Vhl* knockdown mice (Fig. 8A). It has already been shown that TNF, produced by glial cells, can be a mediator of cell death in glaucoma through activation of the initiator caspase-8 or through direct neurotoxicity for retinal cells (Tezel, 2008). And an increase in HIF1 transcriptional activity can enhance caspase-8 mediated apoptosis in thymocytes (Biju et al., 2004). Thus, caspase-8 might be a relevant factor in the degenerating retina of the *Vhl* knockdown mouse. Pathways of caspase-mediated apoptosis may converge at the level of the effector caspase-3. In the retina, however, it is still controversially discussed whether caspase-3 is involved in photoreceptor death (Jomary et al., 2001; Doonan et al., 2003). Although gene expression of *caspase-3* was not, or not strongly different between knockdown and control retinas, we detected increased protein expression of pro-caspase-3 in 28-day-old $vhl^{flox/flox}$;α-cre mice (Fig. 8B) supporting a potential role of caspase-3 in the degeneration observed here. In contrast to the other caspases analyzed, expression of capsase-3 was high early during postnatal development and reduced during maturation. Protein levels of caspase-3 were also high at 10 days of age and almost not detectable at 28 days of age in the wild type retina. This supports the hypothesis that caspase 3 is involved in programmed cell death during postnatal development of the mouse retina (Zeiss et al., 2004; O'Driscoll et al., 2006).

In addition to caspase-1 and caspase-8, several other genes known to be regulated by VHL and related to cell death were induced in the knockdown retinas. Very strong induction of expression was observed for example for *Phd3* (*Egln3*) (Fig. 1). PHD3 has been connected to apoptosis in neuronal cells (Lee et al., 2005) and tumors (Tennant and Gottlieb, ; Schlisio et al., 2008). The transcription factor KLF10 was recently shown to be repressed by wild type VHL protein (Ivanov et al., 2008). Therefore, increased expression of *Klf10* in the *Vhl* knockdown retina was probably due to the absence of the VHL repressor protein. KLF10 was also reported to be a transactivator of the *Tgfbi* promotor. Increased KLF10 levels caused increased

expression of *Tgfbi*, a protein associated with the extracellular matrix. Elevated expression of *Tgfbi* can increase sensitivity of cells to various death inducing agents used in chemotherapy (Irigoyen et al., ; Ahmed et al., 2007). It was also shown that elevated levels of TGFBI altered the extracellular matrix facilitating extravasation of metastatic cancer cells (Ma et al., 2008) and that overexpression of a mutant form of TGFBI in the retina caused photoreceptor apoptosis (Bustamante et al., 2008). VHL has been shown before to be involved in the regulation of a proper assembly of the extracellular fibronectin matrix by binding to FN1 (Ohh et al., 1998; Ohh and Kaelin, 1999). Together with increased *Tgfbi* levels, the upregulation of *Fn1* expression in *Vhl* knockdown retinas may point to a problem with extracellular matrix assembly in the absence of VHL. The presence of HIF independent VHL functions in connection to extracellular matrix has already been suggested before (Bishop et al., 2004). Inappropriate formation or destabilization of the extracellular matrix may also facilitate abnormal development of retinal vasculature with vessels penetrating the ONL reaching the photoreceptor segment layer as observed here.

Conclusions

In summary we have shown that downregulation of VHL during development of the retina leads to long-term stabilization of HIF transcription factors and to a strong vascular phenotype with embryonic structures persisting into adulthood. In human patients, mutations in the tumor suppressor gene *Vhl* results in the VHL syndrome, an autosomal dominant disease that manifests itself by hemangioblastomas in the cerebellum, spinal cord and the retina. Tumor development during the disease is thought to be mainly due to overactivation of HIF transcription factors and the subsequent upregulation of angiogenic and growth related genes. Inactivation of *Vhl* in the mouse retina ((Kurihara et al.) and this work) and zebrafish (van Rooijen et al.) led to a severe vascular phenotype and may serve as a model to study retinal consequences of VHL syndrome. In addition to the misregulation of vascular development, lack of VHL also caused severe degeneration of all cell types in the mouse retina. Increased levels of caspases as well as induced expression of genes encoding for proteins connected to the regulation of the integrity of the extracellular matrix point to a complex pattern of the molecular mechanisms involved in the degenerative processes. Although such a severe degenerative phenotype has not been reported for patients, the mouse model may be highly useful to investigate the

connection between a proper retinal vasculature and the physiology, function and survival of the neuronal retina.

Acknowledgements

The authors thank Coni Imsand and Hedwig Wariwoda for excellent technical assistance. This work was supported by the Swiss National Science Foundation (Grant 3100A0–117760), the Fritz Tobler Foundation and the H. Messerli Foundation. Deutsche Forschungsgemeinschaft (DFG, grants Se837/5-2, Se837/6-1, Se837/7-1), the German Ministry of Education and Research (BMBF, grant 0314106).

Figure legends

Fig. 1. Hypoxia-like response in *Vhl* knockdown retinas.

(A) PCR amplification of genomic DNA isolated from retinal tissue at indicated postnatal days to test Cre-mediated excision of floxed *Vhl* sequences. The un-excised allele (floxed) has a length of 460 bp in both $vhl^{flox/flox}$ and $vhl^{flox/flox}$;α-cre mice. The excised allele (excised) was identified as a 260 bp band in $vhl^{flox/flox}$;α-cre mice. (B) Semi-quantitative real time PCR of *Vhl*, *Hif1a*, *Hif2a* (*Epas1*), *Phd2* (*Egln1*), *Phd1* (*Egln2*) and *Phd3* (*Egln3*) in $vhl^{flox/flox}$ (squares) and $vhl^{flox/flox}$;α-cre (triangles) at postnatal days (d) as indicated. Given are mean values ± SD of 3 retinas amplified in duplicates. Values were normalized to *β-actin* and expressed relatively to the first time point (5d) in $vhl^{flox/flox}$ mice. (C) Western blot analysis of whole retinal extracts from 10 and 28 day old $vhl^{flox/flox}$;α-cre (CRE+) and $vhl^{flox/flox}$ (CRE-) mice. β-actin (ACTB) served as a control for equal loading. *: $p<0.05$, **: $p<0.01$, ***: $p<0.001$, ****:$p<0.0001$. Significance between $vhl^{flox/flox}$ and $vhl^{flox/flox}$;α-cre mice was calculated for individual timepoints by an unpaired t test.

Fig. 2. Abnormal ocular vasculature in $vhl^{flox/flox}$;α-cre mice

(A) *In vivo* cSLO imaging of 10–week-old $vhl^{flox/flox}$ and $vhl^{flox/flox}$;α-cre mice with ICG (795 nm) and FA (488 nm) angiography to ocular vessels as indicated. Adjustment of the optical plane allowed the visualization of remnant hyaloidal vessels (second from right) and of the abnormal vasculature in the iris (right) in $vhl^{flox/flox}$;α-cre mice. White arrow: persistent pupillary membrane. (B) Cross-sectional imaging of $vlh^{flox/flox}$ (left) and $vhl^{flox/flox}$;α-cre (right) mice using SD-OCT. *: optic nerve head; black arrow: persistent hyaloidal vessels emerging from optic nerve head.

Fig. 3. Abnormal retinal vasculature in $vhl^{flox/flox}$;α-cre mice

(A) Retinal flat mounts of 35-day-old $vhl^{flox/flox}$ (top) and $vhl^{flox/flox}$;α-cre (bottom) mice stained with isolectin-A4 to visualize blood vessels. Shown are overviews over the whole retinal flatmount and enlarged representative areas (square). Arrows: retinal vessel growth at the retinal periphery. (B) Retinal cross sections of 35-day-old $vhl^{flox/flox}$ (top) and $vhl^{flox/flox}$;α-cre (bottom) mice stained for vessels using isolectin-A4 (green) and microglia using anti-IBA1 antibodies (red). DAPI (blue) stained nuclei

and nomarski images (gray) are shown for orientation. Shown are representative areas of the peripheral inferior retina. Arrow: abnormal vessel growth into the ONL. Arrowheads: microglia located along ingrown vessels and in the photoreceptor segment layer. (C) Semi-quantitative real time PCR for expression of *Vegfa*, *Epo, Pedf* (*Serpinf1*), *Tie1*, *Tie2* (*Tek*) and *Fzd4* in $vhl^{flox/flox}$ (squares) and $vhl^{flox/flox}$;α-cre (triangles) mice at postnatal days (d) as indicated. Given are mean values ± SD of 3 retinas amplified in duplicates. Values were normalized to *β-actin* and expressed relatively to the first time point (5d) in $vhl^{flox/flox}$ mice. RPE: retinal pigment epithelium. OS: photoreceptor outer segments. IS: photoreceptor inner segments. ONL: outer nuclear layer. IPL: inner plexiform layer. INL: inner nuclear layer. GCL: ganglion cell layer. *: $p<0.05$, **: $p<0.01$, ***: $p<0.001$, ****:$p<0.0001$. Significance between $vhl^{flox/flox}$ and $vhl^{flox/flox}$;α-cre mice was calculated for individual timepoints by an unpaired t test.

Fig. 4. Retinal degeneration in $vhl^{flox/flox}$;α-cre mice

Retinal morphology of 2-week-old (A, B), and 10-week-old (C, D) $vhl^{flox/flox}$ and $vhl^{flox/flox}$;α-cre mice as indicated. (A, C): overviews over the whole retinal morphology. (B, D): higher magnification pictures of the central and peripheral retina (as indicated). RPE: retinal pigment epithelium. IS: photoreceptor inner segments. OS: photoreceptor outer segments. ONL: outer nuclear layer. IPL: inner plexiform layer. INL: inner nuclear layer. GCL: ganglion cell layer.

Fig. 5 Rod and cone degeneration in $vhl^{flox/flox}$;α-cre mice

(A) Immunoflourescence stainings detecting rod opsin (left, red) and S-cone opsin (right, red) in cross sections of 10-week old $vhl^{flox/flox}$ and $vhl^{flox/flox}$;α-cre mice. DAPI (blue) stained nuclei and nomarski images (gray) are shown for orientation. Shown are representative areas of the peripheral inferior retina. *: unspecific staining in the choroid. (B) Semi-quantitative real time PCR for expression of s-cone opsin (*Opn1sw),* m-cone opsin (*Opn1mw*)*,* rod opsin (*rho*)*,* rod transducin (*Gnat1*) and cone transducin (*Gnat2*) in $vhl^{flox/flox}$ (squares) and $vhl^{flox/flox}$;α-cre (triangles) mice at postnatal days (d) as indicated. Given are mean values ± SD of 3 retinas amplified in duplicates. Values were normalized to *β-actin* and expressed relatively to the first time point (5d) in $vhl^{flox/flox}$ mice. RPE: retinal pigment epithelium. IS: photoreceptor

inner segments. OS: photoreceptor outer segments. ONL: outer nuclear layer. IPL: inner plexiform layer. INL: inner nuclear layer. GCL: ganglion cell layer. *: $p<0.05$, **: $p<0.01$, ***: $p<0.001$, ****:$p<0.0001$. Significance between *vhl*$^{flox/flox}$ and *vhl*$^{flox/flox}$;α-cre mice was calculated for individual timepoints by an unpaired t test.

Fig. 6. Reduced retinal function in *vhl*$^{flox/flox}$;α-cre mice

Representative scotopic (A, dark-adapted) and photopic (B, light-adapted) single flash ERGs with increasing light intensities were recorded from *vhl*$^{flox/flox}$ control and *vhl*$^{flox/flox}$;α-cre mice as indicated. Vertical line crossing each trace shows the timing of the light flash. (C) Scotopic and (D) photopic b-wave amplitudes from control (black, n=4) and *vhl*$^{flox/flox}$;α-cre mice (red, n=3) as a function of the logarithm of the flash intensity. Boxes indicate the 25% and 75% quantile range, whiskers indicate the 5% and 95% quantiles, and the asterisks indicate the median of the data.

Fig. 7. Activation of LIF response pathway in *vhl*$^{flox/flox}$;α-cre mice

(A) Semi-quantitative real time PCR for expression of *Lif*, *Gfap*, *Edn2*, *Fgf2* and *Cntf* in *vhl*$^{flox/flox}$ (squares) and *vhl*$^{flox/flox}$;α-cre (triangles) mice at postnatal days (d) as indicated. Given are mean values ± SD of 3 retinas amplified in duplicates. Values were normalized to *β-actin* and expressed relatively to the first time point (5d) in *vhl*$^{flox/flox}$ mice. (B) Western blot analysis of whole retinal extracts from 10 and 28 day old *vhl*$^{flox/flox}$;α-cre (CRE+) and *vhl*$^{flox/flox}$ (CRE-) mice. Shown are protein levels of GFAP, p-STAT3, STAT3, and ACTB as a control for equal loading. *: $p<0.05$, **: $p<0.01$, ***: $p<0.001$, ****:$p<0.0001$. Significance between *vhl*$^{flox/flox}$ and *vhl*$^{flox/flox}$;α-cre mice was calculated for individual timepoints by an unpaired t test.

Fig. 8. Activation of apoptosis pathways and pro-caspases in *vhl*$^{flox/flox}$;α-cre mice

(A) Semi-quantitative real time PCR for expression of *Klf10*, *Tgfbi*, *Fn1*, *Tnf, Casp1, Casp3, Casp8 and Casp9* in *vhl*$^{flox/flox}$ (squares) and *vhl*$^{flox/flox}$;α-cre (triangles) mice at postnatal days (d) as indicated. Given are mean values ± SD of 3 retinas amplified in duplicates. Values were normalized to *β-actin* and expressed relatively to the first time point (5d) in *vhl*$^{flox/flox}$ mice. (B) Western blot analysis of whole retinal extracts from 10 and 28 day old *vhl*$^{flox/flox}$;α-cre (CRE+) and *vhl*$^{flox/flox}$ (CRE-) mice. Shown are protein levels of CASP1, CASP3, CASP8, CASP9 and ACTB as a control for equal

loading. *: p<0.05, **: p<0.01, ***: p<0.001, ****:p<0.0001. Significance between *vhl*$^{flox/flox}$ and *vhl*$^{flox/flox}$;α-cre mice was calculated for individual timepoints by an unpaired t test.

References

Ahmed AA, Mills AD, Ibrahim AE, Temple J, Blenkiron C, Vias M, Massie CE, Iyer NG, McGeoch A, Crawford R, Nicke B, Downward J, Swanton C, Bell SD, Earl HM, Laskey RA, Caldas C, Brenton JD (2007) The extracellular matrix protein TGFBI induces microtubule stabilization and sensitizes ovarian cancers to paclitaxel. Cancer Cell 12:514-527.

Applebury ML, Antoch MP, Baxter LC, Chun LL, Falk JD, Farhangfar F, Kage K, Krzystolik MG, Lyass LA, Robbins JT (2000) The murine cone photoreceptor: a single cone type expresses both S and M opsins with retinal spatial patterning. Neuron 27:513-523.

Barnstable CJ, Tombran-Tink J (2004) Neuroprotective and antiangiogenic actions of PEDF in the eye: molecular targets and therapeutic potential. Prog Retin Eye Res 23:561-577.

Biju MP, Neumann AK, Bensinger SJ, Johnson RS, Turka LA, Haase VH (2004) Vhlh gene deletion induces Hif-1-mediated cell death in thymocytes. Mol Cell Biol 24:9038-9047.

Bishop T, Lau KW, Epstein AC, Kim SK, Jiang M, O'Rourke D, Pugh CW, Gleadle JM, Taylor MS, Hodgkin J, Ratcliffe PJ (2004) Genetic analysis of pathways regulated by the von Hippel-Lindau tumor suppressor in Caenorhabditis elegans. PLoS Biol 2:e289.

Braun RD, Linsenmeier RA (1995) Retinal oxygen tension and the electroretinogram during arterial occlusion in the cat. Invest Ophthalmol Vis Sci 36:523-541.

Budihardjo I, Oliver H, Lutter M, Luo X, Wang X (1999) Biochemical pathways of caspase activation during apoptosis. Annu Rev Cell Dev Biol 15:269-290.

Burgi S, Samardzija M, Grimm C (2009) Endogenous leukemia inhibitory factor protects photoreceptor cells against light-induced degeneration. Mol Vis 15:1631-1637.

Bustamante M, Tasinato A, Maurer F, Elkochairi I, Lepore MG, Arsenijevic Y, Pedrazzini T, Munier FL, Schorderet DF (2008) Overexpression of a mutant

form of TGFBI/BIGH3 induces retinal degeneration in transgenic mice. Mol Vis 14:1129-1137.

Chollangi S, Wang J, Martin A, Quinn J, Ash JD (2009) Preconditioning-induced protection from oxidative injury is mediated by leukemia inhibitory factor receptor (LIFR) and its ligands in the retina. Neurobiol Dis 34:535-544.

Doonan F, Donovan M, Cotter TG (2003) Caspase-independent photoreceptor apoptosis in mouse models of retinal degeneration. J Neurosci 23:5723-5731.

Fischer MD, Huber G, Beck SC, Tanimoto N, Muehlfriedel R, Fahl E, Grimm C, Wenzel A, Reme CE, van de Pavert SA, Wijnholds J, Pacal M, Bremner R, Seeliger MW (2009) Noninvasive, in vivo assessment of mouse retinal structure using optical coherence tomography. PLoS One 4:e7507.

Fruttiger M (2002) Development of the mouse retinal vasculature: angiogenesis versus vasculogenesis. Invest Ophthalmol Vis Sci 43:522-527.

Grimm C, Wenzel A, Acar N, Keller S, Seeliger M, Gassmann M (2006) Hypoxic preconditioning and erythropoietin protect retinal neurons from degeneration. Adv Exp Med Biol 588:119-131.

Grimm C, Hermann DM, Bogdanova A, Hotop S, Kilic U, Wenzel A, Kilic E, Gassmann M (2005) Neuroprotection by hypoxic preconditioning: HIF-1 and erythropoietin protect from retinal degeneration. Semin Cell Dev Biol 16:531-538.

Grimm C, Wenzel A, Groszer M, Mayser H, Seeliger M, Samardzija M, Bauer C, Gassmann M, Reme CE (2002) HIF-1-induced erythropoietin in the hypoxic retina protects against light-induced retinal degeneration. Nat Med 8:718-724.

Guicciardi ME, Gores GJ (2009) Life and death by death receptors. Faseb J 23:1625-1637.

Haase VH, Glickman JN, Socolovsky M, Jaenisch R (2001) Vascular tumors in livers with targeted inactivation of the von Hippel-Lindau tumor suppressor. Proc Natl Acad Sci U S A 98:1583-1588.

Huang LE, Gu J, Schau M, Bunn HF (1998) Regulation of hypoxia-inducible factor 1alpha is mediated by an O2-dependent degradation domain via the ubiquitin-proteasome pathway. Proc Natl Acad Sci U S A 95:7987-7992.

Huber G, Beck SC, Grimm C, Sahaboglu-Tekgoz A, Paquet-Durand F, Wenzel A, Humphries P, Redmond TM, Seeliger MW, Fischer MD (2009) Spectral

domain optical coherence tomography in mouse models of retinal degeneration. Invest Ophthalmol Vis Sci 50:5888-5895.

Irigoyen M, Pajares MJ, Agorreta J, Ponz-Sarvise M, Salvo E, Lozano MD, Pio R, Gil-Bazo I, Rouzaut A TGFBI expression is associated with a better response to chemotherapy in NSCLC. Mol Cancer 9:130.

Ito M, Yoshioka M (1999) Regression of the hyaloid vessels and pupillary membrane of the mouse. Anat Embryol (Berl) 200:403-411.

Ivan M, Kondo K, Yang H, Kim W, Valiando J, Ohh M, Salic A, Asara JM, Lane WS, Kaelin WG, Jr. (2001) HIFalpha targeted for VHL-mediated destruction by proline hydroxylation: implications for O2 sensing. Science 292:464-468.

Ivanov SV, Ivanova AV, Salnikow K, Timofeeva O, Subramaniam M, Lerman MI (2008) Two novel VHL targets, TGFBI (BIGH3) and its transactivator KLF10, are up-regulated in renal clear cell carcinoma and other tumors. Biochem Biophys Res Commun 370:536-540.

Iwai K, Yamanaka K, Kamura T, Minato N, Conaway RC, Conaway JW, Klausner RD, Pause A (1999) Identification of the von Hippel-lindau tumor-suppressor protein as part of an active E3 ubiquitin ligase complex. Proc Natl Acad Sci U S A 96:12436-12441.

Joly S, Lange C, Thiersch M, Samardzija M, Grimm C (2008) Leukemia inhibitory factor extends the lifespan of injured photoreceptors in vivo. J Neurosci 28:13765-13774.

Jomary C, Neal MJ, Jones SE (2001) Characterization of cell death pathways in murine retinal neurodegeneration implicates cytochrome c release, caspase activation, and bid cleavage. Mol Cell Neurosci 18:335-346.

Kamura T, Koepp DM, Conrad MN, Skowyra D, Moreland RJ, Iliopoulos O, Lane WS, Kaelin WG, Jr., Elledge SJ, Conaway RC, Harper JW, Conaway JW (1999) Rbx1, a component of the VHL tumor suppressor complex and SCF ubiquitin ligase. Science 284:657-661.

Kibel A, Iliopoulos O, DeCaprio JA, Kaelin WG, Jr. (1995) Binding of the von Hippel-Lindau tumor suppressor protein to Elongin B and C. Science 269:1444-1446.

Kurihara T, Kubota Y, Ozawa Y, Takubo K, Noda K, Simon MC, Johnson RS, Suematsu M, Tsubota K, Ishida S, Goda N, Suda T, Okano H von Hippel-

Lindau protein regulates transition from the fetal to the adult circulatory system in retina. Development 137:1563-1571.

Lee S, Nakamura E, Yang H, Wei W, Linggi MS, Sajan MP, Farese RV, Freeman RS, Carter BD, Kaelin WG, Jr., Schlisio S (2005) Neuronal apoptosis linked to EglN3 prolyl hydroxylase and familial pheochromocytoma genes: developmental culling and cancer. Cancer Cell 8:155-167.

Ma C, Rong Y, Radiloff DR, Datto MB, Centeno B, Bao S, Cheng AW, Lin F, Jiang S, Yeatman TJ, Wang XF (2008) Extracellular matrix protein betaig-h3/TGFBI promotes metastasis of colon cancer by enhancing cell extravasation. Genes Dev 22:308-321.

Marquardt T, Ashery-Padan R, Andrejewski N, Scardigli R, Guillemot F, Gruss P (2001) Pax6 is required for the multipotent state of retinal progenitor cells. Cell 105:43-55.

O'Driscoll C, Donovan M, Cotter TG (2006) Analysis of apoptotic and survival mediators in the early post-natal and mature retina. Exp Eye Res 83:1482-1492.

Ohh M, Kaelin WG, Jr. (1999) The von Hippel-Lindau tumour suppressor protein: new perspectives. Mol Med Today 5:257-263.

Ohh M, Yauch RL, Lonergan KM, Whaley JM, Stemmer-Rachamimov AO, Louis DN, Gavin BJ, Kley N, Kaelin WG, Jr., Iliopoulos O (1998) The von Hippel-Lindau tumor suppressor protein is required for proper assembly of an extracellular fibronectin matrix. Mol Cell 1:959-968.

Peruzzi B, Athauda G, Bottaro DP (2006) The von Hippel-Lindau tumor suppressor gene product represses oncogenic beta-catenin signaling in renal carcinoma cells. Proc Natl Acad Sci U S A 103:14531-14536.

Samardzija M, Wenzel A, Aufenberg S, Thiersch M, Reme C, Grimm C (2006a) Differential role of Jak-STAT signaling in retinal degenerations. Faseb J 20:2411-2413.

Samardzija M, Wenzel A, Thiersch M, Frigg R, Reme C, Grimm C (2006b) Caspase-1 ablation protects photoreceptors in a model of autosomal dominant retinitis pigmentosa. Invest Ophthalmol Vis Sci 47:5181-5190.

Schlichtenbrede FC, MacNeil A, Bainbridge JW, Tschernutter M, Thrasher AJ, Smith AJ, Ali RR (2003) Intraocular gene delivery of ciliary neurotrophic factor

results in significant loss of retinal function in normal mice and in the Prph2Rd2/Rd2 model of retinal degeneration. Gene Ther 10:523-527.

Schlisio S, Kenchappa RS, Vredeveld LC, George RE, Stewart R, Greulich H, Shahriari K, Nguyen NV, Pigny P, Dahia PL, Pomeroy SL, Maris JM, Look AT, Meyerson M, Peeper DS, Carter BD, Kaelin WG, Jr. (2008) The kinesin KIF1Bbeta acts downstream from EglN3 to induce apoptosis and is a potential 1p36 tumor suppressor. Genes Dev 22:884-893.

Seeliger MW, Grimm C, Stahlberg F, Friedburg C, Jaissle G, Zrenner E, Guo H, Reme CE, Humphries P, Hofmann F, Biel M, Fariss RN, Redmond TM, Wenzel A (2001) New views on RPE65 deficiency: the rod system is the source of vision in a mouse model of Leber congenital amaurosis. Nat Genet 29:70-74.

Seeliger MW, Beck SC, Pereyra-Munoz N, Dangel S, Tsai JY, Luhmann UF, van de Pavert SA, Wijnholds J, Samardzija M, Wenzel A, Zrenner E, Narfstrom K, Fahl E, Tanimoto N, Acar N, Tonagel F (2005) In vivo confocal imaging of the retina in animal models using scanning laser ophthalmoscopy. Vision Res 45:3512-3519.

Senger DR, Galli SJ, Dvorak AM, Perruzzi CA, Harvey VS, Dvorak HF (1983) Tumor cells secrete a vascular permeability factor that promotes accumulation of ascites fluid. Science 219:983-985.

Tanimoto N, Muehlfriedel RL, Fischer MD, Fahl E, Humphries P, Biel M, Seeliger MW (2009) Vision tests in the mouse: Functional phenotyping with electroretinography. Front Biosci 14:2730-2737.

Tennant DA, Gottlieb E HIF prolyl hydroxylase-3 mediates alpha-ketoglutarate-induced apoptosis and tumor suppression. J Mol Med.

Tezel G (2008) TNF-alpha signaling in glaucomatous neurodegeneration. Prog Brain Res 173:409-421.

Thiersch M, Lange C, Joly S, Heynen S, Le YZ, Samardzija M, Grimm C (2009) Retinal neuroprotection by hypoxic preconditioning is independent of hypoxia-inducible factor-1 alpha expression in photoreceptors. Eur J Neurosci 29:2291-2302.

Ueki Y, Wang J, Chollangi S, Ash JD (2008) STAT3 activation in photoreceptors by leukemia inhibitory factor is associated with protection from light damage. J Neurochem 105:784-796.

van Rooijen E, Voest EE, Logister I, Bussmann J, Korving J, van Eeden FJ, Giles RH, Schulte-Merker S von Hippel-Lindau tumor suppressor mutants faithfully model pathological hypoxia-driven angiogenesis and vascular retinopathies in zebrafish. Dis Model Mech 3:343-353.

Zeiss CJ, Neal J, Johnson EA (2004) Caspase-3 in postnatal retinal development and degeneration. Invest Ophthalmol Vis Sci 45:964-970.

Figure 1

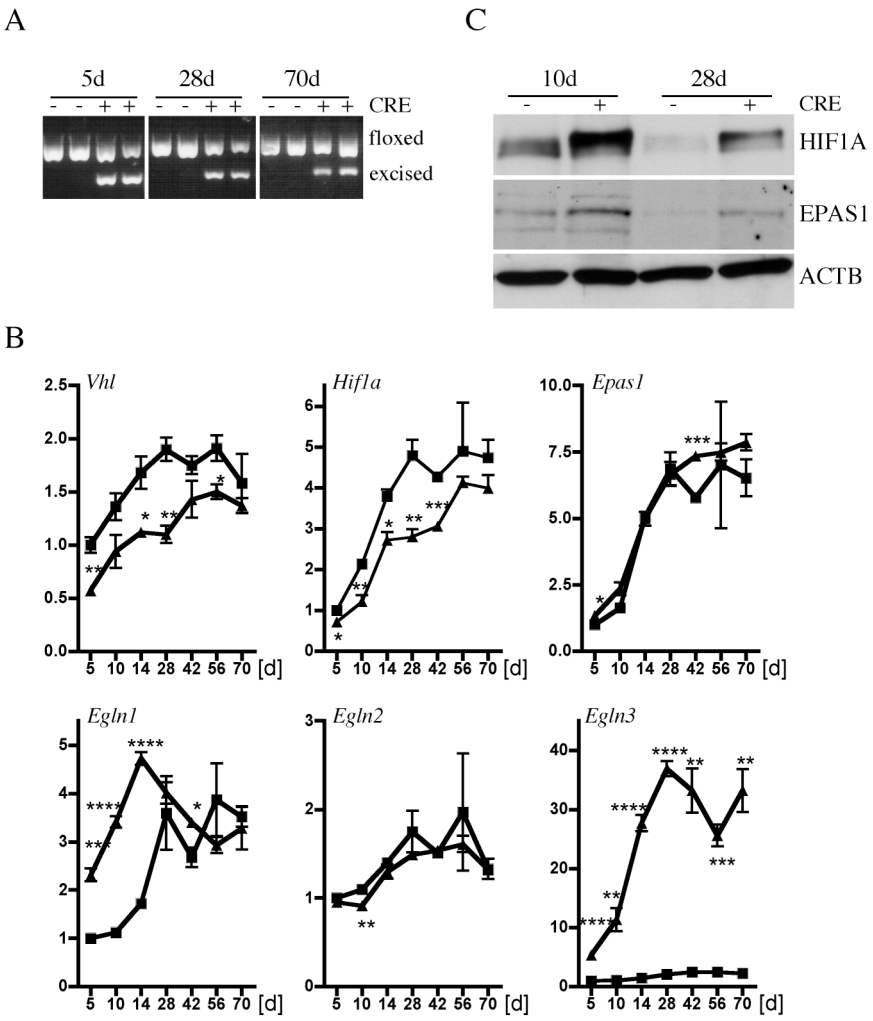
A
5d
28d
70d
- - + + - - + + - - + +
CRE
floxed
excised
C
10d
28d
- + - +
CRE
HIF1A
EPAS1
ACTB
B
Vhl
Hif1a
Epas1
Egln1
Egln2
Egln3
5 10 14 28 42 56 70 [d]

Figure 2

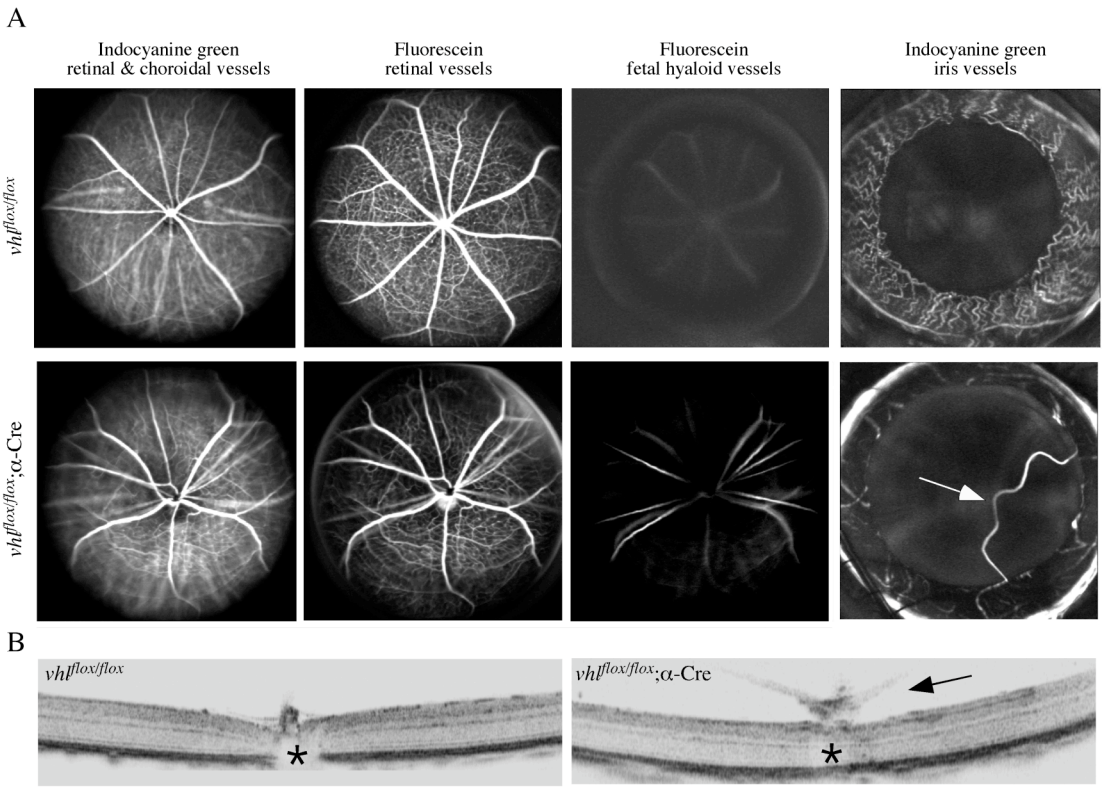
A
Indocyanine green
retinal & choroidal vessels
Fluorescein
retinal vessels
Fluorescein
fetal hyaloid vessels
Indocyanine green
iris vessels
vhl flox/flox
vhl flox/flox;α-Cre
B
vhl flox/flox
vhl flox/flox;α-Cre

Figure 3

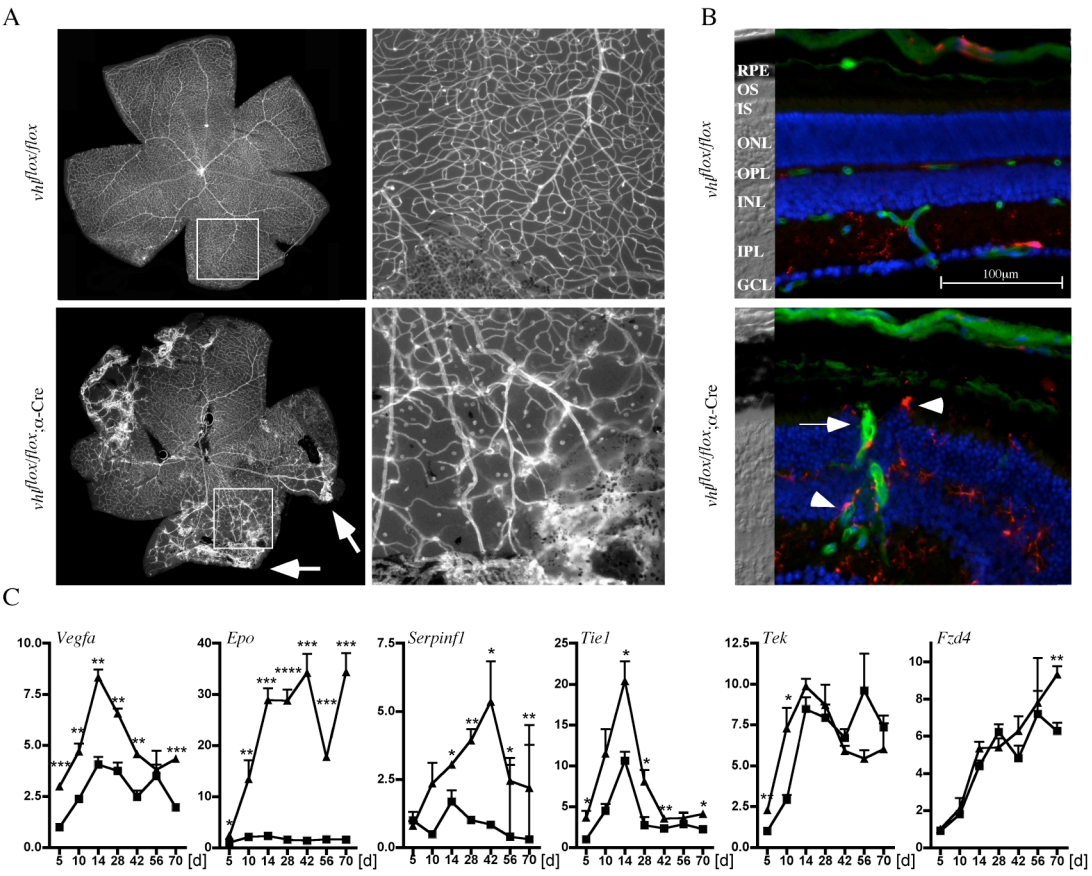
A
B
vhlflox/flox
vhlflox/flox,α-Cre
RPE
OS
IS
ONL
OPL
INL
IPL
GCL
100µm
C
Vegfa
Epo
Serpinf1
Tie1
Tek
Fzd4
[d]

Figure 4

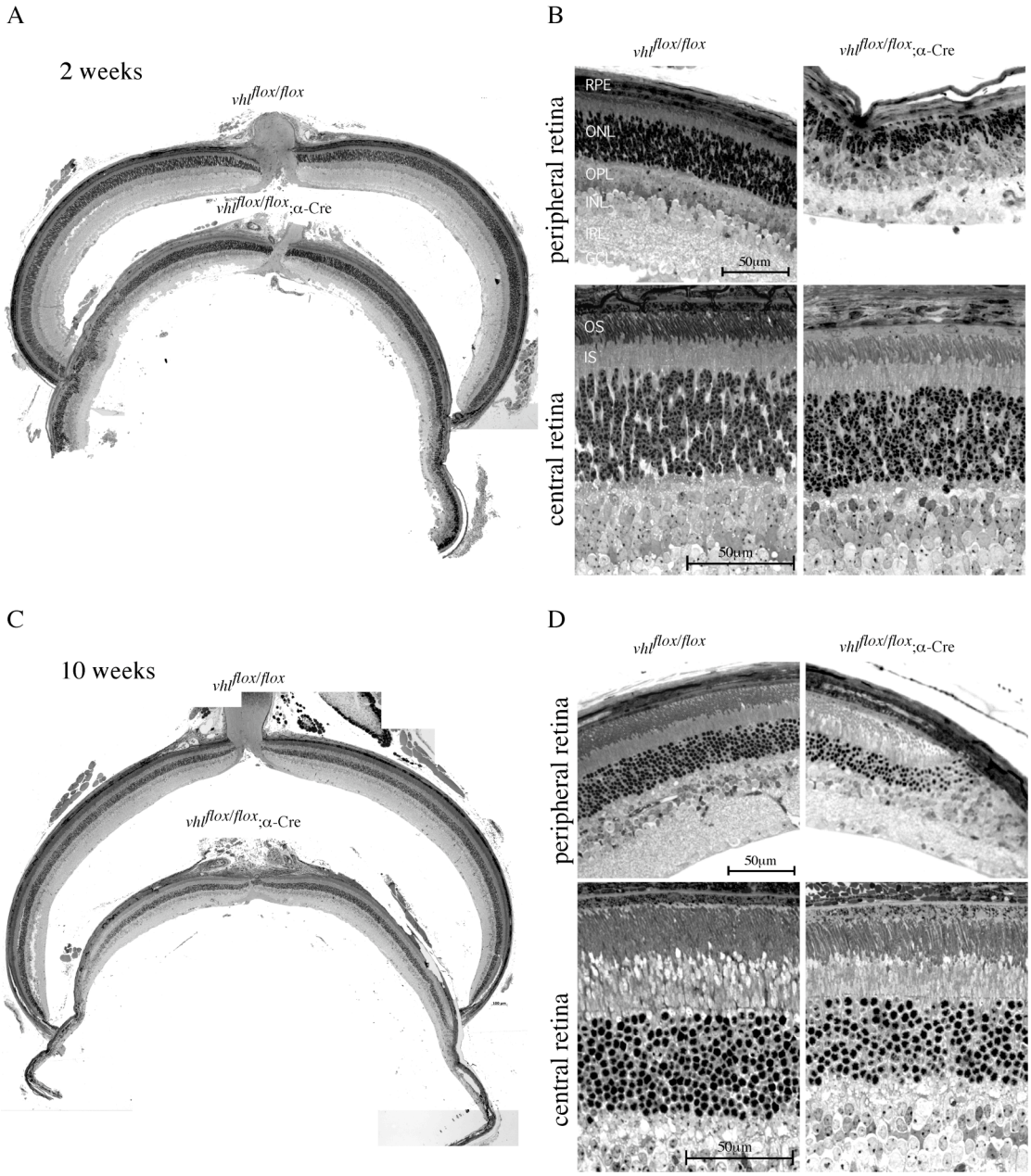
A
2 weeks
vhl flox/flox
vhl flox/flox;α-Cre
B
vhl flox/flox
vhl flox/flox;α-Cre
peripheral retina
central retina
RPE
ONL
OPL
INL
IPL
GCL
OS
IS
50µm
C
10 weeks
vhl flox/flox
vhl flox/flox;α-Cre
D
vhl flox/flox
vhl flox/flox;α-Cre
peripheral retina
central retina
50µm

Figure 5

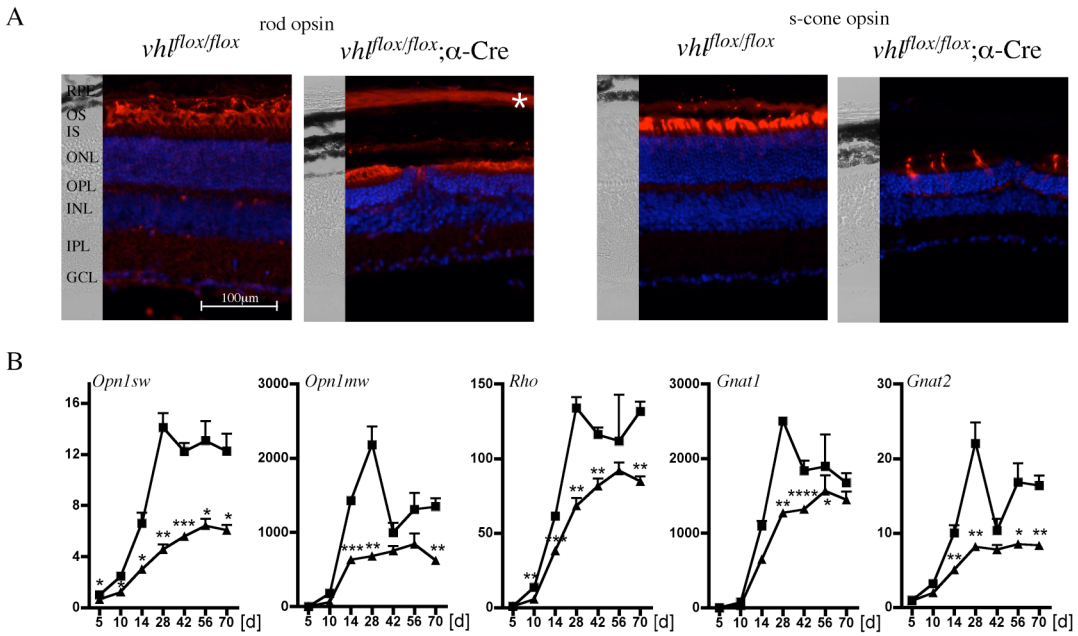
A
rod opsin
vhl flox/flox
vhl flox/flox;α-Cre
s-cone opsin
vhl flox/flox
vhl flox/flox;α-Cre
RPE
OS
IS
ONL
OPL
INL
IPL
GCL
100µm
*
B
Opn1sw
Opn1mw
Rho
Gnat1
Gnat2
[d]
5 10 14 28 42 56 70

Figure 6

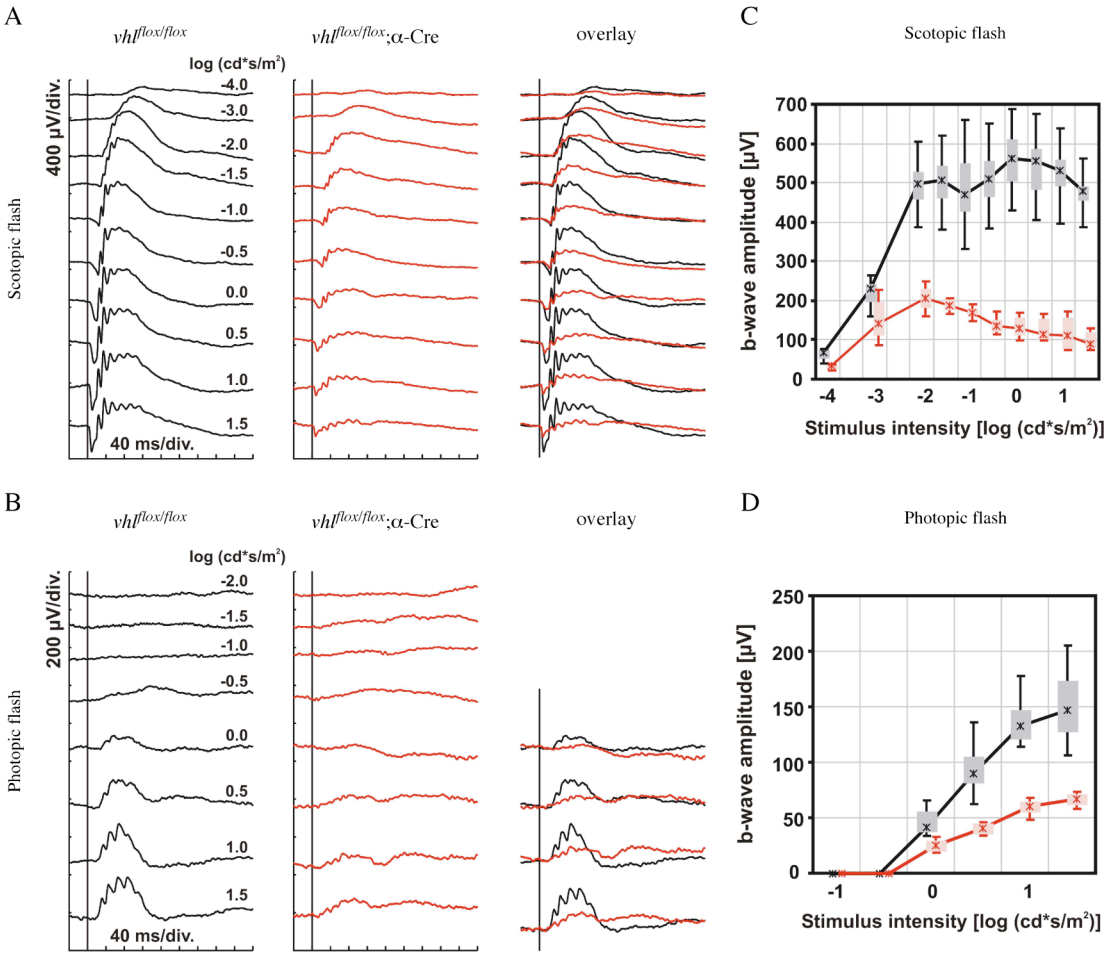
A
vhl flox/flox
vhl flox/flox;α-Cre
overlay
log (cd*s/m²)
-4.0
-3.0
-2.0
-1.5
-1.0
-0.5
0.0
0.5
1.0
1.5
400 µV/div.
40 ms/div.
Scotopic flash
B
vhl flox/flox
vhl flox/flox;α-Cre
overlay
log (cd*s/m²)
-2.0
-1.5
-1.0
-0.5
0.0
0.5
1.0
1.5
200 µV/div.
40 ms/div.
Photopic flash
C
Scotopic flash
b-wave amplitude [µV]
Stimulus intensity [log (cd*s/m²)]
D
Photopic flash
b-wave amplitude [µV]
Stimulus intensity [log (cd*s/m²)]

Figure 7

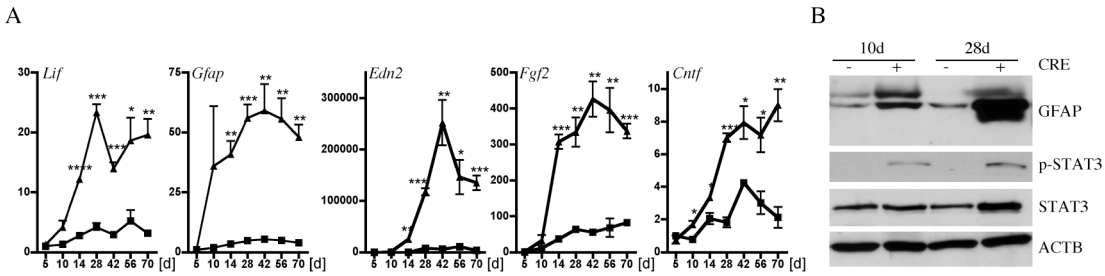
A
B
Lif
Gfap
Edn2
Fgf2
Cntf
5 10 14 28 42 56 70 [d]
10d
28d
- + - +
CRE
GFAP
p-STAT3
STAT3
ACTB

Figure 8

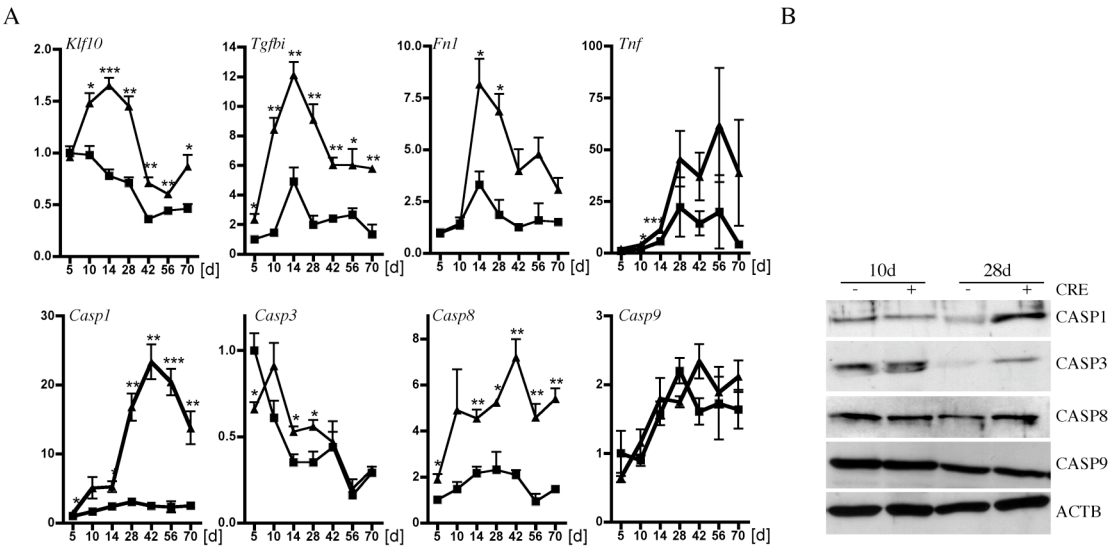
A
B
Klf10
Tgfbi
Fn1
Tnf
Casp1
Casp3
Casp8
Casp9
5 10 14 28 42 56 70 [d]
10d
28d
CRE
CASP1
CASP3
CASP8
CASP9
ACTB

Table 1. Primers used for real-time PCR

Gene	Upstream (5' – 3')	Downstream (5' – 3')	Annealing	Product
β-actin	cgacatggagaagatctggc	caacggctccggcatgtgc	62	153
Casp1	ggcaggaattctggagcttcaa	gtcagtcctggaaatgtgcc	60	138
Casp3	ctggaatgtcatctcgctct	actgtctgtctcaatgccac	60	353
Casp8	ccacacaagaagcaggagacca	agcaggctcaagtcatcttccag	68	329
Casp9	ccaatgggactcacagcaaagg	ttctcaatggacacggagcatc	62	554
Cntf	agccttgactcagtggatggtg	atcagcctctttttcagggacc	58	276
Edn2	agacctcctccgaaagctg	ctggctgtagctggcaaag	60	64
Egln1	cattgttggcagaaggtgtg	caaaggactacagggtctcca	62	70
Egln2	gaacccacatgaggtgaagc	aacacctttctgtcccgatg	60	124
Egln3	tgtctggtacttcgatgctga	gcaagagcagattcagtttttct	60	84
Epas1	ggagctcaaaaggtgtcagg	caggtaaggctcgaacgatg	60	61
Epo	gccctgctagccaattcc	gccctgctagccaattcc	60	128
Fgf2	ggctgctggcttctaagtgt	tccgtgaccggtaagtgttg	62	87
Fn1	accagtgccaagattcagag	cttggtgatgtgtgaaggct	60	245
Fzd4	ctacaacgtgaccaagatgc	gggaatttgctgcagttcag	57	277
Gfap	ccaccaaactggctgatgtctac	ttctctccaaatccacacgagc	62	240
Gnat1	gaggatgctgagaaggatgc	tgaatgttgagcgtggtcat	58	209
Gnat2	gcatcagtgctgaggacaaa	ctaggcactcttcgggtgag	58	192
Hif1α	tcatcaggttgccacttccccac	ccgtcatctgttagcaccatcac	60	198
Klf10	cgtctagtgtctcagtgctc	gacttccagtcgcagctcat	62	243
Lif	aatgccacctgtgccatacg	caacttggtcttctctgtcccg	60	216
Opn1mw	tgtacatggtcaacaatcgga	acaccatctccagaatgcaag	58	153
Opn1sw	ctctgctacctccaagtgtgg	aagtatagggccccagcaga	58	154
Rho	cttcacctggatcatggcgtt	ttcgttgttgacctcaggcttg	62	130
Tgfbi	tcctcatgcgactgctgacc	cgacttgccgcagatcttcc	64	224
Tie1	tccagacaaggtcacacacacg	tcgcacgatgagccgaaagaag	60	256
Tek	ccatcaccataggaagggactttg	taggaaggacgcttgttgacgcatc	60	215
Tnf	ccacgctcttctgtctactga	ggccatagaactgatgagagg	62	92
Serpinf1	tccacagcacctacaaggag	taagccacgccaaggagaag	62	280
Vegfa	acttgtgttgggaggaggatgtc	aatgggtttgtcgtgtttctgg	60	171
Vhl	gagggacccgttccaataat	ttggcaaaaataggctgtcc	60	364

3.2. Additional publications

3.2.1. Leukemia inhibitory factor extends the lifespan of injured photoreceptors *in vivo*

Sandrine Joly[1], Christina Lange[1], Markus Thiersch[1], Marijana Samardzija[1] and Christian Grimm[1,2]

[1]Lab for Retinal Cell Biology, Department Ophthalmology, University of Zurich
[2]Zurich Center for Integrative Human Physiology (ZIHP)

Author contribution:
Design: Sandrine Joly (SJ) and Christian Grimm (CG)
Experiment: SJ, **Christina Lange (CL)** (real time PCR), Markus Thiersch (MT), Marijana Samardzija (MS) and CG
Interpretation: SJ, **CL** (real time PCR data), MT, MS and CG
Manuscript: CG
Manuscript correction: SJ, **CL**, MT, MS and CG

Summary:
In this paper we show that during retinal degeneration in the VPP mouse *Lif* and monocyte chemoattractive protein (*Mcp1*) were induced strongly with a peak around post natal day 42. Whereas ablation of MCP1 did not influence degeneration in the VPP mouse, lack of LIF dramatically accelerated photoreceptor degeneration in this model. The retinas of *Lif* knockout mice (*Lif* $^{-/-}$) were normal in morphology and immunofluorescence stainings showed that all retinal cells are present and normal in *Lif* $^{-/-}$ mice. With *in situ* hybridization for *Lif* combined with a Müller cell specific marker (glutamine synthetase) we showed that the degenerating retina induces *Lif* expression in a subset of Müller cells. By Western blotting and real time PCR analyses we showed that in the degenerating retina of the VPP mouse a signaling cascade involving STAT3, glial fibrillary acid protein (*Gfap*), endothelin 2 (*Edn2*), fibroblast growth factor 2 (*Fgf2*), suppressor of cytokine signaling 3 (*Socs3*) and *Jak3*

is induced. This signaling cascade was absent in *Lif* $^{-/-}$;VPP double transgenic mice. To analyze whether this whole signaling cascade is evoked and controlled by LIF, we injected recombinant LIF (rLIF) intravitreally into the eyes of *Lif* $^{-/-}$ mice. Real time PCR analysis revealed that application of rLIF restored the whole signaling cascade and induced expression of *Edn2*, *Stat3*, *Gfap* and *Fgf2* in *Lif* $^{-/-}$ mice. We hypothesized that EDN receptor b (EDNRb) signaling might induce a positive feed forward loop resulting in an increase in *Lif* expression. This was supported by the strong induction of *Lif*, *Edn2* and *Fgf2* and the protection against light damage after intravitreal injection of a EDNRb agonist (BQ3020) in wild typ mice. In contrary, an EDNRb antagonist (BQ788) increased cell death in the VPP mouse. Furthermore, neither *Edn2* nor *Fgf2* were induced upon BQ3020 injection in *Lif* $^{-/-}$ mice confirming the LIF-dependent feed forward loop.

To analyze whether LIF signaling involves photoreceptors, we injected rLIF intravitreally to photoreceptor-devoid rd1 and to cone only *Nrl* $^{-/-}$ mice. Since LIF did not induce the upregulation of *Edn2*, *Gfap* and *Fgf2* in rd1 but in *Nrl* $^{-/-}$ mice, we concluded that LIF signaling needs the presence of rod and/or cone photoreceptors. Finally we proposed a mechanism in which LIF is induced by an unknown molecule in a subset of Muller glia cells. It then signals to photoreceptors and induces *Edn2*. EDN2 in turn signals back to Muller cells to induce the survival factor *Fgf2*, which acts on photoreceptors to protect them from damage.

Leukemia Inhibitory Factor Extends the Lifespan of Injured Photoreceptors *In Vivo*

Sandrine Joly, Christina Lange, Markus Thiersch, Marijana Samardzija, and Christian Grimm

Laboratory for Retinal Cell Biology, Department of Ophthalmology, Center for Integrative Human Physiology and Neuroscience Center Zurich, University of Zurich, 8091 Zurich, Switzerland

Survival and death of photoreceptors in degenerative diseases of the retina is controlled by a multitude of genes and endogenous factors. Some genes may be involved in the degenerative process itself whereas others may be part of an endogenous defense system. We show in two models of retinal degeneration that photoreceptor death strongly induces expression of leukemia inhibitory factor (LIF) in a subset of Muller glia cells in the inner nuclear layer of the retina. LIF expression is essential to induce an extensive intraretinal signaling system which includes Muller cells and photoreceptors and is characterized by an upregulation of Edn2, STAT3, FGF2 and GFAP. In the absence of LIF, Muller cells remain quiescent, the signaling system is not activated and retinal degeneration is strongly accelerated. Intravitreal application of recombinant LIF induces the full molecular pathway including the activation of Muller cells in wild-type and *Lif*$^{-/-}$ mice. Interruption of the signaling cascade by an Edn2 receptor antagonist increases whereas activation of the receptor decreases photoreceptor cell death. Thus, LIF is essential and sufficient to activate an extensive molecular defense response to photoreceptor injury. Our data establish LIF as a Muller cell derived neuronal survival factor which controls an intrinsic protective mechanism that includes Edn2 signaling to support photoreceptor cell survival and to preserve vision in the injured retina.

Key words: **leukemia inhibitory factor; Edn2; retina; photoreceptor degeneration; neuroprotection; endogenous rescue pathway**

Introduction

Human vision depends on the absorption of photons by rod and cone photoreceptors which convert the light information into a signal which is transported by connecting neurons to the brain. This highly specialized process requires sophisticated molecular interactions between a variety of intra- and intercellular retinal components. Thus, the retina has to maintain a high integrity of its cellular architecture and of the molecular machinery of visual cells. Mutations and/or exogenous stimuli disturb the retinal integrity and may lead to photoreceptor apoptosis and retinal degeneration (Remé et al., 1998). Cells of the retina can react to unfavorable (stress) conditions or to injury with the production of various cytokines and growth factors in an attempt to protect neurons and to preserve retinal function. This might best be seen in experimental paradigms of preconditioning in which a subtoxic stimulus induces the differential expression of specific genes. This increases the resistance of the tissue to a subsequent stronger stress and thus promotes cell survival (Kamphuis et al., 2007; Zhu et al., 2007; Thiersch et al., 2008). Ischemic or hypoxic exposure are classical preconditioning schemes but light exposure below damaging threshold has also been successfully applied (O'Driscoll et al., 2008) demonstrating the existence of several activatable survival pathways in the retina.

Exposure to high levels of white light induces photoreceptor degeneration (Remé et al., 1998) and activates a signaling cascade which includes leukemia inhibitory factor (LIF), Janus kinase 2 (Jak2), signal transducer and activator of transcription 1 (STAT1) and STAT3 (Samardzija et al., 2006a). A similar retinal response has been observed in models of inherited retinal degeneration (Samardzija et al., 2006a). Since recombinant LIF can protect photoreceptor cells against light-induced degeneration (Ueki et al., 2008), the increased expression of endogenous LIF in response to damaging light suggests that LIF might be part of a retinal defense mechanism to increase survival of visual cells. Such an endogenous protective response has recently been postulated by Rattner and Nathans. In their study, they propose that injured photoreceptors produce endothelin 2 (Edn2) which signals onto Muller cells. Activated Muller cells and/or other cells may then produce and release fibroblast growth factor 2 (FGF2) to support survival of viable photoreceptors (Rattner and Nathans, 2005).

Here we focused on the role of LIF in the degenerating retina of the VPP mouse, a model for autosomal dominant retinitis pigmentosa (Naash et al., 1993; Grimm et al., 2004). We show that lack of LIF prevents Edn2 expression, STAT3 phosphorylation, FGF2 production and activation of Muller glia cells and strongly accelerates retinal degeneration. This suggests that LIF is the key factor regulating an endogenous defense mechanism to ensure survival and function of retinal cells. Since LIF expression

Received Oct. 23, 2008; revised Oct. 31, 2008; accepted Nov. 1, 2008.

This work was supported by the Swiss National Science Foundation (Grant 3100A0-117760), a grant from the European Community (EVI-GenoRet; LSHG-CT-512036), the Fritz Tobler Foundation, the Vontobel Foundation, and the H. Messerli Foundation. We thank Coni Imsand, Hedwig Wariwoda, and Philipp Huber for excellent technical assistance and Muna Naash (VPP), Bettina Holtmann, and Michael Sendtner (*Lif*$^{-/-}$) for providing transgenic mouse lines.

Correspondence should be addressed to Christian Grimm, Laboratory for Retinal Cell Biology, Department of Ophthalmology, University of Zurich, Frauenklinikstrasse 24, 8091 Zurich, Switzerland. E-mail: cgrimm@opht.uzh.ch.

DOI:10.1523/JNEUROSCI.5114-08.2008

 0270-6474/08/2813765-10$15.00/0

Table 1. Primers used for genotyping and real-time PCR

Gene/allele	Forward	Reverse
Genotyping		
VPP	AGACTGACATGGGGAGGAATTCCCAGA	CAGCTGCTCGAAGTGACTCCGACC
Lif/wt	AAATGCCACCTGTGCCATACGC	CAACTTGGTCTTCTCTGTCCCG
Lif/KO	CTCTAAGCCTGAACTCTCTCATCC	GATTCGCAGCGCAGCGCATCGCCTT
Ccl-2/wt	GGAGCATCCACGTGTTGGC	ACAGCTTCTTTGGGACACC
Ccl-2/KO	CTTGGGTGGAGAGGCTATTC	AGGTGAGATGACAGGAGATC
Rd1	CATCCCACCTGAGCTCACAGAAAG	GCCTACAACAGAGGAGCTTCTAGC
Nrl/wt	GTGTTCCTTGGCTGGAAAGA	CTGTTCACTGTGGGCTTTCA
Nrl/KO	TGAATACAGGGACGACACCA	GTTCTAATTCCATCAGAAGCTGAC
Real-time PCR		
Edn1	TCCCGTGATCTTCTCTCTGC	AGTTCGGCTCCCAAGACAG
Edn2	AGACCTCCTCCGAAAGCTG	CTGGCTGTAGCTGGCAAAG
Ednrb	ACCTACAAGTTGCTCGCAGAGG	AAAACCTATGGCTTCGGGGAC
Smad1	TGGTTCCAAGCAGAAGGAGGTC	GCTCATTTTGTCCCAGGTTGC
Gfap	CCACCAAACTGGCTGATGTCTAC	TTCTCTCCAAATCCACACGAGC
Mcl1	GTGACTCTTATTTCTTTCGGTGCC	CATCCCAGCCTCTTTGTTTGAC
Casp-1	GGCAGGAATTCTGGAGCTTCAA	GTCAGTCCTGGAAATGTGCC
Fgf2	TGTGTCTATCAAGGGAGTGTGTGC	ACCAACTGGAGTATTTCCGTGACCG
Cntf	CTCTGTAGCCGCTCTATCTG	GGTACACCATCCACTGAGTC
Bdnf	CAAAGCCACAATGTTCCACCAG	GATGTCGTCGTCAGACCTCTCG
Gdnf	AGATGAAGTTATGGGATGTCGTGG	GGCATATTGGAGTCACTGGTCAG
Bcl-2	TTGTGGCCTTCTTTGAGTTCG	ATTTCTACTGCTTTAGTGAACC
Survivin	AACTACCGCATCGCCACCTTCAAG	AGCCAGGGGAGTGCTTTCTATG
Jak1	TGAGCTTTGATCGGATCCTT	GCAGGGTCCCAGAATAGATATG
Jak2	GAACCTACAGATACGGAGTGTCC	CAAAATCATGCCGCCACT
Jak3	CACAGTGCATGGCCTATGAT	AGGTGTGGGGTCTGAGAGG
Tyk2	CCTGTGTCACCTTGCTCTCA	GGAATGAGGGATGCAGTTCT
Socs3	GGAGACAGATGAGGCTGGTGA	GGACCTACTGACCGAGAGAT
Stat3	CAAAACCCTCAAGAGCCAAGG	TCACTCACAATGCTTCTCCGC
Lif-R	ACTGAAGTGGAACGACAGAGG	CTTTACCACTCAGCATTGTGTTG
Gnat1	GAGGATGCTGAGAAGGATGC	TGAATGTTGAGCGTGGTCAT
Lif	AATGCCACCTGTGCCATACG	CAACTTGGTCTTCTCTGTCCCG
Mcp-1	GGCTCAGCCAGATGCAGTTA	CTGCTGCTGGTGATCCTCTT

Primers for *Gnat1* were from Znoiko et al. (2005).

is specifically induced in a subset of Muller glia cells, Muller cells may coordinate the molecular response to injury and initiate an elaborate and LIF-dependent crosstalk between various retinal cells of the INL and ONL.

Materials and Methods

Mice, light exposure, intravitreal injections, and detection of cell death. Animals were treated in accordance with the regulations of the Veterinary Authority of Zurich and with the statement of "The Association for Research in Vision and Ophthalmology" for the use of animals in research. VPP mice [generous gift from Muna Naash (Naash et al., 1993)] were on a mixed SV129BL/6 background. *Lif*$^{-/-}$ mice (Escary et al., 1993) were kindly provided by Bettina Holtmann and Michael Sendtner (University of Wuerzburg, Germany). *Ccl-2*$^{-/-}$ (Jackson Laboratory), BALB/c mice (Harlan) and 129S6/SvEvTac (Taconic) were purchased from commercial suppliers. All mice except BALB/c and 129S6/SvEvTac (both *Rpe65*$_{450Leu}$) expressed the *Rpe65*$_{450Met}$ variant (Samardzija et al., 2006b). Double mutant mice were generated by classical breeding schemes. Primer pairs for genotyping are listed in Table 1. For rd1 genotyping, PCR products were digested with *Dde*I to detect presence or absence of the mutation as described earlier (Hafezi et al., 1998).

For light exposure, 8-week-old wild-type mice were dark-adapted overnight and their pupils were dilated with 1% Cyclogyl (Alcon) and 5% phenylephrine (Ciba Vision) 45 min before exposure to 5000 lux of white fluorescent light for 2 h. After exposure, mice were returned to darkness for 12 h.

Intravitreal injections were performed on anesthetized animals with a 34G needle mounted on a 10 μl Hamilton syringe. Injection site was just behind the limbus on the superior part of the eye. Intravitreal placement of the needle was observed through the pupil. One microliter of rLIF in PBS (10 ng/μl; Millipore), BQ-3020 in H_2O (1 μg/μl; American Peptide), BQ-788 in 10%DMSO in PBS (2 μg/μl; American Peptide) or of vehicle alone was injected within 5–10 s and the empty needle was kept in place for additional 30 s before it was slowly withdrawn. BQ-3020 injections were done in 129S6/SvEvTac mice ($n = 21$) 24 h before exposure to 2 h of 13,000 lux of white light. Analysis of cell death was 24 h after exposure. BQ-788 injections were done in VPP mice ($n = 9$) at PND 35 and analysis of cell death was 48 h thereafter. Cell death was analyzed by measuring free nucleosomes in each (total) retina individually using the cell death detection kit (Roche) according to the manufacturer's recommendations. Retinal cell death in compound injected eyes was expressed as fold-difference to cell death in the sham injected contralateral eyes of the same animal.

Microscopy and immunofluorescence. For light microscopy, eyes were fixed in 2.5% glutaraldehyde in 0.1 M cacodylate buffer, pH 7.3, at 4°C overnight. For each eye, the superior and the inferior retina were prepared, washed in cacodylate buffer, incubated in osmium tetroxide for 1 h, dehydrated, and embedded in Epon 812. Sections (0.5 μm) were prepared from the lower central retina and counterstained with methylene blue.

For immunofluorescence, mice were perfused with 4% paraformaldehyde in PBS. Eyes were removed and post fixed for 10 min in 4% paraformaldehyde. Cornea and lens were removed and eyecups were post-fixed in 4% paraformaldehyde for additional 15 min at room temperature. The tissue was then incubated in 10% sucrose (in PBS) for 10 min, 20% sucrose for 30 min and 30% sucrose overnight at 4°C. Eyecups were embedded in Tissue Tec OCT (Mioles), frozen in liquid nitrogen and stored at −70°C until further use. Twelve micrometer sections were cut, dried and washed in PBST (PBS + 1% Triton X-100) for 3 × 5 min at room temperature (RT). After blocking in PBS + 10% horse serum (HS) for 1 h at RT, sections were incubated with the respective primary antibodies anti-Calbindin (AB1778), anti Brn-3a (MAB1585), anti-CHX10 (AB9014), anti-glutamine synthetase (MAB302; all Millipore), anti-Iba-1 (#019-19741, Wako), anti-PKCβ (sc-209, Santa Cruz; kindly provided by S. Neuhauss, University of Zurich, Zurich, Switzerland), anti-Calretinin or anti-Disabled-3 (both kindly provided by E. Strettoi, Neuroscience Institute, Italian National Research Council, Pisa, Italy). Sections were washed 3 × 10 min in PBS and Cy3- or Cy2-conjugated secondary antibodies (Jackson ImmunoResearch) were applied in PBS + 10% HS (dilution 1:500) for 1–2 h at RT. Sections were washed 3 × 10 min in PBS, mounted and analyzed using a Zeiss fluorescent microscope.

In situ *hybridization.* For *in situ* hybridization, nonfixed tissue was frozen in Tissue Tec OCT (Mioles). Twelve micrometer sections were cut and air dried for 20 min at room temperature and 10 min at 50°C. Sections were post-fixed for 10 min at room temperature in 4% paraformaldehyde (in PBS) followed by 3 washing steps with PBS (5 min each). Samples were acetylated for 20 min at room temperature in 100 mM triethanolamine, 2.5 μl/ml acetic anhydride followed by 3 washing steps with PBS (5 min each). Prehybridization was done at room temperature for 2 h in 50% formamide, 5xSSC, 1xDenhardt's, 1 mg/ml yeast tRNA, 0.1% Tween 20, 0.1% CHAPS, 5 mM EDTA. Hybridization was done for 16 h at 65°C in 15 ml of the same solution including 7–15 μg of DIG-labeled sense or antisense RNA probe. Slides were washed 5 times in SSC with increasing stringency and blocked in 100 mM Tris, pH 7.5, 150 mM NaCl and 1% blocking reagent (Roche # 1096176) for 1 h at room temperature. Incubation with anti-DIG antibody (Roche) in blocking buffer was for 16 h at 4°C. Slides were washed twice in 100 mM Tris, 150 mM NaCl at room temperature for 20 min each, equilibrated for 5 min in 100 mM Tris, pH 9.5, 150 mM NaCl, 50 mM $MgCl_2$, 0.25 mg/ml levamisole (Sigma, L9756) and incubated in the same solution including 1 μl/ml NBT and 3.5 μl/ml BCIP for up to 16 h at room temperature. After color had developed, reaction was stopped in 10 mM Tris (pH 8.0)/1 mM EDTA, slides were mounted and analyzed.

Combined in situ *hybridization/immunofluorescence. In situ* hybridization was performed as described above on perfused (4% PFA) and cryopreserved tissue (see Microscopy and immunofluorescence) using RNase free reagents. After color development slides were washed 2 × in PBS for 5 min each. Slides were then postfixed in 4% PFA for 10 min at RT, washed 2 × in PBS (5 min each) and the primary antibodies were applied in 5% HINGS (heat inactivated goat serum) for 3 h at RT. Slides were

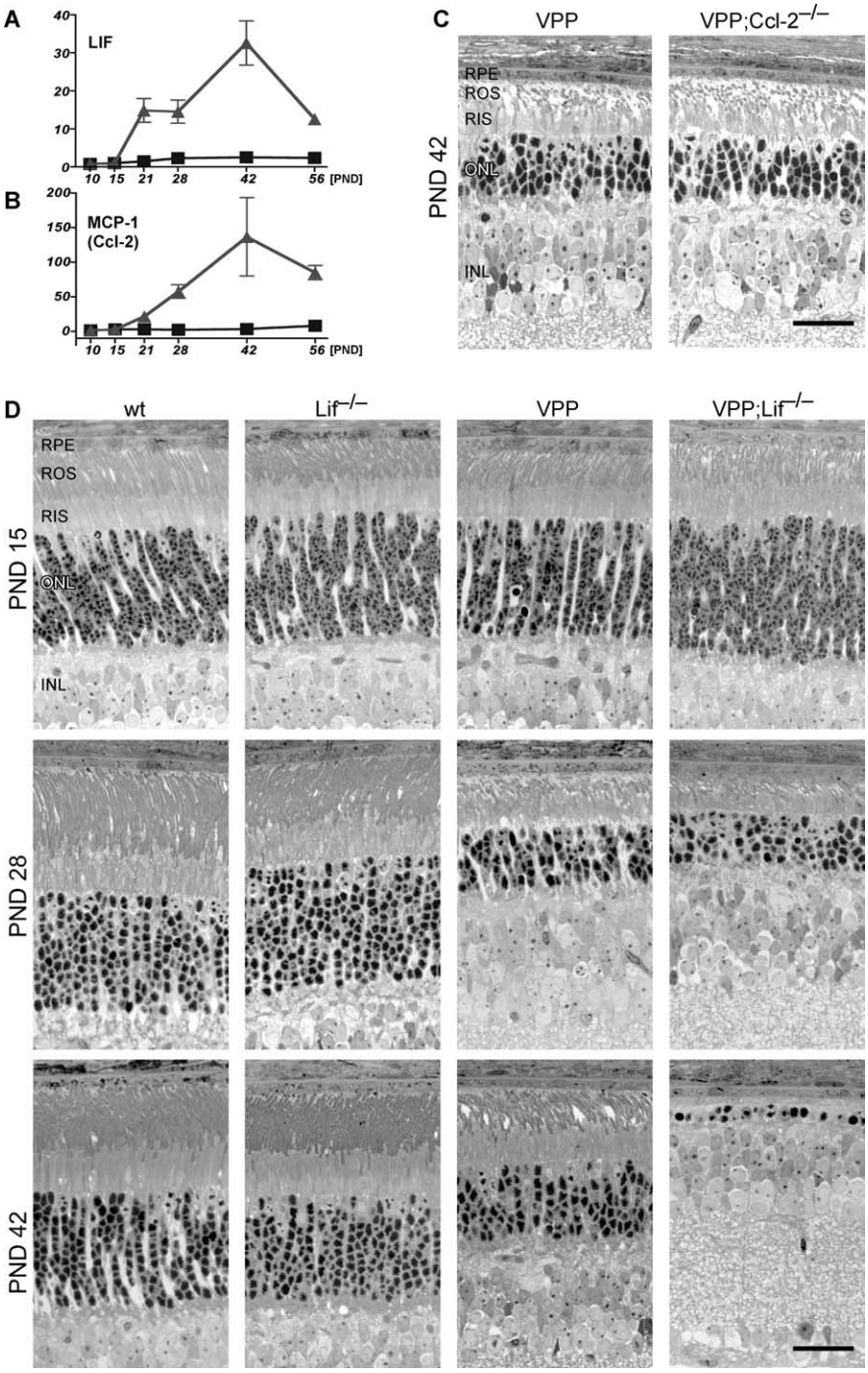

Figure 1. Lack of LIF accelerates photoreceptor degeneration in the VPP retina. ***A***, ***B***, Retinas from wt (squares) or VPP (triangles) mice were isolated at different postnatal days (PND) as indicated. Gene expression of LIF (***A***) and MCP-1 (Ccl-2) (***B***) was analyzed by real-time PCR and normalized to β-actin expression. Expression of both factors was strongly induced in VPP mice starting around PND 15, concomitantly with the onset of photoreceptor degeneration. Shown are the mean mRNA levels ($\pm$SD) of three independent retinas per time point and strain ($n = 3$) relative to the levels of wild-type (wt) at PND 10 which was set to 1. ***C***, Retinal morphology of VPP (left) and VPP;Ccl-2$^{-/-}$ mice (right) at PND 42. Lack of Ccl-2 did not influence the degeneration as reflected by the indistinguishable retinal morphologies. Both genotypes retained 5–6 rows of photoreceptor nuclei in the ONL compared with the 10–12 rows in wild-type retinas (***D***). ***D***, Retinal morphology of wild-type (wt), Lif$^{-/-}$, VPP and VPP;Lif$^{-/-}$ mice was analyzed at PND 15, PND 28 and PND 42 as indicated. Retinal morphology was similar in wt and Lif$^{-/-}$ at all ages tested. Retinas of VPP mice developed normally until the age of 15 d. As expected (Samardzija et al., 2006b), many VPP photoreceptors degenerated until PND 28 before the degeneration slowed down. Photoreceptors of VPP;Lif$^{-/-}$ mice displayed a similar degeneration until PND 28 but had a much more severe progression thereafter as seen by the single row of photoreceptors remaining at PND 42. Shown are representative panels of at least three independent retinas. RPE, Retinal pigment epithelium; ROS, rod outer segments; RIS, rod inner segments; ONL, outer nuclear layer; INL, inner nuclear layer. Scale bars, 25 μm.

rinsed 1x in PBS, washed 3x in PBS (5 min each) and blocked in 20% HINGS at RT for 1 h. The respective secondary antibodies were applied in 5% HINGS at RT for 1 h. Slides were rinsed in PBS, washed 3 $\times$ in PBS (5 min each) and mounted.

Western blotting. Retinas were homogenized by sonication in 100 mM Tris/HCl, pH 8.0, and analyzed for protein content using Bradford reagent. Standard SDS-PAGE (12%) and Western blotting of 40 μg of total retinal extracts were performed. For immunodetection, the following antibodies were used: anti-STAT3 (#9132 Cell Signaling Technology), anti-Akt (#9272, Cell Signaling Technology), anti-gp130 (sc-656, Santa Cruz), anti-GFAP (G-3893, Sigma), anti-CRALBP (gift from John Saari, University of Washington, Seattle, WA), anti-β-actin (sc-1616, Santa Cruz Biotechnology), anti-phospho-STAT3$_{Tyr705}$ (#9131, Cell Signaling Technology), anti-phospho-Akt$_{Tyr473}$ (#9271, Cell Signaling Technology). Blots were incubated overnight at 4°C with primary antibodies followed by a one hour incubation at RT with HRP-conjugated secondary antibodies. Immunoreactivity was visualized using the Western Lightning Chemiluminescence reagent (Perkin-Elmer).

RNA isolation, cDNA synthesis, and real-time PCR. Retinas were removed through a slit in the cornea and snap frozen in liquid nitrogen. Total retinal RNA was prepared using the RNeasy RNA isolation kit (Qiagen) including a DNase treatment to digest residual genomic DNA. One microgram of total RNA were used for reverse transcription using oligo(dT) and M-MLV reverse transcriptase (Promega). cDNAs from individual animals were amplified in duplicates with respective primer pairs (Table 1) in a Light-Cycler instrument 480 (Roche Diagnostics AG) using SYBR Green I Master Mix (Roche Diagnostics AG). mRNA levels were normalized to β-actin and relative gene expression was calculated using the value of one (out of three) wild-type probe as calibrator. For statistical analysis we used ANOVA with Tukey's multiple comparison test (where more than two conditions were compared), ANOVA with Dunnett's multiple comparison test (where several conditions were compared with a control) or a one-tailed *t* test for the comparison of the treatment in *Lif*$^{-/-}$ animals, respectively. *p* values of <0.05 were considered statistically significant.

Results

Lack of LIF accelerates photoreceptor degeneration in a model of retinitis pigmentosa

The degenerating retina of VPP mice induces the expression of several factors connected to an inflammatory or immune response like LIF (Fig. 1*A*) (Samardzija et al., 2006a), monocyte chemoattractant protein-1 (MCP-1) (Fig. 1*B*), Casp-1, interleukin-1β (IL-1β) (Samardzija et al., 2006c), complement component 1qα (C1qα) (Rohrer et al., 2007) and comple-

13768 • J. Neurosci., December 17, 2008 • 28(51):13765–13774 Joly et al. • LIF Increases Photoreceptor Survival *In Vivo*

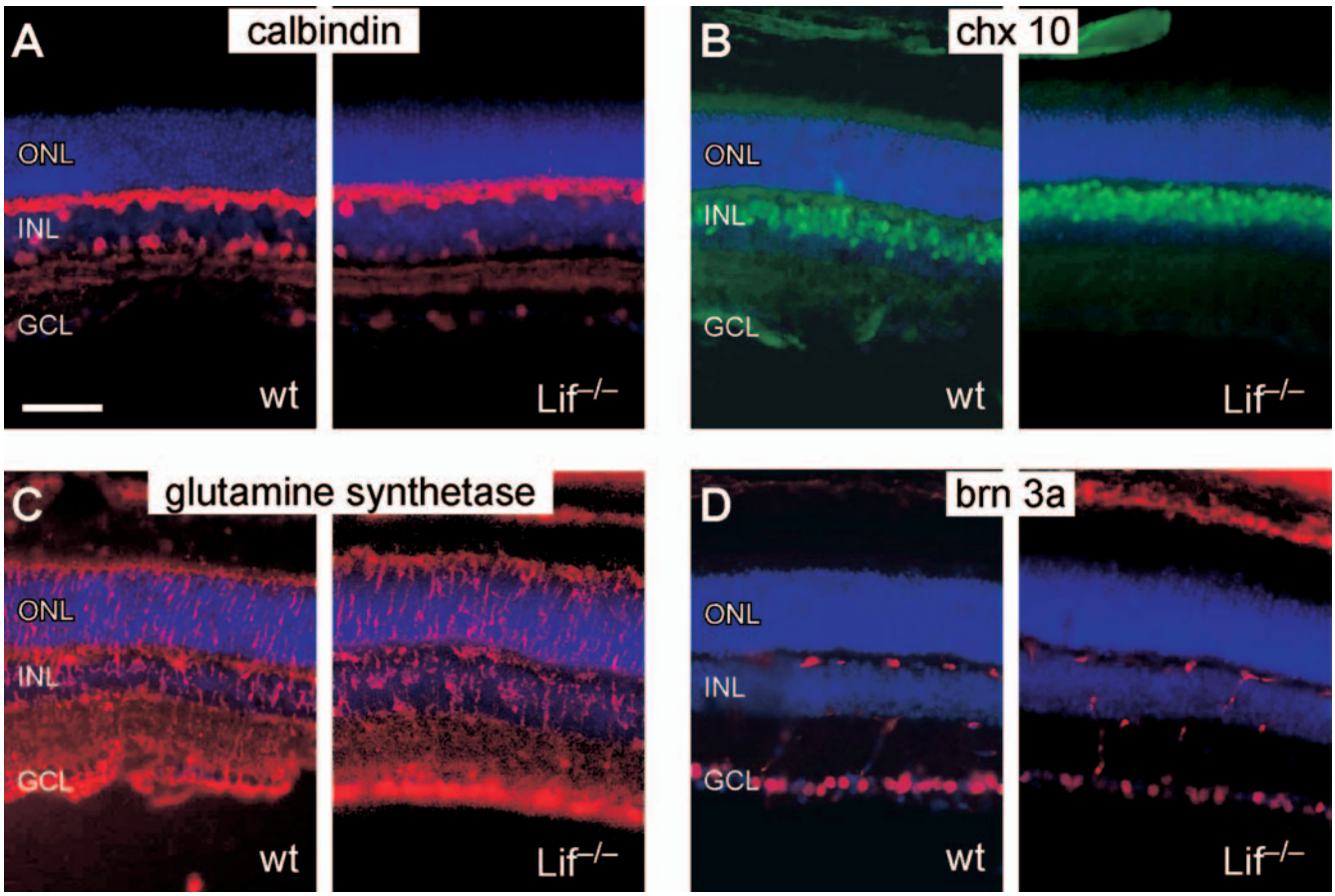

Figure 2. ***A–D***, Lif $^{-/-}$ retinas are similar to wild-type. Retinas of 28-day-old wild-type (wt) and Lif $^{-/-}$ mice, respectively, were stained with antibodies specific for horizontal cells (calbindin, ***A***), bipolar cells (CHX10, ***B***), Muller glia cells (glutamine synthetase, ***C***) and ganglion cells (Brn3a, ***D***). Staining patterns did not differ between wild-type and mutant retinas. GCL, Ganglion cell layer. Other abbreviations as in Figure 1. Scale bar, 50 μm.

ment factor H (CFH, data not shown). To analyze their potential role in the physiology or pathophysiology of the retina, we genetically inhibited MCP-1 and LIF signaling. For this purpose, we generated double mutant mice expressing the VPP transgene on a null background for either the MCP-1 chemokine (*Ccl-2*$^{-/-}$) or the LIF cytokine (*Lif*$^{-/-}$), respectively. Even though MCP-1 was upregulated >100-fold in the VPP retina, lack of functional MCP-1 did not noticeably influence the course of the disease process (Fig. 1*C*). In contrast, genetic ablation of LIF strongly accelerated retinal degeneration and the death of photoreceptors in VPP mice (Fig. 1*D*). Whereas retinas of VPP mice showed the expected slow degeneration with ~6 rows of photoreceptor cells left at PND 42, retinas of VPP mice lacking LIF showed a severely accelerated degeneration with only one row of visual cells remaining 42 d after birth (Fig. 1*D*). Onset and first phase of the degeneration was similar to VPP mice as suggested by the normal retinal appearance at PND 15 and by the only slightly reduced number of photoreceptor nuclei at PND 28.

Although LIF has been implicated in retinal development (Elliott et al., 2006) and lack of LIF was recently reported to increase microvessel density in the retina (Kubota et al., 2008), retinal morphology of *Lif*$^{-/-}$ mice was similar to wild-type mice at all ages tested. Retinal cell layers were well established and distribution of rods and cones was inconspicuous (Fig. 1*D*). In addition, immunofluorescence stainings with antibodies specific for horizontal cells (anti-calbindin), bipolar cells (anti-CHX10), Muller cells (anti-glutamine synthetase) and ganglion cells (anti-Brn3a) resulted in similar staining patterns in wild-type and knock-out mice (Fig. 2). Normal retinal architecture of *Lif*$^{-/-}$ mice is further supported by the equal numbers of retinal ganglion cells in wt and LIF knock-out animals (additional file 1). In addition, retinal function of *Lif*$^{-/-}$ mice was comparable to wild-type animals (data not shown).

Photoreceptor injury induces LIF expression in a subset of Muller glia cells

We used *in situ* hybridization to localize the cells expressing LIF cytokine in response to photoreceptor injury. Whereas most cells did not show enhanced signal intensity compared with controls, few scattered cells were strongly positive for LIF expression in the INL of VPP mice at PND 28 (Fig. 3*A–C*). A very similar expression pattern was also found in retinas of wild-type mice at 12 h after exposure to damaging light (Fig. 3*D–F*,*G*,*J*). This suggests that the same subset of cells might be responsible for LIF upregulation in both models of retinal degeneration. Hybridization of wild-type control retinas with antisense probe did not result in such a staining pattern (Fig. 3*F*) demonstrating that the signal was specific for degenerating retinas. To identify the retinal cell type expressing LIF, we combined *in situ* hybridization with immunofluorescence using antibodies specific for individual retinal cell types. Whereas the *in situ* LIF signal did not colocalize with calbindin (horizontal cells), calretinin (amacrine cells), disabled-3 (type 2 amacrine cells), PKC-β (cone bipolar cells) or Iba-1 (microglia cells) (additional file 2), it labeled a subset of

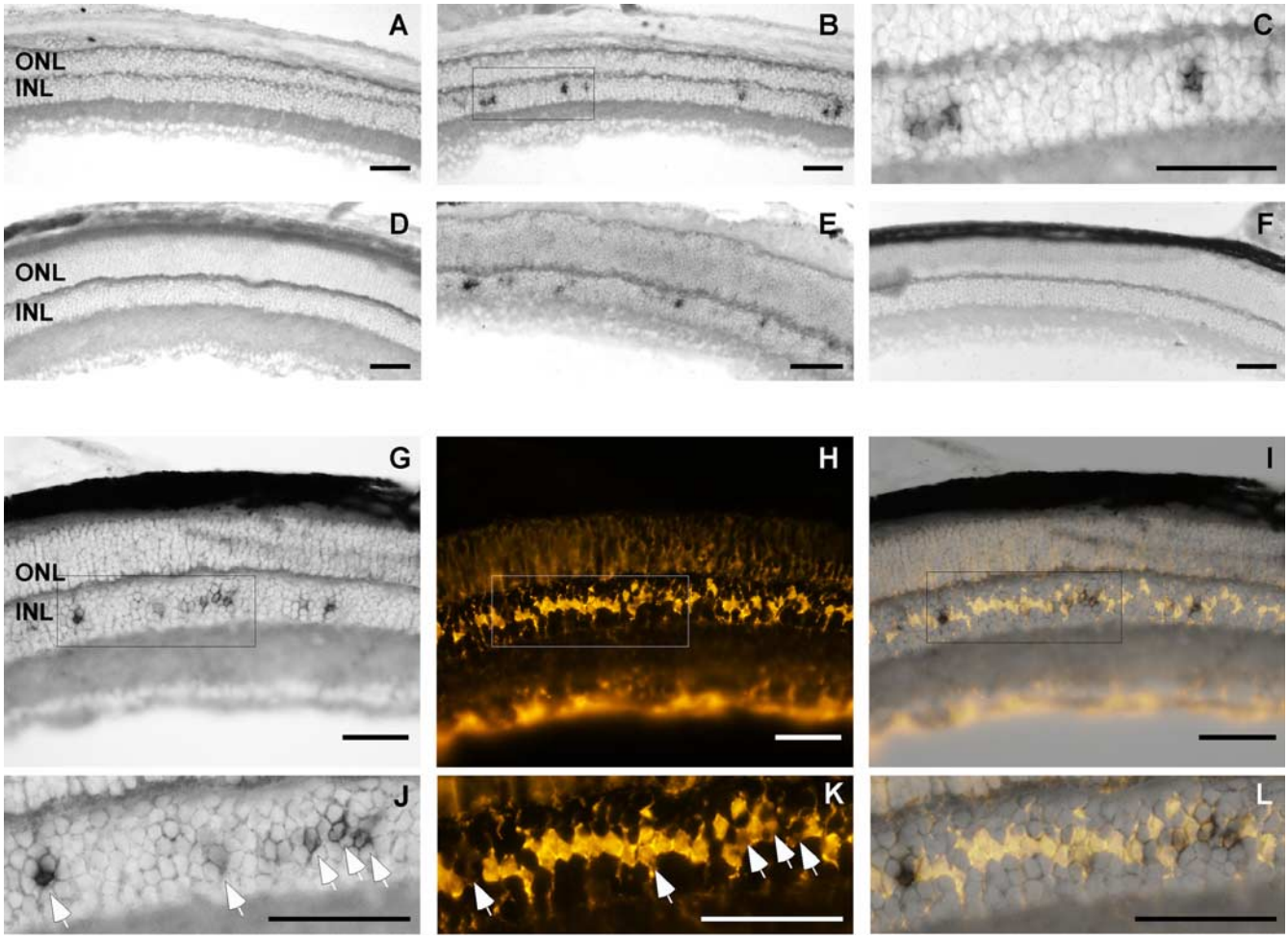

Figure 3. The degenerating retina induces LIF expression in a subset of Muller glia cells. ***A–F***, *In situ* hybridization localizes LIF-expressing cells in the INL. Retinal sections of 28-day-old VPP mice (***A–C***), of wild-type BALB/c mice 12 h after light exposure (***D***, ***E***), or of untreated wild-type mice (***F***) were hybridized with LIF sense (***A***, ***D***) or LIF antisense (***B***, ***C***, ***E***, ***F***) riboprobes. ***C***, Higher magnification of boxed area in ***B***. LIF antisense probes specifically stained scattered cells in the INL in retinas undergoing photoreceptor degeneration (***B***, ***E***) but not in a healthy retina (***F***). ***G–L***, Combined *in situ* and immunofluorescence stainings identified LIF-expressing cells as a subset of Muller glias. Retinal sections of wild-type 129S6/SvEvTac mice 12 h after light exposure were hybridized with LIF antisense riboprobes (***G***, ***J***) and anti-glutamine synthetase antibodies (***H***, ***K***). The merged pictures (***I***, ***L***) identified LIF-expressing cells as a subset of Muller glia cells. ***J–L***, Higher magnifications of boxed area in ***G***. Arrows, cells positive for LIF and GS. Abbreviations as in Figure 1. Scale bars, 50 μm.

cells which stained positive for glutamine synthetase (GS) (Fig. 3*G–L*). This clearly demonstrates that a subset of Muller glia cells upregulated LIF in response to retinal stress. It is interesting to note that the intensity of the GS staining correlated inversely with the intensity of the LIF signal (Fig. 3*J*,*K*).

Lack of LIF prevents activation of Muller glia cells and blocks phosphorylation of STAT3

Muller cell activation is one of the most common hallmarks in a degenerating retina. In virtually all cases studied, retinal Muller cells increase expression of glial fibrillary acid protein (GFAP) in response to a degenerative process (Lewis and Fisher, 2003; Bringmann et al., 2006). This has also been observed in the VPP mouse retina (Fig. 4) (Samardzija et al., 2006a). In contrast to VPP mice on a LIF wild-type background, increased expression of GFAP was completely abolished in retinas of *VPP;Lif*$^{-/-}$ (Fig. 4). The similar expression levels of cellular retinaldehyde-binding protein (CRALBP) (Fig. 4) and the immunofluorescence staining for glutamine synthetase (GS) (Fig. 2), both Muller cell markers, show that the missing glial response was not due to a generally reduced presence of Muller cells in LIF knock-out animals.

Similarly to GFAP in Muller cells, phosphorylation of the anti-apoptotic STAT3 protein has been commonly observed during degenerative processes in the retina (Mechoulam and Pierce, 2005; Samardzija et al., 2006a; Yang et al., 2007; Ueki et al., 2008). As for the increased GFAP expression, phosphorylation of STAT3 was completely blocked in retinas of *VPP;Lif*$^{-/-}$ mice (Fig. 4). Since STAT3 protein was expressed at normal levels (Fig. 4) and the enzymatic machinery to phosphorylate STAT3 was intact in the *Lif*$^{-/-}$ retina (see below), a block of upstream signaling events in the absence of LIF cytokine must account for the lack of STAT3 phosphorylation and the missing Muller cell activation in the double transgenic animals.

Akt, another kinase implicated in retinal degeneration and cell survival (Johnson et al., 2005; Jomary et al., 2006) was slightly activated in degenerating VPP retinas as evidenced by the small increase in phosphorylation observed by Western blotting (Fig. 4). Similar to STAT3, the absence of LIF prevented increased phosphorylation of Akt in response to the degeneration in the *VPP;Lif*$^{-/-}$ retina.

LIF is required for proper signaling in the stressed retina

Recently, Rattner and Nathans (2005) identified photoreceptor-derived Edn2 as a potential signaling molecule regulating a Muller glia cell response to light-mediated injury. Similar to the light-

13770 • J. Neurosci., December 17, 2008 • 28(51):13765–13774

damaged retina (data not shown), the VPP retina strongly upregulated expression of Edn2 (Fig. 5*A*). Basal expression of Edn2 seemed to depend largely on LIF since Edn2 expression was reduced to 2% of wild-type levels in *Lif*$^{-/-}$ mouse retinas. In VPP mice lacking LIF (*VPP;Lif*$^{-/-}$ double mutants), Edn2 expression was not upregulated and remained at the low basal levels observed in the *Lif*$^{-/-}$ retina, despite the accelerated retinal degeneration in the double mutant mice. Edn1 and Ednrb were expressed at similar levels in all mouse strains tested.

In the injured retina of the VPP mouse, GFAP was induced on the mRNA (Fig. 5*B*) and protein (Fig. 4) levels. Similar to Edn2, however, GFAP expression was strongly reduced in retinas of mice lacking LIF (11% of wt) (Fig. 5*B*) and in contrast to VPP mice (2.7-fold elevated mRNA levels) no increased expression of GFAP was detectable in retinas of double mutant mice which is in line with our protein expression data (Fig. 4). LIF influenced also expression of Casp-1 since basal mRNA levels of this protease were reduced by a factor of 2 in retinas of *Lif*$^{-/-}$ mice (Fig. 5*B*). Similar to Edn2 and GFAP, Casp-1 expression was activated in VPP retinas but not in *VPP;Lif*$^{-/-}$ double mutant mice. Expression of other stress related genes like *Smad1* (data not shown) and *Mcl1* (Fig. 5*B*) were not affected by the lack of LIF and/or the presence of the VPP transgene (Fig. 5*B*).

FGF2 is often implicated in a paracrine pathway of photoreceptor neuroprotection in various models of degeneration (Wen et al., 1995; Gao and Hollyfield, 1996; Joly et al., 2007) and is thought to be produced in an attempt to protect cells in unfavorable conditions. As such, FGF2, was also strongly upregulated in the VPP retina (10.2-fold, Fig. 5*C*). Strikingly, however, VPP retinas lacking LIF completely failed to induce FGF2 expression which remained at the same low basal level (38% of wt) as observed in *Lif*$^{-/-}$ single mutant mice (43% of wt). Expression of other neurotrophic factors like BDNF, GDNF and CNTF remained at basal levels in the different strains with a slight upregulation of CNTF in the double transgenic retina (1.7-fold induction, Fig. 5*C*). Similarly, expression of the anti-apoptotic genes survivin and Bcl-2, both may be regulated in a STAT3 dependent manner (Kim et al., 2006; Weerasinghe et al., 2007) remained at basal levels in the retinas of all strains tested. Thus, the lack of FGF2 induction might have been the main reason for the accelerated photoreceptor degeneration in the VPP mouse lacking LIF.

Retinal degeneration in the VPP mouse not only induced phosphorylation of STAT3 (Fig. 4) but also STAT3 gene expression (1.9-fold) and the expression of at least two additional members of the Jak/STAT signaling pathway (Jak3, 2.6-fold and SOCS3, 3.4-fold). Again, lack of LIF in *VPP;Lif*$^{-/-}$ mice completely blocked activation of this signaling cascade (Fig. 5*D*).

In summary, all genes (Edn2, GFAP, Casp-1, FGF2, STAT3, Jak3, SOCS3) or proteins (pSTAT3, p-Akt, GFAP), which were activated in response to VPP-mediated retinal degeneration showed basal expression in the absence of LIF. This strongly suggests an essential and early role of LIF in the retinal response to photoreceptor injury.

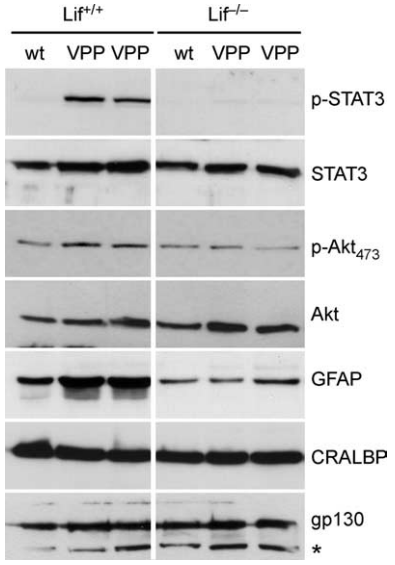

Figure 4. Lack of LIF prevents activation of STAT3, Akt and GFAP. Total retinal extracts of wt, VPP, Lif$^{-/-}$ and VPP;Lif$^{-/-}$ retinas of 28-day-old mice were tested by Western blotting using specific antibodies as indicated. The VPP transgene on a LIF wild-type background (left) induced a strong phosphorylation of STAT3, a weak activation of Akt and a robust upregulation of GFAP. Retinas of VPP mice on a LIF knock-out background (right) did not show any signs of STAT3 phosphorylation and did not increase expression of phospho-Akt and GFP. *Nonspecific signal.

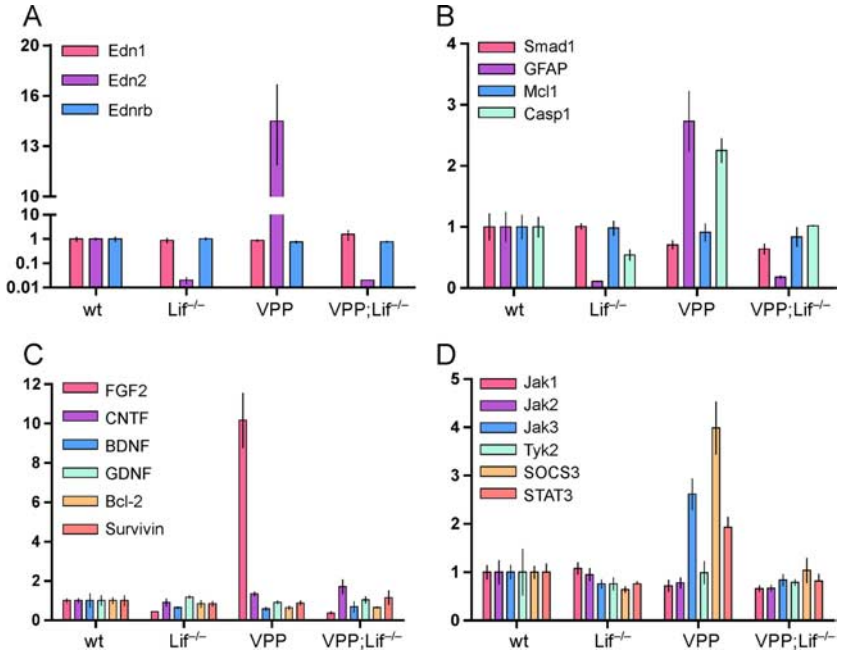

Figure 5. Lack of LIF prevents induction of a genomic response to retinal injury. Total retinal RNA was prepared from 28-day-old wt, VPP, Lif$^{-/-}$ and VPP;Lif$^{-/-}$ mice. cDNA from 3 independent retinas per genotype was amplified in duplicates by real-time PCR. One wild-type sample served as calibrator and the mean of all wild-type samples was set to 1 for each gene amplified. Shown are means ± SD of endothelin-related genes (***A***), stress-related genes (***B***), growth and survival factors (***C***), and of genes relevant for the Jak/STAT signaling pathway (***D***) relative to wild-type levels. Lack of LIF caused very low basal expression levels of Edn2, GFAP and FGF2. In the presence of LIF, VPP-mediated retinal degeneration induced expression of Edn2, GFAP, Casp-1, FGF2, Jak3, SOCS3 and STAT3. The absence of LIF prevented induction of all of these genes in the VPP retina and expression levels remained at similar low levels as in Lif$^{-/-}$ single mutant mice.

Signaling can be restored by the application of rLIF

The missing activation of gene expression and protein phosphorylation in *Lif*$^{-/-}$ mice could be specifically caused by the absence of LIF cytokine or by a general defect in the knock-out animals. To discriminate between these possibilities, we analyzed gene

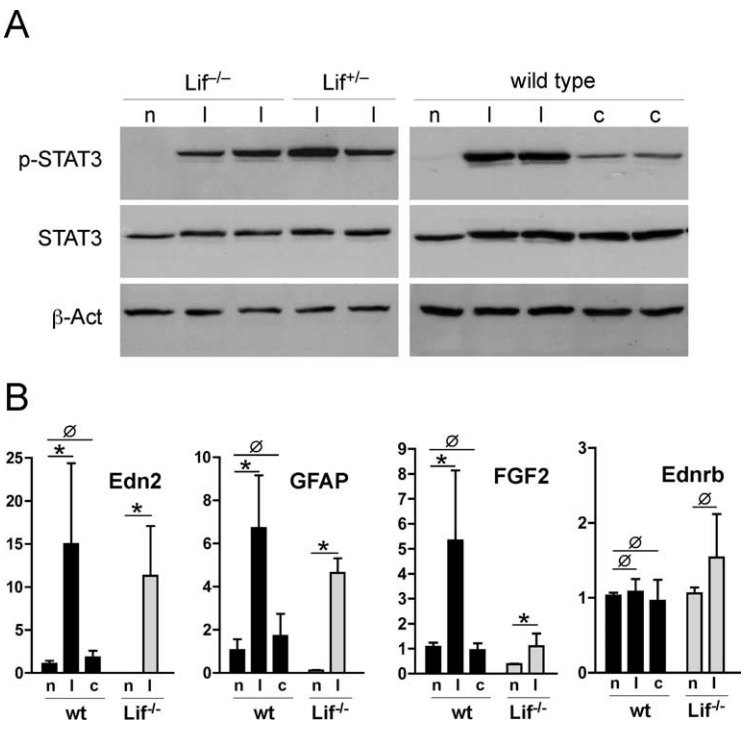

Figure 6. ***A***, ***B***, Injection of rLIF restores signaling in Lif$^{-/-}$ mice. A total of 1 μl (10 ng) of rLIF (l) or of vehicle control (PBS) (c) was injected intravitreally and levels of proteins or mRNAs were analyzed after 24 h by Western blotting (***A***) or by real-time PCR (***B***). ***A***, Injection of rLIF induced phosphorylation of STAT3 in wild-type, Lif$^{+/-}$ and Lif$^{-/-}$ mice. Control PBS injections showed only a minor response. ***B***, Gene expression of noninjected mice (n) or of mice at 24 h after injection of rLIF (l) or vehicle (PBS) (c) in wild-type (black bars) or Lif$^{-/-}$ mice (gray bars). Shown are means ± SD of $n = 3–4$ per genotype and treatment. Levels in noninjected wild-type animals were set to 1. *$p < 0.05$; $^{\varnothing}p > 0.05$. n, Noninjected; l, rLIF-injected; c, vehicle-injected.

expression after intravitreal injection of rLIF into wild-type and *Lif*$^{-/-}$ mice. rLIF induced phosphorylation of STAT3 similarly in all mice tested (Fig. 6*A*) and strongly activated gene expression of Edn2, GFAP and FGF2 in both wild-type and *Lif*$^{-/-}$ retinas (Fig. 6*B*). Although FGF2 mRNA levels in *Lif*$^{-/-}$ retinas treated with rLIF injections did not reach levels of treated wild-type retinas, induction over nontreated retinas was nevertheless similar (5-fold in wild-type and threefold in Lif$^{-/-}$ retinas) in the two mouse strains. It is interesting to note that rLIF induced expression of Edn2 14-fold in wild-type retinas and >3200-fold in *Lif*$^{-/-}$ animals resulting in similar expression levels in the two animals after rLIF application. Control injections of carrier (PBS) resulted only in a subtle response with low levels of STAT3 phosphorylation (Fig. 6*A*) but not in a significant alteration of gene expression (Fig. 6*B*). These data show that the molecular equipment required to transduce LIF-mediated signaling was present and functional in *Lif*$^{-/-}$ retinas. This suggests that lack of gene activation was a specific consequence of the absence of LIF.

Activation of Ednrb induces the molecular response and protects photoreceptors

The receptor for Edn2 has been found to be expressed on Muller cells and potentially astrocytes in the mouse retina (Rattner and Nathans, 2005). To test whether direct stimulation of Ednrb might be able to activate the molecular response to injury we injected the Ednrb agonist BQ-3020 into the vitreous of wild-type and *Lif*$^{-/-}$ mice (Fig. 7). BQ-3020 efficiently induced expression of FGF2, Edn2 and LIF in wild-type retinas. In contrast, the Ednrb agonist failed to significantly induce FGF2 in *Lif*$^{-/-}$ mice and caused only a 70-fold increase of Edn2 expression in the knock-outs compared with the 3200-fold increase after rLIF application (Fig. 6*B*). This supports our conclusion that the signaling system can efficiently be activated only in the presence of LIF. Note that the strong upregulation of LIF in wt mice may have further supported the production of Edn2 by a positive feed forward loop resulting in a signal amplification which was only possible in wild-type but not *Lif*$^{-/-}$ animals.

Modulation of Ednrb activation was directly relevant for photoreceptor survival. Application of the Ednrb agonist resulted in a strong tendency toward protection of photoreceptors against light damage (Fig. 7*D*), whereas injection of an Ednrb antagonist (BQ-788) into eyes of VPP mice significantly increased retinal cell death (Fig. 7*E*).

LIF-induced signaling and Muller cell activation may act through rod photoreceptor cells

To investigate a potential role of photoreceptors for the signaling mechanisms induced by LIF expression, we injected rLIF into the vitreous of mice which are almost devoid of photoreceptors [3-month-old rd1 (Bowes et al., 1990)] or which have a cone-only retina [*Nrl*$^{-/-}$ (Mears et al., 2001)]. Most importantly, although expression of genes was induced upon injections, the response did not differ between rLIF and PBS-injected retinas in these two mouse strains which both lack rod photoreceptors (Fig. 8*A–F*), in contrast to injections into wild-type mice (Fig. 6*B*). This strongly suggests that a specific LIF-mediated retinal response requires rod photoreceptors.

However, it is interesting to note that basal gene expression and the response to injections differed between rd1 and *Nrl*$^{-/-}$ retinas in several points. (1) Basal expression of Edn2 in the aged rd1 mouse was >1300-fold reduced (7×10^{-4} relative to wt, Fig. 8*A*) which is comparable to the low levels of rod specific Gnat1 (rod transducin) mRNA (1×10^{-4} relative to wt) (Fig. 8*F*). This suggests that Edn2 is mainly expressed in photoreceptor cells. Since these cells are no longer present in rd1 mice, Edn2 expression levels are strongly reduced. Since the cone retinas of *Nrl*$^{-/-}$ mice showed only fivefold reduced levels of Edn2 mRNA (Fig. 8*A*) Edn2 may be expressed by both rods and cones in a wild-type retina. (2) Injections (rLIF and PBS) induced expression of GFAP much stronger in the rd1 mouse retina than in the *Nrl*$^{-/-}$ retina (Fig. 8*B*). (3) Basal levels of FGF2 mRNA were higher in the *Nrl*$^{-/-}$ retina (Fig. 8*C*). (4) The mRNA for Ednrb was increased in rd1 (and *Nrl*$^{-/-}$) retinas (Fig. 8*D*) compared with wild-type. This suggests that the receptor for Edn2 is expressed mainly in cells different from photoreceptors which is in line with the findings from Rattner and Nathans (2005). (5) LIF-R mRNA was reduced only sixfold in the rd1 mouse and 2.5-fold in the *Nrl*$^{-/-}$ mouse (Fig. 8*E*) suggesting that also cells apart from photoreceptors may express the receptor for LIF.

Discussion

Cells and tissues are equipped with endogenous protective mechanisms to cope with photoreceptor injury. Knowledge of these mech-

13772 • J. Neurosci., December 17, 2008 • 28(51):13765–13774 Joly et al. • LIF Increases Photoreceptor Survival *In Vivo*

anisms may allow a targeted and sustained activation of intrinsic molecular pathways which could protect cells against death in a variety of degenerative diseases. Protection against cell death may ensure functionality of the tissue which is especially important in tissues depending on quiescent post-mitotic cells like brain and retina. Here we show that the retina contains a LIF-controlled signaling system which apparently aims at the maintenance of the viability of injured photoreceptors. Activation of the system involves at least photoreceptors and Muller glia cells. The absence of LIF completely blocks this endogenous defense pathway, prevents activation of Muller glia cells in response to a stress situation and keeps several signaling and survival factors at basal expression levels. This results in a drastically accelerated degeneration of visual cells.

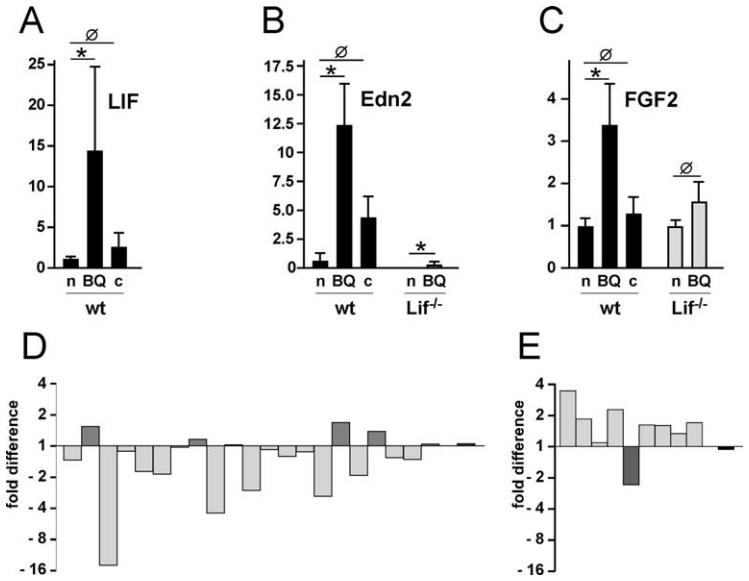

Figure 7. Modulation of Ednrb signaling influences cell survival. ***A–C***, A total of 1 μl (1 μg/μl) of BQ-3020 (BQ) or of vehicle control (H_2O) (c) was injected intravitreally into wild-type (wt) or Lif $^{-/-}$ mice as indicated. Noninjected mice (n) served as controls. Gene expression was analyzed 24 h after injection by real-time PCR on cDNA derived from total retinal RNA. $n = 3$ per treatment. ***D***, Cell death after light exposure in retinas pretreated with BQ-3020. The left eye of each wild-type mouse was injected with BQ-3020 and the right eye with vehicle (sham). Each bar represents the fold difference in cell death between compound and sham treated eyes of a single mouse. The last bar shows the result in a wild-type mouse not exposed to light. Of the 21 mice analyzed, BQ-3020 treated retinas of 15 animals were less severely affected by the light exposure than the contralateral sham treated retinas. This resulted in a strong tendency toward protection by the activation of Ednrb ($p = 0.0536$; paired Student's t test). ***E***, Cell death in retinas of VPP mice treated with BQ-788, an Ednrb antagonist. The left eye of each mouse was injected with BQ-788 and the right eyes with vehicle (sham). Analysis was 2 d after injection. Each bar represents the fold difference in cell death between compound and sham treated eyes of individual VPP mice. The last bar shows the result in a wild-type mouse to test potential toxicity of the compound. Of the 9 mice analyzed, BQ-788 treated retinas of 8 animals were more severely affected by the VPP mediated degeneration than the contralateral sham treated retinas. This resulted in a significantly lower survival of photoreceptors after the inhibition of Ednrb signaling ($p = 0.0351$; paired Student's t test). $^*p < 0.05$; $^{\varnothing}p > 0.05$. n, Noninjected; BQ, BQ-3020-injected; c, vehicle-injected.

Retinal response to injury

Rattner and Nathans (2005) recently proposed a specific retinal response to injury which involves the production and secretion of Edn2 by injured photoreceptors leading to the activation of Muller glia cells via Ednrb and to an increased expression of FGF2. FGF2 is a potent neurotrophic factor that is upregulated in various situations of retinal stress (Gao and Hollyfield, 1996; Hackett et al., 1997; Grimm et al., 2002) and that can protect retinal cells against various insults (Unoki and LaVail, 1994; Liu et al., 1998; Yamada et al., 2001; Schuettauf et al., 2004; O'Driscoll et al., 2007, 2008).

Intriguingly, this response seems not to be initiated by the damaged photoreceptors themselves but rather by a specific subset of Muller glia cells which react with the expression of LIF to photoreceptor injury (Fig. 3). What sets the LIF-expressing Muller cells apart from other Muller cells needs to be investigated. Our combined *in situ* and immunofluorescence stainings suggest that cells expressing high levels of LIF have reduced GS levels. Whether this is an artificial observation due to the staining procedure needs to be analyzed but it is interesting that GS might be down regulated in pathological situations possibly through the action of FGF2 (Kruchkova et al., 2001).

The presence of LIF is required to express Edn2 to normal levels and to induce it in the stressed retina. Since Ednrb is expressed by Muller cells (which also express LIF), Edn2 signaling may induce a positive feed forward loop resulting in an increased stimulation LIF production. This is supported by the strong stimulation of LIF expression after injection of the Ednrb agonist BQ-3020 in wild-type retinas (Fig. 7). In addition to LIF, BQ-3020 application also induced Edn2 and FGF2 expression suggesting that the full response is inducible through activation of Ednrb. Indeed, activation of Ednrb protected cells against light damage and antagonizing the receptor increased cell death in the VPP mouse (Fig. 7). This demonstrates a direct relevance of the LIF-dependent Edn2 signaling for photoreceptor survival and tissue integrity. The existence of a LIF-dependent positive feed forward loop is further supported by the reduced molecular response in retinas of *Lif*$^{-/-}$ mice after BQ-3020 application (Fig. 7).

Since LIF-R and gp130, the two receptor subunits required for LIF binding are ubiquitously expressed in the retina including photoreceptors (Ueki et al., 2008) LIF may directly target visual cells to increase Edn2 production. This notion is supported by our observation that injection of rLIF into eyes of mice without photoreceptors (aged rd1 mice) did not provoke a similar strong response (Fig. 8).

In the presence of increased LIF, the transcription factor STAT3 is strongly phosphorylated and expression of the receptor kinase Jak3 is induced. STAT3 is a downstream mediator of gp130 signaling (Ernst and Jenkins, 2004) and is able to upregulate Jak3 expression (Mangan et al., 2004). In the absence of LIF, STAT3 protein is not activated and expression of Jak3 is not elevated suggesting that LIF may indeed signal through STAT3/Jak3. Since lack of LIF also prevents upregulation of Edn2 expression, the regulation of these molecules may be correlated and directly or indirectly be coordinated by LIF-mediated stimulation of LIF-R.

Similarly to Edn2, STAT3, Jak3 and GFAP, induction of the survival factor FGF2 depends on LIF. It has been shown that injection of rLIF protects the retina against a toxic insult (Ueki et al., 2008), that injection of rLIF upregulates endogenous FGF2 in the retina (Fig. 6), that increased expression of endogenous FGF2 protects against retinal degeneration (O'Driscoll et al., 2008) and that lack of FGF2 activation correlates with accelerated photore-

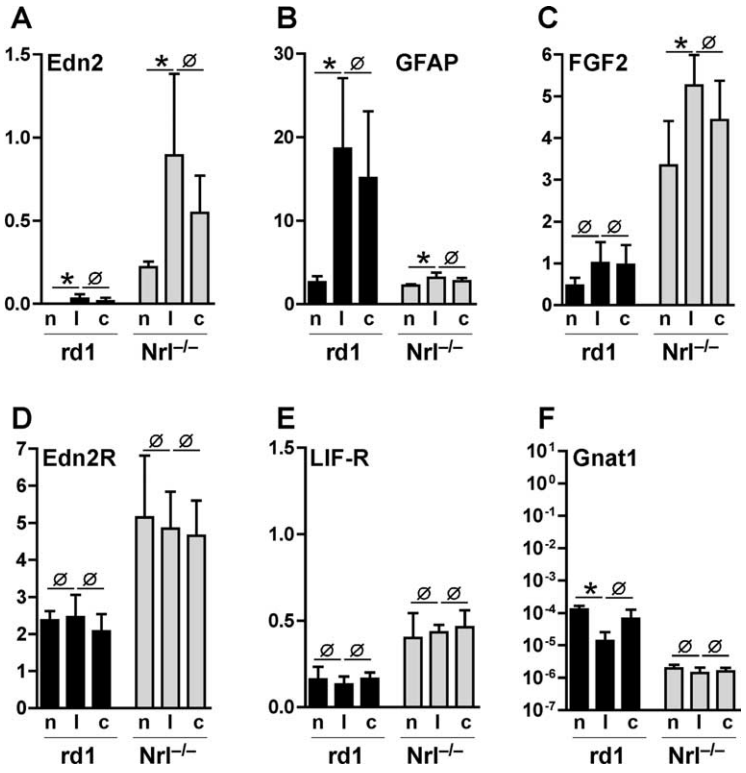

Figure 8. LIF-mediated signaling involves rod photoreceptors. One microliter (10 ng) of rLIF (l) or of vehicle control (PBS) (c) was injected intravitreally into rd1 or Nrl $^{-/-}$ mice as indicated and relative gene expression of Edn2 (***A***), GFAP (***B***), FGF2 (***C***), Ednrb (***D***) LIF-R (***E***), and Gnat1 (***F***) was tested by real-time PCR on cDNA derived from total retinal RNA. Values were expressed relative to RNA levels of untreated wild-type retinas (set to 1, data not shown). Note the logarithmic scale for Gnat1. Shown are means ± SD of $n = 6$ (rd1) or $n = 4$ (Nrl $^{-/-}$) per treatment. *$p < 0.05$; $^{\varnothing}p > 0.05$. n, Noninjected; l, rLIF-injected; c, PBS-injected.

ceptor death (Figs. 1, 5). Thus, is seems highly likely that FGF2 is a major factor in the LIF-controlled protective mechanism. Since independent studies have reported expression of FGF2 by Muller cells (Walsh et al., 2001) and by photoreceptors (Rattner and Nathans, 2005), respectively, regulation of FGF2 expression by LIF needs further detailed investigation.

Together, our results show that LIF is not only essential but also sufficient to serve as the molecular switch to activate an endogenous protective response which may depend on the production of the survival factor FGF2.

Rod photoreceptors are required for a specific LIF-mediated response

Injection of rLIF specifically induced expression of Edn2, GFAP and FGF2 (Fig. 6). Since similar injections in the absence of rod photoreceptors did not cause a significantly different response from control injections (Fig. 8), our results suggest that rod photoreceptors play an essential and specific role in the LIF response pathway. The strong but not exclusive production of Edn2 in rod photoreceptors is demonstrated by the 1300-fold reduced basal Edn2 levels in rd1 compared with wild-type mice. Since rd1 mice at this age (3 months) retain some photoreceptors, mostly cones, in the far peripheral retina (data not shown) and since the all-cone retinas of *Nrl*$^{-/-}$ mice show only fivefold reduced levels of Edn2 mRNA (Fig. 8), cones might also express Edn2 which can be stimulated by retinal injury, although not in a LIF specific way. This conclusion is supported by the lack of significant Edn2 induction in the 661W cone cell line after rLIF application *in vitro* (data not shown).

One of the most common response to retinal injury is the upregulation of the intermediate filament protein GFAP in Muller glia cells (Sarthy and Fu, 1989; Lewis and Fisher, 2003; Nakazawa et al., 2007). This is also evident during the degenerative process in the retina of the VPP mouse (Fig. 4). As for Edn2 and FGF2, expression and upregulation of GFAP depends on the presence of LIF (Figs. 4, 5). The missing induction of GFAP expression in *VPP;Lif*$^{-/-}$ mice suggests that photoreceptor degeneration cannot activate Muller cells and/or astrocytes in the absence of LIF. Injection of rLIF was sufficient to increase expression of GFAP (Fig. 6) but the upregulation was only specific in the presence of rod photoreceptors (Fig. 8). Thus, LIF may not directly target glial cells but may stimulate Muller cells through production of Edn2 in rod photoreceptors.

An endogenous, LIF-mediated neuroprotective response in the retina

Based on our data and on published results (Rattner and Nathans, 2005), we suggest a model pathway which may be used by retinal cells to protect tissue integrity and to preserve photoreceptor function in the presence of damaging stress like excessive light exposure or gene mutations. We propose that a subset of Muller glia cells senses photoreceptor damage and reacts with the upregulation of LIF. Only in the presence of increased LIF, photoreceptors induce expression of Edn2 which may then signal back to Muller glia cells. This may cause a gliosis-like reaction and the stimulation of GFAP expression. Concomitantly, the survival factor FGF2 is produced in Muller cells and/or photoreceptors aiming at the protection of visual cells from further damage (additional file 3). Whether Edn2 expression occurs in healthy or already damaged photoreceptors is currently unknown. Although it was shown that Edn2 is mainly produced in the region affected by a toxic insult (Rattner and Nathans, 2005), the specific response observed after intravitreal injection of rLIF in wild-type animals suggests that also healthy photoreceptors can activate this response pathway. It is thus probable that Edn2 production is a general response of photoreceptors to increased local concentrations of LIF.

Our work establishes LIF as the key molecule in the induction of an endogenous molecular pathway aiming at the protection of photoreceptor cells *in vivo*. This pathway may be part of a tissue defense system which increases the survival of visual cells in situations of environmental or mutational stress. Even though the endogenous potency of the system may not be sufficient to secure the viability of the cells over an extended period of time (photoreceptors in the VPP mouse die eventually), an artificial increase of its efficacy may nevertheless offer the opportunity to significantly prolong the lifespan of visual cells in human patients.

References

Bowes C, Li T, Danciger M, Baxter LC, Applebury ML, Farber DB (1990) Retinal degeneration in the rd mouse is caused by a defect in the beta subunit of rod cGMP-phosphodiesterase. Nature 347:677–680.

Bringmann A, Pannicke T, Grosche J, Francke M, Wiedemann P, Skatchkov SN, Osborne NN, Reichenbach A (2006) Muller cells in the healthy and diseased retina. Prog Retin Eye Res 25:397–424.

Elliott J, Cayouette M, Gravel C (2006) The CNTF/LIF signaling pathway

regulates developmental programmed cell death and differentiation of rod precursor cells in the mouse retina in vivo. Dev Biol 300:583–598.

Ernst M, Jenkins BJ (2004) Acquiring signalling specificity from the cytokine receptor gp130. Trends Genet 20:23–32.

Escary JL, Perreau J, Duménil D, Ezine S, Brûlet P (1993) Leukaemia inhibitory factor is necessary for maintenance of haematopoietic stem cells and thymocyte stimulation. Nature 363:361–364.

Gao H, Hollyfield JG (1996) Basic fibroblast growth factor: increased gene expression in inherited and light-induced photoreceptor degeneration. Exp Eye Res 62:181–189.

Grimm C, Wenzel A, Groszer M, Mayser H, Seeliger M, Samardzija M, Bauer C, Gassmann M, Remé CE (2002) HIF-1-induced erythropoietin in the hypoxic retina protects against light-induced retinal degeneration. Nat Med 8:718–724.

Grimm C, Wenzel A, Stanescu D, Samardzija M, Hotop S, Groszer M, Naash M, Gassmann M, Remé C (2004) Constitutive overexpression of human erythropoietin protects the mouse retina against induced but not inherited retinal degeneration. J Neurosci 24:5651–5658.

Hackett SF, Schoenfeld CL, Freund J, Gottsch JD, Bhargave S, Campochiaro PA (1997) Neurotrophic factors, cytokines and stress increase expression of basic fibroblast growth factor in retinal pigmented epithelial cells. Exp Eye Res 64:865–873.

Hafezi F, Abegg M, Grimm C, Wenzel A, Munz K, Stürmer J, Farber DB, Remé CE (1998) Retinal degeneration in the rd mouse in the absence of c-fos. Invest Ophthalmol Vis Sci 39:2239–2244.

Johnson LE, van Veen T, Ekström PA (2005) Differential Akt activation in the photoreceptors of normal and rd1 mice. Cell Tissue Res 320:213–222.

Joly S, Pernet V, Chemtob S, Di Polo A, Lachapelle P (2007) Neuroprotection in the juvenile rat model of light-induced retinopathy: evidence suggesting a role for FGF-2 and CNTF. Invest Ophthalmol Vis Sci 48:2311–2320.

Jomary C, Cullen J, Jones SE (2006) Inactivation of the Akt survival pathway during photoreceptor apoptosis in the retinal degeneration mouse. Invest Ophthalmol Vis Sci 47:1620–1629.

Kamphuis W, Dijk F, Bergen AA (2007) Ischemic preconditioning alters the pattern of gene expression changes in response to full retinal ischemia. Mol Vis 13:1892–1901.

Kim KW, Mutter RW, Cao C, Albert JM, Shinohara ET, Sekhar KR, Lu B (2006) Inhibition of signal transducer and activator of transcription 3 activity results in down-regulation of Survivin following irradiation. Mol Cancer Ther 5:2659–2665.

Kruchkova Y, Ben-Dror I, Herschkovitz A, David M, Yayon A, Vardimon L (2001) Basic fibroblast growth factor: a potential inhibitor of glutamine synthetase expression in injured neural tissue. J Neurochem 77:1641–1649.

Kubota Y, Hirashima M, Kishi K, Stewart CL, Suda T (2008) Leukemia inhibitory factor regulates microvessel density by modulating oxygen-dependent VEGF expression in mice. J Clin Invest 118:2393–2403.

Lewis GP, Fisher SK (2003) Up-regulation of glial fibrillary acidic protein in response to retinal injury: its potential role in glial remodeling and a comparison to vimentin expression. Int Rev Cytol 230:263–290.

Liu C, Peng M, Laties AM, Wen R (1998) Preconditioning with bright light evokes a protective response against light damage in the rat retina. J Neurosci 18:1337–1344.

Mangan JK, Rane SG, Kang AD, Amanullah A, Wong BC, Reddy EP (2004) Mechanisms associated with IL-6-induced up-regulation of Jak3 and its role in monocytic differentiation. Blood 103:4093–4101.

Mears AJ, Kondo M, Swain PK, Takada Y, Bush RA, Saunders TL, Sieving PA, Swaroop A (2001) Nrl is required for rod photoreceptor development. Nat Genet 29:447–452.

Mechoulam H, Pierce EA (2005) Expression and activation of STAT3 in ischemia-induced retinopathy. Invest Ophthalmol Vis Sci 46:4409–4416.

Naash M, Hollyfield JG, al-Ubaidi MR, Baehr W (1993) Simulation of human autosomal dominant retinitis pigmentosa in transgenic mice expressing a mutated murine opsin gene. Proc Natl Acad Sci U S A 90:5499–5503.

Nakazawa T, Takeda M, Lewis GP, Cho KS, Jiao J, Wilhelmsson U, Fisher SK, Pekny M, Chen DF, Miller JW (2007) Attenuated glial reactions and photoreceptor degeneration after retinal detachment in mice deficient in glial fibrillary acidic protein and vimentin. Invest Ophthalmol Vis Sci 48:2760–2768.

O'Driscoll C, Wallace D, Cotter TG (2007) bFGF promotes photoreceptor cell survival in vitro by PKA-mediated inactivation of glycogen synthase kinase 3beta and CREB-dependent Bcl-2 up-regulation. J Neurochem 103:860–870.

O'Driscoll C, O'Connor J, O'Brien CJ, Cotter TG (2008) Basic fibroblast growth factor-induced protection from light damage in the mouse retina in vivo. J Neurochem 105:524–536.

Rattner A, Nathans J (2005) The genomic response to retinal disease and injury: evidence for endothelin signaling from photoreceptors to glia. J Neurosci 25:4540–4549.

Remé CE, Grimm C, Hafezi F, Marti A, Wenzel A (1998) Apoptotic cell death in retinal degenerations. Prog Retin Eye Res 17:443–464.

Rohrer B, Demos C, Frigg R, Grimm C (2007) Classical complement activation and acquired immune response pathways are not essential for retinal degeneration in the rd1 mouse. Exp Eye Res 84:82–91.

Samardzija M, Wenzel A, Aufenberg S, Thiersch M, Remé C, Grimm C (2006a) Differential role of Jak-STAT signaling in retinal degenerations. FASEB J 20:2411–2413.

Samardzija M, Wenzel A, Naash M, Remé CE, Grimm C (2006b) Rpe65 as a modifier gene for inherited retinal degeneration. Eur J Neurosci 23:1028–1034.

Samardzija M, Wenzel A, Thiersch M, Frigg R, Remé C, Grimm C (2006c) Caspase-1 ablation protects photoreceptors in a model of autosomal dominant retinitis pigmentosa. Invest Ophthalmol Vis Sci 47:5181–5190.

Sarthy PV, Fu M (1989) Transcriptional activation of an intermediate filament protein gene in mice with retinal dystrophy. DNA 8:437–446.

Schuettauf F, Vorwerk C, Naskar R, Orlin A, Quinto K, Zurakowski D, Dejneka NS, Klein RL, Meyer EM, Bennett J (2004) Adeno-associated viruses containing bFGF or BDNF are neuroprotective against excitotoxicity. Curr Eye Res 29:379–386.

Thiersch M, Raffelsberger W, Frigg R, Samardzija M, Wenzel A, Poch O, Grimm C (2008) Analysis of the retinal gene expression profile after hypoxic preconditioning identifies candidate genes for neuroprotection. BMC Genomics 9:73.

Ueki Y, Wang J, Chollangi S, Ash JD (2008) STAT3 activation in photoreceptors by leukemia inhibitory factor is associated with protection from light damage. J Neurochem 105:784–796.

Unoki K, LaVail MM (1994) Protection of the rat retina from ischemic injury by brain-derived neurotrophic factor, ciliary neurotrophic factor, and basic fibroblast growth factor. Invest Ophthalmol Vis Sci 35:907–915.

Walsh N, Valter K, Stone J (2001) Cellular and subcellular patterns of expression of bFGF and CNTF in the normal and light stressed adult rat retina. Exp Eye Res 72:495–501.

Weerasinghe P, Garcia GE, Zhu Q, Yuan P, Feng L, Mao L, Jing N (2007) Inhibition of Stat3 activation and tumor growth suppression of non-small cell lung cancer by G-quartet oligonucleotides. Int J Oncol 31:129–136.

Wen R, Song Y, Cheng T, Matthes MT, Yasumura D, LaVail MM, Steinberg RH (1995) Injury-induced upregulation of bFGF and CNTF mRNAS in the rat retina. J Neurosci 15:7377–7385.

Yamada H, Yamada E, Ando A, Esumi N, Bora N, Saikia J, Sung CH, Zack DJ, Campochiaro PA (2001) Fibroblast growth factor-2 decreases hyperoxia-induced photoreceptor cell death in mice. Am J Pathol 159:1113–1120.

Yang Z, Quigley HA, Pease ME, Yang Y, Qian J, Valenta D, Zack DJ (2007) Changes in gene expression in experimental glaucoma and optic nerve transection: the equilibrium between protective and detrimental mechanisms. Invest Ophthalmol Vis Sci 48:5539–5548.

Zhu Y, Zhang Y, Ojwang BA, Brantley MA Jr, Gidday JM (2007) Long-term tolerance to retinal ischemia by repetitive hypoxic preconditioning: role of HIF-1alpha and heme oxygenase-1. Invest Ophthalmol Vis Sci 48:1735–1743.

Znoiko SL, Rohrer B, Lu K, Lohr HR, Crouch RK, Ma JX (2005) Downregulation of cone-specific gene expression and degeneration of cone photoreceptors in the Rpe65−/− mouse at early ages. Invest Ophthalmol Vis Sci 46:1473–1479.

3.2.2. Retinal neuroprotection by hypoxic preconditioning is independent of hypoxia-inducible factor-1α expression in photoreceptors

Markus Thiersch[1], Christina Lange[1], Sandrine Joly[1], Severin Heynen[1], Yun Zheng Le[3], Marijana Samardzija[1] and Christian Grimm[1,2]

[1]Lab for Retinal Cell Biology, Department Ophthalmology, University of Zurich
[2]Zurich Center for Integrative Human Physiology (ZIHP)
[3]Health Sciences Center, University of Oklahoma, Oklahoma City, OK, USA

Author contribution:
Design: MT and CG
Experiment: MT, **CL** (Lasercapture microdissection, assistance with morphology, assistance with maintaince and injection of mice), SJ, Severin Heynen (SH), MS
Interpretation: MT, **CL**, SJ, SH, MS and CG
Manuscript: MT
Manuscript correction: **CL**, SJ, SH, MS and CG

Summary:
Hypoxic preconditioning stabilizes HIF1A in the retina and protects photoreceptors from light-induced cell death. In this paper we determined whether this stabilization of HIF1A in photoreceptor cells is essential for the protection seen after hypoxic preconditioning. We show that *Hif1a* is expressed in each cell layer of the retina. To knock down *Hif1a* specifically in rod photoreceptors, we crossed *Hif1a*-floxed mice (HIF-1$\alpha^{F/F}$) to mice expressing Cre recombinase under the opsin promotor (LMOPC1) and to mice in which Cre is under control of the Tamoxifen-inducible prp promotor (PrP-Cre-ER^{T}(28.4)). HIF1A knock-down was more efficient in HIF-1$\alpha^{F/F}$ crossed to PrP-Cre-ER^{T}(28.4) (PrPCre$^{(HIF-\Delta)}$) than in HIF-1$\alpha^{F/F}$ crossed to LMOPC1 (OpnCre$^{(HIF-\Delta)}$). The knock-down was specific for the ONL, but mild reduction of *Hif1a* gene expression was also seen in the INL and the GCL. Hypoxia induced HIF1A target genes like proyl hydroxylase 2 (*Egln1*), BCL2/adenovirus E1B

interacting protein 3 (*Bnip3*), *Vegf*, solute carrier family 2 member 1 (*Slc2a1* or *Glut1*) and adrenomedullin (*Adm*) were reduced significantly in the PrpCre$^{(HIF-\Delta)}$ mice in contrast to the OpnCre$^{(HIF-\Delta)}$, where only *Egln1* and *Glut1* showed a significant reduction. Tamoxifen injection and/or hypoxia alone did not alter retinal morphology of neither HIF-1$\alpha^{F/F}$, OpnCre$^{(HIF-\Delta)}$ nor PrPCre$^{(HIF-\Delta)}$ mice. We therefore exposed the HIF1A knock down mice to light with or without hypoxic preconditioning. Although these mice did not have HIF1A in photoreceptors, hypoxic preconditioning protected them from light damage indicating that protection of visual cells by hypoxic preconditioning does not depend on HIF1A in photoreceptors. From this we concluded that either the stabilization of other HIF transcription factors (e.g. HIF2A) in photoreceptors is responsible for the protection or HIF1A activates target genes in other cell layers that act in a paracrine manner to protect photoreceptors from light damage. Indeed we saw stabilization of HIF2A after hypoxic preconditioning in both OpnCre$^{(HIF-\Delta)}$ and PrPCre$^{(HIF-\Delta)}$ mice. Furthermore, other hypoxic target genes, like BCL2 like 10 (*Bcl2l10*), metallothionein 1 (*Mt1*) and 2 (*Mt2*), epidermal growth factor (*Egf*) and *Epo,* were still induced in both HIF1A knock-downs after hypoxic preconditioning.

Retinal neuroprotection by hypoxic preconditioning is independent of hypoxia-inducible factor-1α expression in photoreceptors

Markus Thiersch,[1] Christina Lange,[1] Sandrine Joly,[1] Severin Heynen,[1] Yun Zheng Le,[2] Marijana Samardzija[1] and Christian Grimm[1]
[1]Department of Ophthalmology, Laboratory of Retinal Cell Biology, Center for Integrative Human Physiology and Neuroscience Center Zurich, University of Zurich, Frauenklinikstrasse 24, CH-8091 Zurich, Switzerland
[2]Health Sciences Center, University of Oklahoma, Oklahoma City, OK, USA

Keywords: cell survival, degeneration, HIF, hypoxia, retina

Abstract

Hypoxic preconditioning stabilizes hypoxia-inducible factor (HIF) 1α in the retina and protects photoreceptors against light-induced cell death. HIF-1α is one of the major transcription factors responding to low oxygen tension and can differentially regulate a large number of target genes. To analyse whether photoreceptor-specific expression of HIF-1α is essential to protect photoreceptors by hypoxic preconditioning, we knocked down expression of HIF-1α specifically in photoreceptor cells, using the cyclization recombinase (Cre)–lox system. The Cre-mediated knockdown caused a 20-fold reduced expression of *Hif-1α* in the photoreceptor cell layer. In the total retina, RNA expression was reduced by 65%, and hypoxic preconditioning led to only a small increase in HIF-1α protein levels. Accordingly, HIF-1 target gene expression after hypoxia was significantly diminished. Retinas of *Hif-1α* knockdown animals did not show any pathological alterations, and tolerated hypoxic exposure in a comparable way to wild-type retinas. Importantly, the strong neuroprotective effect of hypoxic preconditioning against light-induced photoreceptor degeneration persisted in knockdown mice, suggesting that hypoxia-mediated survival of light exposure does not depend on an autocrine action of HIF-1α in photoreceptor cells. Hypoxia-mediated stabilization of HIF-2α and phosphorylation of signal transducer and activator of transcription 3 (STAT 3) were not affected in the retinas of *Hif-1α* knockdown mice. Thus, these factors are candidates for regulating the resistance of photoreceptors to light damage after hypoxic preconditioning, along with several potentially neuroprotective genes that were similarly induced in hypoxic knockdown and control mice.

Introduction

Photoreceptor degeneration is common to many blinding diseases, including retinitis pigmentosa and age-related macular degeneration. Whereas retinitis pigmentosa is a monogenetic disorder primarily affecting photoreceptors, the pathology of age-related macular degeneration is complex and involves the death of cells of the retinal pigment epithelium and of photoreceptors, changes in Bruch's membrane, formation of Drusen and – in the wet form of the disease – neovascularization. To mimic photoreceptor degeneration as part of the retinal pathology in these diseases, mice are exposed to cytotoxic levels of white light, which triggers apoptosis in photoreceptors (Wenzel *et al.*, 2005). Different strategies, such as hypoxic and ischemic preconditioning, have been shown to inhibit cell death and to protect non-neuronal as well as neuronal tissues – including the retina – from apoptosis (Gage & Stanton, 1996; Barone *et al.*, 1998; Roth *et al.*, 1998; Gidday *et al.*, 1999; Grimm *et al.*, 2002; Tanaka *et al.*, 2002; Zhang *et al.*, 2002; Sharp *et al.*, 2004; Zhu *et al.*, 2007). The underlying pro-survival mechanisms are not completely understood. However, it is clear that cells respond to hypoxia with the differential regulation of genes driven by several major transcription factors. Among those, hypoxia-inducible factors (HIFs) are the most prominent proteins regulating the tissue response to low oxygen levels. The HIF family consists of three identified members, with HIF-1 being the best-characterized protein (Bruick & McKnight, 2002). It is a heterodimeric transcription factor consisting of the HIF-1α and HIF-1β subunits. Both proteins are ubiquitously expressed, with HIF-1α being post-translationally regulated by oxygen availability (Wang & Semenza, 1993, 1995). Under normoxic conditions, prolylhydroxylases (PHDs) hydroxylate HIF-1α at specific proline residues (Bruick & McKnight, 2001; Ivan *et al.*, 2001; Jaakkola *et al.*, 2001), providing the substrate for the von Hippel-Lindau protein, which initiates the cumulative binding of ubiquitin to the protein. This finally results in the efficient degradation of HIF-1α via the proteosomal degradation pathway (Salceda & Caro, 1997; Huang *et al.*, 1998). Additionally,

Correspondence: Dr C. Grimm, as above.
E-mail: cgrimm@opht.uzh.ch

Received 30 October 2008, revised 7 April 2009, accepted 19 April 2009

factor inhibiting HIF (FIH) hydroxylates HIF-1α at an asparagine residue in the transactivation domain to inhibit the binding of transcriptional cofactors (Mahon *et al.*, 2001). Under hypoxic conditions, the hydroxylases fail to hydroxylate HIF-1α, resulting in its stabilization and activation. Stabilized HIF-1α is transferred into the nucleus, where it binds its partner HIF-1β to form HIF-1, which differentially regulates the expression of many genes involved in apoptosis, cell survival, angiogenesis and metabolism (Bruick & McKnight, 2002).

Many reports have connected HIF-1α to tissue protection and neuroprotection (Ran *et al.*, 2005; Siddiq *et al.*, 2005; Hill *et al.*, 2008; Rosenberger *et al.*, 2008). Recently, it was reported that cardioprotection against ischemia–reperfusion after ischemic preconditioning requires HIF-1α expression (Cai *et al.*, 2008) and that neuronal ablation of HIF-1α enhances pathological effects after cerebral ischemia (Baranova *et al.*, 2007). In the retina, HIF-1α was found, in association with heat shock protein 27, nitric oxide synthase or heme oxygenase-1, to protect against ischemia after ischemic preconditioning (Whitlock *et al.*, 2005; Kaur *et al.*, 2006; Zhu *et al.*, 2007). Additionally, the level of HIF-1α stabilization after hypoxic preconditioning correlated with the degree of photoreceptor protection from light-induced degeneration (Grimm *et al.*, 2002). Part of this neuroprotective response was attributed to erythropoietin (Grimm *et al.*, 2002), which, as newer data indicate, may mainly be regulated by HIF-2 and not by HIF-1 (Rankin *et al.*, 2007). This suggests that HIF-2 may have neuroprotective activity affecting cell survival after a toxic insult. To date, the impact of HIF-1α on retinal neuroprotection after hypoxic preconditioning has not been analysed in detail. Using tissue-specific knockdown mice, we analysed whether photoreceptors require intrinsic activity of HIF-1α to survive light exposure after hypoxic preconditioning.

Materials and methods

Animals

Animals were treated in accordance with the regulations of the Veterinary Authority of Zurich and with the statement of 'The Association for Research in Vision and Ophthalmology' for the use of animals in research. Mice carrying a floxed exon 2 of HIF-1α (HIF-1$\alpha^{F/F}$) (Ryan *et al.*, 2000) were kindly provided by R. Johnson (UCSD, San Diego, CA, USA) and M. Gassmann (University of Zurich, Zurich, Switzerland), and PrP-Cre-ER^{T}(28.4) mice (Weber *et al.*, 2001) were obtained from P. Chambon (IGBMC, Strasbourg, France). LMOPC1 mice [expressing cyclization recombinase (Cre) under the control of the rod opsin promoter] have been described previously (Le *et al.*, 2006). To generate conditional knockdown mice, HIF-1$\alpha^{F/F}$ mice were bred with PrP-Cre-ER^{T}(28.4) mice or with LMOPC1 mice, according to classical breeding schemes. All mouse strains analysed were maintained on a homozygous Rpe65$_{450Leu}$ background (Wenzel *et al.*, 2003). To simplify matters, LMOPC1:HIF-1$\alpha^{\Delta/\Delta}$ mice were named OpnCre$^{(HIF\text{-}\Delta)}$, and HIF-1$\alpha^{F/F}$ control mice were named OpnCre$^{(HIF\text{-}wt)}$. PrP-Cre-ER^{T}(28.4) mice required tamoxifen (TAM) to induce Cre activity. TAM was dissolved in sunflower oil (Sigma-Aldrich, Buchs, Switzerland) to obtain a concentration of 10 mg/mL. TAM (1 mg/40 g) was injected intraperitoneally into 3-week-old animals twice a day for five consecutive days. Control injections were performed with oil only. After injections, mice were allowed to recover for 2 weeks before experiments were performed. In keeping with the above nomenclature, TAM-treated knockdown animals [PrP-Cre-ER^{T}(28.4):HIF$^{\Delta/\Delta}$] were named PrpCre$^{(HIF\text{-}\Delta)}$, and oil-treated PrP-Cre-ER^{T}(28.4):HIF$^{F/F}$ control mice were named PrpCre$^{(HIF\text{-}wt)}$. For tissue isolation and analysis, mice were killed by CO_2 anesthesia followed by cervical dislocation.

Hypoxic preconditioning and light exposure

Hypoxic preconditioning (6–7% O_2 for 6 h) was performed as described previously (Grimm *et al.*, 2002). After hypoxia, mice were killed at the indicated time points for tissue collection or were dark adapted for 4 h before light onset. For light exposure, pupils of mice were dilated in dim red light using 1% cyclogyl (Alcon, Cham, Switzerland) and 5% phenylephrine (Ciba Vision, Niederwangen, Switzerland) 45 min prior to illumination. After light exposure (13 000 lux; 2 h), animals remained in darkness overnight and were analysed after 36 h or at the time points indicated.

Morphology and cell death detection

To analyse morphology, mice were killed 36 h after light exposure. Eyes were enucleated and processed for light microscopy as previously described (Samardzija *et al.*, 2006). A digitalized Axiovision microscope (Carl Zeiss Microscopy, Jena, Germany) using ×40 objective lenses with a numerical aperture of 1.3 was used to examine slides. Representative images were taken from the inferior temporal retina. To balance for staining variabilities, contrast and brightness were sometimes slightly adjusted. As a semiquantitative assessment of apoptosis, nucleosomal release was determined at 36 h after light exposure, using a cell death detection kit (Roche Diagnostics, Basel, Switzerland), according to the manufacturer's recommendation.

RNA isolation and real-time PCR

Retinas were isolated immediately after hypoxic preconditioning, frozen in liquid nitrogen and stored at −80°C. Normoxic controls were treated in parallel and collected at the same time points. Total retinal RNA was extracted using the RNeasy isolation kit (Qiagen, Hilden, Germany), including a DNase treatment to digest residual genomic DNA. cDNA was prepared from equal amounts of total retinal RNA using oligo(dT) primers and Moloney murine leukemia virus reverse transcriptase (Promega, Madison, WI, USA). Five nanograms of cDNA was amplified in a LightCycler 480 instrument (Roche Diagnostics AG, Rotkreuz, Switzerland) using LightCycler 480 SYBR Green I Master Mix (Roche Diagnostics AG, Rotkreuz, Switzerland) and appropriate primer pairs (Table 1). cDNA levels were normalized to β-actin, and relative values were calculated using a respective calibrator. At least eight independent samples were used for each condition in PrpCre mice and five in OpnCre mice.

Western blotting

Retinas were sonified in 0.1 M Tris-HCl (pH 8.0) at 4°C, and protein content was determined using a BCA Protein Assay Kit (Pierce, Rockford, IL, USA). Protein extracts were mixed with sodium dodecylsulfate (SDS) sample buffer and incubated for 10 min at 95°C. Proteins were separated by SDS polyacrylamide gel electrophoresis and blotted onto a nitrocellulose membrane. After blocking with 5% non-fat dry milk (Bio-Rad, Munich, Germany) in 10 mM Tris-HCl (pH 8), 150 mM NaCl and 0.05% Tween-20, membranes were incubated with primary antibodies at 4°C overnight. Primary antibodies used were as follows: rabbit anti-HIF-1α (Novus Biologicals NB, Littleton, CA, USA; 100–479; 1 : 1000); rabbit anti-phospho-signal transducer and activator of transcription 3 (STAT3) (Cell Signaling, Danvers, MA, USA; #9131; 1 : 500); rabbit anti-STAT3 (Cell Signalling; #9132; 1 : 1000); rabbit anti-HIF-2α (Novus Biologicals; 100–480; 1 : 500); and goat anti-β-actin (Santa Cruz,

TABLE 1. Primer pairs used for polymerase chain reaction

Gene	Forward primer	Reverse primer	Size of product (bp)
β-Actin	CAACGGCTCCGGCATGTGC	CTCTTGCTCTGGGCCTCG	153
Adm	TTCGCAGTTCCGAAAGAAGT	GGTAGCTGCTGGATGCTTGTA	77
Bcl2l10	GAACTTTCTGTATAATCTGCTCATGG	TGAAGAAGCGGCAAAAGC	89
Bnip3	CCTGTCGCAGTTGGGTTC	GAAGTGCAGTTCTACCCAGGAG	93
Chx10	CCAGAAGACAGGATACAGGTG	GGCTCCATAGAGACCATACT	111
Egf	CATGCCCCACAGGATTTG	GGGCAGGAAACAAGTTCGT	64
Egln1	CATTGTTGGCAGAAGGTGTG	CAAAGGACTACAGGGTCTCCA	70
Epo	GCCCTGCTAGCCAATTCC	GGCGACATCAATTCCTTCTG	128
Glut1	ATGGATCCCAGCAGCAAG	CCAGTGTTATAGCCGAACTGC	92
Gnat1	GAGGATGCTGAGAAGGATGC	TGAATGTTGAGCGTGGTCAT	209
Hif-1α	TCATCAGTTGCCACTTCCCCAC	CCGTCATCTGTTAGCACCATCAC	198
Hif-2α	GGAGCTCAAAAGGTGTCAGG	CAGGTAAGGCTCGAACGATG	61
Mt1	GAATGGACCCCAACTGCTC	GCAGCAGCTCTTCTTGCAG	104
Mt2	TCTTCAAACCGATCTCTCGTCG	CAGCAGCTTTTCTTGCAGGAAG	94
Opn4	CCAGCTTCACAACCAGTCCT	CAGCCTGATGTGCAGATGTC	111
Vegf	ACTTGTGTTGGGAGGAGGATGTC	AATGGGTTTGTCGTGTTTCTGG	171

Santa Cruz, CA, USA; sc1616; 1 : 1000). After incubation with horseradish peroxidase-labeled secondary antibodies for 1 h at room temperature, the protein bands were visualized by the application of a chemiluminescent substrate (PerkinElmer, Boston, MA, USA) and exposure to a Super RX film (Fujifilm, Dielsdorf, Switzerland). For protein analyses, at least four individual samples were used for each condition.

Immunofluorescence

Eyes were isolated and incubated for 10 min in phosphate-buffered saline (PBS) containing 4% paraformaldehyde. The cornea and lens were removed, and the remaining tissue, including the retina, was incubated for another 15 min in 4% paraformaldehyde. Eyecups were then kept in 30% sucrose and embedded in cryoprotective medium (Jung, Nussloch, Germany). Twelve-micrometer sections were cut, and cryoslides were blocked in a humid chamber with PBS containing 3% normal goat serum and 0.3% Triton X-100. Slides were incubated with rabbit anti-HIF-1α antibody (Novus Biologicals; 100–654; 1 : 100). After being washed with PBS, slides were incubated with Cy3-labeled secondary antibodies (Jackson ImmunoResearch Europe, Newmarket, UK), for 1 h at room temperature, washed with PBS, counterstained with 4′,6-diamidino-2-phenylindole dilactate (Molecular Probes, Invitrogen, Carlsbad, CA, USA) and mounted with Mowiol 4-88 Reagent (VWR International AG, Lucerna, Switzerland). Immunofluorescent stainings were analysed with a digitalized Axiovision microscope (Carl Zeiss Microscopy) using ×20 objective lenses with a numerical aperture of 0.5. Stainings on normoxic and hypoxic samples were performed in parallel on the same slide.

Laser capture microdissection

For laser capture microdissection (LCM), eyes were enucleated, embedded in RNase-free cryoprotective medium (Jung) and stored at −80°C. Samples were cut (12 μm) and transferred to nuclease-free and human nucleic acid-free membrane slides (Molecular Machines & Industries, Glattbrugg, Switzerland). Prior to LCM, samples were incubated with acetone (5 min), 99.9% ethanol (30 s) and xylol (5 min). After acetone and xylol incubation, slides were dried for 5 and 30 min, respectively. Laser-captured tissues were collected in tubes with an adhesive lid (Molecular Machines & Industries) and stored at −80°C. RNA was isolated using the RNeasy Micro Kit (Qiagen) according to the manufacturer's recommendations, including a DNase treatment to digest residual genomic DNA. cDNA synthesis and analyses were performed as described above.

Statistical analyses

For statistical validations of gene expression, we used unpaired, two-tailed Student *t*-tests for the individual comparisons between wild-type and knockdown mice in normoxia or hypoxia, respectively. *F*-values, *t*-ratios (*t*), degrees of freedom (d.f.) and number of samples (*n*) are given for each analysis in the main text. One-way ANOVA with Bonferroni post-tests was used to compare the cell death of normoxic and hypoxic wild-type or knockdown mice, respectively, with controls. *F*-values, total (treatment plus residual) d.f., *t*-ratios (*t*) for each post-test, and number of samples (*n*), as well as whether *P*-values were above or below the level of significance ($P > 0.05$ or $P < 0.05$) are given in the Results. All calculations were performed using PRISM software (GraphPad Prism Software Inc., San Diego, CA, USA).

Results

HIF-1α is expressed in all retinal cell layers

The *Hif-1α* gene is ubiquitously expressed in almost all eukaryotic cells. To analyse the mRNA expression of *Hif-1α* and its family member *Hif-2α* in the different layers of the mouse retina, we isolated the outer nuclear layer (ONL), the inner nuclear layer (INL) and the ganglion cell layer (GCL) by LCM of normoxic adult PrpCre$^{(HIF\text{-}wt)}$ mice, and analysed gene expression by reverse transcription polymerase chain reaction. Whereas mRNAs of the control genes *Gnat1* (encoding transducin) (ONL), *Chx10* (encoding visual system homeobox 2) (INL) and *Opn4* (encoding melanopsin) (GCL) were mainly detected in their expected layers, *Hif-1α* and *Hif-2α* were expressed in all layers of the retina (Fig. 1A).

To analyse the protein distribution of HIF-1α, we performed immunostaining on normoxic and hypoxic retinas. In normoxic mice, HIF-1α protein is rapidly degraded and is therefore hardly detectable. Nevertheless, immunostaining for HIF-1α showed some residual protein in the normoxic GCL (Fig. 1B). During hypoxia, HIF-1α protein is stabilized, and a strong accumulation of HIF-1α was observed in the GCL and INL (Fig. 1B), as reported previously (Ozaki *et al.*, 1999; Zhu *et al.*, 2007). In addition, we also observed intense HIF-1α staining in the ONL, supporting our RNA data indicating that HIF-1α is expressed in all retinal cell layers.

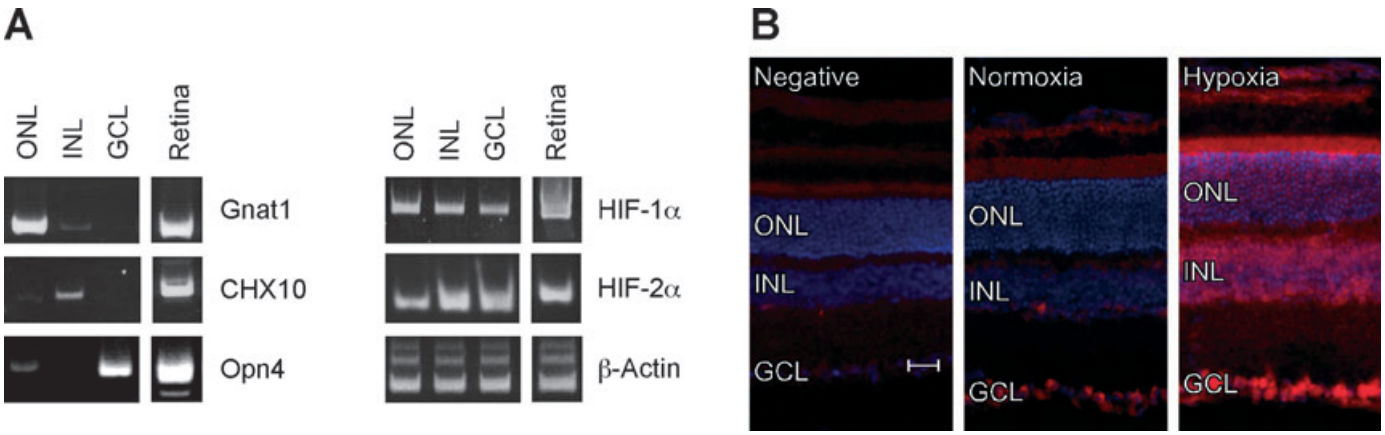

FIG. 1. Distribution of HIF-1α mRNA and protein in the retina. (A) HIF-1α and HIF-2α mRNA expression in the outer nuclear layer (ONL), inner nuclear layer (INL) and ganglion cell layer (GCL) isolated by laser capture microdissection. Captured fragments of three mice were pooled and analysed by conventional real-time polymerase chain reaction. HIF-1α and HIF-2α expression was observed in all retinal cell layers. *Gnat1* (ONL marker), *Chx10* (INL marker) and *Opn4* (GCL marker) served as indicators for the purity of the isolated tissue fragments (note that minor cross-contaminations were detected). Total retinal RNA was used as positive control. (B) Protein distribution of HIF-1α in the retina of normoxic mice and immediately after hypoxia (6% O_2; 6 h). Immunofluorescence staining indicates stable HIF-1α protein in the GCL during normoxia and the stabilization of HIF-1α protein in the whole retina during hypoxia. A normoxic retina served as a negative control, incubated with the secondary antibody (Cy3 anti-rabbit) alone. Scale bar: 25 μm.

Deletion of Hif-1α in photoreceptor cells

The stabilization of HIF-1α in the ONL during hypoxia suggests that it might be needed by photoreceptors to cope with hypoxic stress. To investigate the role of HIF-1α in photoreceptor cells, we generated two mouse strains with photoreceptor-specific deletions of *Hif-1α* (see Materials and methods). PrpCre mice express TAM-inducible Cre under the control of the prion protein promoter (Prp), whereas OpnCre mice express Cre under the control of the rod opsin promoter. Both mouse lines have been reported to express Cre specifically in photoreceptor cells (Weber *et al.*, 2001; Le *et al.*, 2006). To generate $PrpCre^{(HIF-\Delta)}$ mice, $PrpCre^{(HIF-wt)}$ mice were treated with TAM to delete *Hif-1α* in the adult retina, leaving postnatal retinal development undisturbed. Oil-treated $PrpCre^{(HIF-wt)}$ mice served as controls. After a recovery phase of 2 weeks after the last TAM (or oil) injection, we performed experiments in $PrpCre^{(HIF-\Delta)}$ and $PrpCre^{(HIF-wt)}$ mice at 6 weeks of age. Likewise, $OpnCre^{(HIF-\Delta)}$ mice, which start to delete the floxed target sequence at postnatal day (PND) 7 (Le *et al.*, 2006) and $OpnCre^{(HIF-wt)}$ control mice were 6 weeks of age when used for experiments.

To determine the knockdown efficiency in the two strains, we isolated total retinal mRNA and protein of at least five independent mice. In normoxic $OpnCre^{(HIF-\Delta)}$ mice, *Hif-1α* mRNA levels were significantly ($P = 0.019$, $F = 3.409$, $t = 2.919$, d.f. = 8, $n = 5$ for each strain) reduced, to nearly 50% of those of control mice (Fig. 2A, left panel).

As this analysis included RNA from cells of the INL and GCL, which do not (or do not strongly) express Cre, most of the detected *Hif-1α* mRNA in retinas of $OpnCre^{(HIF-\Delta)}$ mice was likely to be expressed in cells other than photoreceptors. Under hypoxic conditions, *Hif-1α* RNA levels were not significantly ($P = 0.117$, $F = 2.470$, $t = 1.756$, d.f. = 8, $n = 5$ for each strain) different from those of controls, suggesting an incomplete deletion of the *Hif-1α* gene in photoreceptors. In $PrpCre^{(HIF-\Delta)}$ mice, *Hif-1α* RNA levels were strongly and significantly reduced to 35% of those of controls in both normoxic ($P = 0.0003$, $F = 6.263$, $t = 4.810$, d.f. = 14, $n = 8$ for each strain) and hypoxic ($P = 0.0001$, $F = 2.355$, $t = 8.655$, d.f. = 14, $n = 8$ for each strain) retinas (Fig. 2A, right panel). LCM was used to test the specificity of *Hif-1α* deletion in retinas of $PrpCre^{(HIF-\Delta)}$ mice. The ONL had 20-fold reduced *Hif-1α* RNA levels as compared to controls (Fig. 2B). As expression of *Hif-1α* is not regulated at the gene level, these data indicate that only between 5 and 10% of the cells in the ONL still express both or one allele of *Hif-1α*, respectively. Thus, at least 90% of photoreceptors are genuine *Hif-1α* knockout cells, whereas the other cells are either heterozygous or wild type for *Hif-1α*. In contrast, cells of the INL and GCL of $PrpCre^{(HIF-\Delta)}$ mice showed only a two-fold reduced expression of *Hif-1α* mRNA, indicating that *Hif-1α* deletion was restricted mainly but not exclusively to photoreceptor cells. Although most cells in the ONL are knockouts, on a tissue level (whole retina), $PrpCre^{(HIF-\Delta)}$ mice are, rather, knockdowns for HIF-1α. The reason for the reduced *Hif-1α* RNA levels in the INL and GCL is not known, but they may be due to Cre activity in some cells other than photoreceptors. The general integrity of gene expression in Cre-expressing $PrpCre^{(HIF-\Delta)}$ mice was not affected, as suggested by the normal RNA levels of *Chx10* in the INL and *Gnat1* in the ONL (data not shown).

To investigate the effect of the *Hif-1α* deletion on protein levels, we performed western blotting of normoxic or hypoxic preconditioned $PrpCre^{(HIF)}$ and $OpnCre^{(HIF)}$ mice (Fig. 2C). As expected, we observed only very faint bands in normoxic animals and strong stabilization of HIF-1α in hypoxic control animals. The comparison between hypoxic $PrpCre^{(HIF-wt)}$ and $PrpCre^{(HIF-\Delta)}$ mice showed that the HIF-1α protein levels were dramatically reduced in knockdown mice (Fig. 2C). In fact, they seemed to reach almost the basal levels of normoxic mice, indicating that the knockdown efficiency was very high at the protein level. In contrast, $OpnCre^{(HIF-\Delta)}$ mice showed less pronounced reduction of HIF-1α protein expression during hypoxia when compared to control levels.

In conclusion, $PrpCre^{(HIF-\Delta)}$ mice showed a very strong reduction of *Hif-1α* expression, predominantly in photoreceptor cells. $OpnCre^{(HIF-\Delta)}$ mice presented a less severe reduction, with more HIF-1α protein remaining in the retina after hypoxic exposure.

Reduced HIF-1α target gene expression in knockdown mice

Hif-1α regulates the expression of many genes during hypoxia. To analyse the effect of reduced HIF-1α protein levels on *Hif-1α* target gene expression after hypoxic preconditioning, we determined mRNA expression levels in normoxic and hypoxic retinas (Fig. 3). The EGL

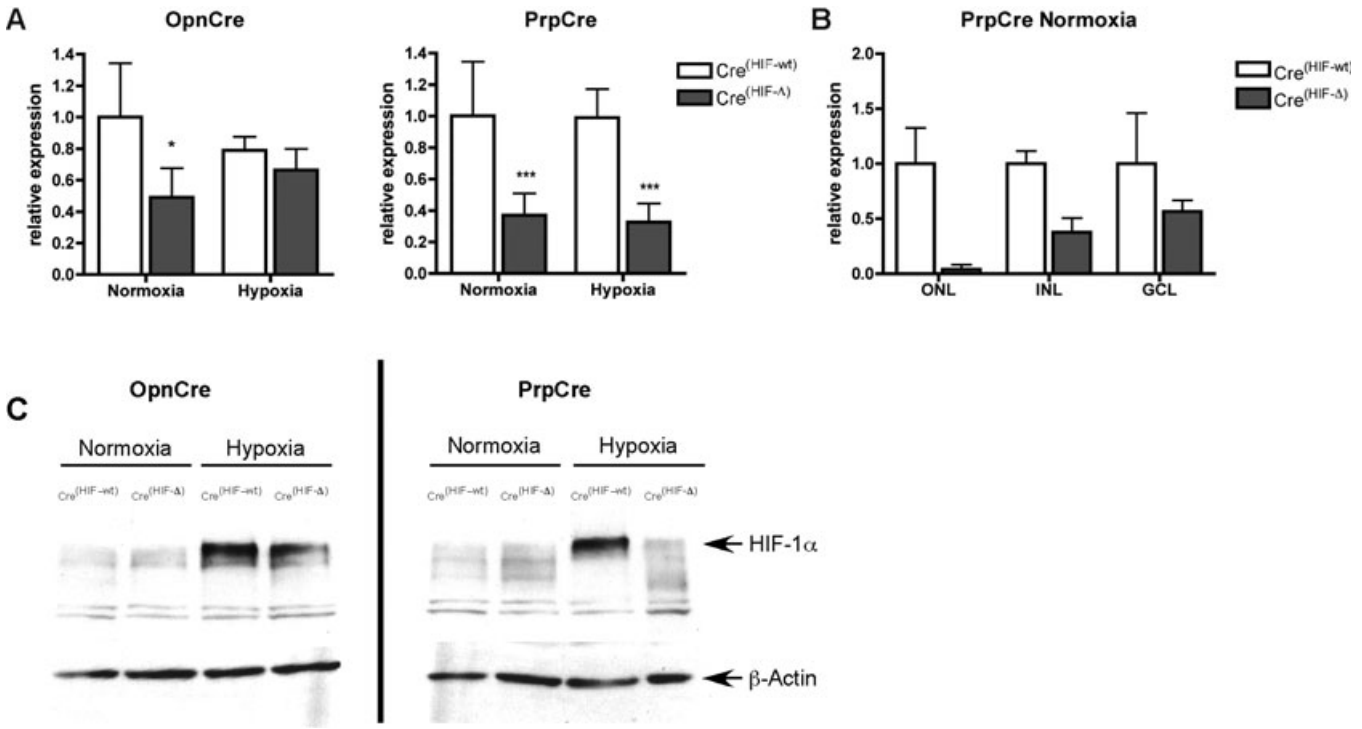

FIG. 2. Efficiency of HIF-1α knockdown in the outer nuclear layer (ONL). Gene and protein expression was analysed in mice held in normoxia or in mice immediately after exposure to hypoxia (6% O_2; 6 h). (A) Total retinal levels of *Hif-1α* mRNA were analysed by real-time polymerase chain reaction in opsin-Cre-mediated (left panel) and PrpCre-mediated (right panel) HIF-1α knockdowns (gray bars) and compared to their respective wild-type controls (white bars). *β*-Actin served as reference, and data were normalized to levels of normoxic $Cre^{(HIF\text{-}wt)}$ mice (first bar of each panel). Under normoxic conditions, $OpnCre^{(HIF\text{-}\Delta)}$ mice displayed HIF-1α mRNA levels that were significantly (*$P = 0.0193$, $n = 5$) reduced, by 50%. After hypoxia, no significant ($P = 0.117$, $n = 5$) differences were detectable. HIF-1α deletion in $PrpCre^{(HIF\text{-}\Delta)}$ mice was very efficient, and significantly reduced expression of *Hif-1α* to 35% of control levels under both normoxic (***$P = 0.0003$, $n = 8$) and hypoxic (***$P = 0.0001$, $n = 8$) conditions. Means ± standard deviations are given. Statistical validations were performed using unpaired, two-tailed *t*-tests. (B) *Hif-1α* RNA expression in normoxic $PrpCre^{(HIF\text{-}\Delta)}$ (gray bars) mice as compared with normoxic $PrpCre^{(HIF\text{-}wt)}$ (white bar) mice in the ONL, inner nuclear layer (INL) and ganglion cell layer (GCL) after laser capture microdissection. For each retinal layer, tissue was pooled from three individual mice. *β*-Actin expression served as reference, and data were normalized to expression levels of $PrpCre^{(HIF\text{-}wt)}$ in each individual layer (set to 1). *Hif-1α* RNA expression was reduced 20-fold in the ONL of $PrpCre^{(HIF\text{-}\Delta)}$ mice but only two-fold in the INL and GCL. Mean values ± standard deviations of three mice are shown. (C) Western blot analysis of retinal HIF-1α protein expression in normoxic and hypoxic HIF-1α knockdown and wild-type mice as indicated. Only faint protein bands were observed under normoxic conditions. After hypoxia, HIF-1α protein expression was increased in retinas of control $OpnCre^{(HIF\text{-}wt)}$ and $PrpCre^{(HIF\text{-}wt)}$ mice. In hypoxic $OpnCre^{(HIF\text{-}\Delta)}$ mice, HIF-1α protein levels were only slightly diminished, but hypoxic $PrpCre^{(HIF\text{-}\Delta)}$ mice showed severely reduced HIF-1α protein expression. Representative blots of four mice are shown.

nine homolog 1 gene (*Egln1*) encodes PHD2, which is required for the oxygen-dependent degradation of HIF-1α (Bruick & McKnight, 2001; Ivan *et al.*, 2001; Jaakkola *et al.*, 2001). In $PrpCre^{(HIF\text{-}wt)}$ mice and $OpnCre^{(HIF\text{-}wt)}$ mice, *Egln1* RNA levels were induced fivefold to sixfold immediately after hypoxia (Fig. 3). The *Egln1* induction was significantly suppressed by more than 50% in $PrpCre^{(HIF\text{-}\Delta)}$ mice ($P < 0.0001$, $t = 7.142$, $F = 1.501$, d.f. = 14, $n = 8$ for each strain) and by about 30% in $OpnCre^{(HIF\text{-}\Delta)}$ mice ($P = 0.0072$, $F = 2.562$, $t = 3.579$, d.f. = 8, $n = 5$ for each strain). Similarly reduced mRNA levels after hypoxia were found in the $PrpCre^{(HIF\text{-}\Delta)}$ strain for other HIF-1α target genes, such as the pro-apoptotic gene *Bnip3* (encoding BCL2/adenovirus E1B interacting protein 3) ($P = 0.0001$, $F = 2.981$, $t = 6.261$, d.f. = 14, $n = 8$ for each strain), the potentially anti-apoptotic genes *Vegf* (encoding vascular endothelial growth factor) ($P = 0.0011$, $F = 2.980$, $t = 4.085$, d.f. = 14, $n = 8$ for each strain) and *Adm* (encoding adrenomedullin) ($P = 0.0002$, $F = 1.284$, $t = 4.884$, d.f. = 14, $n = 8$ for each strain) as well as *Glut1* [encoding solute carrier family 2 (facilitated glucose transporter), member 1] ($P < 0.0001$, $F = 1.157$, $t = 9.052$, d.f. = 14, $n = 8$ for each strain). RNA levels were also reduced in the hypoxic $OpnCre^{(HIF\text{-}\Delta)}$ mice, but reached significance only for *Egln1* (see above) and *Glut1* ($P = 0.0362$, $F = 2.023$, $t = 2.514$, d.f. = 8, $n = 5$ for each strain). The milder reduction of hypoxic mRNA expression in $OpnCre^{(HIF\text{-}\Delta)}$ mice than in $PrpCre^{(HIF\text{-}\Delta)}$ mice nicely reflects the different knock-down efficiencies in the two strains.

Normal retinal development and retinal resistance to hypoxia in mice with reduced HIF-1α levels

It has been reported that TAM treatment in patients after breast cancer surgery can very occasionally cause mild pathogenic changes in the retina (Heier *et al.*, 1994; Tang *et al.*, 1997; Bourla *et al.*, 2007). On the other hand, small doses of TAM have been shown to promote neuroprotection (Zhang *et al.*, 2007; Wakade *et al.*, 2008). However, neither TAM nor oil treatment had an obvious effect on retinal morphology in control mice up to 4 months post-injection (Fig. 4A). Additionally, wild-type mice treated with oil and TAM were equally susceptible to light-induced retinal degeneration 2 weeks after TAM application (data not shown), indicating that TAM neither impaired normal retinal morphology nor protected the retina against a toxic light insult *per se*.

As HIF-1α has been shown to be important for coping with hypoxic conditions in neurons (Vangeison *et al.*, 2008), and as the retina

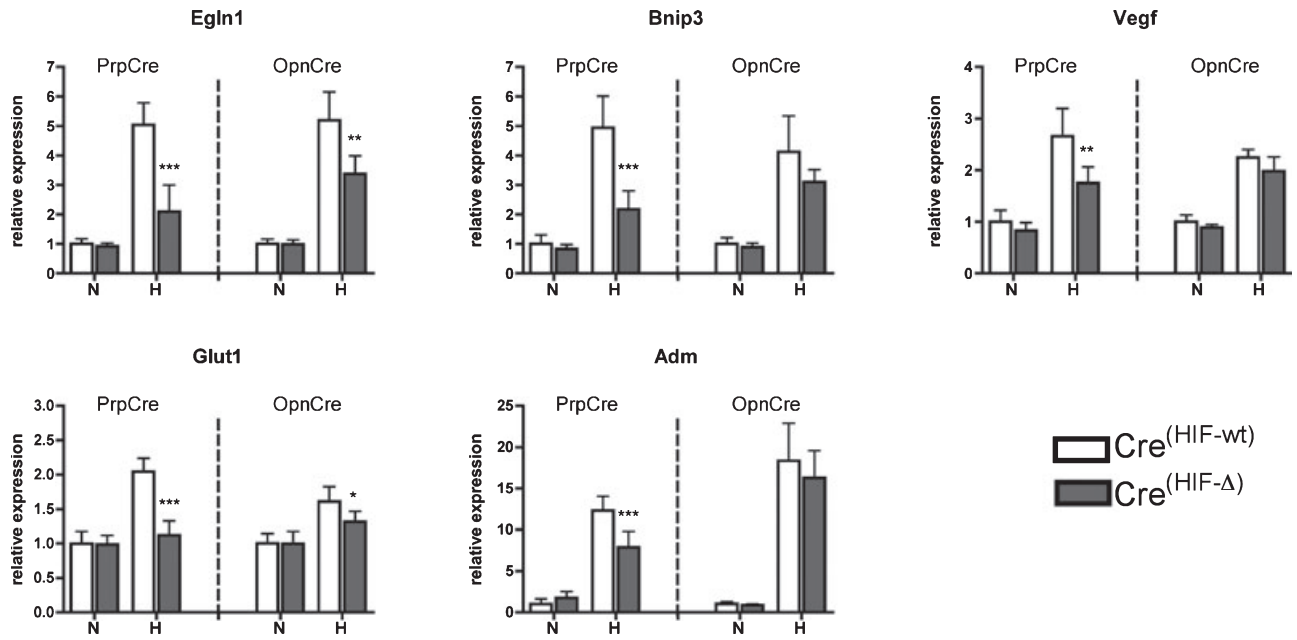

FIG. 3. Expression of HIF-1α target genes in total retina. mRNA levels of HIF-1α target genes were determined immediately after hypoxia or in normoxic controls in total retinal RNA. mRNA expression in OpnCre$^{(HIF-\Delta)}$ and PrpCre$^{(HIF-\Delta)}$ mice (gray bars) was compared to that in OpnCre$^{(HIF-wt)}$ and PrpCre$^{(HIF-wt)}$ control mice (white bars). Expression levels of normoxic (N) Cre$^{(HIF-wt)}$ mice (first bars) were set to '1'. β-Actin expression served as a reference. Expression levels in normoxic Cre$^{(HIF-wt)}$ and Cre$^{(HIF-\Delta)}$ mice were comparable. During hypoxia (H), all tested HIF-1α target genes were induced in control mice. In hypoxic PrpCre$^{(HIF-\Delta)}$ mice, the induction of all tested HIF-1α target genes was significantly repressed (***P = 0.0002; **P = 0.0011; n = 5). Hypoxic OpnCre$^{(HIF-\Delta)}$ mice showed a milder effect, which reached significance only for *Egln1* (**P = 0.0072, n = 5) and *Glut1* (*P = 0.0362, n = 5). Means ± standard deviations are shown. Statistical validations were performed using unpaired, two-tailed t-tests.

becomes borderline hypoxic during dark phases (Cringle *et al.*, 2002), we investigated whether the absence of HIF-1α from photoreceptors in PrpCre$^{(HIF-\Delta)}$ mice during normoxia or hypoxia would be harmful to the retina even without subsequent exposure to damaging light. PrpCre$^{(HIF-wt)}$ and PrpCre$^{(HIF-\Delta)}$ mice were kept in a standard animal facility with a 12 : 12-h day/night cycle for 4 months. During this time, no obvious morphological alterations appeared, and the retinas of control and knockdown mice were similar (Fig. 4B, upper panels). Surprisingly, even a short period of severe hypoxia (6%, 6 h) followed by a recovery period of 4 weeks did not induce any noticeable changes in the retina of PrpCre$^{(HIF-\Delta)}$ mice (Fig. 4B, lower panels).

During postnatal development, HIF-1α is strongly upregulated from PND5 to PND14 (Ozaki *et al.*, 1999; Grimm *et al.*, 2005). Although excision of a large percentage of floxed sequences by the opsin-driven Cre requires several weeks, recombination in OpnCre mice starts around PND7 (Le *et al.*, 2006). We therefore investigated whether early loss of HIF-1α in some photoreceptors might influence retinal development. However, we did not observe any changes in the retinal morphology of OpnCre$^{(HIF-\Delta)}$ mice at 6 weeks of age (Fig. 4C). Also, retinal susceptibility to light damage seemed to be unimpaired (Fig. 5).

We conclude that photoreceptors can cope with acute (6% oxygen for 6 h) or mild (normal light/dark cycle) hypoxic stress in the almost complete absence of their own HIF-1α. We next investigated the influence of photoreceptor-specific HIF-1α in a pathological situation by analysing photoreceptor survival after hypoxic preconditioning and light exposure.

Neuroprotection after hypoxic preconditioning is independent of HIF-1α stabilization in photoreceptor cells

To determine whether HIF-1α in photoreceptor cells is required to establish the neuroprotective effect of hypoxic preconditioning, we compared light-induced photoreceptor death in hypoxic preconditioned control and knockdown mice. To quantify apoptosis, we measured the release of nucleosomes as indicators of ongoing apoptosis at 36 h after the toxic light insult (Fig. 5A and B). Non-exposed dark control mice of all strains showed only basal levels of free nucleosomes (Fig. 5A and B). Similarly, retinal morphology was normal (Fig. 5C, upper panels). Normoxic PrpCre$^{(HIF-wt)}$ mice [$P < 0.05$, $F = 6.349$, d.f. = 15, $t = 2.903$, $n = 3$ (control), $n = 7$ (normoxia)] and PrpCre$^{(HIF-\Delta)}$ mice [$P < 0.0001$, $F = 264.4$, d.f. = 12, $t = 18.18$, $n = 3$ (control), $n = 5$ (normoxia)] showed significant cell death when compared to their respective controls. Thus, these mice were susceptible to light damage, as expected (Fig. 5A). Hypoxic preconditioning protected against light-induced apoptosis independently of the presence of HIF-1α in photoreceptors. Cell death in both light-exposed PrpCre$^{(HIF-wt)}$ mice [$P > 0.05$, $F = 6.349$, d.f. = 15, $t = 0.4745$, $n = 3$ (control), $n = 6$ (hypoxia)] and light-exposed PrpCre$^{(HIF-\Delta)}$ mice [$P > 0.05$, $F = 264.4$, d.f. = 12, $t = 0.3677$, $n = 3$ (control), $n = 5$ (hypoxia)] was not significantly different from that in dark controls. Similar results were obtained with the OpnCre mice. Again, light exposure did not cause significantly elevated levels of free nucleosomes in hypoxic preconditioned OpnCre$^{(HIF-wt)}$ mice [$P > 0.05$, $F = 3.541$, d.f. = 15, $t = 0.002733$, $n = 3$ (control), $n = 4$ (hypoxia)] or OpnCre$^{(HIF-\Delta)}$ mice ($P > 0.05$, $F = 2.745$, d.f. = 13, $t = 0.008509$, $n = 3$ (control), $n = 4$ (hypoxia)] as compared to controls (Fig. 5B). These data were morphologically confirmed by the presence of a large number of pycnotic photoreceptor nuclei (Fig. 5C, middle panels, arrowheads) and disintegrated outer and inner segments in light-exposed normoxic wild-type and knockdown mice. Hypoxic preconditioning, however, strongly protected retinal morphology against light damage independently of the presence of HIF-1α in photoreceptors. Only a few scattered pycnotic nuclei were present, leaving the majority of photoreceptor cells unaffected by light exposure (Fig. 5C, lower panels). Analyses of

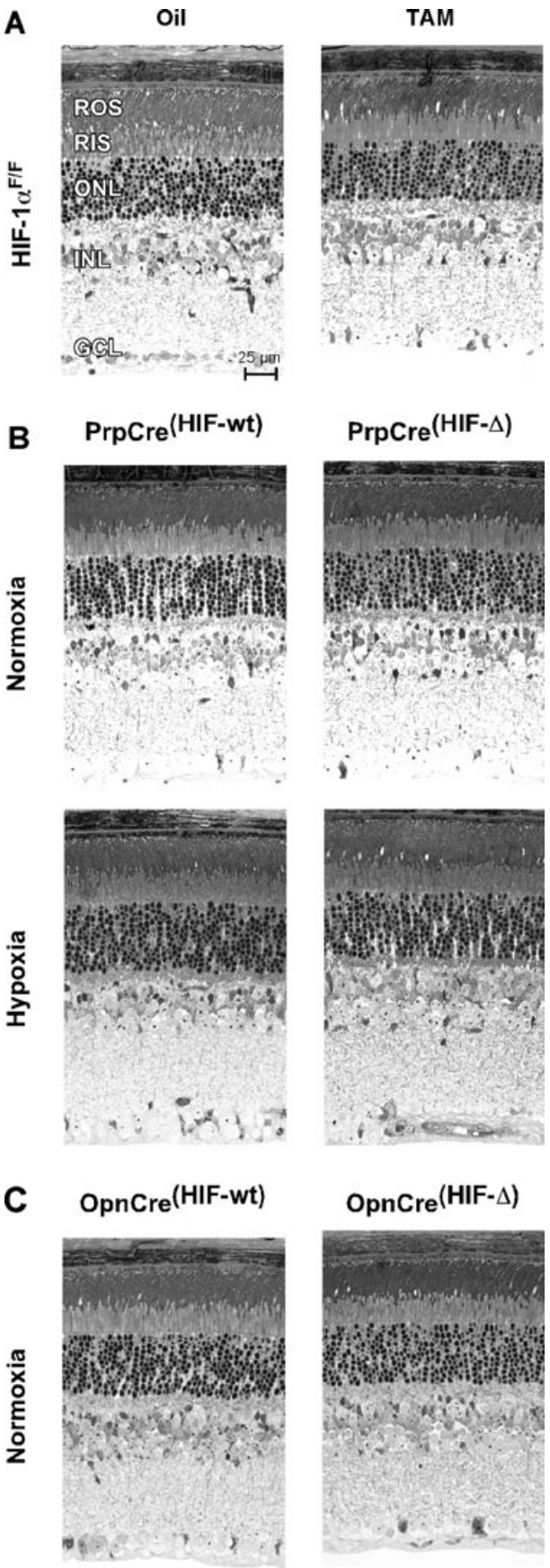

heterozygous *Hif-1α* knockout mice lacking 50% of total *Hif-1α* RNA and protein in the retina showed similar results (data not shown).

Although we successfully deleted HIF-1α from most photoreceptor cells, hypoxic preconditioning still conferred a strong neuroprotective effect, rescuing photoreceptors from light damage. This indicates that protection of visual cells by hypoxic preconditioning does not depend on HIF-1α stabilization in photoreceptors.

Alternative mechanisms for neuroprotection after hypoxic preconditioning

Hypoxia activates several transcription factors in addition to HIF-1α (Kenneth & Rocha, 2008), leading to the potential regulation of a variety of HIF-1α-independent genes. Here we analysed selected genes with potential neuroprotective properties, which have been found to be differentially regulated during hypoxia in the wild-type retina (Thiersch *et al.*, 2008). In *Hif-1α* wild-type mice, we found strong, hypoxia-driven induction of the anti-apoptotic gene *Bcl2l10* (encoding B-cell lymphoma 2-like 10), of *Mt1/2* (encoding metallothioneins 1 and 2), *Egf* (encoding endothelial growth factor) and *Epo* (encoding erythropoietin) (Fig. 6A, white bars). This induction was not affected in *Hif-1α* knockdown mice (Fig. 6A, gray bars). The only exception was *Egf*, whose expression was even slightly induced in hypoxic PrpCre$^{(HIF-\Delta)}$ mice ($P = 0.0156$, $F = 2.332$, $t = 2.751$, d.f. = 14, $n = 8$ for each strain). This suggests that these genes might be controlled by transcription factors different from HIF-1. Potential candidates are HIF-2 or STAT3, which were activated by hypoxic exposure in both control and knockdown mice (Fig. 6B). Metal-regulatory transcription factor 1 (MTF-1), which is strongly expressed in the normoxic and hypoxic retina (Supporting information, Fig. S1), might be involved in the hypoxic regulation of *Mt1* and *Mt2* expression (see Discussion). The genes not affected by the *Hif-1α* knockdown included *Epo*, which has been especially reported to have strong neuroprotective properties (Sakanaka *et al.*, 1998; Bernaudin *et al.*, 1999; Brines *et al.*, 2000; Siren *et al.*, 2001; Grimm *et al.*, 2002) and to be controlled mainly by HIF-2α (Morita *et al.*, 2003; Gruber *et al.*, 2007; Rankin *et al.*, 2007). Therefore, *Epo* might function in photoreceptor protection also in the absence of HIF-1α in photoreceptors. In conclusion, the knockdown of *Hif-1α* in photoreceptors reduced the induction of HIF-1α target genes during hypoxia without affecting the neuroprotective capacity of hypoxic preconditioning. Several genes with neuroprotective potential (e.g. *Mt1/2*, *Bcl2l10* and *Egf*; Fig. 6A), which are not affected by the HIF-1α knockdown, could potentially participate in the protection of the retina against light-induced retinal degeneration.

FIG. 4. Intraperitoneal tamoxifen (TAM) application and the ablation of HIF-1α in photoreceptor cells has no effect on the retinas of normoxic and hypoxic mice. (A) Mice carrying the floxed exon 2 of HIF-1α without Cre (HIF-1α$^{F/F}$) were intraperitoneally injected with oil or TAM as indicated. The treatment did not result in any morphological alterations up to 4 months post-application. (B) PrpCre-mediated knockdown of HIF-1α did not affect retinal morphology in normoxic mice or after 6 h of hypoxia (6% O_2). Representative panels of control (PrpCre$^{(HIF-wt)}$) and knockdown (PrpCre$^{(HIF-\Delta)}$) mice kept in normoxia for 4 months after treatment (upper panels) or of mice at 4 weeks after exposure to hypoxia (lower panels) are shown. (C) An early but moderate deletion of HIF-1α during development did not interfere with retinal development, and mice showed normal retinal morphology at 6 weeks of age. GCL, ganglion cell layer; INL, inner nuclear layer; ONL, outer nuclear layer; RIS, rod inner segments; ROS, rod outer segments. Scale bar: 25 μm.

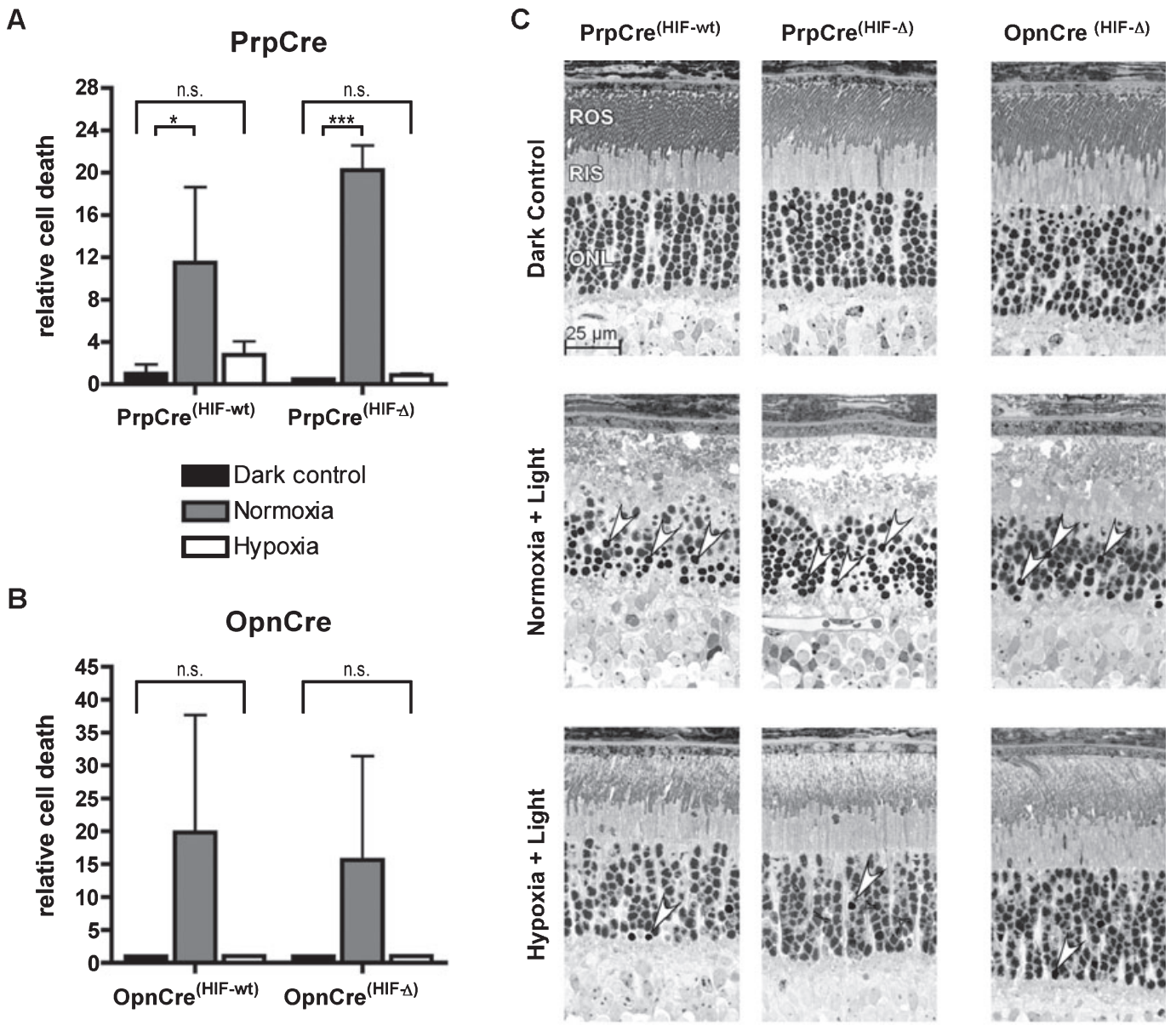

FIG. 5. Role of HIF-1α in retinal neuroprotection. Normoxic or hypoxia-pretreated mice were exposed to 13 000 lux for 2 h and analysed after 36 h. Dark-adapted, normoxic mice served as negative controls. (A) Relative nucleosomal release was measured as an indicator of apoptotic processes in the retina. Values are expressed relative to PrpCre$^{(HIF\text{-}wt)}$ mice, which were set to '1'. Both normoxic PrpCre$^{(HIF\text{-}wt)}$ and normoxic PrpCre$^{(HIF\text{-}\Delta)}$ mice were susceptible [$*P < 0.05$, $***P < 0.001$; $n = 3$ for dark control, $n = 7$ for normoxic PrpCre$^{(HIF\text{-}wt)}$ mice, $n = 5$ for normoxic PrpCre$^{(HIF\text{-}\Delta)}$ mice, one-way ANOVA with Bonferroni post-test] to light damage as indicated by the increased release of nucleosomes (gray bars). Hypoxic preconditioned PrpCre$^{(HIF\text{-}\Delta)}$ mice showed no increased apoptosis after light exposure [not significant (n.s.), $P > 0.05$, $n = 3$ for dark control, $n = 6$ for hypoxic PrpCre$^{(HIF\text{-}wt)}$ mice, $n = 5$ for hypoxic PrpCre$^{(HIF\text{-}\Delta)}$ mice, one-way ANOVA with Bonferroni post-test]. (B) OpnCre mice were analysed as in A. Hypoxic preconditioning resulted in full protection of OpnCre$^{(HIF\text{-}wt)}$ and OpnCre$^{(HIF\text{-}\Delta)}$ mice (white bars), with no increased cell death as compared with controls [n.s., $P > 0.05$, $n = 3$ for dark control, $n = 4$ for hypoxic OpnCre$^{(HIF\text{-}wt)}$ mice, $n = 4$ for hypoxic OpnCre$^{(HIF\text{-}\Delta)}$ mice, one-way ANOVA with Bonferroni post-test]. (C) Retinal morphology after light exposure. Dark controls (upper panels) showed normal retinal structure before light exposure. Normoxic PrpCre$^{(HIF\text{-}wt)}$, PrpCre$^{(HIF\text{-}\Delta)}$ and OpnCre$^{(HIF\text{-}\Delta)}$ mice exposed to light (middle panels) showed severe degeneration of photoreceptor cells, as indicated by the presence of pycnotic nuclei (arrowheads) and the complete disruption of inner and outer segments. All hypoxic preconditioned mice (lower panel) were strongly protected against light damage. Means ± standard deviations are shown; numbers of samples (n) are indicated above. ONL, outer nuclear layer; RIS, rod inner segments; ROS, rod outer segments. Scale bar: 25 μm.

Discussion

Hypoxic preconditioning is a successful strategy with which to inhibit tissue degeneration. The reported correlation between HIF-1α stabilization and retinal neuroprotection (Grimm *et al.*, 2002; Zhu *et al.*, 2007) suggested that the activation of HIF-1α plays an important role in pro-survival mechanisms activated by hypoxic preconditioning. Here, we analysed the impact of the transcription factor HIF-1α on neuroprotection using *Hif-1α* knockdown mice.

Characterization of photoreceptor-specific Hif-1α knockdown mice

Consistent with a previous report (Zhu *et al.*, 2007), we found HIF-1α to be expressed and stabilized in all retinal layers during hypoxic preconditioning. To delete HIF-1α predominantly in photoreceptor cells, we employed two different mouse strains expressing Cre under different promoters. TAM-inducible PrpCre deleter mice activate Cre efficiently and predominantly in photoreceptor cells (Weber *et al.*,

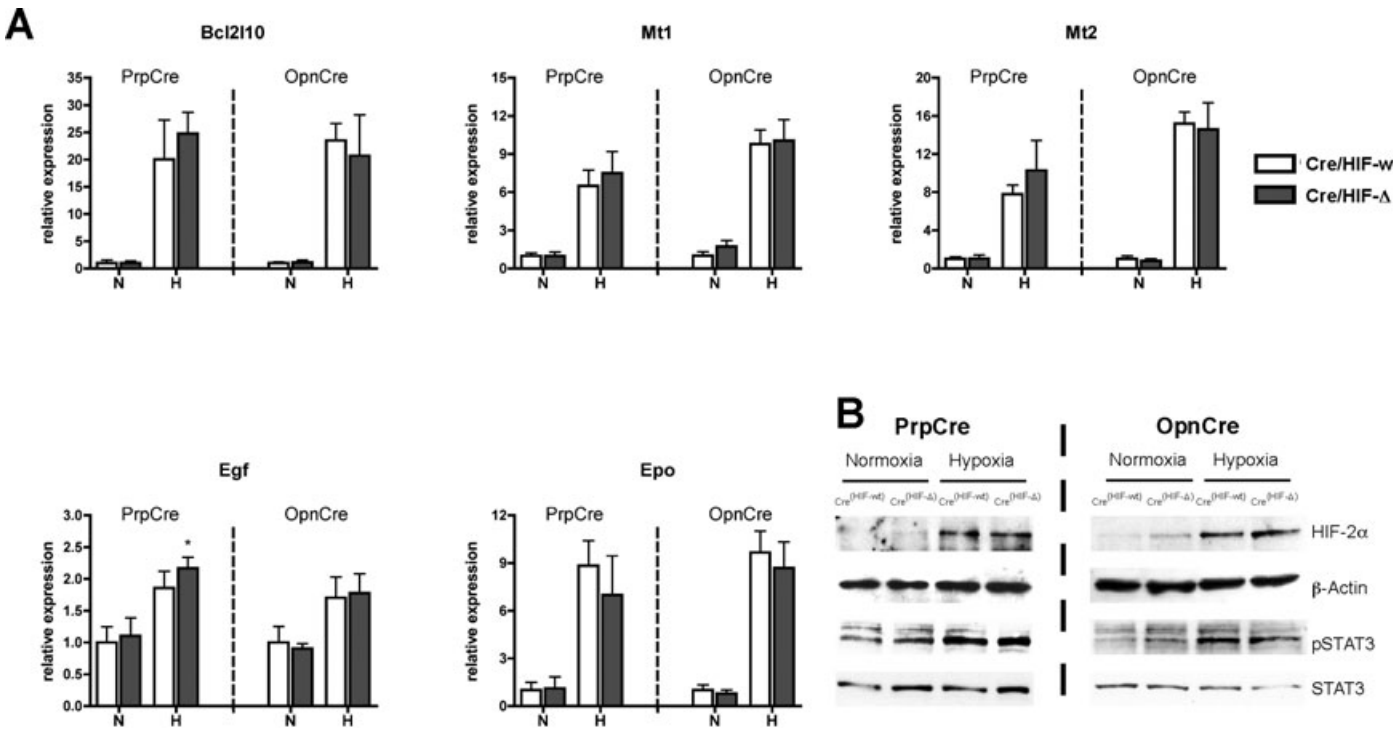

FIG. 6. Hypoxia-mediated upregulation of pro-survival genes and transcription factors in retinas of HIF-1α knockdown mice. Mice were (H) or were not (N) exposed to hypoxia, and mRNA or protein expression was analysed immediately after hypoxia. (A) Expression of selected potential pro-survival genes analysed by real-time PCR. Expression levels of normoxic (N) $Cre^{(HIF\text{-}wt)}$ mice of each strain were set to '1' (first bar). β-Actin served as a reference. Expression levels of normoxic $Cre^{(HIF\text{-}wt)}$ and $Cre^{(HIF\text{-}\Delta)}$ mice were comparable. All genes were strongly induced after hypoxia (H) in control mice as well as in $PrpCre^{(HIF\text{-}\Delta)}$ and $OpnCre^{(HIF\text{-}\Delta)}$ mice, with only slight differences (*$P = 0.0156$, $n = 8$; unpaired, two-tailed t-tests). Means ± standard deviations of eight mice (PrpCre strains) or of five mice (OpnCre strains) are shown. (B) Protein extracts were analysed by western blotting. Comparable induction of HIF-2α and pSTAT3 in $OpnCre^{(HIF\text{-}\Delta)}$ and $PrpCre^{(HIF\text{-}\Delta)}$ mice as well as in $OpnCre^{(HIF\text{-}wt)}$ and $PrpCre^{(HIF\text{-}wt)}$ control mice was observed in hypoxia-pretreated mice. β-Actin and STAT3 were used as loading controls. Representative blots of four mice are shown.

2001). In our hands, this strain almost completely deleted HIF-1α in photoreceptors, which was also evidenced by highly reduced HIF-1α target gene transcription after hypoxia. Deletion with the OpnCre line was less effective, resulting in higher HIF-1α levels and less reduced target gene transcription after hypoxia. The knockdown of *Hif-1α* had no influence on retinal morphology of untreated or hypoxic preconditioned mice. As different studies showed a correlation of HIF-1α induction and retinal neuroprotection (Grimm *et al.*, 2002; Whitlock *et al.*, 2005; Zhu *et al.*, 2007), we used these mice to analyse the role of HIF-1α in hypoxic preconditioning-mediated protection and survival of photoreceptor cells after exposure to high levels of white light.

HIF-1α in photoreceptor cells is not essential to cope with severe hypoxia or to drive retinal neuroprotection after hypoxic preconditioning

Our experiments show that photoreceptors do not need to express HIF-1α to be protected against light exposure after hypoxic preconditioning. With our approach, however, we cannot exclude the possibility that HIF-1α in cells of the INL and/or GCL might contribute to the protection of photoreceptors through the expression of diffusible factors.

The exact role of HIF-1α in neuronal tissues during severe hypoxia or ischemia is controversial. Two studies with a brain-specific deletion of HIF-1α demonstrated somewhat contradictory effects. Whereas Helton *et al.* (2005) showed that lack of HIF-1α in the cortex and hippocampus was rather protective against global ischemia, Baranova *et al.* (2007) reported that the reduction of HIF-1α increased the damage after cerebral ischemia. The knockdowns used in these studies differed in the extent of HIF-1α ablation. Baranova *et al.* used a neuron-specific knockdown, whereas in the mice reported by Helton *et al.*, HIF-1α deletion affected additional cell types, including astrocytes. It is of note that a recent report showed that induction of HIF-1α in astrocytes accelerated hypoxia-induced neuronal cell death, whereas induction of HIF-1α in neurons was beneficial for resistance to severe hypoxia (Vangeison *et al.*, 2008).

In contrast to the neuronal HIF-1α deletion in brain, which showed increased injury after cerebral ischemia (Baranova *et al.*, 2007), $PrpCre^{(HIF\text{-}\Delta)}$ mice showed no retinal abnormalities after exposure to hypoxia. One explanation for this difference may be that hypoxia is less severe than ischemia/reperfusion. Furthermore, hypoxia allows substrate exchange and removal of toxic waste products, owing to the maintained blood flow. Another possible explanation for the retinal resistance to hypoxia is that the retina might have specific mechanisms to deal with low oxygen even in the absence of HIF-1α. The retina is a tissue with a high metabolic rate, and can become borderline hypoxic, especially during the night (Cringle *et al.*, 2002). The constant exposure to mild hypoxia during the night might activate basic hypoxia response mechanisms that are not exclusively HIF-1α-dependent and that have the potential to protect against severe hypoxia.

Alternative mechanisms for hypoxia-induced neuroprotection

Recently, similar HIF-1α-independent protection of brain neurons against cerebral ischemia after hypoxic preconditioning was reported

(Baranova *et al.*, 2007). In that study, HIF-2α was discussed as a possible alternative mechanism to HIF-1α-mediated neuroprotection. In the retina, we also found elevated levels of HIF-2α after hypoxia in control and knockdown mice (Fig. 6B). Recently, it was shown that HIF-2α and not HIF-1α may regulate the expression of *Epo in vivo* (Morita *et al.*, 2003; Gruber *et al.*, 2007; Rankin *et al.*, 2007) and in cell culture experiments (Chavez *et al.*, 2006). In line with these findings, we observed no or only a small decrease in the induction of *Epo* expression in our knockdown strains after hypoxic preconditioning. As *Epo* has proven neuroprotective properties in the brain and the retina (Bernaudin *et al.*, 1999; Brines *et al.*, 2000; Digicaylioglu & Lipton, 2001; Grimm *et al.*, 2002; Weishaupt *et al.*, 2004), *Epo* may be part of the neuroprotective response in the *Hif-1α* knockdown strains.

In addition to HIF-2α, other transcription factors, such as STAT3 and MTF-1, may contribute to the observed protection. STAT3 was strongly phosphorylated after hypoxic preconditioning, and is usually connected to anti-apoptotic activities (Stephanou, 2004). Recently, Ueki *et al.* suggested a prominent role of STAT3 in leukemia inhibitory factor-mediated protection of photoreceptors from light-induced degeneration (Ueki *et al.*, 2008). MTF-1 controls the expression of *Mt1* and *Mt2* (Heuchel *et al.*, 1994), which are expressed in all retinal layers (supporting Fig. S1). Both *Mt1* and *Mt2* were reported to be upregulated in the hypoxic brain, suggesting that expression of the metallothioneins encoded by these genes might be part of a general response to hypoxic exposure (Bernaudin *et al.*, 2002; Tang *et al.*, 2006). Protecting against oxidative stress (Chen *et al.*, 2004; Suemori *et al.*, 2006; Nachman-Clewner *et al.*, 2008), *Mt1* and *Mt2* may thus participate in the hypoxia-induced resistance against light damage. Interestingly, it has recently been suggested that hypoxic induction of *Mt1* and *Mt2* requires a cooperative interaction between MTF-1 and HIF-1α (Murphy *et al.*, 2008). As the *Hif-1α* knockdown did not affect expression of *Mt1* and *Mt2*, our results may suggest that MTF-1 does not strictly depend on HIF-1α but might use alternative factors such as HIF-2α for hypoxic gene expression.

In our earlier analysis of the hypoxic transcriptome of the retina (Thiersch *et al.*, 2008), we found several additional potential pro-survival factors that have been connected to cell survival and/or protection of the retina against toxic insults. Among the genes encoding these, *Bcl2l10* (Song *et al.*, 1999), *Adm* (Garayoa *et al.*, 2000; Miyashita *et al.*, 2006), *Vegf* (Jin *et al.*, 2000; Nishijima *et al.*, 2007) and *Egf* (Hicks *et al.*, 1998) were tested in addition to *Epo*, *Mt1* and *Mt2* for their hypoxic regulation in the *Hif-1α* knockdown retinas. Only the expression of *Vegf* and *Adm* was affected in the PrpCre$^{(HIF-\Delta)}$ mouse. However, as both genes encode secreted factors, we cannot exclude the possibility that their production in cells of the INL and/or GCL contributed to the protection of photoreceptor cells after hypoxic preconditioning. All of these genes were expressed either independently of HIF-1α or in cell layers where HIF-1α has not been knocked down. Although a detailed investigation of these genes is still needed, these factors may well play an active role in protecting photoreceptors against light damage.

The cell-type-specific deletion of HIF-1α is an excellent tool with which to address the role and function of HIF-1α exclusively in photoreceptor cells. However, the neuronal retina consists of three cell layers, which form a functional unit with the retinal pigment epithelium. During hypoxia, HIF-1α is also strongly stabilized in the GCL and INL, where it might drive expression of neuroprotective factors that could directly or indirectly protect photoreceptor cells. Nevertheless, our results demonstrate that photoreceptors do not need to express their own HIF-1α to maintain the structural integrity of the retina, despite the borderline hypoxic conditions experienced by retinal cells during each dark period. Photoreceptors also do not need to express and stabilize HIF-1α to survive a toxic light exposure after hypoxic preconditioning. Other factors, such as HIF-2α, STAT3 and/or MTF-1, may play a role in photoreceptor protection, and it will be of importance to characterize these factors to develop efficient neuroprotective strategies.

Supporting Information

Additional supporting information may be found in the online version of this article:

Fig. S1. Retinal expression of MTF-1.

Please note: Wiley-Blackwell are not responsible for the content or functionality of any supporting materials supplied by the authors. Any queries (other than missing material) should be directed to the corresponding author for the article.

Acknowledgements

The authors thank Coni Imsand, Hedwig Wariwoda and Philipp Huber for excellent technical assistance. Randy Johnson, Max Gassmann and Pierre Chambon are acknowledged for kindly providing HIF-1α$^{F/F}$ and PrpCre mice, respectively. This work was supported by the Swiss National Science Foundation (SNF, grant 3100A0-117760), the Fritz-Tobler Foundation and the European Union (Evi-GenoRet, LSHG-CT-512036).

Abbreviations

Cre, cyclization recombinase; d.f., degrees of freedom; *Egln1,* EGL nine homolog 1 (*Caenorhabditis elegans*) gene; GCL, ganglion cell layer; HIF, hypoxia-inducible factor; INL, inner nuclear layer; LCM, laser capture microdissection; MTF-1, metal response element binding transcription factor 1; ONL, outer nuclear layer; PBS, phosphate-buffered saline; PHD, prolylhydroxylase; PND, postnatal day; Prp, prion protein promoter; SDS, sodium dodecylsulfate; STAT3, signal transducer and activator of transcription 3; TAM, tamoxifen.

References

Baranova, O., Miranda, L.F., Pichiule, P., Dragatsis, I., Johnson, R.S. & Chavez, J.C. (2007) Neuron-specific inactivation of the hypoxia inducible factor 1 alpha increases brain injury in a mouse model of transient focal cerebral ischemia. *J. Neurosci.*, **27**, 6320–6332.

Barone, F.C., White, R.F., Spera, P.A., Ellison, J., Currie, R.W., Wang, X. & Feuerstein, G.Z. (1998) Ischemic preconditioning and brain tolerance: temporal histological and functional outcomes, protein synthesis requirement, and interleukin-1 receptor antagonist and early gene expression. *Stroke*, **29**, 1937–1950.

Bernaudin, M., Marti, H.H., Roussel, S., Divoux, D., Nouvelot, A., MacKenzie, E.T. & Petit, E. (1999) A potential role for erythropoietin in focal permanent cerebral ischemia in mice. *J. Cereb. Blood Flow Metab.*, **19**, 643–651.

Bernaudin, M., Tang, Y., Reilly, M., Petit, E. & Sharp, F.R. (2002) Brain genomic response following hypoxia and re-oxygenation in the neonatal rat. Identification of genes that might contribute to hypoxia-induced ischemic tolerance. *J. Biol. Chem.*, **277**, 39728–39738.

Bourla, D.H., Sarraf, D. & Schwartz, S.D. (2007) Peripheral retinopathy and maculopathy in high-dose tamoxifen therapy. *Am. J. Ophthalmol.*, **144**, 126–128.

Brines, M.L., Ghezzi, P., Keenan, S., Agnello, D., de Lanerolle, N.C., Cerami, C., Itri, L.M. & Cerami, A. (2000) Erythropoietin crosses the blood–brain barrier to protect against experimental brain injury. *Proc. Natl Acad. Sci. USA*, **97**, 10526–10531.

Bruick, R.K. & McKnight, S.L. (2001) A conserved family of prolyl-4-hydroxylases that modify HIF. *Science*, **294**, 1337–1340.

Bruick, R.K. & McKnight, S.L. (2002) Transcription. Oxygen sensing gets a second wind. *Science*, **295**, 807–808.

Cai, Z., Zhong, H., Bosch-Marce, M., Fox-Talbot, K., Wang, L., Wei, C., Trush, M.A. & Semenza, G.L. (2008) Complete loss of ischaemic

preconditioning-induced cardioprotection in mice with partial deficiency of HIF-1 alpha. *Cardiovasc. Res.*, **77**, 463–470.

Chavez, J.C., Baranova, O., Lin, J. & Pichiule, P. (2006) The transcriptional activator hypoxia inducible factor 2 (HIF-2/EPAS-1) regulates the oxygen-dependent expression of erythropoietin in cortical astrocytes. *J. Neurosci.*, **26**, 9471–9481.

Chen, L., Wu, W., Dentchev, T., Wong, R. & Dunaief, J.L. (2004) Increased metallothionein in light damaged mouse retinas. *Exp. Eye Res.*, **79**, 287–293.

Cringle, S.J., Yu, D.Y., Yu, P.K. & Su, E.N. (2002) Intraretinal oxygen consumption in the rat *in vivo*. *Invest. Ophthalmol. Vis. Sci.*, **43**, 1922–1927.

Digicaylioglu, M. & Lipton, S.A. (2001) Erythropoietin-mediated neuroprotection involves cross-talk between Jak2 and NF-kappaB signalling cascades. *Nature*, **412**, 641–647.

Gage, A.T. & Stanton, P.K. (1996) Hypoxia triggers neuroprotective alterations in hippocampal gene expression via a heme-containing sensor. *Brain Res.*, **719**, 172–178.

Garayoa, M., Martinez, A., Lee, S., Pio, R., An, W.G., Neckers, L., Trepel, J., Montuenga, L.M., Ryan, H., Johnson, R., Gassmann, M. & Cuttitta, F. (2000) Hypoxia-inducible factor-1 (HIF-1) up-regulates adrenomedullin expression in human tumor cell lines during oxygen deprivation: a possible promotion mechanism of carcinogenesis. *Mol. Endocrinol.*, **14**, 848–862.

Gidday, J.M., Shah, A.R., Maceren, R.G., Wang, Q., Pelligrino, D.A., Holtzman, D.M. & Park, T.S. (1999) Nitric oxide mediates cerebral ischemic tolerance in a neonatal rat model of hypoxic preconditioning. *J. Cereb. Blood Flow Metab.*, **19**, 331–340.

Grimm, C., Wenzel, A., Groszer, M., Mayser, H., Seeliger, M., Samardzija, M., Bauer, C., Gassmann, M. & Reme, C.E. (2002) HIF-1-induced erythropoietin in the hypoxic retina protects against light-induced retinal degeneration. *Nat. Med.*, **8**, 718–724.

Grimm, C., Hermann, D.M., Bogdanova, A., Hotop, S., Kilic, U., Wenzel, A., Kilic, E. & Gassmann, M. (2005) Neuroprotection by hypoxic preconditioning: HIF-1 and erythropoietin protect from retinal degeneration. *Semin. Cell Dev. Biol.*, **16**, 531–538.

Gruber, M., Hu, C.J., Johnson, R.S., Brown, E.J., Keith, B. & Simon, M.C. (2007) Acute postnatal ablation of Hif-2alpha results in anemia. *Proc. Natl Acad. Sci. USA*, **104**, 2301–2306.

Heier, J.S., Dragoo, R.A., Enzenauer, R.W. & Waterhouse, W.J. (1994) Screening for ocular toxicity in asymptomatic patients treated with tamoxifen. *Am. J. Ophthalmol.*, **117**, 772–775.

Helton, R., Cui, J., Scheel, J.R., Ellison, J.A., Ames, C., Gibson, C., Blouw, B., Ouyang, L., Dragatsis, I., Zeitlin, S., Johnson, R.S., Lipton, S.A. & Barlow, C. (2005) Brain-specific knock-out of hypoxia-inducible factor-1alpha reduces rather than increases hypoxic-ischemic damage. *J. Neurosci.*, **25**, 4099–4107.

Heuchel, R., Radtke, F., Georgiev, O., Stark, G., Aguet, M. & Schaffner, W. (1994) The transcription factor MTF-1 is essential for basal and heavy metal-induced metallothionein gene expression. *EMBO J.*, **13**, 2870–2875.

Hicks, D., Heidinger, V., Mohand-Said, S., Sahel, J. & Dreyfus, H. (1998) Growth factors and gangliosides as neuroprotective agents in excitotoxicity and ischemia. *Gen. Pharmacol.*, **30**, 265–273.

Hill, P., Shukla, D., Tran, M.G., Aragones, J., Cook, H.T., Carmeliet, P. & Maxwell, P.H. (2008) Inhibition of hypoxia inducible factor hydroxylases protects against renal ischemia–reperfusion injury. *J. Am. Soc. Nephrol.*, **19**, 39–46.

Huang, L.E., Gu, J., Schau, M. & Bunn, H.F. (1998) Regulation of hypoxia-inducible factor 1alpha is mediated by an O2-dependent degradation domain via the ubiquitin–proteasome pathway. *Proc. Natl Acad. Sci. USA*, **95**, 7987–7992.

Ivan, M., Kondo, K., Yang, H., Kim, W., Valiando, J., Ohh, M., Salic, A., Asara, J.M., Lane, W.S. & Kaelin, W.G. Jr (2001) HIFalpha targeted for VHL-mediated destruction by proline hydroxylation: implications for O2 sensing. *Science*, **292**, 464–468.

Jaakkola, P., Mole, D.R., Tian, Y.M., Wilson, M.I., Gielbert, J., Gaskell, S.J., Kriegsheim, A., Hebestreit, H.F., Mukherji, M., Schofield, C.J., Maxwell, P.H., Pugh, C.W. & Ratcliffe, P.J. (2001) Targeting of HIF-alpha to the von Hippel–Lindau ubiquitylation complex by O2-regulated prolyl hydroxylation. *Science*, **292**, 468–472.

Jin, K.L., Mao, X.O. & Greenberg, D.A. (2000) Vascular endothelial growth factor: direct neuroprotective effect in in vitro ischemia. *Proc. Natl Acad. Sci. USA*, **97**, 10242–10247.

Kaur, C., Sivakumar, V. & Foulds, W.S. (2006) Early response of neurons and glial cells to hypoxia in the retina. *Invest. Ophthalmol. Vis. Sci.*, **47**, 1126–1141.

Kenneth, N.S. & Rocha, S. (2008) Regulation of gene expression by hypoxia. *Biochem. J.*, **414**, 19–29.

Le, Y.Z., Zheng, L., Zheng, W., Ash, J.D., Agbaga, M.P., Zhu, M. & Anderson, R.E. (2006) Mouse opsin promoter-directed Cre recombinase expression in transgenic mice. *Mol. Vis.*, **12**, 389–398.

Mahon, P.C., Hirota, K. & Semenza, G.L. (2001) FIH-1: a novel protein that interacts with HIF-1alpha and VHL to mediate repression of HIF-1 transcriptional activity. *Genes Dev.*, **15**, 2675–2686.

Miyashita, K., Itoh, H., Arai, H., Suganami, T., Sawada, N., Fukunaga, Y., Sone, M., Yamahara, K., Yurugi-Kobayashi, T., Park, K., Oyamada, N., Sawada, N., Taura, D., Tsujimoto, H., Chao, T.H., Tamura, N., Mukoyama, M. & Nakao, K. (2006) The neuroprotective and vasculo-neuro-regenerative roles of adrenomedullin in ischemic brain and its therapeutic potential. *Endocrinology*, **147**, 1642–1653.

Morita, M., Ohneda, O., Yamashita, T., Takahashi, S., Suzuki, N., Nakajima, O., Kawauchi, S., Ema, M., Shibahara, S., Udono, T., Tomita, K., Tamai, M., Sogawa, K., Yamamoto, M. & Fujii-Kuriyama, Y. (2003) HLF/HIF-2alpha is a key factor in retinopathy of prematurity in association with erythropoietin. *EMBO J.*, **22**, 1134–1146.

Murphy, B.J., Kimura, T., Sato, B.G., Shi, Y. & Andrews, G.K. (2008) Metallothionein induction by hypoxia involves cooperative interactions between metal-responsive transcription factor-1 and hypoxia-inducible transcription factor-1alpha. *Mol. Cancer Res.*, **6**, 483–490.

Nachman-Clewner, M., Giblin, F.J., Dorey, C.K., Blanks, R.H., Dang, L., Dougherty, C.J. & Blanks, J.C. (2008) Selective degeneration of central photoreceptors after hyperbaric oxygen in normal and metallothionein-knockout mice. *Invest. Ophthalmol. Vis. Sci.*, **49**, 3207–3215.

Nishijima, K., Ng, Y.S., Zhong, L., Bradley, J., Schubert, W., Jo, N., Akita, J., Samuelsson, S.J., Robinson, G.S., Adamis, A.P. & Shima, D.T. (2007) Vascular endothelial growth factor-A is a survival factor for retinal neurons and a critical neuroprotectant during the adaptive response to ischemic injury. *Am. J. Pathol.*, **171**, 53–67.

Ozaki, H., Yu, A.Y., Della, N., Ozaki, K., Luna, J.D., Yamada, H., Hackett, S.F., Okamoto, N., Zack, D.J., Semenza, G.L. & Campochiaro, P.A. (1999) Hypoxia inducible factor-1alpha is increased in ischemic retina: temporal and spatial correlation with VEGF expression. *Invest. Ophthalmol. Vis. Sci.*, **40**, 182–189.

Ran, R., Xu, H., Lu, A., Bernaudin, M. & Sharp, F.R. (2005) Hypoxia preconditioning in the brain. *Dev. Neurosci.*, **27**, 87–92.

Rankin, E.B., Biju, M.P., Liu, Q., Unger, T.L., Rha, J., Johnson, R.S., Simon, M.C., Keith, B. & Haase, V.H. (2007) Hypoxia-inducible factor-2 (HIF-2) regulates hepatic erythropoietin in vivo. *J. Clin. Invest.*, **117**, 1068–1077.

Rosenberger, C., Rosen, S., Shina, A., Frei, U., Eckardt, K.U., Flippin, L.A., Arend, M., Klaus, S.J. & Heyman, S.N. (2008) Activation of hypoxia inducible factors (HIF) ameliorates hypoxic distal tubular injury in the isolated perfused rat kidney. *Nephrol. Dial. Transplant.*, **23**, 3472–3478.

Roth, S., Li, B., Rosenbaum, P.S., Gupta, H., Goldstein, I.M., Maxwell, K.M. & Gidday, J.M. (1998) Preconditioning provides complete protection against retinal ischemic injury in rats. *Invest. Ophthalmol. Vis. Sci.*, **39**, 777–785.

Ryan, H.E., Poloni, M., McNulty, W., Elson, D., Gassmann, M., Arbeit, J.M. & Johnson, R.S. (2000) Hypoxia-inducible factor-1alpha is a positive factor in solid tumor growth. *Cancer Res.*, **60**, 4010–4015.

Sakanaka, M., Wen, T.C., Matsuda, S., Masuda, S., Morishita, E., Nagao, M. & Sasaki, R. (1998) In vivo evidence that erythropoietin protects neurons from ischemic damage. *Proc. Natl Acad. Sci. USA*, **95**, 4635–4640.

Salceda, S. & Caro, J. (1997) Hypoxia-inducible factor 1alpha (HIF-1alpha) protein is rapidly degraded by the ubiquitin–proteasome system under normoxic conditions. Its stabilization by hypoxia depends on redox-induced changes. *J. Biol. Chem.*, **272**, 22642–22647.

Samardzija, M., Wenzel, A., Aufenberg, S., Thiersch, M., Reme, C. & Grimm, C. (2006) Differential role of Jak-STAT signaling in retinal degenerations. *FASEB J.*, **20**, 2411–2413.

Sharp, F.R., Ran, R., Lu, A., Tang, Y., Strauss, K.I., Glass, T., Ardizzone, T. & Bernaudin, M. (2004) Hypoxic preconditioning protects against ischemic brain injury. *NeuroRx*, **1**, 26–35.

Siddiq, A., Ayoub, I.A., Chavez, J.C., Aminova, L., Shah, S., LaManna, J.C., Patton, S.M., Connor, J.R., Cherny, R.A., Volitakis, I., Bush, A.I., Langsetmo, I., Seeley, T., Gunzler, V. & Ratan, R.R. (2005) Hypoxia-inducible factor prolyl 4-hydroxylase inhibition. A target for neuroprotection in the central nervous system. *J. Biol. Chem.*, **280**, 41732–41743.

Siren, A.L., Fratelli, M., Brines, M., Goemans, C., Casagrande, S., Lewczuk, P., Keenan, S., Gleiter, C., Pasquali, C., Capobianco, A., Mennini, T., Heumann, R., Cerami, A., Ehrenreich, H. & Ghezzi, P. (2001) Erythropoietin prevents neuronal apoptosis after cerebral ischemia and metabolic stress. *Proc. Natl Acad. Sci. USA*, **98**, 4044–4049.

Song, Q., Kuang, Y., Dixit, V.M. & Vincenz, C. (1999) Boo, a novel negative regulator of cell death, interacts with Apaf-1. *EMBO J.*, **18**, 167–178.
Stephanou, A. (2004) Role of STAT-1 and STAT-3 in ischaemia/reperfusion injury. *J. Cell Mol. Med.*, **8**, 519–525.
Suemori, S., Shimazawa, M., Kawase, K., Satoh, M., Nagase, H., Yamamoto, T. & Hara, H. (2006) Metallothionein, an endogenous antioxidant, protects against retinal neuron damage in mice. *Invest. Ophthalmol. Vis. Sci.*, **47**, 3975–3982.
Tanaka, H., Calderone, A., Jover, T., Grooms, S.Y., Yokota, H., Zukin, R.S. & Bennett, M.V. (2002) Ischemic preconditioning acts upstream of GluR2 down-regulation to afford neuroprotection in the hippocampal CA1. *Proc. Natl Acad. Sci. USA*, **99**, 2362–2367.
Tang, R., Shields, J., Schiffman, J., Li, H., Locher, D., Hampton, J., Prager, T. & Pardo, G. (1997) Retinal changes associated with tamoxifen treatment for breast cancer. *Eye*, **11**(Pt 3), 295–297.
Tang, Y., Pacary, E., Freret, T., Divoux, D., Petit, E., Schumann-Bard, P. & Bernaudin, M. (2006) Effect of hypoxic preconditioning on brain genomic response before and following ischemia in the adult mouse: identification of potential neuroprotective candidates for stroke. *Neurobiol. Dis.*, **21**, 18–28.
Thiersch, M., Raffelsberger, W., Frigg, R., Samardzija, M., Wenzel, A., Poch, O. & Grimm, C. (2008) Analysis of the retinal gene expression profile after hypoxic preconditioning identifies candidate genes for neuroprotection. *BMC Genomics*, **9**, 73.
Ueki, Y., Wang, J., Chollangi, S. & Ash, J.D. (2008) STAT3 activation in photoreceptors by leukemia inhibitory factor is associated with protection from light damage. *J. Neurochem.*, **105**, 784–796.
Vangeison, G., Carr, D., Federoff, H.J. & Rempe, D.A. (2008) The good, the bad, and the cell type-specific roles of hypoxia inducible factor-1 alpha in neurons and astrocytes. *J. Neurosci.*, **28**, 1988–1993.
Wakade, C., Khan, M.M., De Sevilla, L.M., Zhang, Q.G., Mahesh, V.B. & Brann, D.W. (2008) Tamoxifen neuroprotection in cerebral ischemia involves attenuation of kinase activation and superoxide production and potentiation of mitochondrial superoxide dismutase. *Endocrinology*, **149**, 367–379.
Wang, G.L. & Semenza, G.L. (1993) Characterization of hypoxia-inducible factor 1 and regulation of DNA binding activity by hypoxia. *J. Biol. Chem.*, **268**, 21513–21518.
Wang, G.L. & Semenza, G.L. (1995) Purification and characterization of hypoxia-inducible factor 1. *J. Biol. Chem.*, **270**, 1230–1237.
Weber, P., Metzger, D. & Chambon, P. (2001) Temporally controlled targeted somatic mutagenesis in the mouse brain. *Eur. J. Neurosci.*, **14**, 1777–1783.
Weishaupt, J.H., Rohde, G., Polking, E., Siren, A.L., Ehrenreich, H. & Bahr, M. (2004) Effect of erythropoietin axotomy-induced apoptosis in rat retinal ganglion cells. *Invest. Ophthalmol. Vis. Sci.*, **45**, 1514–1522.
Wenzel, A., Grimm, C., Samardzija, M. & Reme, C.E. (2003) The genetic modifier Rpe65Leu(450): effect on light damage susceptibility in c-Fos-deficient mice. *Invest. Ophthalmol. Vis. Sci.*, **44**, 2798–2802.
Wenzel, A., Grimm, C., Samardzija, M. & Reme, C.E. (2005) Molecular mechanisms of light-induced photoreceptor apoptosis and neuroprotection for retinal degeneration. *Prog. Retin. Eye Res.*, **24**, 275–306.
Whitlock, N.A., Agarwal, N., Ma, J.X. & Crosson, C.E. (2005) Hsp27 upregulation by HIF-1 signaling offers protection against retinal ischemia in rats. *Invest. Ophthalmol. Vis. Sci.*, **46**, 1092–1098.
Zhang, C., Rosenbaum, D.M., Shaikh, A.R., Li, Q., Rosenbaum, P.S., Pelham, D.J. & Roth, S. (2002) Ischemic preconditioning attenuates apoptotic cell death in the rat retina. *Invest. Ophthalmol. Vis. Sci.*, **43**, 3059–3066.
Zhang, Y., Milatovic, D., Aschner, M., Feustel, P.J. & Kimelberg, H.K. (2007) Neuroprotection by tamoxifen in focal cerebral ischemia is not mediated by an agonist action at estrogen receptors but is associated with antioxidant activity. *Exp. Neurol.*, **204**, 819–827.
Zhu, Y., Zhang, Y., Ojwang, B.A., Brantley, M.A. Jr & Gidday, J.M. (2007) Long-term tolerance to retinal ischemia by repetitive hypoxic preconditioning: role of HIF-1alpha and heme oxygenase-1. *Invest. Ophthalmol. Vis. Sci.*, **48**, 1735–1743.

3.2.3. The differential role of JAK/STAT signaling in retinal degeneration (bookchapter)

Christina Lange[1], Markus Thiersch[1], Marijana Samardzija[1] and Christian Grimm[1,2]

[1]Lab for Retinal Cell Biology, Department Ophthalmology, University of Zurich
[2]Zurich Center for Integrative Human Physiology (ZIHP)

Author contribution:
Design: **CL** and CG
Experiment: **CL** (all data: real time PCR), MT, MS
Interpretation: **CL** (all data), MT, MS and CG
Manuscript: **CL**
Manuscript correction: MT, MS and CG

Summary:
In this bookchapter we looked at the retinal expression of several genes involved in the JAK/STAT signaling pathway in an induced (light exposure) and an inherited (rd1) model for retinal degeneration. We showed that *Stat1, Stat2, Stat3* and *Stat4* are induced in the light exposure model, whereas in the rd1 mouse only *Stat3* showed a slight induction. *Stat5b* showed a slight down-regulation after light exposure and a slight upregulation in the rd1 mouse. Src-homology containing phosphatase 1 (*Shp-1*) was only induced after light but not in the rd1 mouse. In contrast, *Jak3* was induced in both, the induced and the inherited model. Expression of the other Janus kinases remained at basal levels in both models. In conclusion this showed that, depending on the death stimulus, the JAK/STAT pathway can be differentially activated during retinal degeneration.

Adv Exp Med Biol 664:601-607

Chapter 69
The Differential Role of Jak/Stat Signaling in Retinal Degeneration

C. Lange, M. Thiersch, M. Samardzija, and C. Grimm

Abstract Retinal degenerative diseases are a major cause of severe visual impairment or blindness in humans. To develop therapeutic strategies it is of particular importance to understand the molecular mechanisms taking place during the progression of the disease. Genes and proteins of the Janus kinase/Signal Transducer and Activator of Transcription (Jak/STAT) signaling pathway have been shown to play an important role in models of retinal degeneration (RD). Here we investigated the expression of additional genes involved in the Jak/STAT pathway in an induced (light exposure) and an inherited (rd1 mouse) model of RD. We show that STAT mRNAs as well as the Jak2/shp-1 pathway are differentially regulated in the two models. In contrast, we show that Jak3 mRNA is upregulated in both, the light damaged and the degenerative retina of the rd1 mouse. This common answer to probably different apoptotic stimuli suggests a prominent role for Jak3 in the damaged retina and could therefore be interesting for further investigations.

69.1 Introduction

Retinal degenerative diseases like retinitis pigmentosa (RP) are a frequent cause of severe visual impairment or blindness in human patients. They are characterized by the progressive loss of visual cells by apoptosis. Understanding the molecular mechanisms underlying the processes of photoreceptor degeneration and identifying endogenous rescue pathways is of fundamental importance to develop successful therapeutic strategies for this group of diseases.

There are various animal models, induced as well as inherited, to study retinal degenerations. In one model for induced retinal degeneration mice are exposed to bright light which causes photoreceptors to die by apoptosis (Reme et al. 1998; Grimm et al. 2000; Wenzel et al. 2005). Depending on the light intensity used and

C. Lange (✉)
Lab for Retinal Cell Biology, Department of Ophthalmology, University of Zurich, Zurich, Switzerland
e-mail: christina.lange@usz.ch

R.E. Anderson et al. (eds.), *Retinal Degenerative Diseases*, Advances in Experimental Medicine and Biology 664, DOI 10.1007/978-1-4419-1399-9_69,

the duration of exposure, more or less photoreceptors die and are cleared from the subretinal space until 10 days post exposure. The rd1 (retinal degeneration 1) mouse is a model for autosomal recessive RP. It carries a null mutation in the β-subunit of the cGMP-phosphodiesterase. Lack of cGMP-phosphodiesterase activity leads to accumulation of cGMP and Ca^{2+} in the outer segment of rod-photoreceptors (Bowes et al. 1990). In this model, photoreceptors start to die around postnatal day (PND) 10 with nearly no photoreceptors left at PND 21. Although photoreceptors die by an apoptotic process in both models, it is not yet clear how induced models compare to inherited models for retinal degeneration. Understanding the cell death mechanisms that these models share or in which they are different is important in order to develop treatment strategies, which aim at the inhibition of cell death mechanisms or at the activation of cell survival strategies.

Gene expression analysis in mouse retinas has shown that the expression of different genes of the Janus kinase/Signal Transducer and Activator of Transcription (Jak/STAT) signaling pathway changes during retinal degeneration after light exposure and in the rd1 mouse (Samardzija et al. 2006). This points to an important role of individual members of this pathway for cell death or cell survival in injured retinas.

Here we investigated additional genes from the Jak/STAT pathway and analyzed their potential involvement in the induced (light) and the inherited (rd1) model for retinal degeneration.

69.2 Materials and Methods

69.2.1 Mice and Light Exposure

Animals were treated in accordance with the regulations of the Veterinary Authority of Zurich and with the statement of 'The Association for Research in Vision and Ophthalmology' for the use of animals in research. About 6- to 8-week old Balb/c mice (from Harlan) were dark adapted over night (16h) and exposed to white fluorescent light (5,000 lux) for 1 h. After light exposure mice were kept in darkness for different periods of time before sacrifice and removal of the retina. After 24 h in darkness they were returned to cyclic (12 h: 12 h) light. Mice that were dark-adapted but not exposed to light served as controls. Rd1 mice (Harlan) were sacrificed at different ages (PND10 to PND37) for removal of the retina. Here, wild-type Bl/6 mice (from a breeding colony in the animal facility of the University Hospital Zurich) served as controls for normalization.

69.2.2 Semi-Quantitative Real Time Polymerase Chain Reaction (PCR)

Retinas were removed through a slit in the cornea and immediately frozen in liquid nitrogen. Total RNA was prepared using the RNeasy RNA isolation kit (Qiagen)

according to the manufacture's directions including a DNase treatment to digest residual genomic DNA. Equal amounts of RNA were used for reverse transcription using oligo(dT) and M-MLV reverse transcriptase (Promega). Relative quantification of cDNA was carried out by real-time PCR using the LightCycler 480 Sybr Green I Master kit, a LightCycler 480 instrument (Roche) and specific primer pairs (Table 69.1). Three animals per time point were analyzed in duplicates and compared to the expression of the bipolar cell marker visual system homeobox 2 (CHX10) by relative quantification using the Light Cycler 480 software (Roche). CHX10 was chosen because it is expressed in the inner nuclear layer and should not be affected by photoreceptor apoptosis during retinal degeneration. Light exposure samples were normalized to the dark control (DC). Rd1 samples were normalized to the wild-type and to 10 day old rd1 (PND10).

Table 69.1 PCR primers used for real time PCR

Gene	Upstream	Downstream	Product (bp)
Jak1	tgagctttgatcggatcctt	gcagggtcccagaatagatatg	90
Jak2	gaacctacagatacggagtgtcc	caaaatcatgccgccact	96
Jak3	cacagtgcatggcctatgat	aggtgtggggtctgagagg	110
Shp-1	tgactaccagagaggtggagaaagg	agagaccatagacacgctgagtgc	84
STAT1	ttgtgttgaatcccgaacct	tcgaaccactgtgacatcct	95
STAT2	attggaagttgcagcgagag	tgcgccatttggactctt	67
STAT3	caaaaccctcaagaagccaagg	tcactcacaatgcttctccgc	139
STAT4	ttcagagcagctcaacatgc	ggtgaggtgaccatcattgtag	70
STAT5a	aagatcaagctggggcacta	catgggacagcggtcatac	60
STAT5b	cgagctggtctttcaagtca	ctggctgccgtgaacaat	64
Tyk2	cctgtgtcaccttgctctca	ggaatgagggatgcagttct	85

69.3 Results

69.3.1 STATs Are Induced Differently in Retinas of Light-Exposed and rd1 Mice

After light exposure STAT1 and STAT2 were induced with peaks at 12–24 h (4- to 5-fold). STAT3 expression was activated earlier with an induction peak at 6–12 h (5- to 7-fold). STAT4 showed only a minor induction at 6–12 h (2-fold) and STAT5a and b did not change in expression (STAT5a) or were slightly downregulated (STAT5b). In the rd1 mouse none of the STATs showed a major differential expression during the degeneration. Only STAT3 was mildly induced at postnatal day 16 (2- to 3-fold). Of note and in contrast to the light-induced model, STAT5b was rather upregulated than downregulated (Table 69.2).

Table 69.2 Real time semi-quantitative PCR. Given are means ± standard deviation (SD) of 3 retinas per time-point amplified in duplicates. After light exposure STAT1, 2 and 3 were induced. In the rd1 mouse in contrast there was no induction of STATs. DC: dark control. Im: immediately after light exposure. 6h-30d (light exposure): time-point after light exposure. 10d-37d (rd1): day after birth

	STAT1	STAT2	STAT3	STAT4	STAT5a	STAT5b
DC	1.00±0.49	1.00±0.20	1.00±0.16	1.00±0.90	1.00±0.23	1.00±0.12
Im	0.74±0.27	0.93±0.03	0.91±0.07	0.64±0.44	1.03±0.19	0.83±0.15
6h	1.96±0.05	1.58±0.18	6.53±0.81	2.13±2.64	1.18±0.16	0.80±0.13
12 h	4.73±0.28	4.51±0.62	5.95±1.05	2.05±2.49	1.09±0.33	0.63±0.04
24 h	4.69±0.30	4.73±0.66	4.28±0.82	0.75±0.26	1.18±0.12	0.63±0.12
2d	1.78±0.31	1.16±0.04	1.68±0.54	0.63±0.36	0.92±0.23	0.49±0.10
3d	2.27±1.52	1.80±0.97	1.69±0.61	1.05±0.32	1.12±0.12	0.71±0.21
5d	0.82±0.38	0.64±0.21	0.76±0.07	0.59±0.42	0.70±0.06	0.59±0.14
10d	0.88±0.16	1.02±0.07	0.88±0.08	0.45±0.11	1.10±0.23	0.91±0.15
20d	0.61±0.06	0.81±0.11	0.84±0.03	0.77±0.23	1.32±0.14	0.88±0.08
30d	0.64±0.04	0.84±0.11	0.75±0.12	0.87±0.43	1.25±0.26	0.87±0.08
Rd1						
10d	1.00±0.00	1.00±0.00	1.00±0.00	1.00±0.00	1.00±0.00	1.00±0.00
14d	0.78±0.34	1.04±0.29	1.79±0.44	0.85±0.24	1.38±0.24	2.01±0.35
16d	0.81±0.17	0.91±0.22	2.42±0.11	0.57±0.07	1.85±0.10	1.77±0.11
21d	0.73±0.16	0.90±0.16	1.45±0.34	1.43±0.67	1.95±0.29	1.97±0.68
28d	0.82±0.23	0.80±0.08	1.38±0.46	0.66±0.13	1.51±0.14	1.59±0.35
37d	0.56±0.22	0.71±0.35	1.24±0.54	2.37±1.10	1.44±0.68	1.49±0.70

69.3.2 Shp-1 Is Induced After Light Exposure But Not in the rd1 Mouse

After light exposure scr-homology containing phosphatase 1 (shp-1) was induced with a peak (7-fold) at 3 days post exposure. In contrast, shp-1 was not induced and showed rather a tendency for downregulation in the rd1 mouse (Table 69.3).

69.3.3 Jak3 mRNA Is Induced Similarly in the Model of Light Induced Photoreceptor Cell Death and the rd1 Mouse Model

Jak3 showed an induction with a peak (11-fold) at 24 h after light exposure (Table 69.4). The expression of other Janus kinases remained nearly unchanged. Also in the rd1 mouse induction of Jak3 was prominent at the time of the peak of photoreceptor death (14 days after birth) (5-fold). It stayed induced (2- to 3-fold) at least until all photoreceptors have disappeared (37 days after birth) (Table 69.4). Here the expression of the other Janus kinases tended to be downregulated.

Table 69.3 Real time semi-quantitative PCR for shp-1. Given are means ± standard deviation (SD) of 3 retinas per time-point amplified in duplicates. After light exposure shp-1 was induced. In the rd1 mouse there was no induction of shp-1. DC: dark control. Im: immediately after light exposure. 6h-30d (light exposure): time-point after light exposure. 10d-37d (rd1): day after birth

	Shp-1
DC	1.00±0.41
Im	1.18±0.16
6h	1.63±1.14
12 h	2.14±1.09
24 h	3.17±0.63
2d	4.17±0.84
3d	7.42±1.52
5d	2.17±0.14
10d	2.72±0.72
20d	1.73±0.09
30d	2.12±0.54
10d	1.00±0.03
14d	0.87±0.13
16d	0.52±0.05
21d	0.36±0.01
28d	0.49±0.10
37d	0.14±0.02

Table 69.4 Real time semi-quantitative PCR. Given are means ± standard deviation (SD) of 3 retinas per time-point amplified in duplicates. Jak3 was induced in both models. It peaked at 24 h after light exposure and was induced from PND 14 on in the rd1 mouse. DC: dark control. Im: immediately after light exposure. 6h-30d (light exposure): time-point after light exposure. 10d-37d (rd1): day after birth

	Jak1	Jak2	Jak3	Tyk2
DC	1.00±0.22	1.00±0.09	1.00±0.00	1.00±0.31
Im	1.05±0.18	1.44±0.15	0.80±0.06	1.42±0.07
6h	1.31±0.09	1.79±0.24	5.53±0.58	1.35±0.14
12 h	1.10±0.32	1.45±0.18	9.75±1.75	1.47±0.11
24 h	0.63±0.07	1.18±0.09	11.50±2.58	1.71±0.30
2d	0.45±0.03	0.80±0.04	4.07±1.00	1.64±0.42
3d	0.59±0.04	0.75±0.05	4.75±1.17	1.61±0.47
5d	0.47±0.09	0.83±0.17	0.98±0.11	0.99±0.35
10d	1.04±0.10	0.90±0.23	1.34±0.10	1.66±0.27
20d	0.67±0.40	0.69±0.11	1.08±0.10	1.32±0.29
30d	0.81±0.13	0.74±0.17	1.00±0.05	1.19±0.21
Rd1				
10d	1.00±0.00	1.00±0.09	1.00±0.00	1.00±0.09
14d	0.65±0.12	0.93±0.18	5.33±2.74	0.69±0.07
16d	0.43±0.04	0.76±0.07	5.04±0.53	0.67±0.10
21d	0.54±0.02	0.72±0.05	2.84±0.61	0.51±0.01
28d	0.30±0.00	0.60±0.06	2.35±0.38	0.48±0.10
37d	0.21±0.00	0.48±0.17	3.14±1.54	0.31±0.05

69.4 Discussion

Jak2 and STAT3, proteins from the Jak/STAT signaling pathway, have been shown to be involved in photoreceptor apoptosis during retinal degeneration (Samardzija et al. 2006). To further increase our understanding of the role of Jak/STAT signaling in this process, we analyzed the expression profiles of additional Jak/STAT related genes in the light-induced and the inherited rd1 model for retinal degeneration.

Although there were similarities between the two models of retinal degeneration, significant differences support the existence of model-specific signaling systems.

Expression of STAT1, 2 and 3 was upregulated after light exposure but only STAT3 was induced in the rd1 mouse (Table 69.2).

Similarly, the phosphatase shp-1, was induced after light exposure but not in the rd1 mouse (Table 69.3). Shp-1 is known to bind to activated Jak2 to dephosphorylate and therefore inhibit it (Akagi et al. 2004; Minoo et al. 2004; Lyons et al. 2006; Chong and Maiese 2007). We have shown that Jak2 is transiently phosphorylated in response to light peaking at 12 h after light exposure (Samardzija et al. 2006). Thereafter, levels of p-Jak2 are gradually reduced reaching basal levels at 2 days post exposure. During this decline of p-Jak2 levels, expression of shp-1 started to rise. It is therefore likely that shp-1 is upregulated to inhibit Jak2 in the light damaged retina. In the rd1 mouse Jak2 does not appear to be phosphorylated during photoreceptor degeneration (Samardzija et al. 2006). Therefore, a molecular control of Jak2 activity may not be needed which may explain the lack of shp-1 upregulation in the rd1 retina. A different signaling between the rd1 and the light damaged retina has been observed earlier. Whereas erythropoietin (EPO) protects photoreceptors against light damage it does not inhibit the inherited degeneration caused by the rd1 mutation (Grimm et al. 2004). Since EPO is reported to trigger the Jak2/shp-1 pathway (Akagi et al. 2004), lack of protection in the rd1 mouse may indicate that the Jak2 signaling system may be severely disturbed early in the degenerating rd1 retina.

Although both the light damaged and the degenerative rd1 retina upregulate STAT3 expression and phosphorylation (Samardzija et al. 2006), the up- and downstream signaling cascades are not yet clear. A likely candidate up- or downstream is Jak3, which was induced at least from PND 14 on in the rd1 mouse and with a peak at 24 h after light exposure (Table 69.4). Since Jak3 activity is mainly regulated on the gene expression level (Mangan et al. 2006), the strong induction of mRNA levels suggest a prominent role of this kinase in the injured retina. It is possible that Jak3 is part of an immune-related response induced by retinal damage. This response may be responsible for the attraction of immune-cells entering the retina in both models of retinal degeneration (Zeng et al. 2005; Zhang et al. 2005). Jak3 was described to be important for lymphoid development and to be primarily expressed in immune-cells (Leonard and O'Shea 1998). Lack of Jak3 leads to a severe combined immunodeficiency. Preliminary results from laser-capture experiments (data not shown), however, suggest that Jak3 is also expressed in the outer nuclear layer and the ganglion cell layer of the healthy retina. Whether its

expression is indeed relevant for immune-related signaling or whether Jak3 may have other roles for example in the survival of retinal cells is not known and will be studied in detail using Jak3 knockout animals.

Acknowledgments The authors thank Coni Imsand, Hedwig Wariwoda and Philipp Huber for excellent technical assistance. This work was supported by the Swiss National Science Foundation (SNF).

References

Akagi S, Ichikawa H et al (2004) The critical role of SRC homology domain 2-containing tyrosine phosphatase-1 in recombinant human erythropoietin hyporesponsive anemia in chronic hemodialysis patients. J Am Soc Nephrol 15(12):3215–3224

Bowes C, Li T et al (1990) Retinal degeneration in the rd mouse is caused by a defect in the beta subunit of rod cGMP-phosphodiesterase. Nature 347(6294):677–680

Chong ZZ, Maiese K (2007) The Src homology 2 domain tyrosine phosphatases SHP-1 and SHP-2: diversified control of cell growth, inflammation, and injury. Histol Histopathol 22(11): 1251–1267

Grimm C, Wenzel A et al (2000) Gene expression in the mouse retina: the effect of damaging light. Mol Vis 6:252–260

Grimm C, Wenzel A et al (2004) Constitutive overexpression of human erythropoietin protects the mouse retina against induced but not inherited retinal degeneration. J Neurosci 24(25): 5651–5658

Leonard WJ, O'Shea JJ (1998) Jaks and STATs: biological implications. Annu Rev Immunol 16:293–322

Lyons BL, Smith RS et al (2006) Deficiency of SHP-1 protein-tyrosine phosphatase in "viable motheaten" mice results in retinal degeneration. Invest Ophthalmol Vis Sci 47(3):1201–1209

Mangan JK, Tantravahi RV et al (2006) Granulocyte colony-stimulating factor-induced upregulation of Jak3 transcription during granulocytic differentiation is mediated by the cooperative action of Sp1 and Stat3. Oncogene 25(17):2489–2499

Minoo P, Zadeh MM et al (2004) A novel SHP-1/Grb2-dependent mechanism of negative regulation of cytokine-receptor signaling: contribution of SHP-1 C-terminal tyrosines in cytokine signaling. Blood 103(4):1398–1407

Reme CE, Grimm C et al (1998) Apoptotic cell death in retinal degenerations. Prog Retin Eye Res 17(4):443–464

Samardzija M, Wenzel A et al (2006) Differential role of Jak-STAT signaling in retinal degenerations. FASEB J 20(13):2411–2413

Wenzel A, Grimm C et al (2005) Molecular mechanisms of light-induced photoreceptor apoptosis and neuroprotection for retinal degeneration. Prog Retin Eye Res 24(2):275–306

Zeng HY, Zhu XA et al (2005) Identification of sequential events and factors associated with microglial activation, migration, and cytotoxicity in retinal degeneration in rd mice. Invest Ophthalmol Vis Sci 46(8):2992–2999

Zhang C, Shen JK et al (2005) Activation of microglia and chemokines in light-induced retinal degeneration. Mol Vis 11:887–895

4. Concluding discussion

Retinal degeneration diseases like Retinitis Pigmentosa often lead to loss of vision in human patients due to photoreceptor cell death by apoptosis. Until today it is largely unclear what molecular mechanisms lead to photoreceptor apoptosis. A lot of research has been done and is still going on trying to elucidate the cell signaling mechanisms and to find out how such death could be prevented to save vision for patients.

In this thesis I investigated molecular mechanisms of two endogenous survival pathways for photoreceptor protection to identify potential targets for future therapeutical interventions. The first pathway is characterized by the activation of JAK/STAT signaling after photoreceptor injury whereas the second system is induced by hypoxic preconditioning.

The activation of the JAK/STAT signaling pathway by LIF, seems to be a global response to many different kinds of photoreceptor degeneration or retinal stress. It has been detected during light induced degeneration and in at least three mouse models for inherited degeneration (Samardzija et al., 2006a; Joly et al., 2008; Burgi et al., 2009; Lange et al., 2010b; Lange et al., 2010a) (reference Joly et al. refers to chapter 3.2.1. of this work and references Lange et al. refer to chapter 3.1.1. and 3.2.3. of this work) and in retina-specific VHL knockdown mice (chapter 3.1.3.).

In this work we showed that LIF can induce different molecular pathways that use JAK/STAT signaling, one involving EDN2 and FGF2 and another one involving JAK3. We have shown that the second one has no essential function during photoreceptor degeneration and the biological significance of its activation is not clear (Lange et al., 2010b) (chapter 3.1.1.). Since LIF is a secreted protein produced by a subset of Muller cells in the INL, it seems conceivable that newly produced LIF not only reaches photoreceptors but also other retinal cells like ganglion cells. Assuming that upregulation and secretion of LIF is a general response of Muller cells to any retinal stress or damage, it seems possible that a system has been established which can discriminate between the different cell types and regulate a molecular response which is specific and optimal for the injured cell. Thus, it would be interesting to investigate whether LIF-mediated activation of JAK3 may be important for a molecular response of injured ganglion cells, for example during glaucoma. Since

JAK3 is involved in many types of immune responses, it would also be interesting to enlighten its role during ocular immune diseases like autoimmune uveitis.

The LIF-induced pathway involving EDN2 and FGF2 is an endogenous survival pathway that aims at the protection of photoreceptors from damage (chapter 3.2.1.). Even though expression of *Lif* is upregualated early after light exposure (Samardzija et al., 2006a), it is not sufficient to render full protection to photoreceptors after acute light damage, presumably because damage in most cells is already beyond repair at the time of LIF upregulation. Nevertheless, lack of LIF increases the severity of the lesion after light exposure suggesting that the system still has the possibility to protect some cells in the light damage paradigm (Burgi et al., 2009). In slowly progressing inherited degenerations, photoreceptors do not enter the degenerative process as simultanously as in the light-induced model. That means that when Muller cells upregulate *Lif* expression after the first cells suffered damage, LIF protein is already present to protect and support cells, which are still viable. As a consequence, degeneration proceeds slower. In the absence of LIF, such a protection does not happen and cells may enter apoptosis earlier. Indeed, degeneration in the VPP mouse is induced at a similar postnatal stage with or without endogenous LIF, but proceeds much slower in the presence of LIF (Joly et al., 2008) (reference refers to chapter 3.2.1. of this work). This suggests that LIF might only be able to protect cells effectively when the death process has not yet been started. Such a conclusion is supported by the observation that preconditioning with moderate levels of light protects photoreceptors from a subsequent strong light exposure. Here, the cellular stress induced by the preconditioning protocol may elevate LIF levels in the retina to a level which is sufficient to protect cells from the following toxic insult (Chollangi et al., 2009). Furthermore, intravitreal injections of recombinant LIF in mice protected photoreceptors from light induced damage (Ueki et al., 2008). Again, LIF was present before the overwhelming light stress.

The LIF-endogenous survival pathway was also activated during retinal degeneration induced by the absence of the VHL tumor suppressor gene (chapter 3.1.3.). According to the above hypothesis, we would expect that retinal degeneration would proceed much faster in *Vhl* knockdown mice lacking LIF. The observation that not only photoreceptors but also other retinal cells in peripheral cell layers undergo apoptosis in the *Vhl* knockdown mice supports our earlier suggestion (see above) that the LIF-pathway might be a global response to different kinds of retinal cell death. LIF could

therefore be a potential medication for human patients. Interestingly, ciliary neurotophic factor (CNTF), another member of the IL-6 family of cytokines, also signals through the JAK/STAT pathway and has protective capacity. In an innovative approach to deliver CNTF to the human retina of AMD and RP patients (Emerich and Thanos, 2008), capsules containing genetically modified cells that produce CNTF are implanted into the vitreous of the human eye. These studies are in phase 2 clinical trial at the moment (http://www.neurotechusa.com/ect/nt-501.asp).

As mentioned above, several endogenous rescue systems exist in the mouse retina. Thus, protection of the retina may not solely depend on the JAK/STAT system induced by LIF or CNTF. Our lab has shown, for example, that hypoxic preconditioning induces a strong neuroprotective effect (Grimm et al., 2002), which, at least partially, may involve transcription factors of the HIF family (chapter 3.1.2.). Artificial stabilization of HIF1A and HIF2A by the ablation of VHL in normoxic photoreceptors rendered transient protection against light induced degeneration. Further studies will reveal whether this effect is indeed because of HIF stabilization or whether other effects due to the downregulation of VHL may account for the observed protection. Intriguingly, HIF1 originating from photoreceptors does not seem to be essential for neuroprotection, because photoreceptor-specific HIF1 knockdown mice were still protected from a light insult after hypoxic preconditioning (Thiersch et al., 2009) (reference refers to chapter 3.2.2. of this work). The fact that stabilization of HIF2A in addition to HIF1A in photoreceptors rendered at least a transient protection makes HIF2 a more likely candidate for neuroprotection.

EPO, a factor that is most likely produced by HIF2 (Haase, 2010), was shown to be activated after hypoxic preconditioning and to render protection against light induced retinal degeneration and in other models (Ghezzi and Brines, 2004; Grimm et al., 2005). EPO was still activated after hypoxia in photoreceptor-specific HIF1 knockdown mice, which were still protected against light induced degeneration. However, EPO was not activated and mice were only transiently protected after experimental stabilization of HIF1 and HIF2 in photoreceptors of the *Vhl* knockdown mice. This further supports an important role for EPO in the protection of photoreceptors in the retina. The fact that expression of EPO was not induced after photoreceptor specific HIF2A stabilization hints to an activation of EPO in cell layers other than the photoreceptor layer during hypoxic preconditioning. In retinal ischemia

for example, HIF2A activation is restricted to Müller glial cells and astrocytes (Mowat et al., 2010).

However, after systemic application of EPO, protection against light damage was not as complete as with hypoxic preconditioning and no protection was achieved in models of inherited retinal degeneration like the rd1 or the VPP mouse (Grimm et al., 2005). It is therefore very likely that factors induced by hypoxic preconditioning in addition to EPO are important for the protection. Further research will aim at the identification of these additional factors for possible clinical application in the future.

Although our approach of mimiking hypoxia in the normoxic retina by the artificial and long-term stabilization of HIFA transcription factors is valuable for the investigation of HIF- and or VHL-mediated biological mechanisms, it may not be a possible way to protect visual cells in patients. We showed for example that long-term stabilization of HIFs can lead to retinal degeneration (chapter 3.1.2. and 3.1.3.). Additionally, if HIFs are stabilized very early during development of the eye, the retinal vasculature is severely disturbed. If repetitive short-term stabilization of HIFs in all retinal cell layers was accomplished after the development of the retinal vasculature one could possibly circumvent this problem. Although difficult to achieve, such a stabilization could be attempted by the pharmaceutical inhibition of prolyl hydroxylases or the VHL protein. This could provide a good model to test the influences on pure HIF stabilization in the whole retina for light induced degeneration.

It remains unclear what molecular mechanisms account for retinal degeneration in general and in the α-Cre;*Vhl* knockdown mice. The activation of caspases during retinal degeneration has been controversially discussed (Jomary et al., 2001; Donovan and Cotter, 2002). Caspase 1 has been shown to be activated during light induced and two models for inherited retinal degeneration (rd1 and VPP). However, ablation of caspase 1 was only protective in the VPP model (Samardzija et al., 2006b). In our study we showed that during retinal degeneration induced by the absence of the tumor suppressor protein VHL in the $Vhl^{flox/flox}$; α-cre mouse expression of caspase 8 was induced in addition to caspase 1 (chapter 3.1.3.). Whether this activation is due to the cell death in the retina of *Vhl* knockdowns or whether it is directly connected to the absence of VHL remains to be elucidated. Since we never detected active (cleaved)

forms of these caspases, it also needs to be investigated whether these caspases have a role in the degenerative process and how they might function.

An additional interesting observation awaiting further investigation was the upregulation of several genes connected to the extracellular matrix in $Vhl^{flox/flox}$; α-cre mice. The extracellular matrix is important for a variety of processes in the retina including development, intercellular transport, cell-cell communication and tissue stability. The increased expression of some of these genes suggests an alteration of the ECM, which may influence cellular physiology and may also facilitate abnormal vessel growth as observed in the retinas of our knockdown mice. It would thus be very interesting to study the role of such genes in connection with retinal degeneration.

In summary, intense research is still ongoing to understand the mechanisms of how retinal degenerations develop and how endogenous survival systems attempt to protect cells in the retina. Detailed knowledge of these systems may allow to target key molecules in order to preserve vision by therapeutical strategies. Our studies on JAK3, the JAK/STAT pathway, LIF and hypoxia have contributed to this knowledge and provided a closer insight into some of the signaling mechanisms during retinal degeneration.

All together our research and the research of all the other groups working on different aspects of retinal degeneration will hopefully someday help patients to keep useful vision or even to restore some of their lost vision and thus improve their quality of life.

5. Appendix

5.1. References

Aiello LP, Avery RL, Arrigg PG, Keyt BA, Jampel HD, Shah ST, Pasquale LR, Thieme H, Iwamoto MA, Park JE, et al. (1994) Vascular endothelial growth factor in ocular fluid of patients with diabetic retinopathy and other retinal disorders. N Engl J Med 331:1480-1487.

An WG, Kanekal M, Simon MC, Maltepe E, Blagosklonny MV, Neckers LM (1998) Stabilization of wild-type p53 by hypoxia-inducible factor 1alpha. Nature 392:405-408.

Bowes C, Li T, Danciger M, Baxter LC, Applebury ML, Farber DB (1990) Retinal degeneration in the rd mouse is caused by a defect in the beta subunit of rod cGMP-phosphodiesterase. Nature 347:677-680.

Bruick RK, McKnight SL (2001) A conserved family of prolyl-4-hydroxylases that modify HIF. Science 294:1337-1340.

Burgi S, Samardzija M, Grimm C (2009) Endogenous leukemia inhibitory factor protects photoreceptor cells against light-induced degeneration. Mol Vis 15:1631-1637.

Calzada MJ, Esteban MA, Feijoo-Cuaresma M, Castellanos MC, Naranjo-Suarez S, Temes E, Mendez F, Yanez-Mo M, Ohh M, Landazuri MO (2006) von Hippel-Lindau tumor suppressor protein regulates the assembly of intercellular junctions in renal cancer cells through hypoxia-inducible factor-independent mechanisms. Cancer Res 66:1553-1560.

Carmeliet P (2003) Angiogenesis in health and disease. Nat Med 9:653-660.

Chang B, Hawes NL, Pardue MT, German AM, Hurd RE, Davisson MT, Nusinowitz S, Rengarajan K, Boyd AP, Sidney SS, Phillips MJ, Stewart RE, Chaudhury R, Nickerson JM, Heckenlively JR, Boatright JH (2007) Two mouse retinal degenerations caused by missense mutations in the beta-subunit of rod cGMP phosphodiesterase gene. Vision Res 47:624-633.

Chitalia VC, Foy RL, Bachschmid MM, Zeng L, Panchenko MV, Zhou MI, Bharti A, Seldin DC, Lecker SH, Dominguez I, Cohen HT (2008) Jade-1 inhibits Wnt

signalling by ubiquitylating beta-catenin and mediates Wnt pathway inhibition by pVHL. Nat Cell Biol 10:1208-1216.

Chollangi S, Wang J, Martin A, Quinn J, Ash JD (2009) Preconditioning-induced protection from oxidative injury is mediated by leukemia inhibitory factor receptor (LIFR) and its ligands in the retina. Neurobiol Dis 34:535-544.

Donovan M, Cotter TG (2002) Caspase-independent photoreceptor apoptosis in vivo and differential expression of apoptotic protease activating factor-1 and caspase-3 during retinal development. Cell Death Differ 9:1220-1231.

Emerich DF, Thanos CG (2008) NT-501: an ophthalmic implant of polymer-encapsulated ciliary neurotrophic factor-producing cells. Curr Opin Mol Ther 10:506-515.

Fleisch VC, Schonthaler HB, von Lintig J, Neuhauss SC (2008) Subfunctionalization of a retinoid-binding protein provides evidence for two parallel visual cycles in the cone-dominant zebrafish retina. J Neurosci 28:8208-8216.

Frank RN (2004) Diabetic retinopathy. N Engl J Med 350:48-58.

Franze K, Grosche J, Skatchkov SN, Schinkinger S, Foja C, Schild D, Uckermann O, Travis K, Reichenbach A, Guck J (2007) Muller cells are living optical fibers in the vertebrate retina. Proc Natl Acad Sci U S A 104:8287-8292.

Freedman MS, Lucas RJ, Soni B, von Schantz M, Munoz M, David-Gray Z, Foster R (1999) Regulation of mammalian circadian behavior by non-rod, non-cone, ocular photoreceptors. Science 284:502-504.

Ghezzi P, Brines M (2004) Erythropoietin as an antiapoptotic, tissue-protective cytokine. Cell Death Differ 11 Suppl 1:S37-44.

Gnarra JR, Ward JM, Porter FD, Wagner JR, Devor DE, Grinberg A, Emmert-Buck MR, Westphal H, Klausner RD, Linehan WM (1997) Defective placental vasculogenesis causes embryonic lethality in VHL-deficient mice. Proc Natl Acad Sci U S A 94:9102-9107.

Gooley JJ, Lu J, Fischer D, Saper CB (2003) A broad role for melanopsin in nonvisual photoreception. J Neurosci 23:7093-7106.

Grimm C, Wenzel A, Hafezi F, Reme CE (2000a) Gene expression in the mouse retina: the effect of damaging light. Mol Vis 6:252-260.

Grimm C, Wenzel A, Hafezi F, Yu S, Redmond TM, Reme CE (2000b) Protection of Rpe65-deficient mice identifies rhodopsin as a mediator of light-induced retinal degeneration. Nat Genet 25:63-66.

Grimm C, Wenzel A, Acar N, Keller S, Seeliger M, Gassmann M (2006) Hypoxic preconditioning and erythropoietin protect retinal neurons from degeneration. Adv Exp Med Biol 588:119-131.

Grimm C, Hermann DM, Bogdanova A, Hotop S, Kilic U, Wenzel A, Kilic E, Gassmann M (2005) Neuroprotection by hypoxic preconditioning: HIF-1 and erythropoietin protect from retinal degeneration. Semin Cell Dev Biol 16:531-538.

Grimm C, Wenzel A, Groszer M, Mayser H, Seeliger M, Samardzija M, Bauer C, Gassmann M, Reme CE (2002) HIF-1-induced erythropoietin in the hypoxic retina protects against light-induced retinal degeneration. Nat Med 8:718-724.

Gustafsson MV, Zheng X, Pereira T, Gradin K, Jin S, Lundkvist J, Ruas JL, Poellinger L, Lendahl U, Bondesson M (2005) Hypoxia requires notch signaling to maintain the undifferentiated cell state. Dev Cell 9:617-628.

Haase VH (2010) Hypoxic regulation of erythropoiesis and iron metabolism. Am J Physiol Renal Physiol 299:F1-13.

Hattar S, Kumar M, Park A, Tong P, Tung J, Yau KW, Berson DM (2006) Central projections of melanopsin-expressing retinal ganglion cells in the mouse. J Comp Neurol 497:326-349.

Hergovich A, Lisztwan J, Barry R, Ballschmieter P, Krek W (2003) Regulation of microtubule stability by the von Hippel-Lindau tumour suppressor protein pVHL. Nat Cell Biol 5:64-70.

Hu CJ, Wang LY, Chodosh LA, Keith B, Simon MC (2003) Differential roles of hypoxia-inducible factor 1alpha (HIF-1alpha) and HIF-2alpha in hypoxic gene regulation. Mol Cell Biol 23:9361-9374.

Huang LE, Gu J, Schau M, Bunn HF (1998) Regulation of hypoxia-inducible factor 1alpha is mediated by an O2-dependent degradation domain via the ubiquitin-proteasome pathway. Proc Natl Acad Sci U S A 95:7987-7992.

Ivan M, Kondo K, Yang H, Kim W, Valiando J, Ohh M, Salic A, Asara JM, Lane WS, Kaelin WG, Jr. (2001) HIFalpha targeted for VHL-mediated destruction by proline hydroxylation: implications for O2 sensing. Science 292:464-468.

Iwai K, Yamanaka K, Kamura T, Minato N, Conaway RC, Conaway JW, Klausner RD, Pause A (1999) Identification of the von Hippel-lindau tumor-suppressor protein as part of an active E3 ubiquitin ligase complex. Proc Natl Acad Sci U S A 96:12436-12441.

Jaakkola P, Mole DR, Tian YM, Wilson MI, Gielbert J, Gaskell SJ, Kriegsheim A, Hebestreit HF, Mukherji M, Schofield CJ, Maxwell PH, Pugh CW, Ratcliffe PJ (2001) Targeting of HIF-alpha to the von Hippel-Lindau ubiquitylation complex by O2-regulated prolyl hydroxylation. Science 292:468-472.

Jager RD, Mieler WF, Miller JW (2008) Age-related macular degeneration. N Engl J Med 358:2606-2617.

Joly S, Lange C, Thiersch M, Samardzija M, Grimm C (2008) Leukemia inhibitory factor extends the lifespan of injured photoreceptors in vivo. J Neurosci 28:13765-13774.

Joly S, Francke M, Ulbricht E, Beck S, Seeliger M, Hirrlinger P, Hirrlinger J, Lang KS, Zinkernagel M, Odermatt B, Samardzija M, Reichenbach A, Grimm C, Reme CE (2009) Cooperative phagocytes: resident microglia and bone marrow immigrants remove dead photoreceptors in retinal lesions. Am J Pathol 174:2310-2323.

Jomary C, Neal MJ, Jones SE (2001) Characterization of cell death pathways in murine retinal neurodegeneration implicates cytochrome c release, caspase activation, and bid cleavage. Mol Cell Neurosci 18:335-346.

Kamura T, Koepp DM, Conrad MN, Skowyra D, Moreland RJ, Iliopoulos O, Lane WS, Kaelin WG, Jr., Elledge SJ, Conaway RC, Harper JW, Conaway JW (1999) Rbx1, a component of the VHL tumor suppressor complex and SCF ubiquitin ligase. Science 284:657-661.

Keller C, Grimm C, Wenzel A, Hafezi F, Reme C (2001) Protective effect of halothane anesthesia on retinal light damage: inhibition of metabolic rhodopsin regeneration. Invest Ophthalmol Vis Sci 42:476-480.

Kibel A, Iliopoulos O, DeCaprio JA, Kaelin WG, Jr. (1995) Binding of the von Hippel-Lindau tumor suppressor protein to Elongin B and C. Science 269:1444-1446.

Kile BT, Alexander WS (2001) The suppressors of cytokine signalling (SOCS). Cell Mol Life Sci 58:1627-1635.

Koochekpour S, Jeffers M, Wang PH, Gong C, Taylor GA, Roessler LM, Stearman R, Vasselli JR, Stetler-Stevenson WG, Kaelin WG, Jr., Linehan WM, Klausner RD, Gnarra JR, Vande Woude GF (1999) The von Hippel-Lindau tumor suppressor gene inhibits hepatocyte growth factor/scatter factor-induced

invasion and branching morphogenesis in renal carcinoma cells. Mol Cell Biol 19:5902-5912.

Koshiji M, Kageyama Y, Pete EA, Horikawa I, Barrett JC, Huang LE (2004) HIF-1alpha induces cell cycle arrest by functionally counteracting Myc. Embo J 23:1949-1956.

Krebs DL, Hilton DJ (2001) SOCS proteins: negative regulators of cytokine signaling. Stem Cells 19:378-387.

Kurban G, Duplan E, Ramlal N, Hudon V, Sado Y, Ninomiya Y, Pause A (2008) Collagen matrix assembly is driven by the interaction of von Hippel-Lindau tumor suppressor protein with hydroxylated collagen IV alpha 2. Oncogene 27:1004-1012.

Kuznetsova AV, Meller J, Schnell PO, Nash JA, Ignacak ML, Sanchez Y, Conaway JW, Conaway RC, Czyzyk-Krzeska MF (2003) von Hippel-Lindau protein binds hyperphosphorylated large subunit of RNA polymerase II through a proline hydroxylation motif and targets it for ubiquitination. Proc Natl Acad Sci U S A 100:2706-2711.

Lange C, Thiersch M, Samardzija M, Grimm C (2010a) The differential role of Jak/STAT signaling in retinal degeneration. Adv Exp Med Biol 664:601-607.

Lange C, Thiersch M, Samardzija M, Burgi S, Joly S, Grimm C (2010b) LIF-dependent JAK3 activation is not essential for retinal degeneration. J Neurochem 113:1210-1220.

Li Z, Na X, Wang D, Schoen SR, Messing EM, Wu G (2002) Ubiquitination of a novel deubiquitinating enzyme requires direct binding to von Hippel-Lindau tumor suppressor protein. J Biol Chem 277:4656-4662.

Li Z, Wang D, Na X, Schoen SR, Messing EM, Wu G (2003) The VHL protein recruits a novel KRAB-A domain protein to repress HIF-1alpha transcriptional activity. Embo J 22:1857-1867.

Liu C, Peng M, Laties AM, Wen R (1998) Preconditioning with bright light evokes a protective response against light damage in the rat retina. J Neurosci 18:1337-1344.

Mahon PC, Hirota K, Semenza GL (2001) FIH-1: a novel protein that interacts with HIF-1alpha and VHL to mediate repression of HIF-1 transcriptional activity. Genes Dev 15:2675-2686.

Mowat FM, Luhmann UF, Smith AJ, Lange C, Duran Y, Harten S, Shukla D, Maxwell PH, Ali RR, Bainbridge JW (2010) HIF-1alpha and HIF-2alpha are differentially activated in distinct cell populations in retinal ischaemia. PLoS One 5:e11103.

Naash MI, Hollyfield JG, al-Ubaidi MR, Baehr W (1993) Simulation of human autosomal dominant retinitis pigmentosa in transgenic mice expressing a mutated murine opsin gene. Proc Natl Acad Sci U S A 90:5499-5503.

Ohh M, Kaelin WG, Jr. (1999) The von Hippel-Lindau tumour suppressor protein: new perspectives. Mol Med Today 5:257-263.

Ohh M, Park CW, Ivan M, Hoffman MA, Kim TY, Huang LE, Pavletich N, Chau V, Kaelin WG (2000) Ubiquitination of hypoxia-inducible factor requires direct binding to the beta-domain of the von Hippel-Lindau protein. Nat Cell Biol 2:423-427.

Ohh M, Yauch RL, Lonergan KM, Whaley JM, Stemmer-Rachamimov AO, Louis DN, Gavin BJ, Kley N, Kaelin WG, Jr., Iliopoulos O (1998) The von Hippel-Lindau tumor suppressor protein is required for proper assembly of an extracellular fibronectin matrix. Mol Cell 1:959-968.

Okuda H, Saitoh K, Hirai S, Iwai K, Takaki Y, Baba M, Minato N, Ohno S, Shuin T (2001) The von Hippel-Lindau tumor suppressor protein mediates ubiquitination of activated atypical protein kinase C. J Biol Chem 276:43611-43617.

Pause A, Lee S, Worrell RA, Chen DY, Burgess WH, Linehan WM, Klausner RD (1997) The von Hippel-Lindau tumor-suppressor gene product forms a stable complex with human CUL-2, a member of the Cdc53 family of proteins. Proc Natl Acad Sci U S A 94:2156-2161.

Peruzzi B, Athauda G, Bottaro DP (2006) The von Hippel-Lindau tumor suppressor gene product represses oncogenic beta-catenin signaling in renal carcinoma cells. Proc Natl Acad Sci U S A 103:14531-14536.

Pioli PA, Rigby WF (2001) The von Hippel-Lindau protein interacts with heteronuclear ribonucleoprotein a2 and regulates its expression. J Biol Chem 276:40346-40352.

Redmond TM, Yu S, Lee E, Bok D, Hamasaki D, Chen N, Goletz P, Ma JX, Crouch RK, Pfeifer K (1998) Rpe65 is necessary for production of 11-cis-vitamin A in the retinal visual cycle. Nat Genet 20:344-351.

Reme CE, Grimm C, Hafezi F, Marti A, Wenzel A (1998) Apoptotic cell death in retinal degenerations. Prog Retin Eye Res 17:443-464.

Risau W (1997) Mechanisms of angiogenesis. Nature 386:671-674.

Roe JS, Kim H, Lee SM, Kim ST, Cho EJ, Youn HD (2006) p53 stabilization and transactivation by a von Hippel-Lindau protein. Mol Cell 22:395-405.

Salceda S, Caro J (1997) Hypoxia-inducible factor 1alpha (HIF-1alpha) protein is rapidly degraded by the ubiquitin-proteasome system under normoxic conditions. Its stabilization by hypoxia depends on redox-induced changes. J Biol Chem 272:22642-22647.

Samardzija M, Wenzel A, Aufenberg S, Thiersch M, Reme C, Grimm C (2006a) Differential role of Jak-STAT signaling in retinal degenerations. Faseb J 20:2411-2413.

Samardzija M, Wenzel A, Thiersch M, Frigg R, Reme C, Grimm C (2006b) Caspase-1 ablation protects photoreceptors in a model of autosomal dominant retinitis pigmentosa. Invest Ophthalmol Vis Sci 47:5181-5190.

Samardzija M, von Lintig J, Tanimoto N, Oberhauser V, Thiersch M, Reme CE, Seeliger M, Grimm C, Wenzel A (2008) R91W mutation in Rpe65 leads to milder early-onset retinal dystrophy due to the generation of low levels of 11-cis-retinal. Hum Mol Genet 17:281-292.

Samardzija M, Tanimoto N, Kostic C, Beck S, Oberhauser V, Joly S, Thiersch M, Fahl E, Arsenijevic Y, von Lintig J, Wenzel A, Seeliger MW, Grimm C (2009) In conditions of limited chromophore supply rods entrap 11-cis-retinal leading to loss of cone function and cell death. Hum Mol Genet 18:1266-1275.

Schindler C, Levy DE, Decker T (2007) JAK-STAT signaling: from interferons to cytokines. J Biol Chem 282:20059-20063.

Senger DR, Galli SJ, Dvorak AM, Perruzzi CA, Harvey VS, Dvorak HF (1983) Tumor cells secrete a vascular permeability factor that promotes accumulation of ascites fluid. Science 219:983-985.

Shuai K (2006) Regulation of cytokine signaling pathways by PIAS proteins. Cell Res 16:196-202.

Stebbins CE, Kaelin WG, Jr., Pavletich NP (1999) Structure of the VHL-ElonginC-ElonginB complex: implications for VHL tumor suppressor function. Science 284:455-461.

Sun H, Tonks NK (1994) The coordinated action of protein tyrosine phosphatases and kinases in cell signaling. Trends Biochem Sci 19:480-485.

Thiersch M, Raffelsberger W, Frigg R, Samardzija M, Wenzel A, Poch O, Grimm C (2008) Analysis of the retinal gene expression profile after hypoxic preconditioning identifies candidate genes for neuroprotection. BMC Genomics 9:73.

Thiersch M, Lange C, Joly S, Heynen S, Le YZ, Samardzija M, Grimm C (2009) Retinal neuroprotection by hypoxic preconditioning is independent of hypoxia-inducible factor-1 alpha expression in photoreceptors. Eur J Neurosci 29:2291-2302.

Thoma CR, Frew IJ, Hoerner CR, Montani M, Moch H, Krek W (2007) pVHL and GSK3beta are components of a primary cilium-maintenance signalling network. Nat Cell Biol 9:588-595.

Ueki Y, Wang J, Chollangi S, Ash JD (2008) STAT3 activation in photoreceptors by leukemia inhibitory factor is associated with protection from light damage. J Neurochem 105:784-796.

Wang GL, Semenza GL (1993) Characterization of hypoxia-inducible factor 1 and regulation of DNA binding activity by hypoxia. J Biol Chem 268:21513-21518.

Wang JS, Kefalov VJ (2009) An alternative pathway mediates the mouse and human cone visual cycle. Curr Biol 19:1665-1669.

Wenzel A, Grimm C, Samardzija M, Reme CE (2005) Molecular mechanisms of light-induced photoreceptor apoptosis and neuroprotection for retinal degeneration. Prog Retin Eye Res 24:275-306.

Wenzel A, Reme CE, Williams TP, Hafezi F, Grimm C (2001) The Rpe65 Leu450Met variation increases retinal resistance against light-induced degeneration by slowing rhodopsin regeneration. J Neurosci 21:53-58.

Wolf G (2004) The visual cycle of the cone photoreceptors of the retina. Nutr Rev 62:283-286.

Yang H, Minamishima YA, Yan Q, Schlisio S, Ebert BL, Zhang X, Zhang L, Kim WY, Olumi AF, Kaelin WG, Jr. (2007) pVHL acts as an adaptor to promote the inhibitory phosphorylation of the NF-kappaB agonist Card9 by CK2. Mol Cell 28:15-27.

Zhang C, Rosenbaum DM, Shaikh AR, Li Q, Rosenbaum PS, Pelham DJ, Roth S (2002) Ischemic preconditioning attenuates apoptotic cell death in the rat retina. Invest Ophthalmol Vis Sci 43:3059-3066.

Zhou MI, Wang H, Foy RL, Ross JJ, Cohen HT (2004) Tumor suppressor von Hippel-Lindau (VHL) stabilization of Jade-1 protein occurs through plant homeodomains and is VHL mutation dependent. Cancer Res 64:1278-1286.

5.2. List of Abbreviations

11-RDH	11-*cis* retinol dehydrogenase
ABCA	ATP binding cassette protein
ADM	Adrenomedullin
AMD	Age related macular degeneration
ARNT	aryl-hydrocarbon receptor nuclear translocator
atRDH	all-*trans* retinol dehydrogenase
bHLH	basic helix-loop-helix
BNIP3	BCL2/adenovirus E1B interacting protein
cGMP	cyclic guanosine monophosphate
CNTF	cililary neurotophic factor
CRALBP	cellular retinaldehyde binding protein
CRBP	cellular retinol binding protein
EDN2	endothelin 2
EDNRb	endothelin receptor b
EGLN1	egl nine homolog 1, prolyl hydroxylase 2
EPO	erythropoietin
FGF2	fibroblast growth factor 2
FIH	factor inhibiting HIF
GC	Guanylate cyclase
GCAP	guanylate-cyclase-activating protein
GCL	ganglion cell layer
GDP	guanosine-5 diphosphate
GFAP	glial fibrillary acidic protein

GLUT1	also: SLCRA1: solute carrier family 2 member 1
GTP	guanosine-5 triphosphate
HIF	hypoxia inducible factor
hnRNP A2	heterogenous nuclear ribonucleoprotein A2
INL	inner nulear layer
IPL	inner plexiform layer
IRBP	inter photoreceptor retinol binding protein
IS	inner segments
JAK	Janus kinase
KRAB-A	Kruppel associated box A
LGN	lateral geniculate nucleus
LIF	leukemia inhibitory factor
LRAT	lecithin retinol acyl transferase
MCP1	monocyte chemoattractive protein 1
ONL	outer nuclear layer
OPL	outer plexiform layer
OS	outer segments
p53	protein 53
PAS	PER/ARNT/SIM
PDE	phosphodiesterase
PIAS	protein inhibitor of activated STAT
PTP	protein tyrosin phosphatase
Rbx1	ring box 1
Rd1	retinal degeneration 1
Rd10	retinal degeneration 10
REH	retinyl ester hydrolase
RHO	rod opsin
RP	retinitis pigmentosa
RPE	retinal pigment epithelium
RPE65	retinal pigment epithelium 65
SAG	s-antigen
SHP1	scr-homology containing phosphatase 1
SOCS	suppressor of cytokine signaling
STAT	signal transducer and activator of transcription

VEGF	vascular endothelial growth factor
VHL	von Hippel-Lindau
VHLaK	VHL associated KRAB-A domain containing protein
VPP	V20G, P23H, P27L mutations in the inherited mouse model

6. Curriculum vitae

Name		Lange
First name		Christina
Date of birth		August 1 1981
Nationality		German
Address	Office:	Sternwartstrasse 14,
		8091 Zurich, Switzerland
	Private:	Kreuzstrasse 23,
		4600 Olten, Switzerland
Phone:	Office:	0041/442553872
	Private:	0041/622960937
	Mobil:	0041/786480183
Email:	Office:	christina.lange@usz.ch
	Private:	christina.lange@yahoo.de

Education

February 2007 – present: Ph.D. student in the Lab for Retinal Cell Biology, Department Ophthalmology, University Hospital Zurich; title: “Signaling in retinal degeneration and neuroprotection - the role of JAK/STAT and HIF”.

October 2006: Graduated Neuroscience at the ETH Zurich, Zurich, Switzerland: Diploma thesis at the zoological institute of the University of Zurich; title: “Procedural learning during path integration of the desert ant *Cataglyphis fortis*”.

2001 – 2006: study of Biochemistry (main field neuroscience) at the ETH Zurich, Zurich

1994 – 2001: Kantonsschule Rychenberg, Winterthur, Switzerland

before 1994: Primary school in Germany

Awards

2008: Travel award and speaker at the XIIIth international symposium on retinal degeneration, 2008 Emei Shan, China, title: “The role of JAK/STAT signaling in retinal degeneration”

2010: Retina Suisse Award 2010 in the category “Young Researchers” for the best talk, title: “Does normoxic activation of HIF prevent cell death?”, Swiss Eye Resaerch Meeting 2010 Bienne, Switzerland.

Courses

- LTK Module 1: Introductory course in laboratory animal science, Summer Semester (SS) 2007
- Membrane transport: ZIHP course, SS 2007
- Scientific writing: ZIHP course, Autumn Semester (AS) 2007
- Introduction in Bioethics: transferable skills course of LSZGS, AS 2007
- Project Management: transferable skills course of the University of Zurich, SS 2008
- Presentation: transferable skills course of the University of Zürich, SS 2008
- Electrophysiology, ZIHP course, SS 2008
- Mouse physiology, ZIHP course, SS 2008
- Sensory systems, ZIHP course, AS 2008

Original publications

1. Knaden M, **Lange C**, Wehner R (2006) The importance of procedural knowledge in desert-ant navigation. Curr Biol 16:R916-917.
2. Joly S, **Lange C**, Thiersch M, Samardzija M, Grimm C (2008) Leukemia inhibitory factor extends the lifespan of injured photoreceptors in vivo. J Neurosci 28:13765-13774.
3. Thiersch M, **Lange C**, Joly S, Heynen S, Le YZ, Samardzija M, Grimm C (2009) Retinal neuroprotection by hypoxic preconditioning is independent of hypoxia-

inducible factor-1 alpha expression in photoreceptors. Eur J Neurosci 29:2291-2302.

4. **Lange C**, Thiersch M, Samardzija M, Burgi S, Joly S, Grimm C (2010) LIF dependent JAK3 activation is not essential for retinal degeneration. J Neurochem 113:1210-1220.
5. **Lange C**, Tanimoto N, Beck S, Huber G, Samardzija M, Seeliger M, Grimm C (submitted) Retina specific activation of a sustained hypoxia-like response leads to severe retinal degeneration and loss of vision. Neurobiol Dis.
6. **Lange C**, Tanimoto N, Heynen S, Huber G, Beck S, Joly S, Seeliger M, Samardzija M, Grimm C (in preparation) Normoxic activation of hypoxia inducible factors provides transient protection against light induced retinal degeneration.

Bookchapters

1. **Lange C**, Thiersch M, Samardzija M, Grimm C The differential role of Jak/STAT signaling in retinal degeneration. Adv Exp Med Biol 664:601-607.

Presentations

Oral presentations

- March 2008: 7th day of clinical research 2008, University Hospital Zurich, title: "The role of JAK/STAT signaling in retinal degeneration"
- September 2008: XIIIth international symposium on retinal degeneration, 2008 Emei Shan, China, title: "The role of JAK/STAT signaling in retinal degeneration"
- February 2009: Swiss eye research meeting 2009, Biel, Switzerland, title: "The role of JAK/STAT signaling in retinal degeneration"
- June 2009: retreat of the imMed Phd-program, Oberschan, Switzerland, title: "Does normoxic activation of HIF prevent cell death?"
- January 2010: Swiss eye research meeting 2010, Biel, Switzerland, title: "Does normoxic activation of HIF prevent cell death?"

Poster presentations

- March 2008: 7th day of clinical research 2008, University Hospital Zurich, title: "The role of JAK/STAT signaling in retinal degeneration"
- March 2009: 8th day of clinical research 2009, University Hospital Zurich, title: "The differential role of JAK/STAT signaling in retinal degeneration"
- April 2009: Pro Retina Meeting, Potsdam, Germany, title: "The differential role of JAK/STAT signaling in retinal degeneration"
- May 2009: ARVO, Fort Lauderdale, Florida, USA, title: "The differential role of JAK/STAT signaling in retinal degeneration"
- March 2010: 9th day of clinical research 2010, University Hospital Zurich, title: "Normoxic activation of HIFs in photoreceptors provides transcient protection against light induced retinal degeneration"
- April 2010: Pro Retina Meeting, Potsdam, Germany, title: "Normoxic activation of HIFs in photoreceptors provides transcient protection against light induced retinal degeneration"
- May 2010: ARVO, Fort Lauderdale, Florida, USA, title: "Normoxic activation of HIFs in photoreceptors provides transcient protection against light induced retinal degeneration"

7. Acknowledgements

I want to thank the members of my thesis committee (Prof. Dr. Stephan Neuhaus, Prof. Dr. Christian Grimm, Prof. Dr. Wolfgang Berger and Prof. Dr. Stephan Christen) for reviewing this thesis.
Additionally I thank my Doctor father Prof. Dr. Stephan Neuhaus for dealing with all the administrative paperwork connected to my thesis.
Very special thanks go to my supervisor Prof. Dr. Christian Grimm. First of all he was the one who offered me the opportunity to conduct my Ph.D. in his lab. Christian was all the time a helping hand discussing project outlines, correcting manuscripts very fast (!) and supporting me also through the tough times of my Ph.D.
Another special thank you goes to Dr. Marijana Samardzija and Dr. Markus Thiersch. Marijana and Markus introduced me to most of the technical work in the lab and were always very helpful.
Additionally I thank all the other old and current members of the lab (Prof. Dr. Charlotte Remé, Dr. Sandrine Joly, Dr. Karina Guziewicz, Dr. Cavit Agca, Severin Heynen, Christian Caprara, Sandra Bürgi, Corinne Britschgi, Véronique Wettstein, Dr. Kerstin Birke, Hedwig Wariwoda, Coni Imsand, Philip Huber and Christel Beck) for technical help, discussions, beers, Karaoke etc.
Finally I thank all my friends and family especially my dear boyfriend, Dominik Giger, for supporting me all the time during this sometimes tough PhD. Domi thank you for motivating me on and on to finish this thesis; in the end I see why I did it and I don’t regret it at all!

Additionally I thank all the people that are not mentioned by name. It is impossible to list all of them here, but all the people who accompanied me through this time deserve a thank you, too.